A STUDY OF THE COMPOSITE ACTION BETWEEN MASONRY PANELS AND SUPPORTING BEAMS

A Thesis submitted for the Degree of
Doctor of Philosophy
of the
University of Edinburgh

by

AHMED ELTAYEB AHMED, B.Sc.(C.E.)

Department of Civil Engineering and Building Science

JANUARY 1977

DECLARATION

I hereby declare that this Thesis has been composed by me and that the work included has been carried out by myself.

CONTENTS

CONTENTS (continued) *page no*

CONTENTS (continued)

CONTENTS (continued)

ACKNOWLEDGEMENT

The author wishes to express his gratitude to Dr S R Davies for his continuous supervision, valuable suggestions and encouragement during the period of study.

The author would like to thank Dr B P Sinha and colleagues in the Department for their helpful discussions.

Thanks are also due to the technical staff and the photographic unit of the Department and to Miss Linda Murray for her careful typing of the manuscript.

The author also wishes to express his thanks to the British Ceramic Research Unit for providing the bricks.

Thanks are also due to the Sudan Government for awarding the Scholarship and the financial support.

At last but not the least Professor A W Hendry is thankfully acknowledged for giving the opportunity to undertake the research in the Department.

Finally, thanks to my wife for her continuous encouragement during the period of study.

PRINCIPAL NOTATIONS

A	Cross-sectional area of supporting beam
A_s	Area of tension reinforcement
a	Width of smaller section of wall with offset doorway
B	Width of opening
b	Breadth of beam section
C	Vertical stress concentration factor
C_o	Compression force in wall with opening
C_s	Compression force in solid wall
D	Depth of opening
d	Depth of beam section
E_b	Modulus of elasticity of beam
E_w	Modulus of elasticity of wall
f_a	Average stress
f_b	Brickwork design crushing strength
f_c	Maximum principal compressive stress
f'_c	Characteristic compressive strength of brickwork
f_{cu}	Characteristic cube strength
f_m	Maximum compressive stress
f_o	Maximum vertical stress in wall with opening
f_p	Applied stress
f_s	Maximum vertical stress in solid wall
f_{st}	Steel design strength
f_t	Principal tensile stress
f'_t	Tensile strength of brickwork

f_y	Characteristic strength of structural steel
h	Height of wall
h'	Height of arch in wall
I	Second moment of area of beam section
K	Relative axial stiffness parameter
L	Span of wall
ℓ_v	Contact length of vertical force
ℓ_s	Contact length of horizontal shear
M	Bending moment
M_b	Bending moment due to beam self weight and floor loading
M_c	Bending moment at midspan
M_m	Maximum bending moment
M_H	Bending moment due to horizontal shear force
M_T	Total bending moment
M_V	Bending moment due to vertical loading
M_W	Bending moment due to wall self weight and applied loading
T	Axial force in beam
T_o	Axial force in beam supporting wall with opening
T_s	Axial force in beam supporting solid wall
T'	Thrust in arch
t	Wall thickness
U,u	Displacement in x-direction
V,v	Displacement in y-direction
V_x	Shear force
W	Applied load

W_b	Load due to beam self weight and floor loading
W_c	Cracking load
W_u	Ultimate load
w	Intensity of applied load
X	Coordinate
Y	Coordinate
Z	Section modulus
α	Coefficient for axial force in beam dependent upon h/L ratio
α_i	Generalized coordinates
β	Coefficient for maximum vertical stress in wall dependent upon h/L ratio
γ	Coefficient for axial force in beam dependent upon h/L ratio
γ_m	Partial safety factor for strength
δ_H	Deflection due to horizontal force
δ_v	Deflection due to vertical force
δ_s	Deflection due to shear force
ε_y	Vertical strain
θ_o	Inclination of arching thrust at support in wall with opening
θ_s	Inclination of arching thrust at support in solid wall
λ	Coefficient dependent upon shape of contact vertical stress distribution
μ	Coefficient of friction

σ_x	Bending stress
σ_y	Vertical stress
τ_{xy}	Shear stress
τ_j	Joint shear strength
τ_b	Bond shear strength
τ_{ult}	Ultimate shear strength

ABSTRACT

Many shear walls structures are discontinued at the first floor level so as to provide a large open space at the ground floor. The load-bearing walls must therefore be required to transmit their loads to heavy beams of the supporting framed structure. The composite action between the wall and the beam concentrates the vertical loading on the beam very near to the support points and thus producing bending moments which are much less than would be expected when the full loading is acting directly on the beam. The study of this composite action is therefore of economic importance since if it is utilized, the design of the beam will be greatly economized.

The work presented in this thesis includes experimental and analytical investigations of the composite behaviour of walls with and without openings and their supporting beams.

The experimental investigation, described in Chapter 3, comprised of tests on one-third scale model brick panels with and without openings supported on reinforced concrete beams.

The analysis of the problem using a standard finite element program is presented in Chapter 4. This includes a study of influence of the significant design parameters under different boundary conditions. Based on the results obtained, an approximate method of analysis for solid walls has been proposed.

The analysis has been extended in Chapter 5 to include walls with openings. The influence of the size and position of opening has been investigated and an approximate method of analysis suggested.

The effects of the various support conditions have been described in Chapter 6, and a simple design procedure has been proposed in Chapter 7.

CHAPTER 1 : INTRODUCTION

1.1 GENERAL

Composite construction has been known to designers in many forms, from the simplest material composite in reinforced concrete beams, to the more complex structural composite in multistorey building. The simple reinforced concrete beam is an example of a structural member in which two or more elements of different materials designed to resist different types of stress, act together to carry the total load, or resist the total deflection. The more complex multi-storey framed building is built up from members of different kinds, columns, beams, ties, slabs and walls, which are fitted together to form the complex structure. Looking at the multi-storey framed building in this way, the beams and stanchions of its frame, are as much reinforcements of the cellular web of its walls and floors as are the steel rods in the concrete mass of a reinforced concrete beam.

It was customary in the design of these framed structures to ignore the stiffening effects of the infill panels and to consider their presence as additional loads on the supporting beams. In 1955, however, the Building Research Station carried out a series of tests on the steel frame of the new Government Offices, Whitehall Gardens, the intention being to obtain the complete stress history of part of the frame during the placing of the floor and walls, and for the subsequent loading of the completed building[1]. Variable results were obtained ranging

from a stress reduction of up to 90 percent or more in beams, due to their interaction with walls, and from 50 to 80 percent in both beams and stanchions of a frame subjected to a racking test, due to the interaction of the frame and the panel infilling. It is of course in a broad sense apparent that these stress reductions were produced as a result of the composite action between the elements of the framed building. However, it is necessary to determine how these reductions take place and to what extent.

A considerable amount of work has also been done on the investigation of the lateral stiffness of infill frames under racking loads. The infilled frame is one in which the restraint against the lateral forces is provided by the composite action of an infill panel and the bounding frame. From the observed results obtained from these tests, and full scale tests on multi-storey buildings, including the Empire State Building[31], the importance of the phenomenon of composite action in buildings, has been emphasized. The stiffening effects resulting from this composite action is undoubtedly of economic and technical importance. From the economic view point, it permits reduced dimensioning and saving in material required for the structural skeleton. From the technical view point, it affects the structural behaviour. The beams and stanchions act mainly in tension and compression, instead of bending, so that the load distribution on the various members, as well as the distribution of their internal stresses, may deviate considerably from the accepted assumptions. A study of the composite action is thus of

importance for economy as well as for closer approximation of the actual behaviour of the structure.

Among the different aspects of composite structures frequently encountered in civil engineering practice, is the wall on beam problem. Such types of problem is found particularly in multi-storey buildings in which it is often necessary to discontinue the load-bearing walls at the first floor level so as to provide an open space for parking area, garages or shops. The walls, therefore, must be required to transmit their loads to heavy beams of the supporting framed structure, as shown in Plate 1. A further problem in multi-storey buildings has been the need to provide reasonably large, open, public areas. Generally, in hotels these spaces are required in the upper floors. A solution can be adopted in this case in which a cellular-type of structure is used. In this, the load-bearing walls and the floors, form compositely a box-type structure. Another form of the composite wall is encountered when house buildings are carried on foundation beams supported on short bored piles in expansive soils.

Until recently, it was customary in practice to design beams and lintels carrying brickwork walls so as to be capable of supporting a triangular load of bricks, where the base of the triangle is the span of the beam, provided that the remainder of brickwork is adequately supported, Figure 1.1. If the wall was carrying any superimposed load above the apex of the triangle, it was not clear what portion if any of this extra

PLATE 1

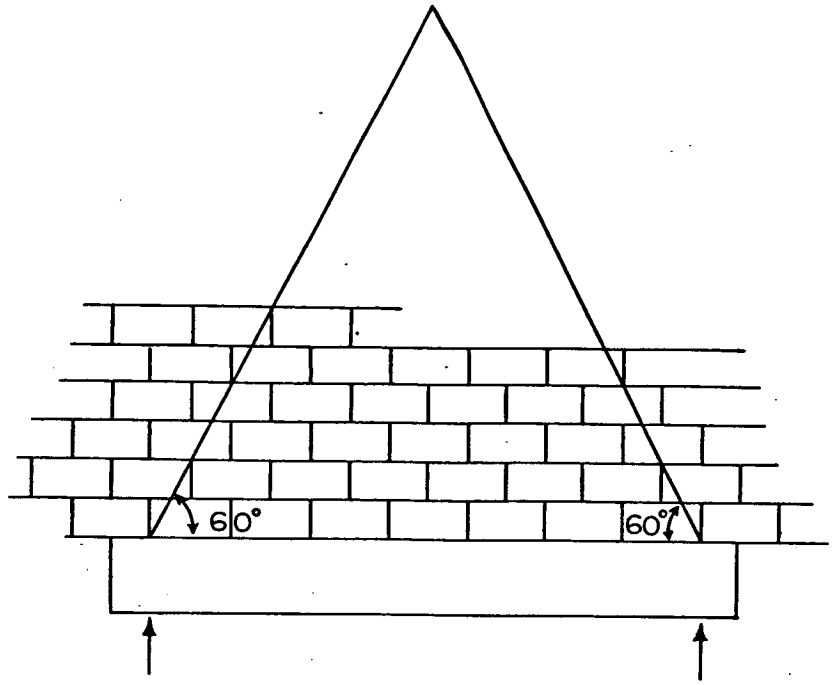

FIG. 1.1 ASSUMED DESIGN LOADING FOR SUPPORTING BEAM.

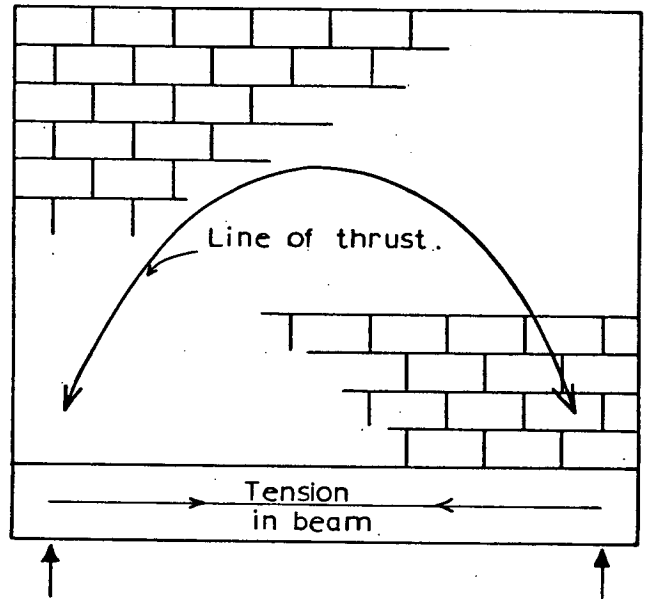

FIG. 1.2 TIED ARCH ACTION

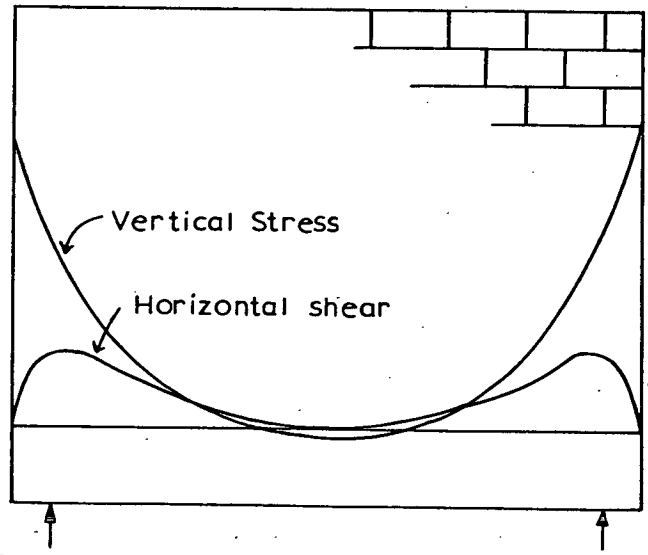

FIG. 1.3 STRESS DISTRIBUTION ALONG WALL/BEAM INTERFACE.

load should be taken into account, and it was frequently ignored. However, this is far from the actual behaviour.

In 1952, Wood[2] investigated the composite action of brick panels supported on reinforced concrete beams, and found that due to arching effects in the brickwork, the brick panel and supporting beam in fact formed a composite deep beam, with the supporting beam acting as reinforcement for the panel as a whole. A great overall stiffness is thus achieved, and a small amount of work is done by the applied loads. The steel stresses in the supporting beam were remarkably low, that it was found possible to recommend a design moment for the supporting beam as low as WL/100, in the case of solid panels or panels with central openings. Wood also concluded that the bending moments induced in the beam depend on the relative stiffness of the beam and wall. The greater the stiffness of the beam, the more load is transmitted to the beam at midspan, and that with very flexible beam a considerable degree of arching can be expected to take place, in the limit, the panel may become self-supporting. Although this fact has been established by many research workers, the definitions assigned to the term 'relative stiffness', are found to differ from one to the other. This point is discussed further in Chapter 4.

The achievement of composite action clearly depends on the extent to which bond or shearing forces can be developed between the beam and the panel, particularly near the beam supports. This will be influenced by the high local compressive stresses,

and hence the greater frictional resistance produced near the supports by the arching action in the wall - Figure 1.2. Typical stress distributions at the wall/beam interface are shown in Figure 1.3. The concentration of stresses near the beam supports has the beneficial effects of considerably reducing the bending moments and the beam deflections. On the panel, however, the effect is adverse, and most frequently the vertical stress concentration, leads to the panel failure by tensile splitting and crushing of corner bricks over the supports.

When an opening is located in the panel at midspan, provided an arch can still form through brickwork or a lintel, the stress distribution in the wall and hence the loading on the beam, are not markedly affected. However, with openings occurring near a support, a secondary arch tends to form in the solid part of the panel, and there is a partial breakdown in composite action. The secondary arch creates very high local stresses adjacent to the opening, and may lead to high shear loads in the beam and consequently high bending moments and deflection.

The problem, therefore, reduces to :

1. The determination of the degree of stress concentration in the panel, particularly at the bottom corners over the supports; and

2. The determination of the load intensity and distribution on the beam.

This thesis describes a study of the composite behaviour of vertically loaded walls, with and without openings, and the influence of significant design parameters, under different boundary conditions. Although the finite element method has been used for the initial analysis, approximate methods are developed which would be suitable for incorporation as a design procedure.

Beside the analytical study, experimental investigation was also carried out on one third scale model brick walls, with and without openings, supported on reinforced concrete beams. The results obtained from these tests, are compared with values obtained by the finite element and the approximate methods.

The study has been focused on the investigation of beams on point supports, since this is considered in practice as the most severe case. The effects, however, of other support conditions, such as the finite support width, the fixity and continuity of the support, with loading on top of wall as well as at the supporting beam level, are also investigated.

Finally, on the basis of the proposed approximate method, a design procedure for the composite system has been derived and compared with existing design methods.

CHAPTER 2 : COMPOSITE ACTION BETWEEN MASONRY WALLS AND THEIR SUPPORTING BEAMS

2.1 REVIEW OF PREVIOUS WORK

During the last 25 years much research has been devoted to the study of the structural interaction in composite masonry-concrete construction. In this Chapter, a review of pertinent research will be presented.

In 1952, Wood[2] presented results of the earliest experimental investigations on the composite action of walls and their supporting beams. Full-scale brickwork panels, with and without openings, supported on reinforced concrete beams, were tested under uniform vertical loading. Remarkably low stresses were recorded in the reinforcement of the beams. On the basis of these low stresses, Wood established moment coefficients by taking equivalent bending moments on a freely-supported beam. For the calculation of beam reinforcement, these moments are to be taken as WL/50 based on total load for panels where there are door or window openings near the supports, and WL/100 in the absence of such openings or their occurrance at midspan.

Wood also proposed another design method for beams supporting walls without openings. The method was based on the deep beam theory, and was referred to as the 'limiting moment-arm method'. It suggests that a limiting moment-arm approximately equal to 0.7 x span is used in deep panels,

otherwise a moment-arm of 2/3 x depth is permissible.

In both methods, the minimum wall height was limited to 0.6 x span and the peak stresses in the wall were totally ignored. However, evaluation of these stresses was considered in a later paper presented by Wood and Simms[3] in 1969. Additional full-scale tests on brickwork panels supported on reinforced concrete beams, were carried out at the Building Research Station. The tests showed that arching action was taking place in the wall and eventually leading to crushing of bricks close to the supports. Their analysis was based on the assumption that vertical loading on the beam at the wall failure, is uniformly distributed very close to the supports. In the proposed design method, the beam bending moment is related to the degree of the stress concentration in the wall and it includes the effect of the horizontal shear forces at the wall/beam interface. The final design formula was presented as follows :

$$R \cdot F \geq \frac{(176 + K)(154 - K(\frac{K-8}{92}))}{3452\ K}$$

where WL/K is the design moment, R is a reduction factor relating the average and the allowable wall stresses, and F is a reduction factor for slenderness ratio.

In 1961, Rosenhaupt[4,5] suggested a numerical approach for the analysis of simply supported composite walls, based on the Airy stress function and the finite difference technique.

In the analysis he neglected the bending regidity (EI) of the beam compared to that of the wall. From his work he concluded that the shearing stresses at the wall/beam boundary induce the composite action of the structure, and that the tensile stresses concentrate in the foundation beam and the compressive stresses are distributed over the whole height of the masonry. The vertical compression forces are transferred by the wall to the supports, where high vertical stresses concentrate. He also concluded that the vertical shear stresses are taken by the masonry part of the wall and that the horizontal shear stresses between the supporting beam and panel, concentrate near the supports.

In 1962, Rosenhaupt[6] also presented the results of tests on model masonry walls resting on point-supported reinforced concrete beams. The tests showed that the concentration of vertical compression and shear in the masonry above the beam supports may cause failure of the structure before the beam failure in axial tension. The concentration of the vertical stress was found to increase with the increase in wall height. However, the inclusion of vertical edge ties was found to relieve the wall from the vertical stress concentration and reduce the shear stresses within the masonry. As a result the deflection in the elastic stage is reduced and the failure resistance of the wall is increased.

In 1964, Raab[27] applied the lattice analogy method, proposed by Hrennikoff[32] to the analysis of composite walls.

In the method, the continuous material of the elastic body is replaced by a framework of linear elements. The cross-sectional properties of the bars which comprises the lattices of the framework are chosen so as to insure that the framework and the elastic body distort under load in the same manner.

Raab performed the analysis on four different cases of the composite problem, and he concluded that the assumption made by Rosenhaupt[4] that the supporting beam has no flexural stiffness can be accepted in many applications with but minor objections. The results also indicate that the neglect of the weight of the wall material might represent a significant departure from the conditions of reality.

In 1965, Rosenhaupt and Sokal[7] presented in a paper the results of tests on masonry walls on continuous reinforced concrete beams. They concluded that a masonry wall built on a continuous beam behaves like a composite diaphragm girder, the foundation beam acting as a tension tie. The main difference between the behaviour of the composite girder and that of an orindary elastic continuous beam lies in the distribution of the reactions. The reactions at the interior supports are much smaller than those of ordinary beams, as a result, the external moments are positive throughout the length of the wall. The results also indicated that, crushing of the masonry above the supports is the main cause of failure of the composite structure. Vertical stanchions at the supports increase the failure load but do not change the mode of failure

that occurs after separation between stanchion and masonry through vertical cracks.

An alternative numerical approach for the solution of the composite problem, was presented by Coull[8], in 1966. The analysis was based on the minimization of the strain energy of the system using the variational method. The procedure consisted of expressing the stresses in the wall by a power series in the horizontal direction, the coefficients of the series being function of the height only. On solving a typical wall on beam problem, Coull chose a simple stress polynomial as a result of which the horizontal and shear stresses had the same form at all levels in the wall. This seems unlikely in practice, however, the accuracy could have been improved if more terms were used which, as Coull pointed out, would be at the expense of extra computational difficulty involved in the solution of the resulting set of simultaneous differential equations. From the analysis he concluded that the wall stresses are mainly affected by the wall height-to-span ratio and the relative stiffness (K) of the wall and beam as given by :

$$K = \left(\frac{C}{d}\right)^3 \left(\frac{t}{b}\right)\left(\frac{E_W}{E_b}\right)$$

in which C, t and E_W are the wall semi-span, thickness and modulus of elasticity respectively and d, b and E_b are respectively the beam depth, its breadth and elastic modulus.

In 1967, Plowman, Sutherland and Couzens[9] carried out a series of full-scale tests on composite cantilever box beams having reinforced concrete slabs as flanges and reinforced brick walls as webs. The results indicated that in all tests failure was slow and was due to diagonal cracking and crushing of the brickwork in the vertically reinforced specimens, and pulling away of the bottom slab in those diagonally reinforced. The horizontal reinforcement used in conjunction with vertical steel increased the failing load in these specimens but had no effect on the deflection or the behaviour at working loads. As conclusion, they suggested that box beams with brickwork webs incorporating either vertical or diagonal reinforcement can be used as structural units with satisfactory factors of safety.

In 1969, Colbourne[10] presented a more accurate analysis of the composite system, based on idealization of the system by a lattice or grid type of structure as shown in Figure 2.1.

The lattice consists of a set of bars joined at their ends by frictionless pins. The bars have an axial stiffness of (Eah) where E and h are the wall elastic modulus and height respectively. The shear bar shown in the diagram by the thin lines are considered to be rigid in bending and are connected to the pins in such a way that they receive no axial force. Each pair of shear bars is hinged at the centre, and a torsion spring of stiffness ($\frac{1}{2}$ Ea^2h) is provided at the intersection points of the bars. The beam is represented by a set of rigid

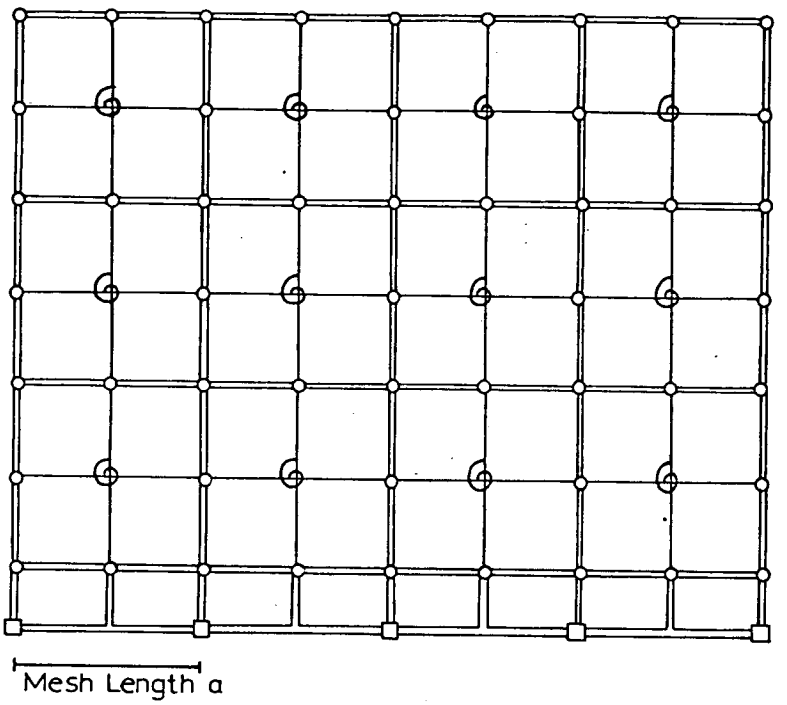

FIG. 2.1 THE LATTICE ANOLOGY

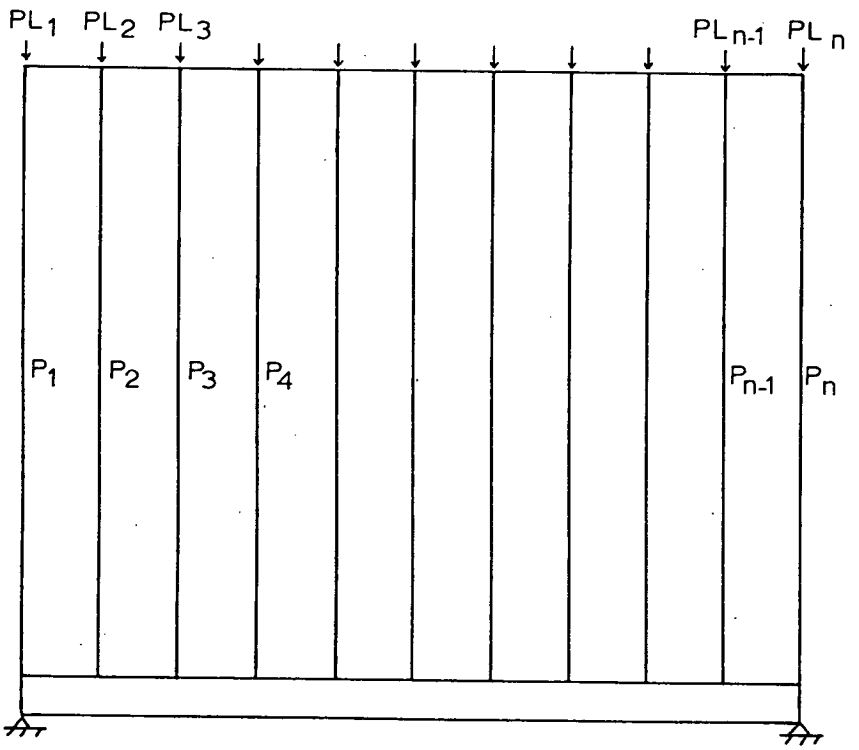

FIG. 2.2 THE SHEAR LAG IDEALIZATION.

bars capable of stretching with axial stiffness (E^bA^b) but remain rigid in bending. These bars, are joined at the mesh points by springs of bending stiffness (E^bI^b), in which E^b, A^b and I^b are respectively the beam elastic modulus, cross-sectional area and second moment of area. Shear connection between the beam and the wall is provided by vertical peices rigidly fixed to the beam main bars.

The resulting equilibrium equations derived on the basis of this technique are identical to those derived by the finite difference method.

In 1969, Burhouse[11] published the results of tests carried out at the Building Research Station. The tests consisted of full-scale brickwork panels, supported either on reinforced concrete beams or encased steel joists. The effect of the wall height-to-span ratio was mainly investigated. In the majority of tests, primary failure occurred as a result of crushing of the brickwork at a lower corner of the panel, and was followed by failure of the supporting beam. In comparing working loads based on a load factor of 5, with those given by CP111, Burhouse suggested that working loads on walls forming part of composite beams should be less then those given by CP111, which assumes a rigid foundation.

In 1971, Yettram and Hirst[12] presented a paper in which they described a numerical method for the solution of the composite problem. The method consists of dividing the wall

into equally spaced vertical stringers, Figure 2.2. These are assumed to carry the direct load and are connected by shear-carrying panels, acting between them. Solution of a typical wall on beam problem using the method, showed that as the beam stiffness increases, the bending moment substantially increases all across the span of the beam, to the limit of WL/8 for an exceedingly stiff beam.

A more rigorous analytical procedure for the analysis of composite walls, with and without openings, was presented by Levy and Spira[13], in 1973. The analysis was based on the determination of stress functions using the finite difference method. They also proposed an approximate solution based on a relative stiffness parameter, K, given by the following relationship :

$$K = 2\left(\frac{E_c I}{E_w t}\right)^{1/3}$$

where $E_c I$ is the bending rigidity of the beam, and E_w and t are respectively the wall elastic modulus and thickness. The maximum vertical stress (σ) in the wall was related to the parameter, K, by the following expression :

$$\sigma = -0.15\,\frac{RK}{t}$$

in which R is the reaction.

Presence of vertical ties was shown to reduce both the compression in the wall, and the bending moment in the supporting beam.

Smith and Riddington[14] in 1973 published a paper in which they proposed a design method for steel beams supporting brickwork walls. The method was based on the assumption that the length of contact between the wall and the beam, is governed mainly by a relative stiffness parameter, K, given as follows :

$$K = 4\sqrt{\frac{E_w\, tL^3}{EI}}$$

The smaller the value of K, in other words, the stiffer being the beam, the longer is the length of contact. In view of this, and results from model tests of plaster walls on steel beams, the following design formula was proposed :

$$I \propto \frac{W^4}{9.5\, Lt^3 P_b}$$

In which, I is the second moment of area of the beam, t is the wall thickness, and P_b is the permissible vertical stress in the wall.

Since the late sixties, the finite element technique has been used by many research workers for the solution of the composite problem. In 1969, Male and Arbon[15] published a paper in which this method was used to analyse walls, with and without openings, resting on simply supported foundation beams. The beam was idealized by four layers of rectangles, subdivided into triangles. The wall, on the other hand, was represented by coarser subdivisions. The element used in the program, was

the three node, two degrees of freedom per node, triangular element. From the analysis, it was shown that for full composite action to develop, shear stresses across the boundary between wall and beam, must be efficiently transmitted. Moreover, tensile connectors should be provided when the load is applied at the beam level. The presence of a central opening in the wall, was shown not to greatly influence the stress distribution in the wall. However, when the opening was situated near to the supports, very high tensile stresses occurred in the vicinity of the opening.

The finite element method, was also used by Green[16,17] for the analysis of shear walls supported on framed structures. The stiffness matrix of the standard flexural element was modified to include the effect of the horizontal force at the wall-beam boundary. A study of the effect of different parameters on the behaviour of the composite structure was undertaken. These variables included the beam stiffness, the beam support width, and the size and position of the opening in the wall. Tests on perspex models were also conducted. From the analysis, Green estimated the minimum tie force in the beam as WL/4.4. The finite support width was found to influence the stress distribution in the wall and the forces in the beam. The stress concentration over the supports, was reduced to the order of 1.5, when the finite support width had been introduced. Furthermore, the effect of the central opening in the wall was found to be negligible. The axial force in beams supporting walls with offset openings was however 75% more.

In 1973, Saw[18] also applied the finite element method for the analysis of the interactive behaviour between walls and their supporting beams. The element used for idealizing the wall, was derived from 144 basic rectangular finite elements. The element formulated,termed 'macro' had four corner nodes with two degrees of freedom at each node. In order to combine the beam line elements with those of the wall, the stiffness matrix of the standard line element was modified so as to relate the forces and the displacements at the wall-beam boundary. Results obtained by solving a typical wall on beam problem, using a total of 42 nodes with 30 macro elements in conjunction with 5 line elements, were comparable with those obtained by Male and Arbon[15], using a total of 313 nodes with 576 triangular elements.

Riddington[19] in 1974 made a study on the interaction between walls and their supporting beams, using the finite element method. A finite element program allowing for the automatic generation of separation cracks at the wall-beam interface, was developed. This was either achieved by reducing the modulus of elasticity of wall-beam interface elements to zero, or separating nodes on the wall-beam interface. The separation cracks were formed automatically by first analysing the structure with all nodes connected, and then starting from the centre of the beam, the elements above the beam were checked for vertical tensile stresses. If a tension element was found, the analysis and separation were repeated until no

further elements became tensile. By adopting rectangular finite elements with two degrees of freedom per node, for both wall and beam, Riddington carried out parametric study of the composite problem. From the analysis and the results obtained from model tests on plaster and araldite walls on steel beams, together with results from tests conducted at the Building Research Establishment, a simplified design procedure for the composite structure, has been proposed.

In 1974, Yettram and Hirst[20] carried out an elastic analysis on the composite action of walls supported on encastre beams and portal frames. They used both the finite element and the shear lag[12] methods. In applying the finite element program to a standard wall on beam problem, the interelement nodal forces taken as an output were converted to average stress at nodes by dividing by the relevant element edge areas. This method compared favourably with the shear lag method. The analysis revealed that the beam stiffness and the flexural rigidity of the columns, had a considerable influence on the stress pattern of the wall. The effect of the columns was most marked at the ends of the supporting beam, the mid-span bending moment, being affected relatively little.

An alternative elastic approach based on the evaluation of the displacements in the wall and beam, was presented by Ramesh et al[21]. Their procedure consisted of expressing the displacement functions of both wall and beam in the form of multiple Fourier series. Their experimental investigations

comprised of model and full scale tests on brickwork walls on reinforced concrete beams. The tests showed that, the failure load of a wall loaded at the beam level, depends on the amount of reinforcement in the vertical tensile connectors.

Based on the results obtained by Ramesh et al[21], Achyutha[22] proposed an approximate method of analysis for the reinforced wall-beam structure. This assumed an analogous truss in which the beam was represented by the bottom cord of the truss, and the tensile connectors by the vertical members with length equal to half the wall height. The stresses in the reinforcement of the supporting beam, were calculated using the total concrete area including the equivalent concrete area due to steel reinforcement.

In 1976, Chandrashekhara and Jacob[23] presented in a paper the results of photoelastic analysis on composite walls, with and without openings. Columbia resin (CR-39) was used to represent the supporting beam, and Araldite (CY 230) to represent the wall. The modular ratio obtained by such combination at 115^{o}C was 23.5. The tests showed that the interface stresses depend on the beam stiffness and the presence of openings in the wall. The literature has shown that not much work has been done on walls with openings to enable detailed design recommendations to be made. However, apart from the experimental investigations carried out by Wood[2], Rosenhaupt and Mueller[24], reported in 1963, the results of investigations on the effects of settling supports,

on masonry walls with openings. They conducted a series of tests on half-scale models of concrete block walls on continuous reinforced concrete beams. They concluded that the statical action of a masonry wall with ties, is comparable to that of a truss, and that the wall strength can be predicted by the truss analogy. The results also indicated that, the strength of a wall with openings can be more than that of a solid wall, if reinforced concrete ties or vertical prestressing are provided on all sides of the openings.

In a later paper published by Rosenhaupt, Bresford and Blakey[25] in 1963, the truss analogy concept was shown to constitute a definite aid for proportioning of the tie members, and details of pretensioning required for composite walls containing openings and built on settling supports.

2.2 SUMMARY AND THE SCOPE OF THE PRESENT WORK

In the preceding review, the contribution of many research workers to the analysis of wall on beam problems has been outlined. Some researchers chose an essentially experimental approach to investigate some aspects of the problem, such as the effect of the wall height-to-span ratio, the influence of openings, or the differential support settlement in continuous walls on expansive soils. Various analytical studies based on different elasticity theories, and occasionally in conjunction with experiments, have also been introduced. In the majority of cases, these analytical procedures made simplifying assumptions

and this considerably detracts from the value of the results obtained. Rosenhaupt, for example, assumed that no direct forces occur between wall and beam except at the support points, and only shear forces are transferred at the interface. He also assumed that the bending rigidity of the beam is negligible, compared to the stiffness of the wall. This is rather an extreme assumption, since it has the effect of eliminating the normal stress between the wall and the beam. The entire load is therefore carried at the bottom corners of the wall, and the exact solution of the problem must contain singularities at these points. Since the finite difference is used to calculate the stresses immediately over the supports, the results are inversely proportional to the mesh-size used, so that the method cannot predict reasonable values at points of stress concentration.

In the variational method of Coull, the horizontal and shear stresses will have the same form at all levels in the wall when simple stress polynomials are used. This does not seem likely in practice. The method is thus considered to be very approximate.

The lattice analogy of Colbourne, and the shear lag method of Yettram and Hirst, are particularly suitable for walls without openings. Furthermore, the computer programs developed for these methods are in most cases, available only to their writers. Also very few of these analytical methods have outlined direct design procedures. However, among the existing

methods of design, the moment coefficients method proposed by Wood, is the most widely used. In itself, the method is entirely empirical and makes no allowance for the variation in the wall-beam stiffness. The other method proposed by Wood, although satisfactory for low modular ratio, could seriously underestimate the beam stresses when applied to higher modular ratio[26].

The design method proposed by Smith and Riddington[14,19] was based on the assumption that the wall would separate from the beam when arching action occurred. The length of contact used in the design method was determined experimentally and analytically using the finite element method. In the tests carried out by the present author, no separation failure was observed. No such type of failure was also reported by Rosenhaupt, but Burhouse observed separation failure in walls of 0.33 height-to-span ratio, which is outside the proposed design limit of 0.6. In determination of the cracks by the finite element method, the occurrence of the vertical tensile stress in the bottom elements of the wall is not an indication to the presence of these cracks. This is because these stresses are very small and in practice the bond between the wall and the beam can withstand them. The method therefore can be assumed as an approximate one.

The aim of the present investigations, is to study the composite behaviour of walls and their supporting beams, and

hence develop a simple design method for the structure. The versatile finite element method is employed in the analysis using a computer program developed at the M.I.T. A parameter study is undertaken with variables which include the wall-height-to-span ratio, the beam stiffness, the support width, and the modular ratio. The effect of the size and position of the opening in the wall is also studied. From this analysis simple design methods are developed. The analysis of experimental results from tests on third scale model brickwork walls on reinforced concrete beams is also included.

CHAPTER 3 : COMPOSITE BEHAVIOUR OF BRICKWORK WALLS ON REINFORCED CONCRETE BEAMS

3.1 INTRODUCTION

In order to study the behaviour of any masonry system, a very large number of tests are needed. This is due to the unit of masonry composite, brick and mortar, being a highly variable and complex material. Possible variations in construction are unlimited and strength parameters vary from one locality to another. The investigation of the composite behaviour of walls on beams in particular, requires a very large number of tests, because of the large number of variables involved in the complex problem. It would therefore be expensive and time-consuming to carry out tests on complete structures or anything approaching full scale. Model tests instead are therefore more economical and efficient. In view of this, Murthy and Hendry[28] have established that the strength of full size brickwork structures for a given strength of brick and mortar can be reproduced by means of model tests provided that the thickness of mortar joints is scaled down and the strength of 1-inch mortar cubes is considered in place of the 2.78 inch cubes used in full size tests. In the present work, although the test walls were constructed using one-third scale model bricks, the resulting structure was assumed to be full scale as far as comparison with the theoretical analysis was concerned. In regard to this, it has been shown by

Benjamin and Williams[29] that brick masonry system can be studied by means of models and that errors caused by model scaling are not significant compared to variations resulting from workmanship. Each model wall/beam can therefore be considered as a structure in itself.

In this Chapter, an investigation of the behaviour of one-third scale model brickwork walls with and without openings, carried on simply supported reinforced concrete beams, is described. Two different studies are presented. The first study is concerned with analyses of solid walls with different height-to-span ratios supported on beams with varying stiffness. The second series of tests, is concerned with analysis of the behaviour of walls containing openings. In this study the parameters involved are limited to the influence of size and orientation of openings. Assessment of the pattern of cracking, the modes of failure and the ultimate strength of the composite structure is included as well as comparison with theoretical results predicted by the finite element and the approximate analyses proposed in Chapter 4.

3.2 MATERIALS

3.2.1 Bricks

One-third scale model bricks were used in the construction of walls. The bricks were tested in accordance with BS 3921-1969, (Part 2). Table 3.1 gives summary of their properties.

TABLE 3.1 BRICK PROPERTIES

Property	Range	Mean	Standard Deviation
length (mm)	74.94 - 78.49	76.33	0.036
width (mm)	34.93 - 36.58	36.07	0.022
height (mm)	23.11 - 24.64	23.50	0.015
compressive strength (N/mm^2)	22.94 - 36.20	29.54	5.36
tensile strength (N/mm^2)*	2.63 - 1.29	1.85	-
water absorption (%)	10.86 - 12.43	12.15	1.23

* KHOO TEST (44)

TABLE 3.2 PROPERTIES OF STEEL REINFORCEMENT

Diameter of Rod (mm)	Yield Stress (N/mm^2)	Ultimate Strength (N/mm^2)	Modulus of Elasticity (KN/mm^2)
6	304	460	214
4.5	252	400	173

TABLE 3.3 PROPERTIES OF WALL SEGMENTS

Test No	Dimensions (mm)	Modulus of Elasticity (KN/mm^2)	Crushing Strength (N/mm^2)
1	322 x 250	-	13.10
2	322 x 295	4.90	12.78
3	325 x 295	4.76	12.74
4	326 x 254	5.60	14.61
5	326 x 254	5.95	13.93

3.2.2 Sand

Fine Leighton Buzzard sand was used in the mortar mix used for construction of walls. The grading curve is shown in Figure 3.1. The sand used in the concrete mix was river sand.

3.2.3 Cement

Rapid hardening Portland cement (Ferrocrete) was used in the mortar mix and also in the concrete mix for all beams and lintels.

3.2.4 Mortar

The mortar used in the construction of walls was prepared from a mix of 1:3 cement:sand by volume. The water/cement ratio was varied in such a way to produce the consistency and workability desired. The cubes were tested simultaneously with the walls. The average crushing strength of 25 mm mortar cubes was 19.87 N/mm^2.

3.2.5 Concrete

A concrete mix of 1:1:2 cement : sand : gravel by volume was used in casting and supporting beams, ties and lintels. The maximum aggregate size was 4.5 mm, the fine aggregate river sand, and the water/cement ratio 0.55. The cubes were tested simultaneously with the walls. The average

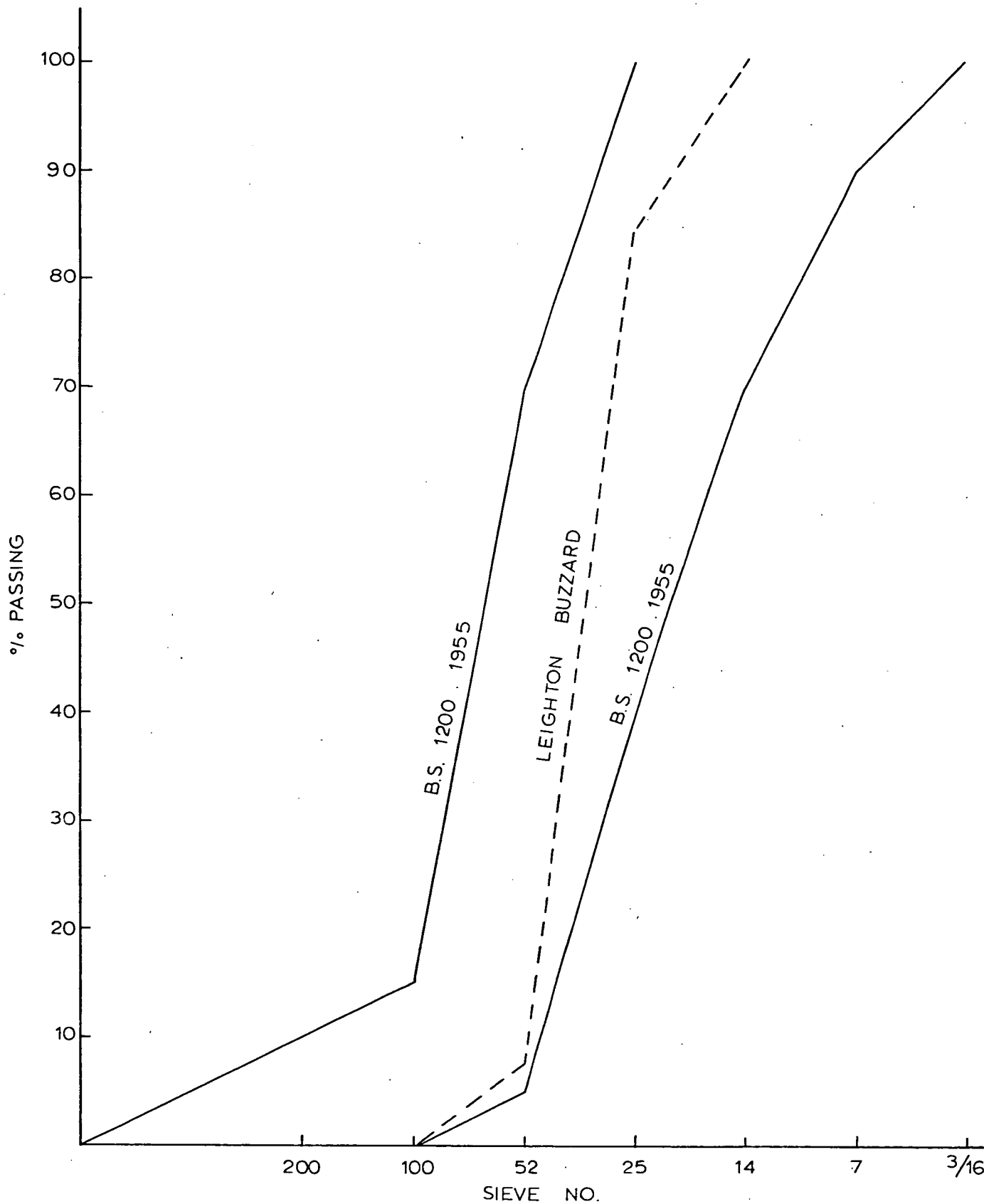

FIG (3.1) GRADING CURVE OF LEIGHTON BUZZARD SAND

crushing strength of 100 mm concrete cubes at 28 days was 51.5 N/mm^2.

3.2.6 Reinforcing Steel

The reinforcement used was ordinary mild steel. The yield stress and the ultimate strength together with the modulus of elasticity are given in Table 3.2.

3.2.7 Modulus of Elasticity of Brickwork

The modulus of elasticity and crushing strength of brickwork were determined by testing wall segments under axial compression. The segments were built using the same mortar mix as that used in the construction of the test walls and cured under the same conditions. The specimens were then tested after 14 days. 150 mm demec gauges were used for measuring the deformations on the two faces of the wall segments. The average modulus of elasticity was found to be 5.25 KN/mm^2 and the average crushing strength was 13.43 N/mm^2. The results are summarized in Table 3.3 and the stress-strain curves are given in Appendix A.

3.2.8 Modulus of Elasticity of Concrete

The modulus of elasticity of concrete was determined by three different methods. Firstly by testing (100 x 100 x 500 mm) concrete beams under bending using two point loads applied at third span points. From the measured central deflection the

TABLE 3.4 MAXIMUM BENDING MOMENT IN THE SUPPORTING BEAM

Wall No	Applied Load KN	Average Contact Length (ℓ/L)	Calculated Load KN	Bending Moment ($\frac{WL}{M}$)		
				Experiment	Finite Element	Approximate
1a, b, c	60	0.434	70.7	61	45	58.79
2a, b, c	60	0.462	66.8	48	44	55.08
3a, b, c	80	0.412	81.3	71	43.7	53.84
5a, b, c	80	0.472	70	35.38	35.97	49.72

TABLE 3.6 BEAM AXIAL FORCE AND INTERNAL MOMENT ARM

Wall No	Applied Load (W) KN	Axial Force at Mid-Span ($\frac{T}{W}$)			Moment Arm
		Experimental	Finite Element	Approximate	Total Height
1c	40	0.303	0.262	0.349	0.678
1c	60	0.266	0.262	0.349	0.773
2b	30	0.284	0.255	0.301	0.704
3b	20	0.324	0.253	0.281	0.430
3b	50	0.367	0.253	0.281	0.380
3c	40	0.177	0.253	0.281	0.795
3c	60	0.203	0.253	0.281	0.693
4a	20	0.271	0.253	0.261	0.450
4b	20	0.197	0.255	0.261	0.606
5a	20	0.222	0.270	0.305	0.678
5b	20	0.214	0.270	0.305	0.712
5c	30	0.415	0.270	0.305	0.360

value of the modulus of elasticity obtained using the appropriate deflection equation was 18.55 KN/mm^2. In the second method a 100 mm diameter concrete cylinder was tested under axial compression and the deformations measured using 150 mm demec gauges. The value of E obtained in this case was 24.01 KN/mm^2. In the third method the value of E was obtained by testing a (100 x 100 x 500 mm) prism under axial compression of up to 50 KN and deformation measurements were taken on opposite faces by means of a 300 mm demec gauge. The value obtained in this case was 28.21 KN/mm^2. The stress-strain curves are given in Appendix A. The value used for calculations was 28.21 KN/mm^2.

3.3 EXPERIMENTAL PROCEDURE

3.3.1 Method of Construction

To start with, an estimate of the supporting beam dimensions was made based upon practical considerations such as safe handling of the complete wall/beam structure to the testing machine. A span of 648 mm was chosen with an effective span of 584 mm and a depth/span ratio of 1/9. The steel reinforcement of the supporting beam was calculated using the limiting moment arm method proposed by Wood[2]. The shear reinforcement of all beams was nominal taken as ϕ3 mm at 50 mm near supports and at 100 mm in the central region. Electrical resistance strain gauges type (PL-3) of gauge length 3 mm were attached to the steel reinforcement. The beam was then cast using 1:1:2 concrete mix and left to cure for at least

14 days. Building of the wall on the beam in stretcher bond was aided by means of a vertical wooden board. The board was first marked horizontally to provide guide lines for the brick courses in which the thickness of the mortar joint was scaled down to 3 mm. Before laying the bricks they were first immersed in water for about twenty minutes. Because the walls had to be transported to the testing machine, the first brick course was laid on a 1:1 cement : sand mortar. The remaining courses being laid using 1:3 mortar. After building the wall it was then covered with polythene sheets and left to cure for 14 days. 24 hours before testing, the upper tie was laid on the top of the wall using 1:1 mortar mix.

3.3.2 Testing Procedure

The wall/beam structure was simply supported over a clear span of 584 mm. Uniform load was applied by means of an Avery testing machine through a system of distributing steel beams and rollers at the top of the wall as illustrated in Figure 3.2. Before loading the wall to failure, an initial load of 0.2 N/mm^2 was applied, this load then was increased in increments of 10 KN until failure occurred. Horizontal strain measurements along the vertical centre line of the wall were made by means of vibrating wire gauges on a 75 mm gauge length. Demec gauges over a gauge length of 50 mm, were used for measurements of the vertical strain in the bottom course of brickwork in order to enable an estimate of the loads transmitted to the supporting beam. Strains in the steel reinforcement of

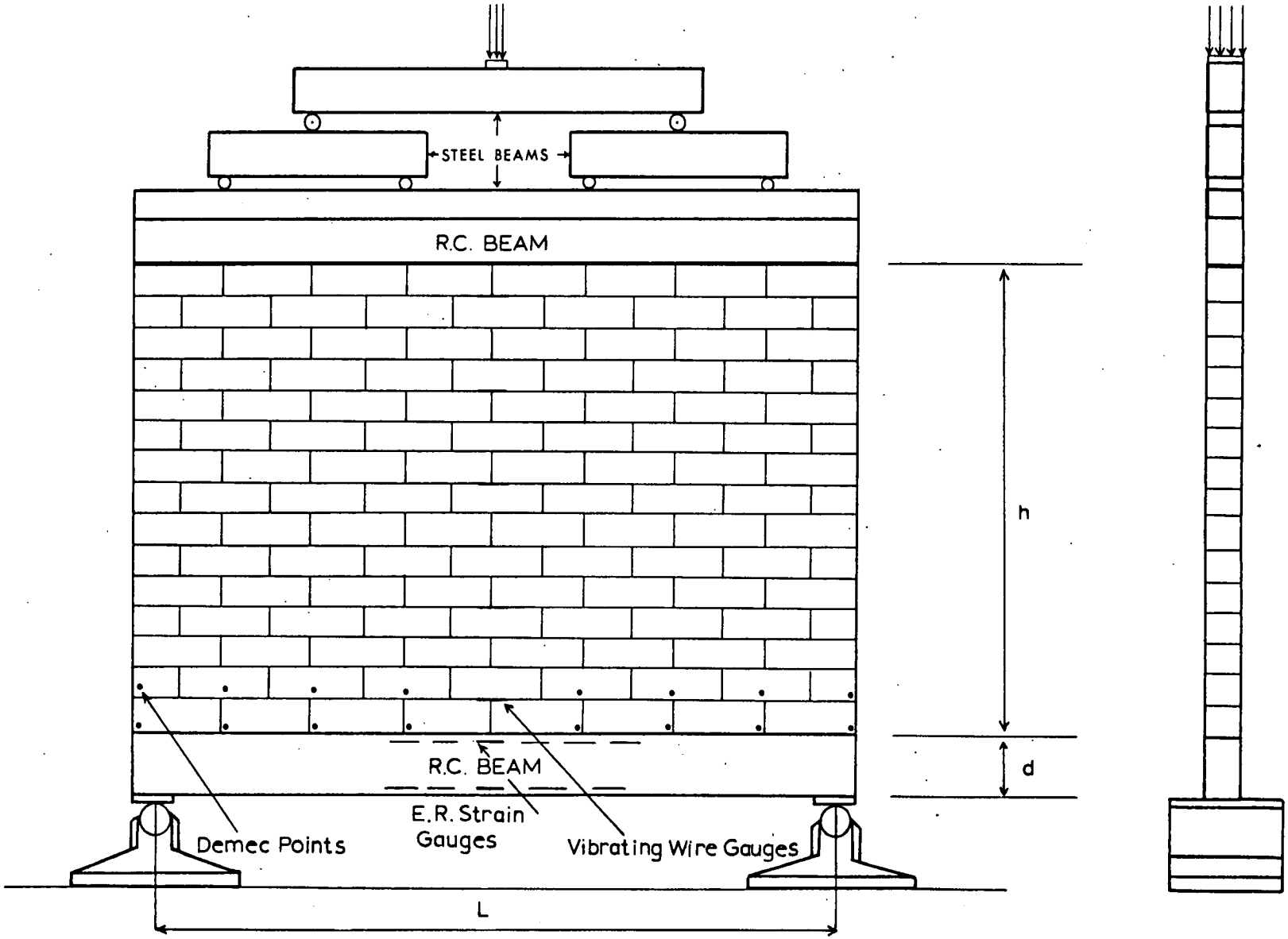

FIG. 3.2 LOADING ARRANGMENT AND POSITION OF STRAIN GAUGES

the supporting beam were measured by electrical resistance strain gauges connected to a 50 channel Solartron data logger. The deflection of the supporting beam was measured by means of dial gauges. In each test, the load was recorded at which the first crack was visible. The pattern of cracking, the modes of failure and the ultimate load were also recorded.

SECTION A : SOLID WALLS

3.A.1 Test Results

In all, 16 walls were tested. The principal details of the test specimens are shown in Table 3.3. The wall height-to-span ratio was varied from 0.48 to 1. With the exception of series 5, the width of the supporting beam in all tests was equal to the wall thickness. In series 5, the beam width was twice the wall thickness. The loads at the appearance of the first crack, the ultimate loads and the modes of failure are summarized in Table 3.8.

The intensity of loading on the supporting beam is obtained from the vertical strain measurements at the bottom course of brickwork just above the top of the beam, (Figure 3.3 - 3.7). From this loading the maximum bending moment in the beam has been calculated based upon neglecting the counter effect produced by the horizontal shear force at the wall/beam interface. The results are summarized in Table 3.4. The vertical stress concentration in the wall expressed as a ratio of the maximum vertical stress to the

average applied stress, is given in Table 3.5. This has been found to increase with increasing wall height and with decreasing supporting beam relative stiffness.

The stress in the steel reinforcement of the supporting beam has been plotted against the applied load in Figures 3.8 - 3.13. The axial force in the supporting beam has been calculated assuming the concrete to be effective in tension before cracking takes place. The force is assumed to act at the centroid of the beam and thus by considering an external moment of WL/8, an internal moment arm is calculated and expressed as a ratio of the total height as shown in Table 3.6.

Typical strain distributions along the centre line of the wall are shown in Figure 3.14. Although the results are insufficient to allow quantitative assessment to be made, they do provide a qualitative prediction of the panel behaviour under the action of the horizontal bending stresses.

The relationship between the applied load and the beam central deflection are given in Figure 3.15 - 3.19. The crack patterns at failure in some of the test specimens are shown in Plates 2 - 4.

3.4 DISCUSSION OF TEST RESULTS

3.4.1 Wall Vertical Stresses

The vertical strain measurements at a series of points on the lowest course of bricks indicate that vertical compression

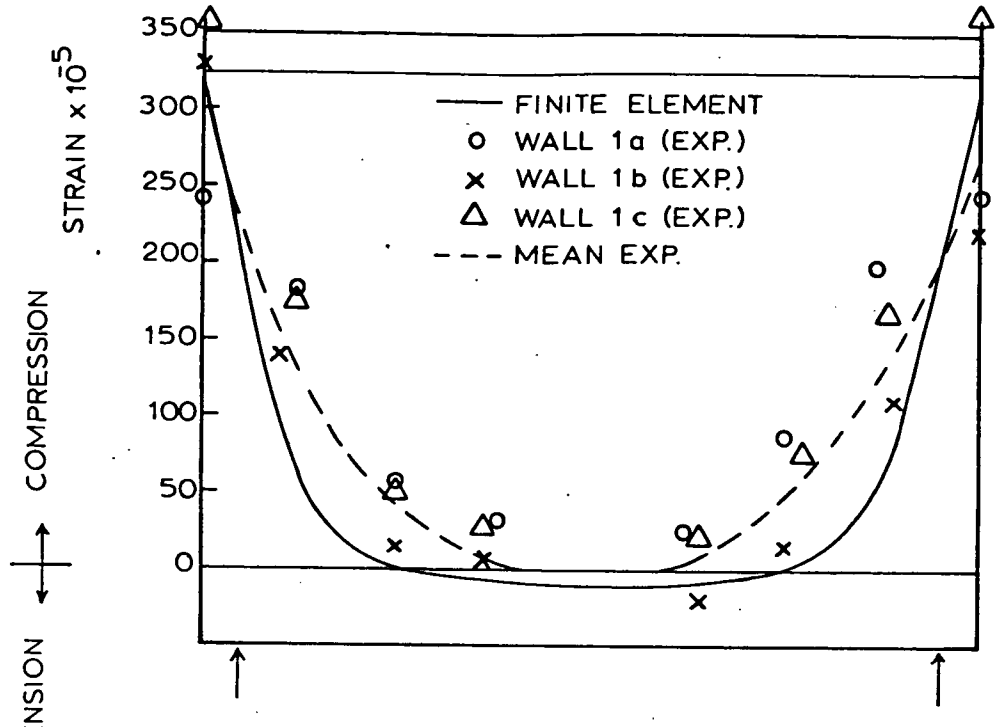

FIG (3·3) VERTICAL STRAIN IN (10^{-5}) IN BOTTOM COURSE OF BRICKWORK IN WALLS (1) AT W= 60 KN.

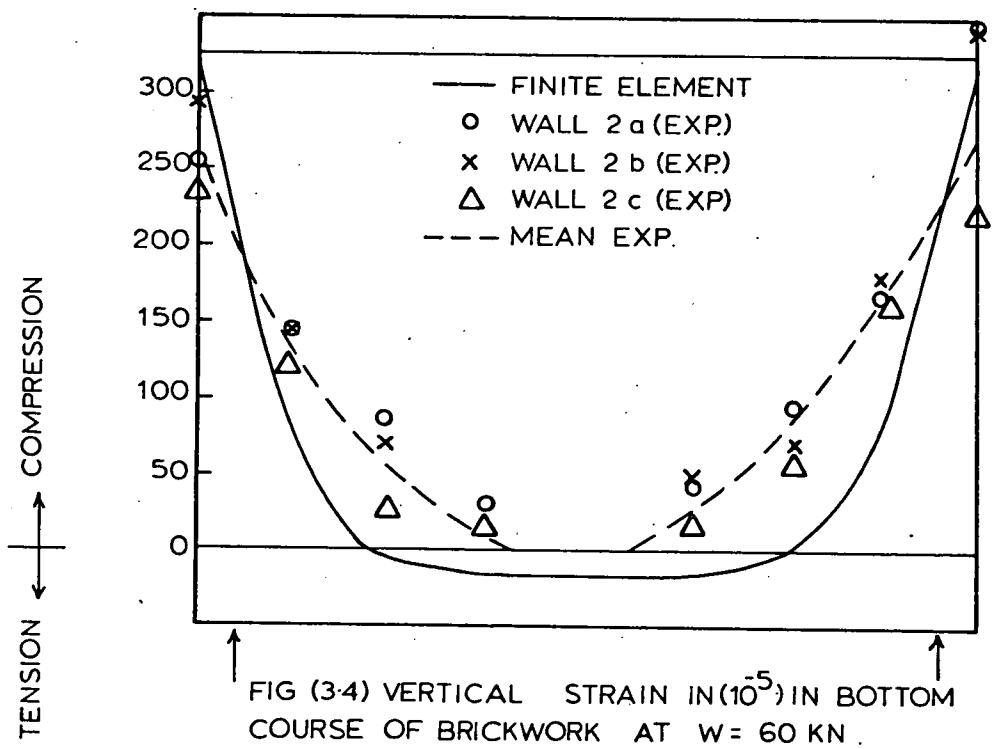

FIG (3·4) VERTICAL STRAIN IN (10^{-5}) IN BOTTOM COURSE OF BRICKWORK AT W= 60 KN.

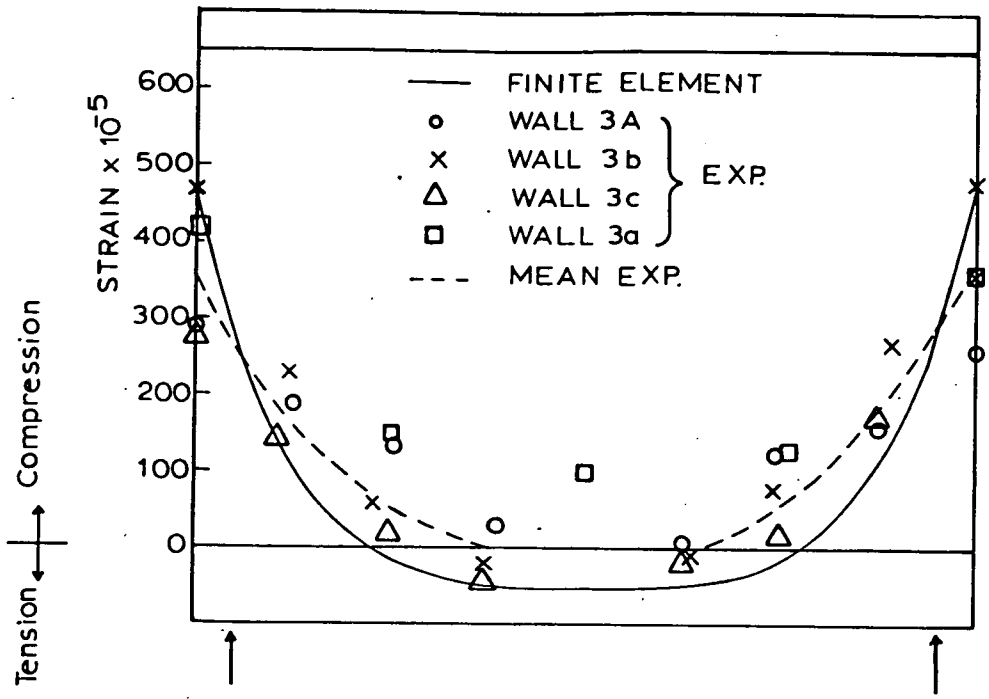

FIG.(3.5) VERTICAL STRAIN (IN 10^{-5}) IN BOTTOM COURSE OF BRICKWORK IN WALLS (3) AT W = 80 KN.

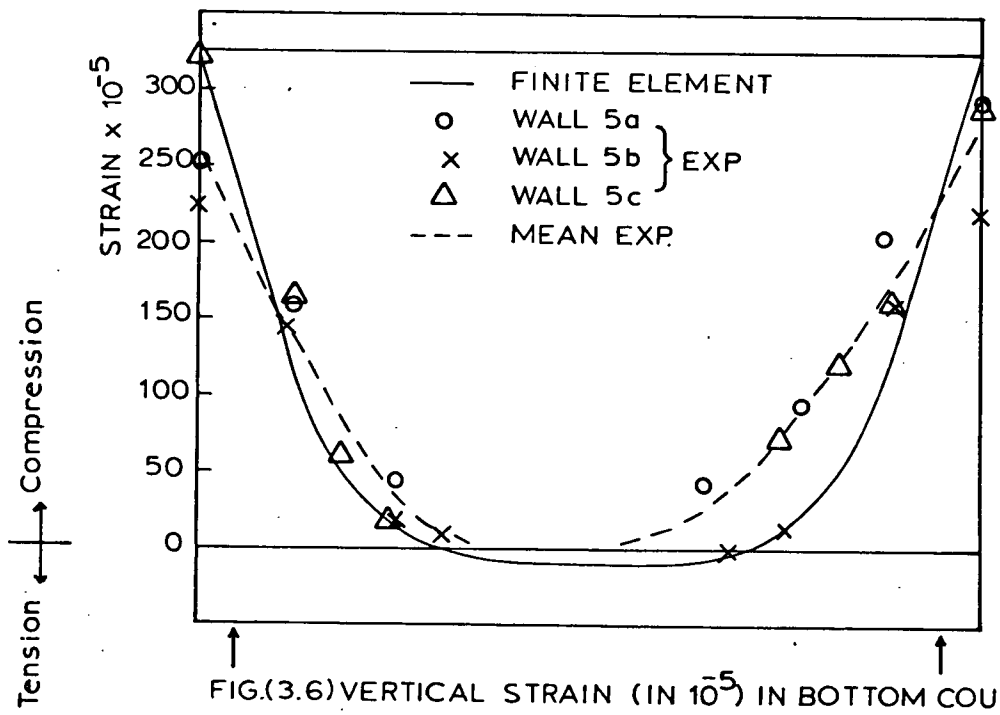

FIG.(3.6) VERTICAL STRAIN (IN 10^{-5}) IN BOTTOM COURSE OF BRICKWORK IN WALLS (5) AT W = 80 KN.

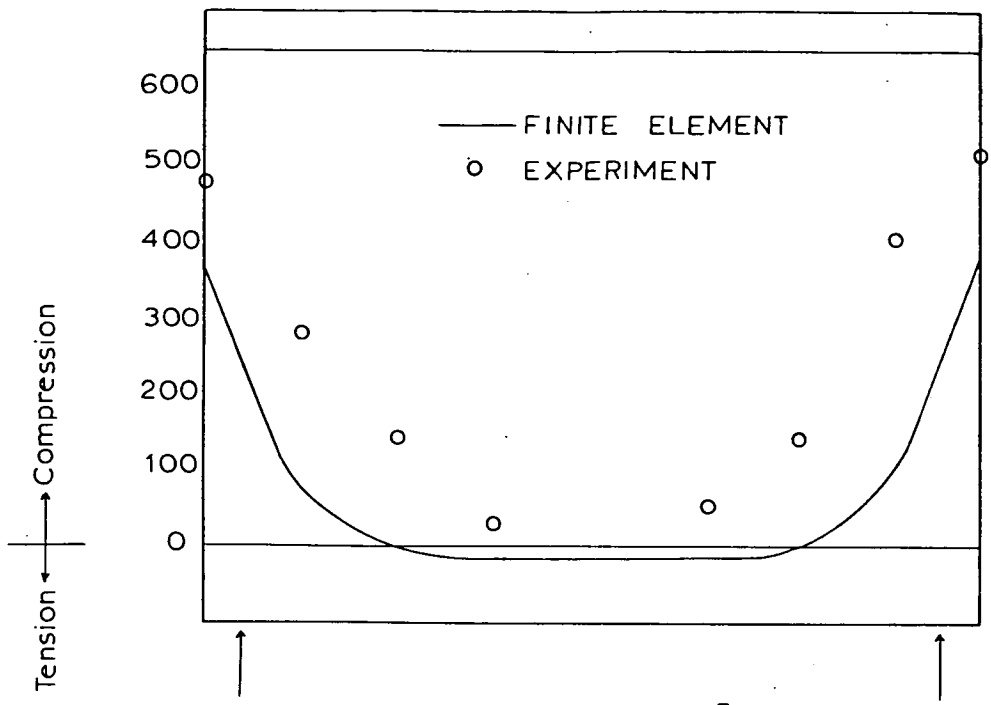

FIG.(3.7) VERTICAL STRAIN (IN 10^{-5}) IN BOTTOM COURSE OF BRICKWORK IN WALL 4A AT W= 70 KN .

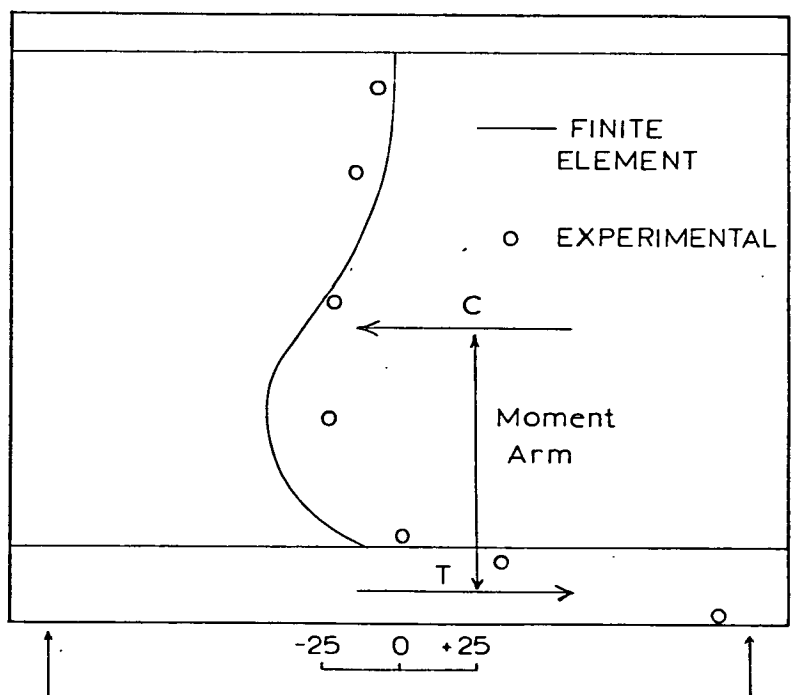

FIG (3.14) HORIZONTAL STRAIN (IN 10^{-5}) IN WALL 5C AT LOAD W = 100 KN

concentrates over the support points, (Figures 3.3 - 3.7). The pattern of the vertical strain distribution is similar in all walls. It shows a remarkable increase in the vertical stress over the supports and for a short length along the beam. In general it is approx. a parabolic curve with its minimum at the centre of the span. For a perfectly elastic, homogenous material, the corresponding vertical stress distribution would be symmetrical about the centre of span and the area under the curve would correspond to the applied load. In practical tests, with a rather variable material, such as brickwork, exact correspondence is not to be expected. In walls of series 4, the maximum stress at the supports is approximately nine times higher than the externally applied stress at the top edge of the wall, Table 3.5. In low walls (series 1), the vertical stress concentration is however of the order of 5 to 6. This indicates that the vertical stress concentration increases with the increase in the wall height-to-span ratio. This is clearly seen from the relationship between the vertical stress concentration and the relative stiffness parameter R derived in Chapter 4. The parameter R is believed to be the significant parameter influencing the degree of arching in the panel and consequently the vertical stress concentration over the support points. It can also be seen from Table 3.5 that the concentration of the vertical stress in walls of series 3 is almost twice that of series 5. It is to be mentioned that the walls of both series are identical excpet in the stiffness of their supporting beams. The beams of series 5 being more

FIG.(3.8) LOAD-REINFORCEMENT STRESS IN BEAM OF WALL (1c)

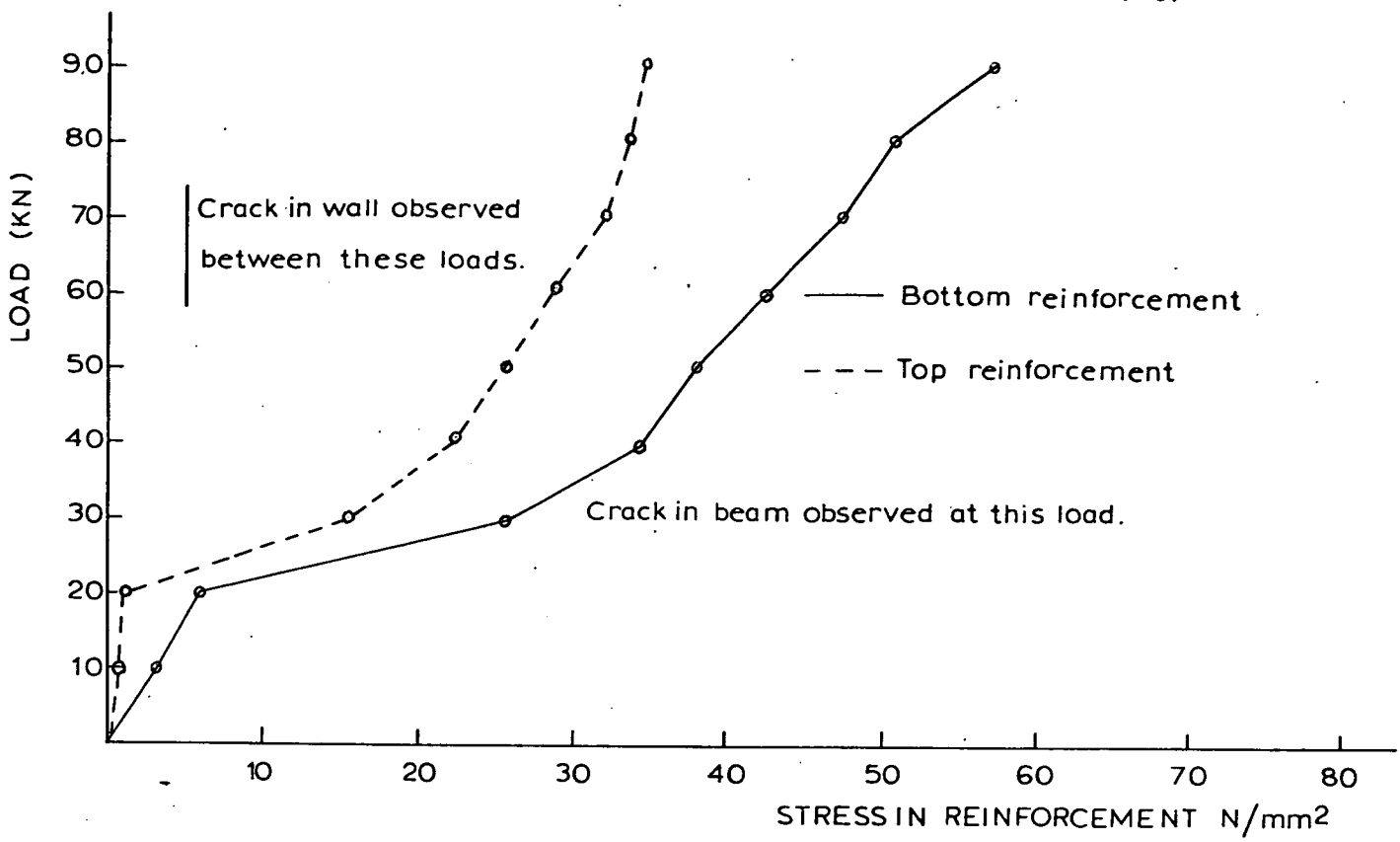

FIG (3.9) LOAD REINFORCEMENT STRESS IN BEAM OF WALL (2b)

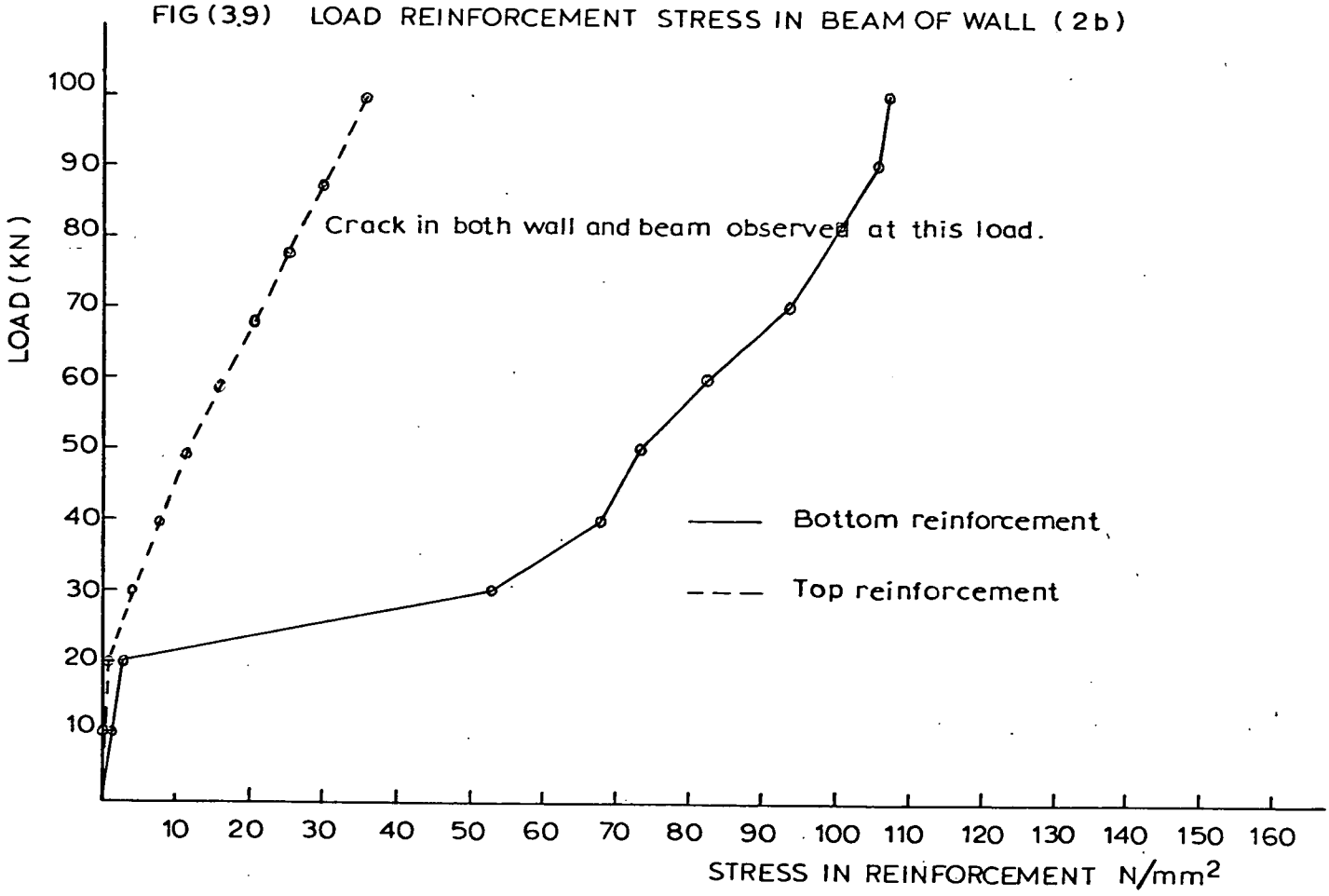

FIG (3.10) LOAD-REINFORCEMENT STRESS IN BEAM OF WALL (3b-c)

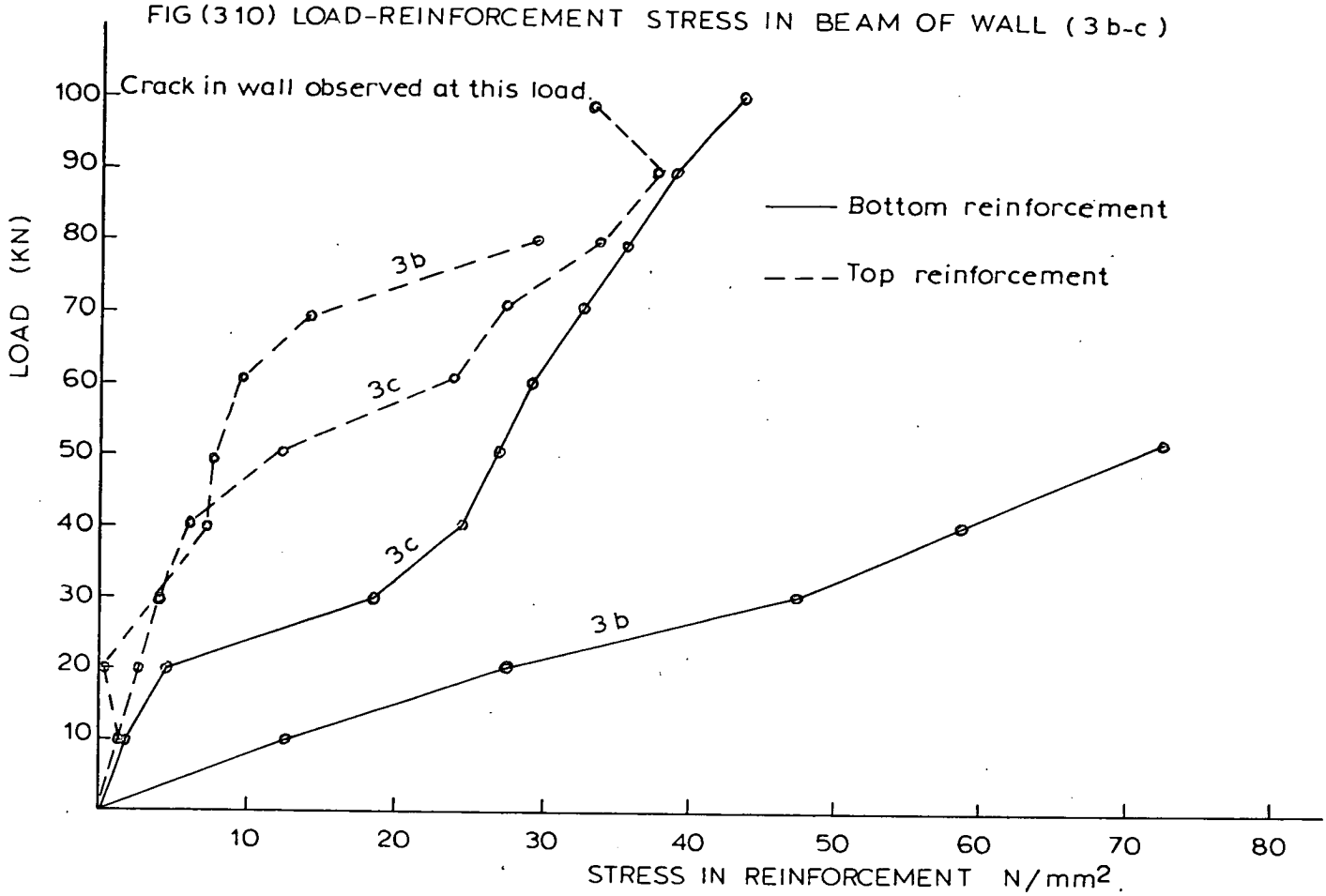

FIG.(3.11) LOAD-REINFORCEMENT STRESS IN BEAM OF WALLS (4a-b).

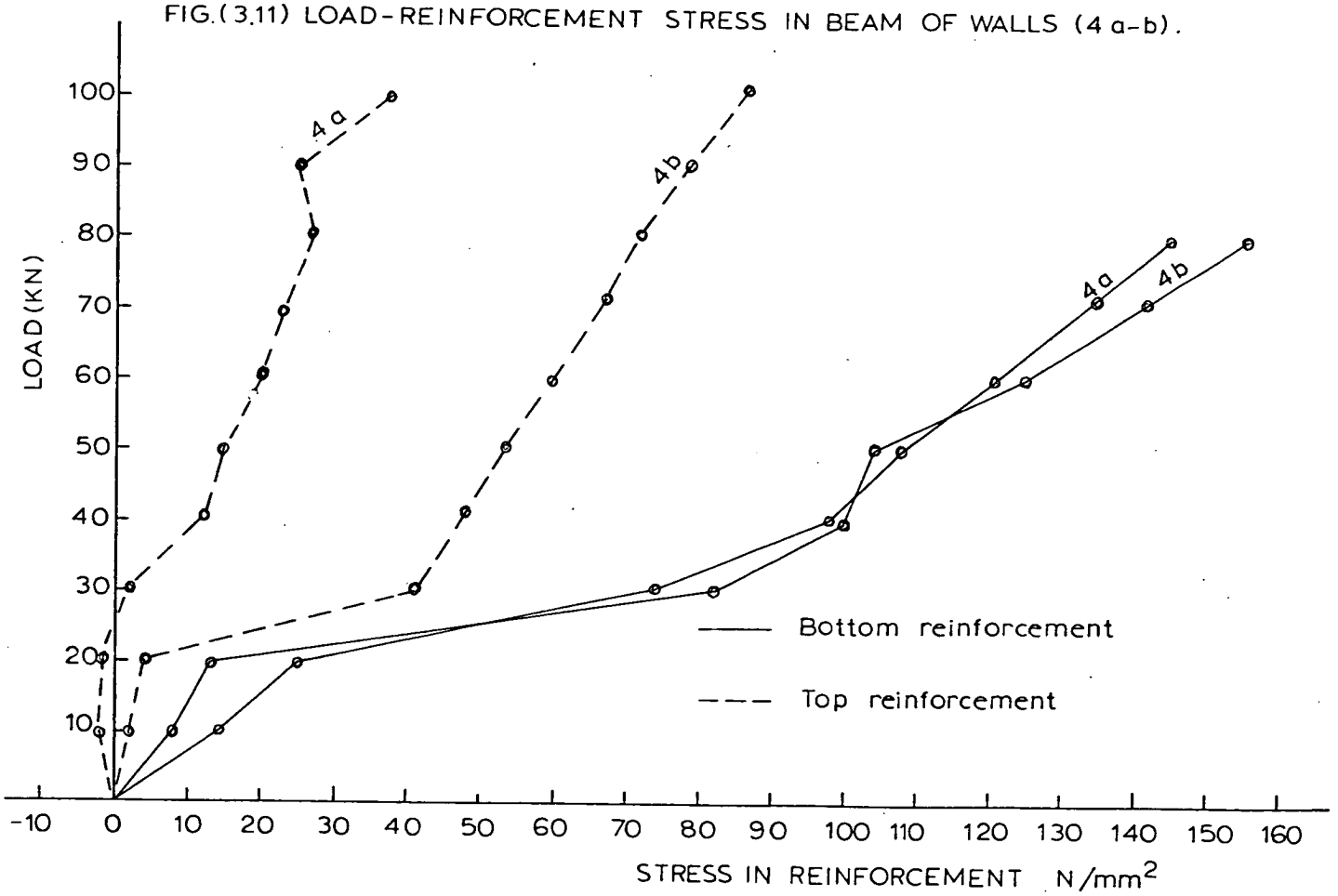

FIG. (3.12) LOAD–REINFORCEMENT STRESS IN BEAM OF WALL (5b)

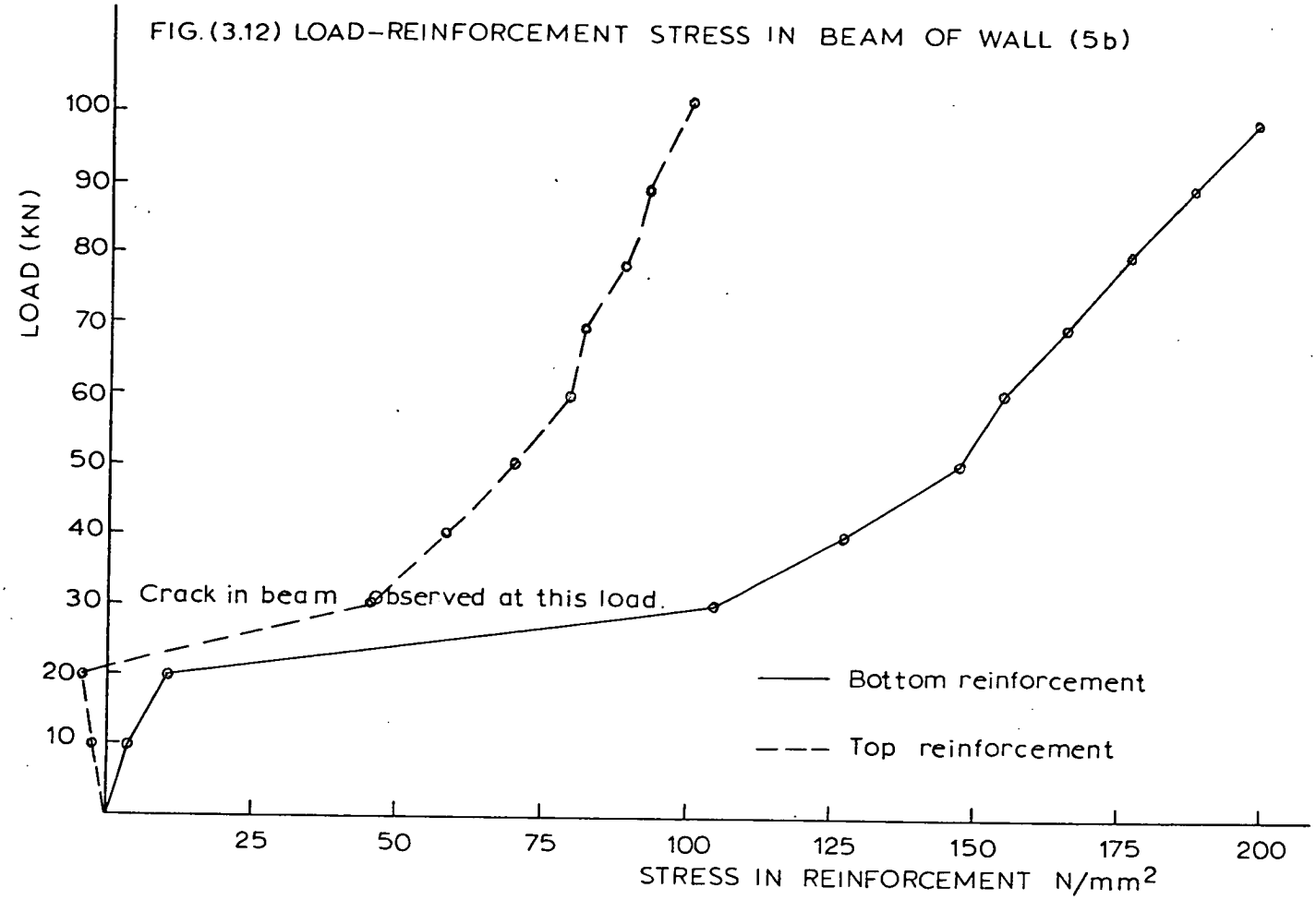

FIG. (313) LOAD-REINFORCEMENT STRESS IN BEAM OF WALLS (5a-c)

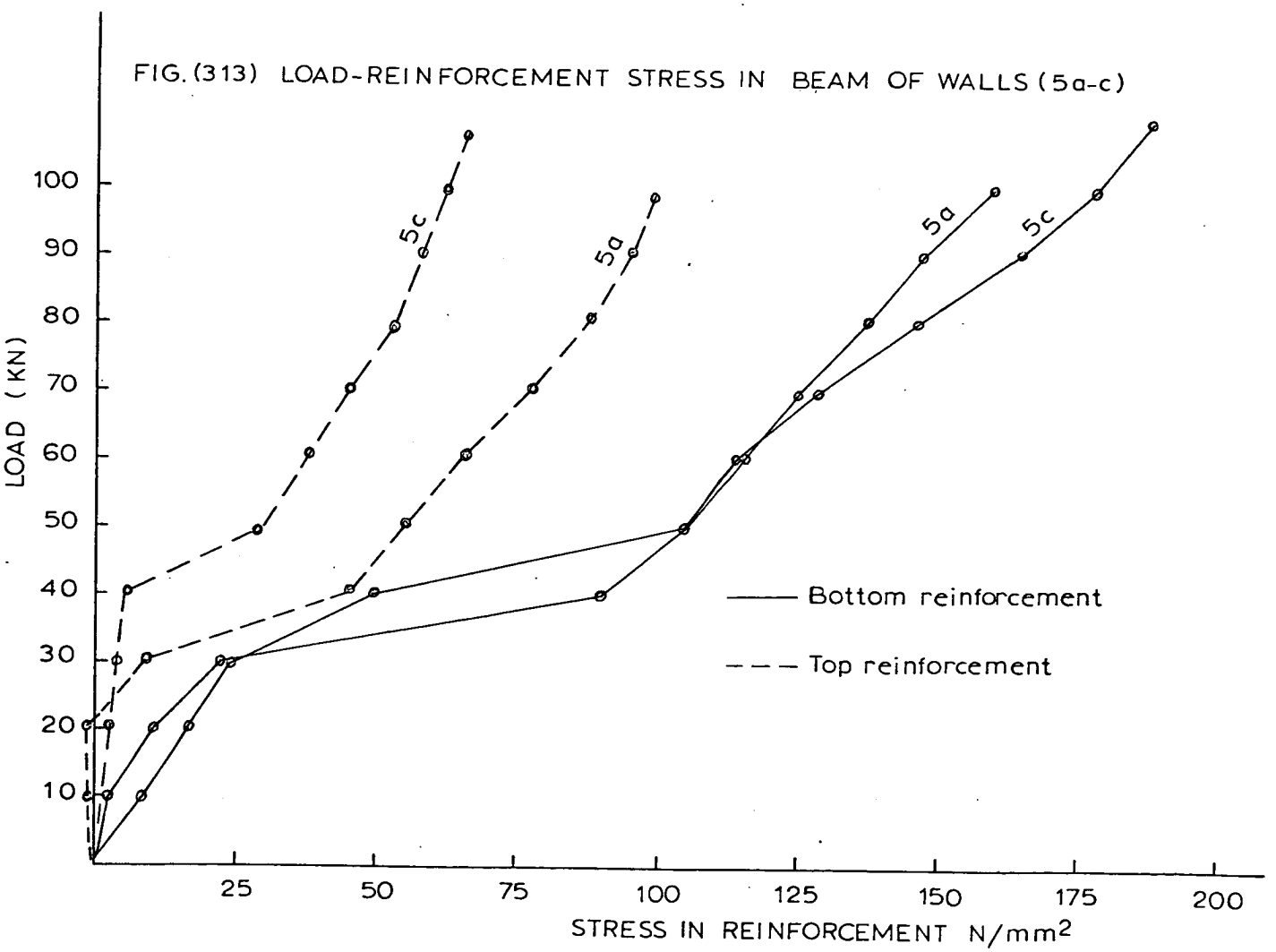

stiff. The vertical strain, and thus the stress, spreads more towards the centre of the span in walls 5, thus reducing the stress concentration over the supports. This tends to confirm that the distribution of the interface vertical stress is influenced by the relative beam stiffness. For an infinitely stiff beam the applied load would therefore act down the wall unaltered to give uniformly distributed load on the supporting beam. The effect of the beam stiffness is being reflected in the relative stiffness parameter R, which actually compares the wall and beam relative stiffness.

3.4.2 Beam Bending Moments

Table 3.4 shows that the maximum bending moment, obtained from the vertical strain distributions, to be of the order of WL/48. In the case of walls of series 5, the moment is increased to WL/35. This is [illegible] because in walls 5, the loading intensity spreads towards the centre of span while in other walls the loading spreads along a short contact length from the supports. Since the counter effect of the horizontal shear force at the wall/beam interface has been neglected, the values of these moments are therefore, overestimated.

3.4.3 Beam Axial Force

Measurements of the strains in the steel reinforcement of the supporting beam, Figures 3.8 -3.13, show that both the

lower and upper reinforcement were in tension throughout all loading stages. Also an investigation on the concrete stresses in the supporting beam, Figures 3.20-3.21, indicates that the top fibres of the beam were also in tension. From this it can be concluded that the composite action was apparently taking place, and the supporting beam was under the combined action of axial tension and bending. The axial force in the supporting beam, calculated for the early stages of loading before cracking of the beam takes place, ranges between W/3.3 to W/5.6. The magnitude of this force depends mainly on the relative axial stiffness parameter K, as will be shown in Chapter 4.

3.4.4 Horizontal Stresses

Typical distribution of the horizontal strain along the wall centre line is shown in Figure 3.14. This shows horizontal compression stresses over the entire height of the panel, and tensile stresses concentrated in the supporting beam. The maximum horizontal tension is much greater than the maximum compression which indicates a departure from the conventional beam theory. The relief of panel from the tensile stresses through the tied arch action, in which the supporting beam takes the tie force, is one of the most significant effects of the composite action. In the absence of the supporting beam, however, these tensile stresses should be carried by the panel itself, and since brickwork is weak in tension, this would lead to the panel failure in lateral tension, as shown in Plate 2.

FIG(315) LOAD DEFLECTION CURVES OF BEAM SOFFIT AT MIDSPAN.

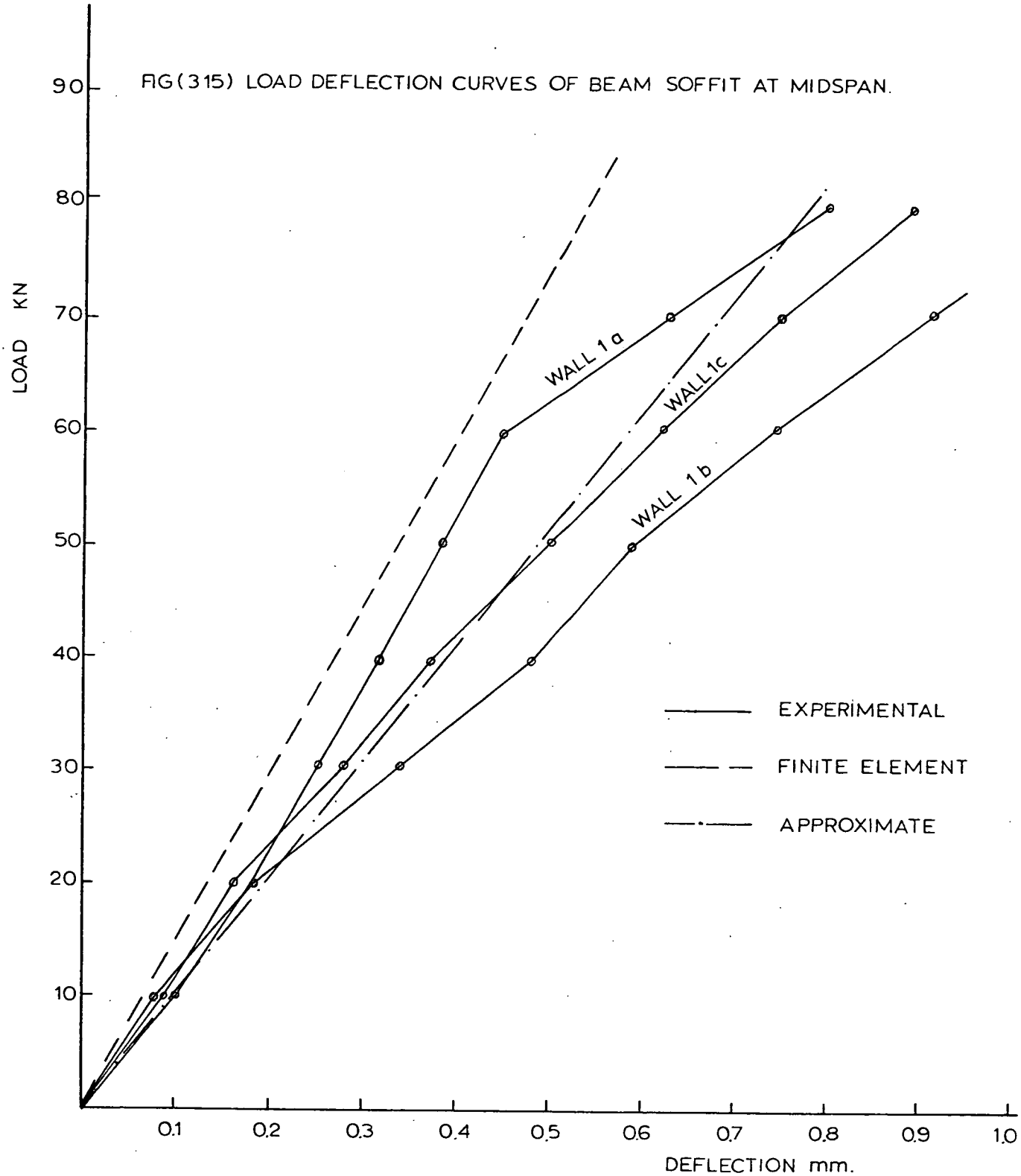

FIG (3.16) LOAD-DEFLECTION CURVES OF BEAM SOFFIT AT MIDSPAN.

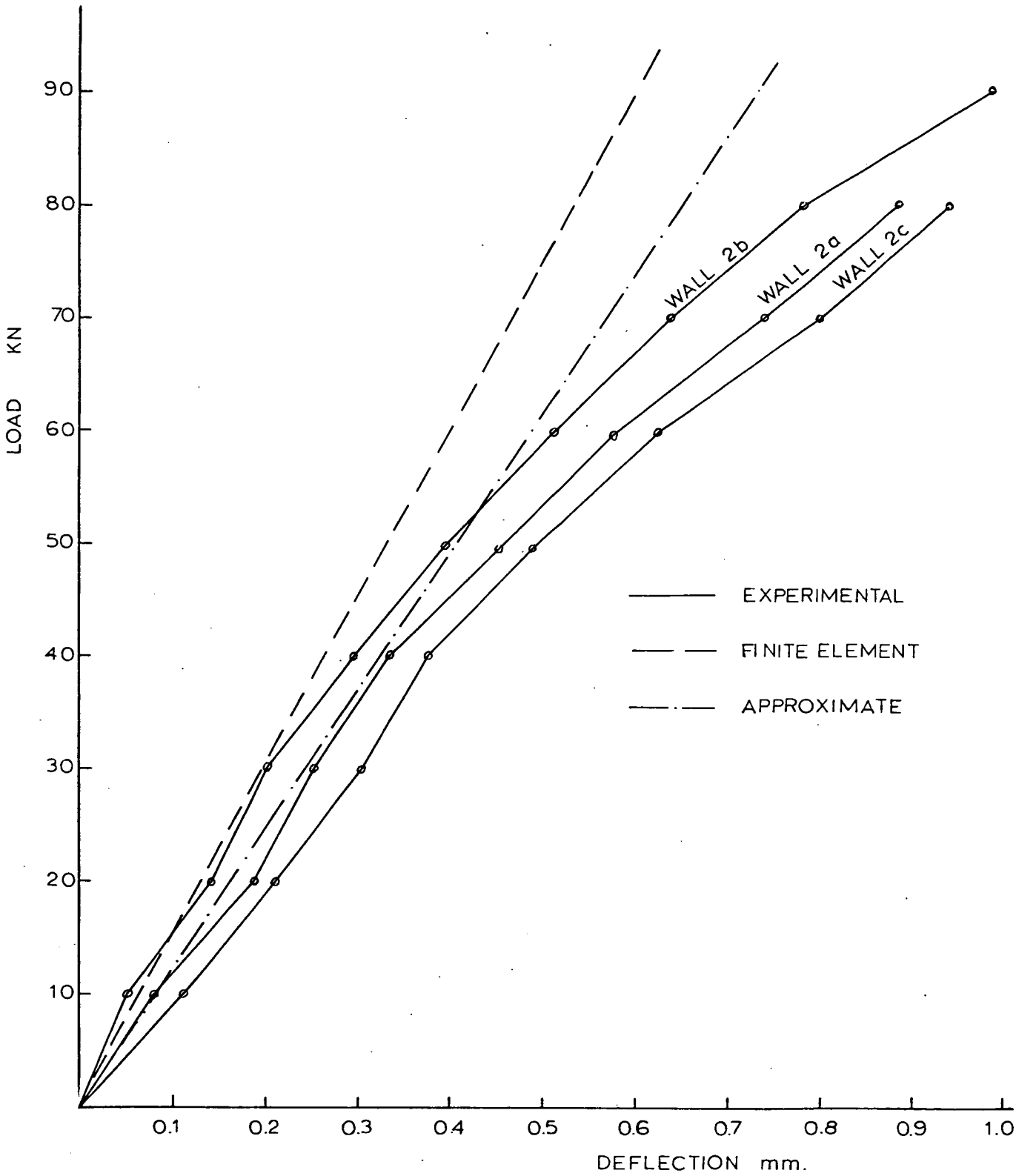

FIG (3.17) LOAD DEFLECTION CURVES OF BEAM SOFFIT AT MIDSPAN

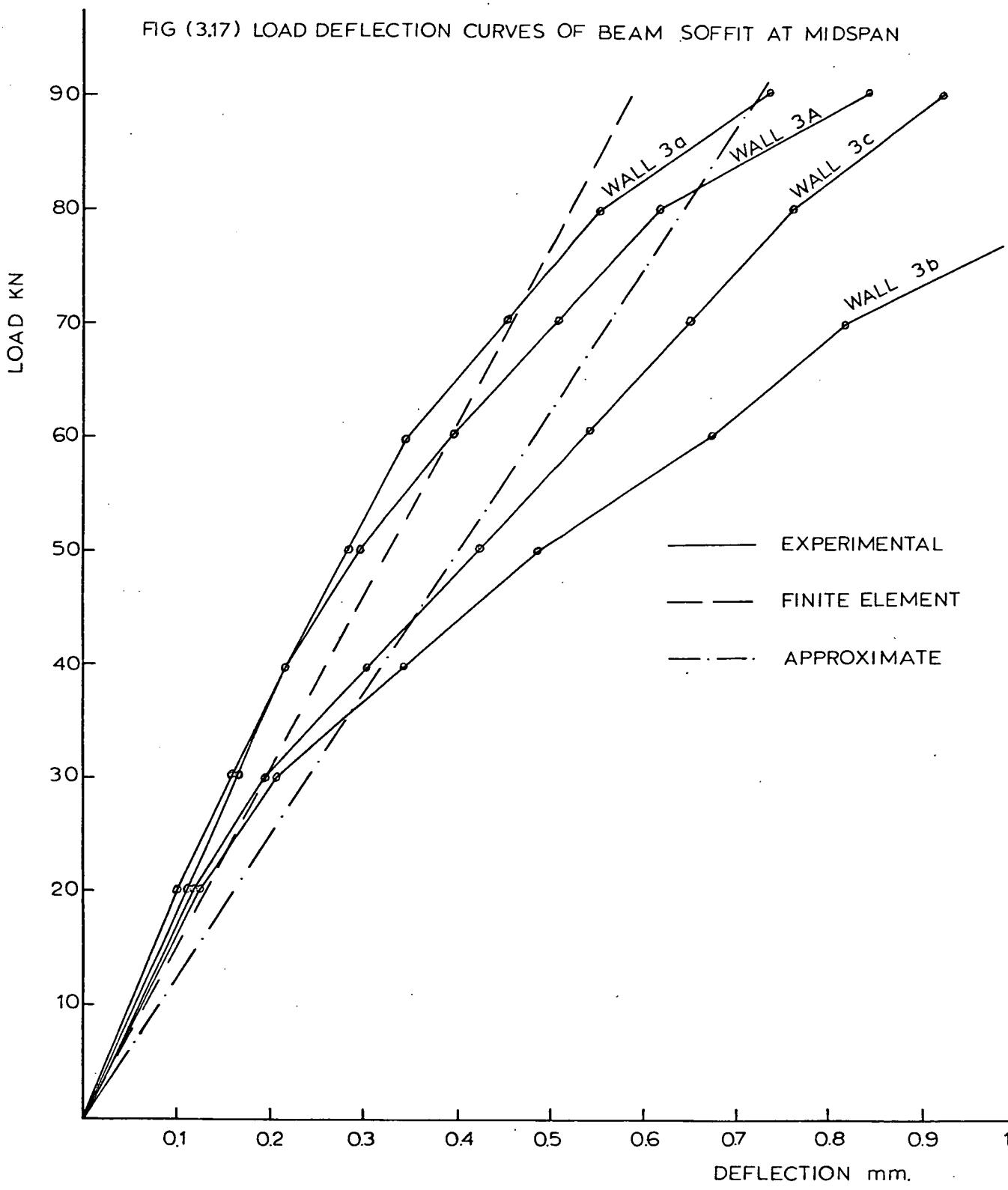

FIG (3.18) LOAD DEFLECTION CURVE OF BEAM SOFFIT AT MIDSPAN.

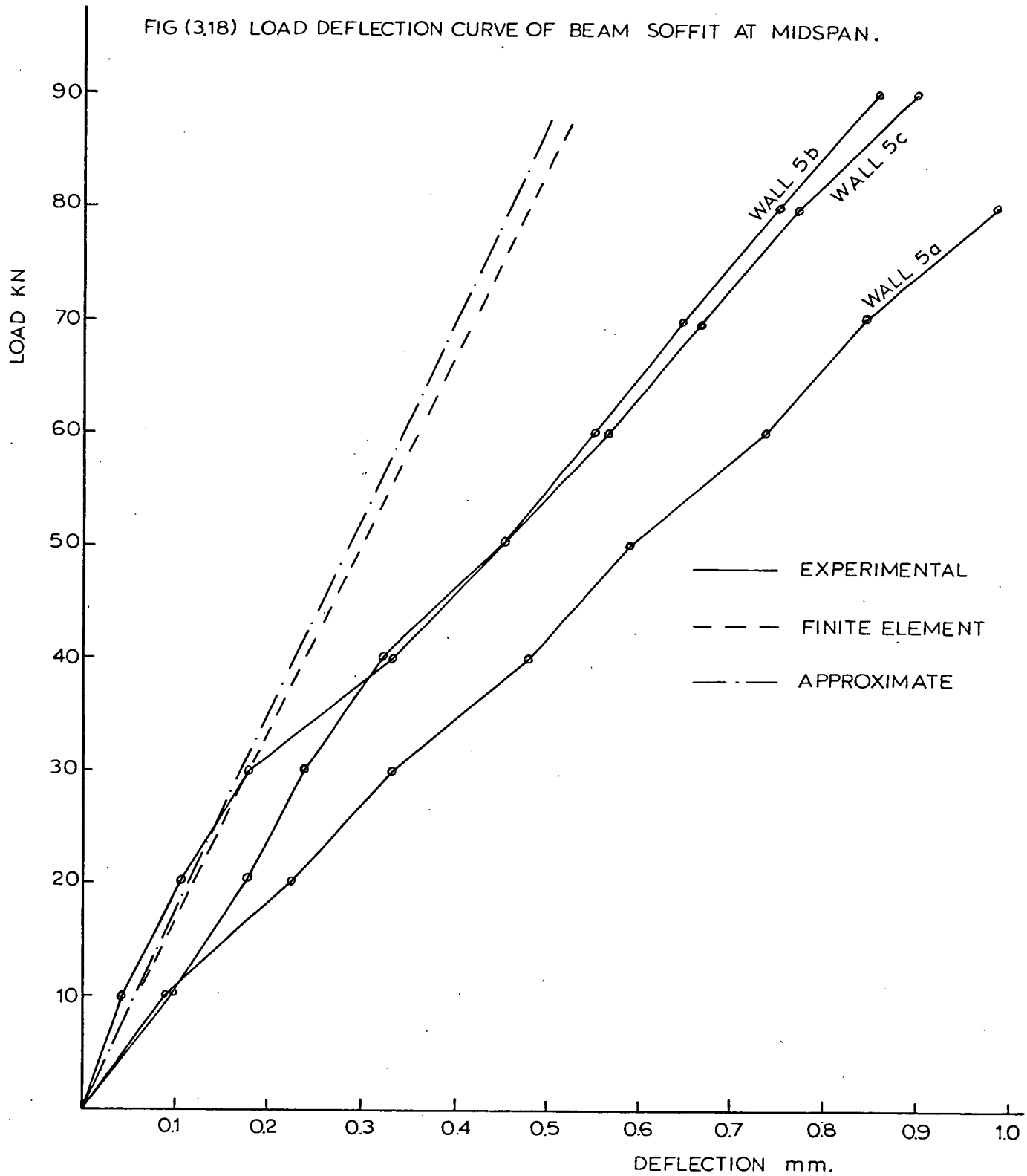

FIG.(3.19) AVERAGE LOAD DEFLECTION OF BEAM SOFFIT AT MIDSPAN.

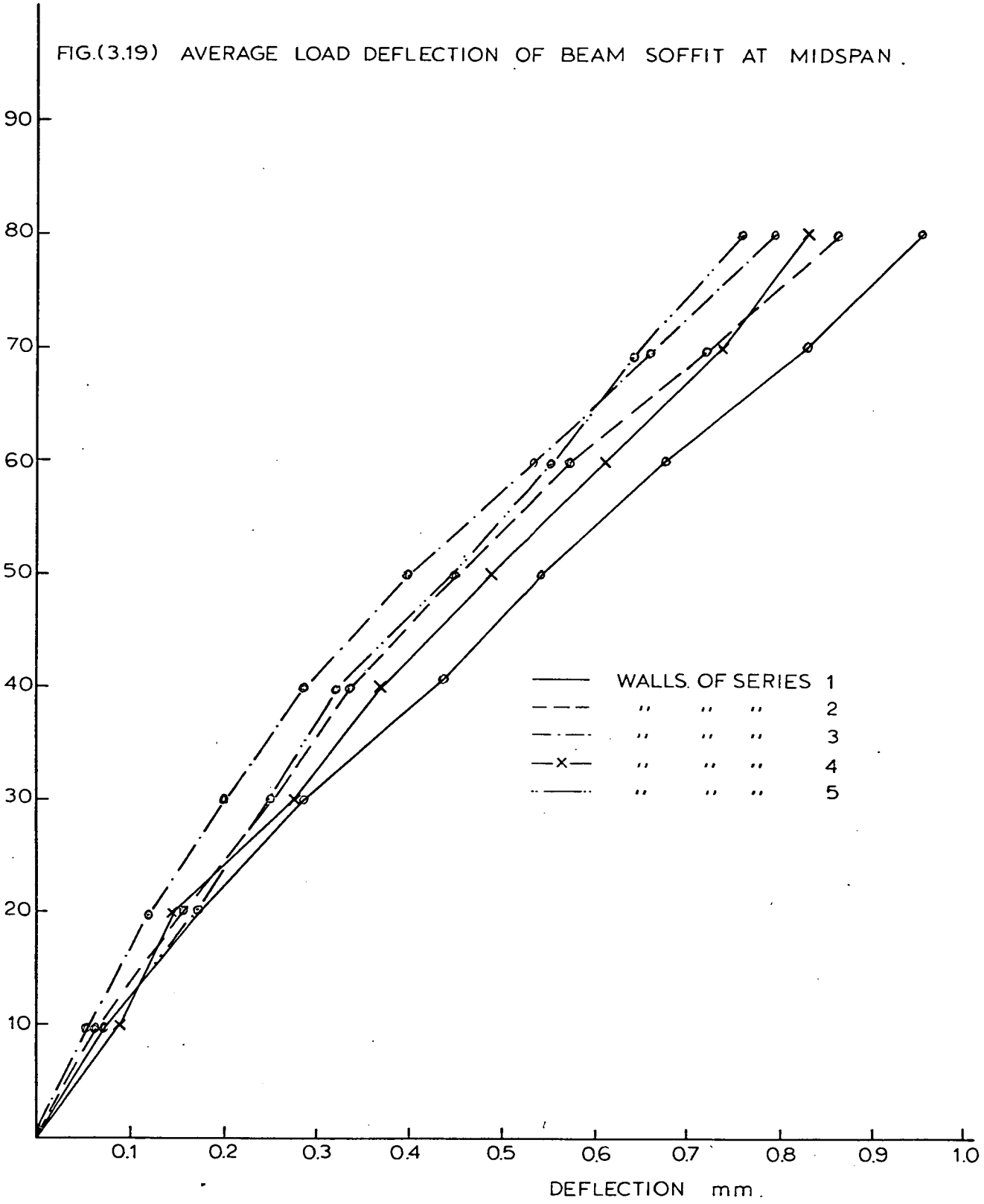

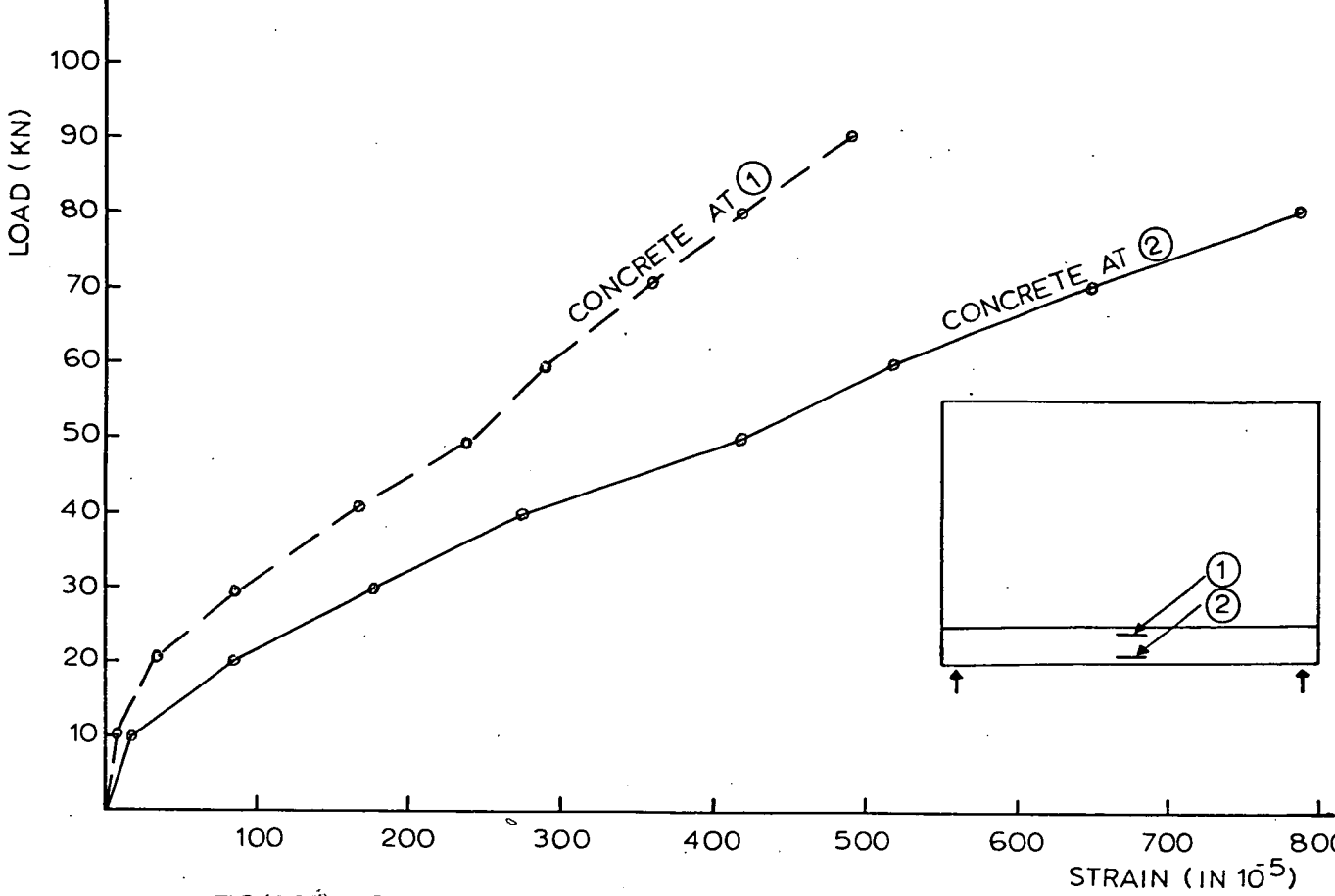

FIG (3.20) LOAD-STRAIN CURVE IN CONCRETE AT POINTS ① AND ② IN BEAM OF WALL 16.

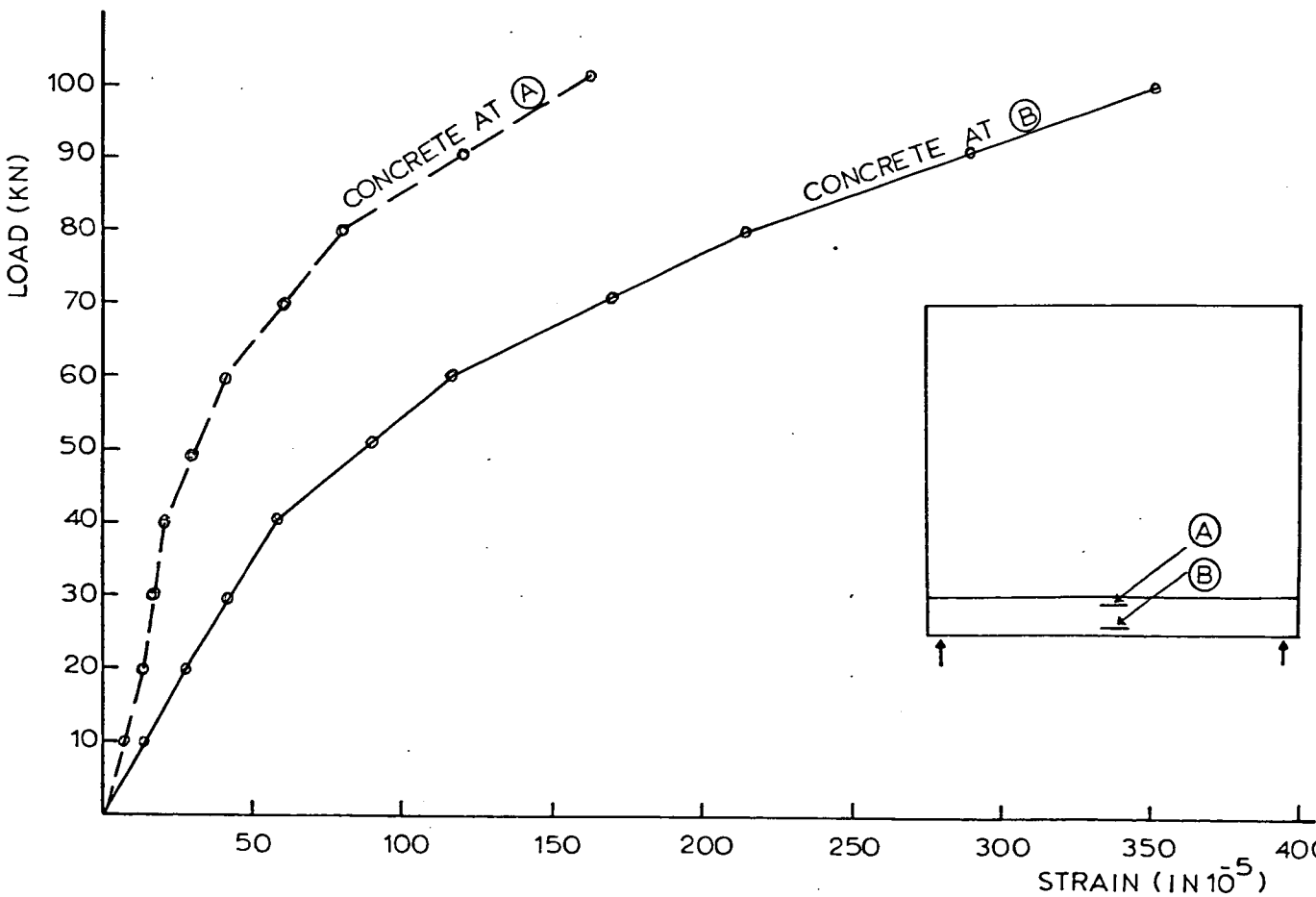

FIG (3.21) LOAD-STRAIN CURVE IN CONCRETE AT POINTS Ⓐ AND Ⓑ IN BEAM OF WALL (3A).

As can also be seen from Figure 3.14, the horizontal stresses in the supporting beam are tensile over the whole cross-section. As these stresses tend to be very low, it is conceivable that the usual assumptions made for reinforced concrete design will no longer hold, and the concrete itself will contribute to the tensile load carrying capacity.

Table 3.6 gives the values of the internal moment arm, expressed as a ratio of the total height. The values vary between 0.6 to 0.8, and as they are calculated on the basis of concrete being effective in tension, it follows that any cracking which occurs on further loading and the consequent transference of resistance against tensile forces to the reinforcement, would lead to an increase in the values of the moment arm in Table 3.6. It is therefore possible that these values can be used for the calculation of areas of steel reinforcement in the supporting beam. It is apparent that the value of 0.66 proposed by Wood[2] is satisfactory.

3.4.5 Deflection

The magnitude of the beam central deflection recorded in tests of series 1 to 4, is of the order of 1/600 of the span at loads approaching failure - Figures 3.15 - 3.19. The reason for the small deflection of the composite beam may be attributable to the counter effect of the horizontal shear force at the wall/beam interface which tends to produce an upward deflection of the supporting beam. As the effect of this force is maximum at midspan,

TABLE 3.5 CONCENTRATION OF VERTICAL STRESS OVER SUPPORTS

Wall No	Applied Stress	Maximum Vertical Stress N/mm^2			f_a/f_p	f_{max}/f_p		
	(f_p) N/mm^2	Left Support	Right Support	Average (f_a)		Experiment	Finite Element	Approx
1a	1.73 2.60	10.03 12.89	9.24 12.89	9.64 12.89	5.57 4.96	5.80 4.96	6.37	6.25
1b	2.60 3.03	17.32 18.62	11.59 14.84	14.46 16.73	5.56 5.52	6.66 6.15	6.37	6.25
1c	1.73 2.17	10.17 14.58	10.94 14.84	10.55 14.71	6.10 6.78	6.32 6.84	6.37	6.25
2a	2.60 3.03	13.54 16.80	18.10 21.74	15.82 19.27	6.08 6.36	6.96 7.17	6.75	6.64
2b	2.17 2.60	12.63 15.49	14.19 17.97	13.41 16.73	6.18 6.43	6.54 6.91	6.75	6.64
2c	2.17 2.60	10.15 12.50	9.11 11.46	9.63 11.98	4.45 4.61	4.68 4.81	6.75	6.64
3A	3.23 4.10	19.49 25.32	20.23 26.15	19.86 25.74	6.15 6.28	6.26 6.38	7.13	6.82
3a	2.45 3.27	13.28 22.0	11.85 18.60	12.56 20.31	5.13 6.21	5.42 6.73	7.13	6.82
3b	3.03 3.46	19.92 24.61	23.05 24.87	21.49 24.84	7.07 7.15	7.61 7.19	7.13	6.82
3c	2.60 3.28	10.42 14.97	11.98 18.36	11.20 16.67	4.31 5.15	4.61 5.60	7.13	6.82
4a	2.60 3.03	21.87 25.26	23.83 26.95	22.85 26.12	8.79 8.60	9.17 8.89	8.60	7.17
5a	3.03 3.46	11.07 13.41	11.59 15.10	11.33 14.23	3.74 4.11	3.83 4.36	4.88	5.81
5b	3.03 3.46	9.90 11.85	10.03 11.72	9.97 11.79	3.29 3.41	3.31 3.42	4.88	5.81
5c	3.03 3.46	14.58 16.80	13.02 15.23	13.8 16.02	4.55 4.63	4.81 4.86	4.88	5.81

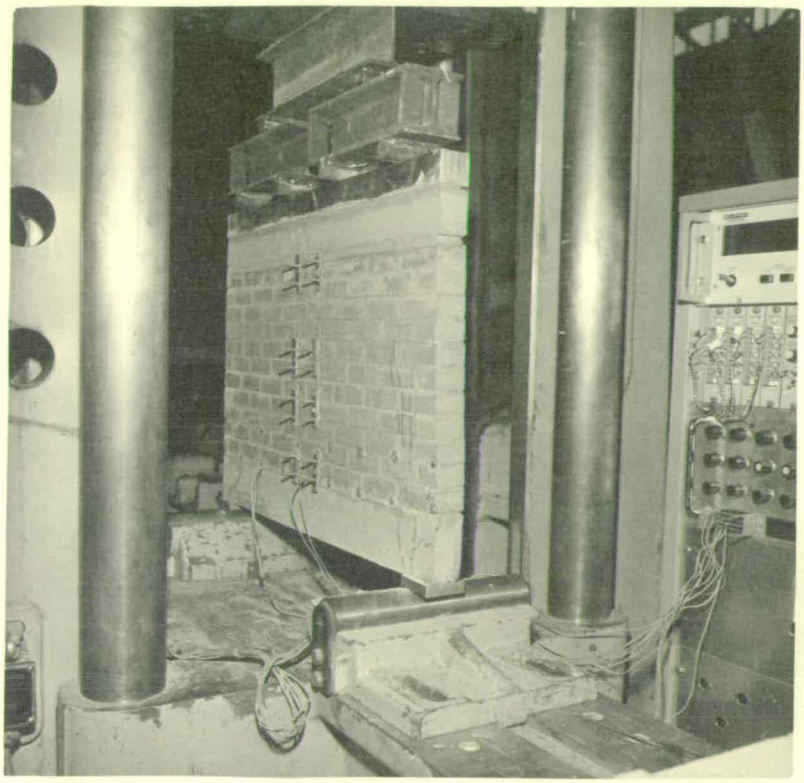

PLATE 2.1 WALL 1c AFTER FAILURE

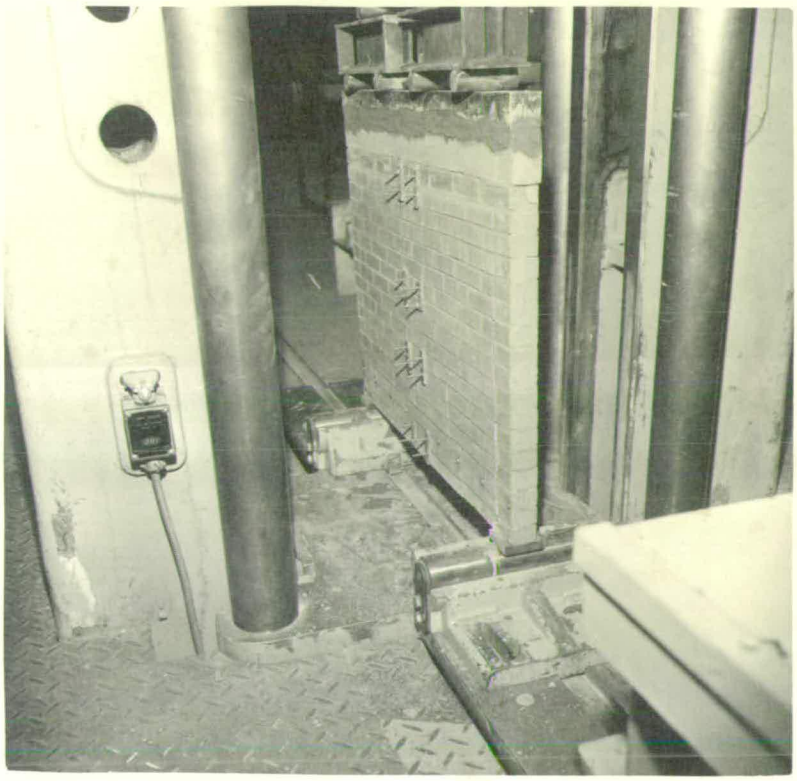

PLATE 2.2 FAILURE OF WALL WITHOUT A SUPPORTING BEAM

the downward central deflection is substantially reduced. The fact that the deflection of beams in series 5 is higher than that in series 3, Figure 3.19, results from the higher effect of the interface horizontal force occurring in the latter. It will be shown later in Chapter 4 that the axial force in the supporting beam is a measure of the magnitude of the horizontal shear force at the interface. With this in mind, reference to Table 3.6 shows that the magnitude of the axial force in beams of series 5, is much more than that in beams of series 3.

3.5 MODES OF FAILURE

The distinct modes of failure exhibited by the test walls were as follows :

1. Diagonal shear in supporting beam and wall over the supports along the entire height.

2. Vertical tensile splitting and crushing of bricks over the supports.

The shear failure in the wall frequently appeared after the first shear cracks had appeared in the supporting beam at the support points. This crack appeared at about 60-80% of the ultimate load. Walls that failed in shear were (1a, 1c, 2a, 2b). In all these walls, the shear crack appeared first in the supporting beam and then extended upward in the wall through the vertical mortar joints and the bricks. It follows that the factors influencing the shear strength of the wall are, the shear

strength of the supporting beam, the height of the wall, the strength of vertical joints and bricks. The support conditions may also have influence on the shear strength of the wall and beam. A wider support relieves the supporting beam from the stress concentration, on the other hand a point support, not usually found in practice, induces high stress concentration, which may initiate beam shear failure.

In relatively high walls (series 3 and 4) or in walls supported on relatively stiff beams (series 5), the criterion of failure was vertical tensile splitting and crushing of corner bricks over the supports. This is, in general, the predominant mode of failure as it is mainly initiated by the high concentration of vertical stress over the supports. The vertical tensile splitting occurs as a result of the different strength and deformation characteristics of bricks and mortar[30]. In general, the uniaxial compressive strength and the modulus of elasticity of mortar are considerably lower than the corresponding values of the bricks. Therefore, if the mortar could deform freely, its lateral strain will be larger than the strain in the bricks. However, because of bond and friction between brick and mortar, the mortar is confined. Thus, an internal state of stress is developed which consists of axial compression and lateral tension in the brick and triaxial compression in the mortar. If the transverse tensile stresses exceed the brick flexural tensile strength, vertical tensile cracking will take place in the bricks. However, the wall at this stage is not to be considered as failed, because it can

withstand more load. Upon further increasing the load, the tensile cracks widen and when the compressive strength of the bricks is exceeded, failure will set in by both vertical splitting and crushing of the corner bricks over the supports - Plates 2, 3 and 4. It can therefore be concluded that for walls in which the primary failure criterion is vertical splitting and crushing of corner bricks, the ultimate strength can be increased by strengthening the corner bricks. This can either be achieved by introducing bricks of very high compressive strength, eg, engineering bricks, or providing horizontal reinforcement in the bed joints in that locality.

The occurrence of tensile cracks at midspan of the supporting beam (walls 1b, 2c, 3c, 4A, 4B, 5a, 5b, 5c) was mainly attributable to the excessive axial force induced in the beam as a result of the tied arch action and the external bending moment. The sudden change in the slope of the load-reinforcement stress curves indicates the formation of these cracks before they were observed. The cracks appeared at about 30-40% of the ultimate load. After cracking of the supporting beam, all tension was absorbed by the reinforcement.

In the present test series, no failure through separation of wall from beam was observed. Such mode of failure is to be anticipated if the frictional resistance of the interface mortar joint is not capable of transferring the horizontal shear force across the wall/beam interface, or the bond strength of the mortar, is sufficiently low so that separation occurs by the vertical

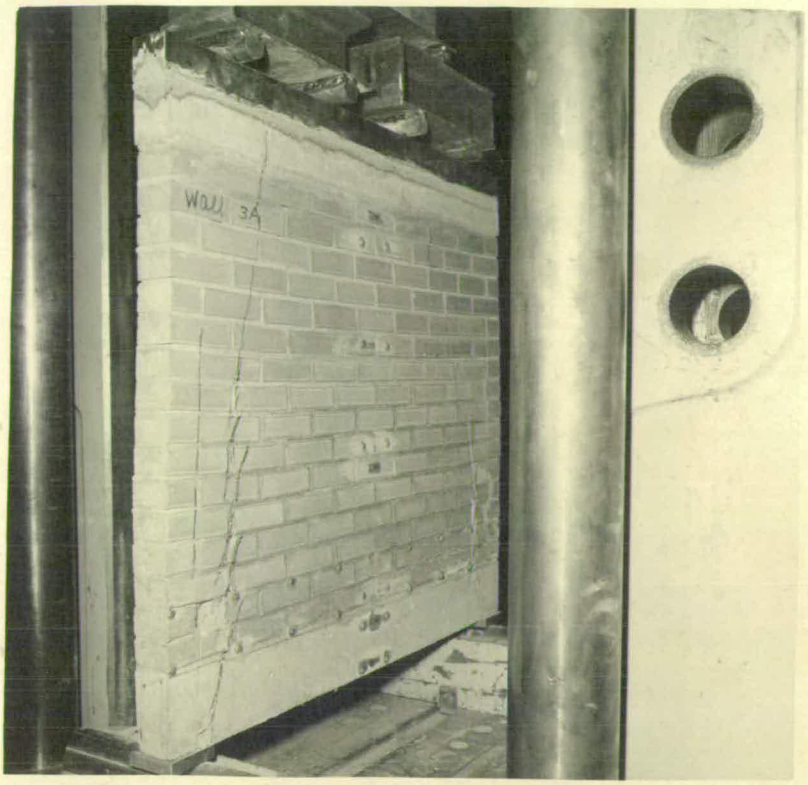

PLATE 3.1 CRACK PATTERN IN WALL 3A

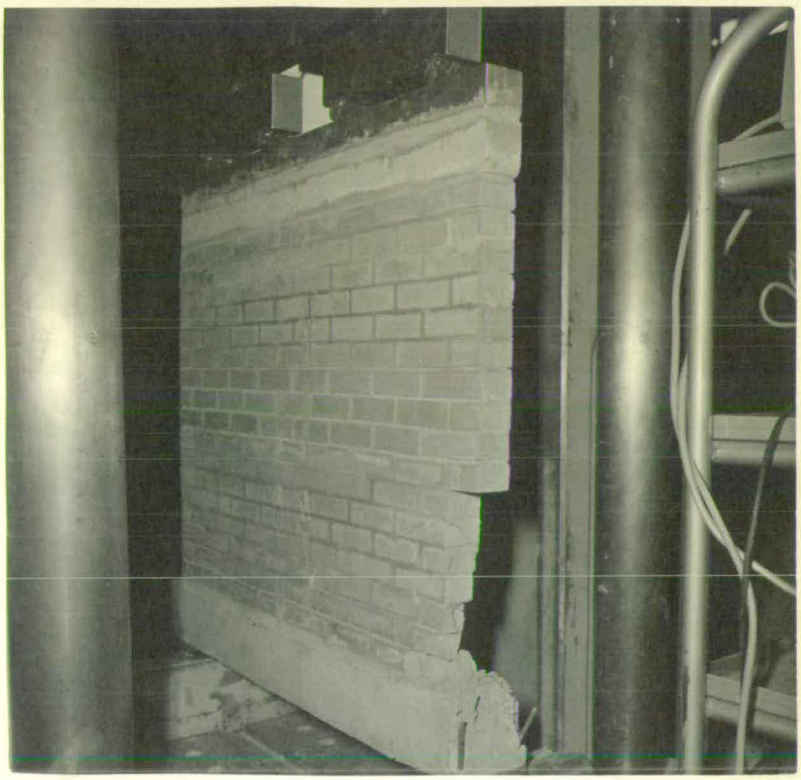

PLATE 3.2 WALL 5a AFTER FAILURE

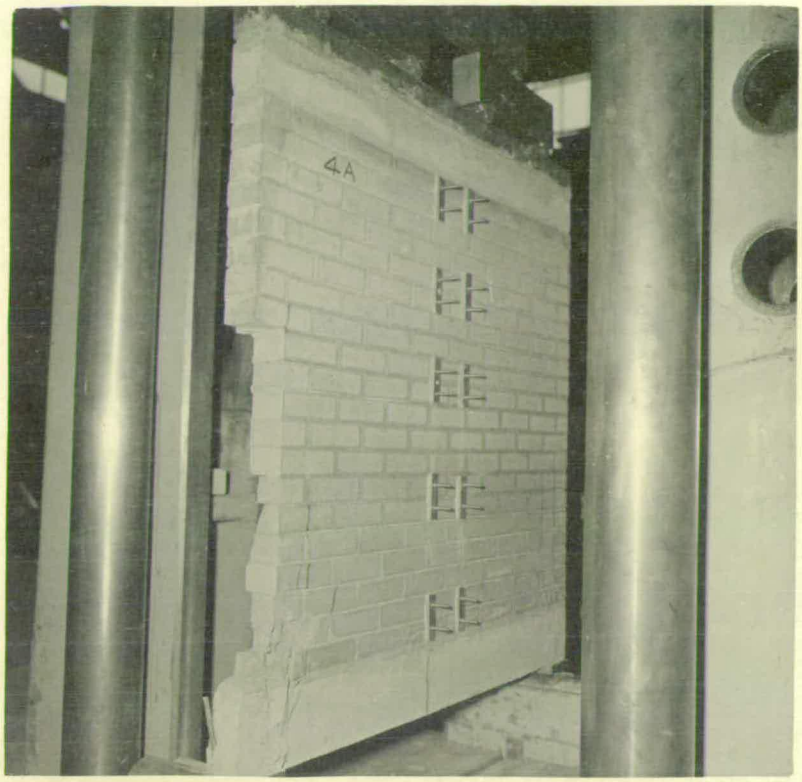

PLATE 4.1 WALL 4A AFTER FAILURE

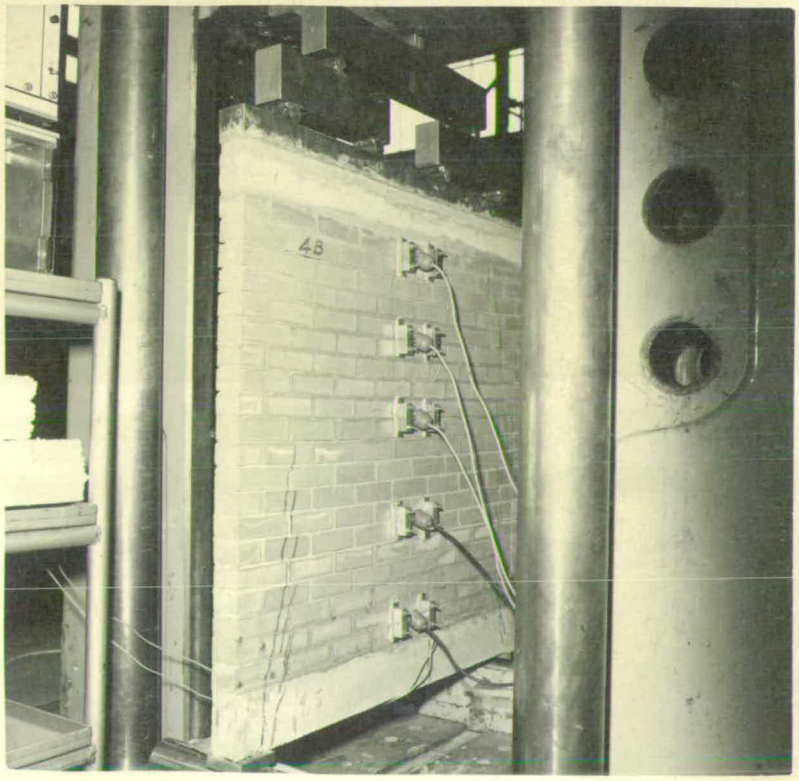

PLATE 4.2 CRACK PATTERN IN WALL 4B

tensile stresses in the central region of the span. However, in all test walls, the interface mortar joint was laid from a 1:1 mortar mix which was strong enough in both friction and bond that separation of components did not occur in any of the test specimens.

3.6 COMPARISON OF RESULTS

Table 3.5 shows comparison of the experimental and theoretical values of the vertical stress concentration in the wall. It is clear that the values predicted by the approximate expression (Equation 4.7.2)are in very good agreement with those predicted by the finite element method. This is to be expected, since the approximate procedure has been suggested based on results predicted by the finite element method. The experimental results are found to be in a satisfactory agreement with both methods. The discrepancy being due to the underestimation of the vertical contact stresses resulting from the strain measurements which were taken slightly above the contact surface. The discrepancy is also attributable to the non-homogeneous nature of the brickwork material. Furthermore, the finite element as well as the approximate procedure are based on elastic theory, and once cracking takes place the system will be non-linear and the prediction of its behaviour by the elastic methods will only be approximate.

Comparison of the maximum bending moment in the supporting

beam predicted by theory and experiment appears in Table 3.4. The experimental values of the bending moments have been obtained from the vertical stress distributions along the contact surface, the effect of the horizontal shear at the wall/beam interface has been neglected. Although this should give higher values of the bending moment compared to the finite element and approximate methods, it appears that the values in beams of series 1 and 3 are slightly lower. This is presumably due to the underestimation of the contact length. In general the finite element method satisfactorily predicted the bending moments in the supporting beam while the approximate method showed slight underestimation.

In Table 3.6, experimental values of the axial force in the supporting beam expressed as a ratio of the applied load, are compared with values predicted by the finite element method and the approximate formula (Equation 4.7.5). The experimental results compare favourably with the finite element method and are also in good agreement with the approximate results. In the calculation of the axial force from the measured strains in the steel reinforcement of the supporting beam, it has been assumed that before cracking occurs, the concrete of the supporting beam is effective in tension. The present finite element analysis and the approximate method consider the same assumption and therefore the predicted values are of the same order of magnitude.

TABLE 3.7 COMPARISON OF ULTIMATE LOAD

TEST NO	FAILURE LOAD KN		% DIFFERENCE
	EXPERIMENTAL	APPROXIMATE	
2a	105	133.5	27.0
2b	100	133.5	33.5
2c	109	133.5	22.5
3A	115	131.3	14.3
3b	105	131.3	25.0
3c	110	131.3	19.3
4A	103.5	124.9	20.7
4B	104	124.9	20.1
5a	150	148.1	-1.3
5b	181	148.1	-18.2
5c	139	148.1	6.5

Comparative plots of the measured deflection at the beam centre and that predicted by the finite element and the approximate expression (Equation 4.7.37) are shown in Figures 3.15 - 3.18. The deflection predicted by the approximate method is in very good agreement with the measured deflection particularly in the elastic stage. The deflection predicted by the finite element method is slightly less than the actual deflection.

Table 3.7 shows comparison between the ultimate load predicted by the approximate expression (Equation 4.7.4) and the actual failure load. In all these walls failure occurred by crushing of the corner bricks over the support. It can be seen that the predicted values are higher than the actual values with a discrepancy varying between -18 to 33 per cent. The discrepancy is as expected since, as will be shown later in Chapter 4, the approximate formula has been derived on the basis of elastic analysis. However, by adopting a suitable load factor, the method can satisfactorily predict the working loads.

3.7 CONCLUSIONS

The results of tests on solid wall/beam structures indicate that :

1. The finite element method and the approximate method, proposed in Chapter 4, have provided a complete solution to the wall on beam problem.

2. The arching action causes concentration of vertical stress above the supports and horizontal shear along the interface joint very near to the supports. It appears that the strength of the corner bricks governs the failure load.

3. Reinforcement of the mortar bed joints may assist in relieving the brickwork from developing tensile cracks in the locality above the supports.

4. The supporting beam is under the combined action of axial tension and bending. Although the test results are insufficiently conclusive to enable proposing method for the calculation of the steel reinforcement in the supporting beam, they indicate that the moment arm method proposed by Wood[2] is satisfactory.

5. Failure of wall in vertical shear can be avoided by adequate shear reinforcement of the supporting beam.

SECTION B

3.9 WALLS WITH OPENINGS

In this section, the behaviour of one-third scale model brick panels combining openings and supported on reinforced concrete beams is investigated. The work comprised of tests on ten walls with either a door or a window opening. The effects of the size and position of the opening are studied.

The materials used in the construction of walls and beams are the same as those used for the solid walls as described earlier in this Chapter. Construction of openings in the wall was guided by timber frames fixed to the back board. Although the dimensions of the walls and beams were not scaled down to one-third of the actual prototype, nevertheless the dimensions of openings were chosen to be proportional to the model dimensions in such a way as to simulate the actual structure. With the exception of wall BIII all walls had reinforced concrete lintels over the openings. Loading procedure and measurements of strains and deflections were performed in the same manner as described in Section A of this Chapter.

3.9.1 Test Results

The details of the walls are shown in Figure 3.23. The results of the vertical strain measurements at the bottom course of bricks are given in Figures 3.24-29. Indirect information obtained from these measurements, are the vertical stress

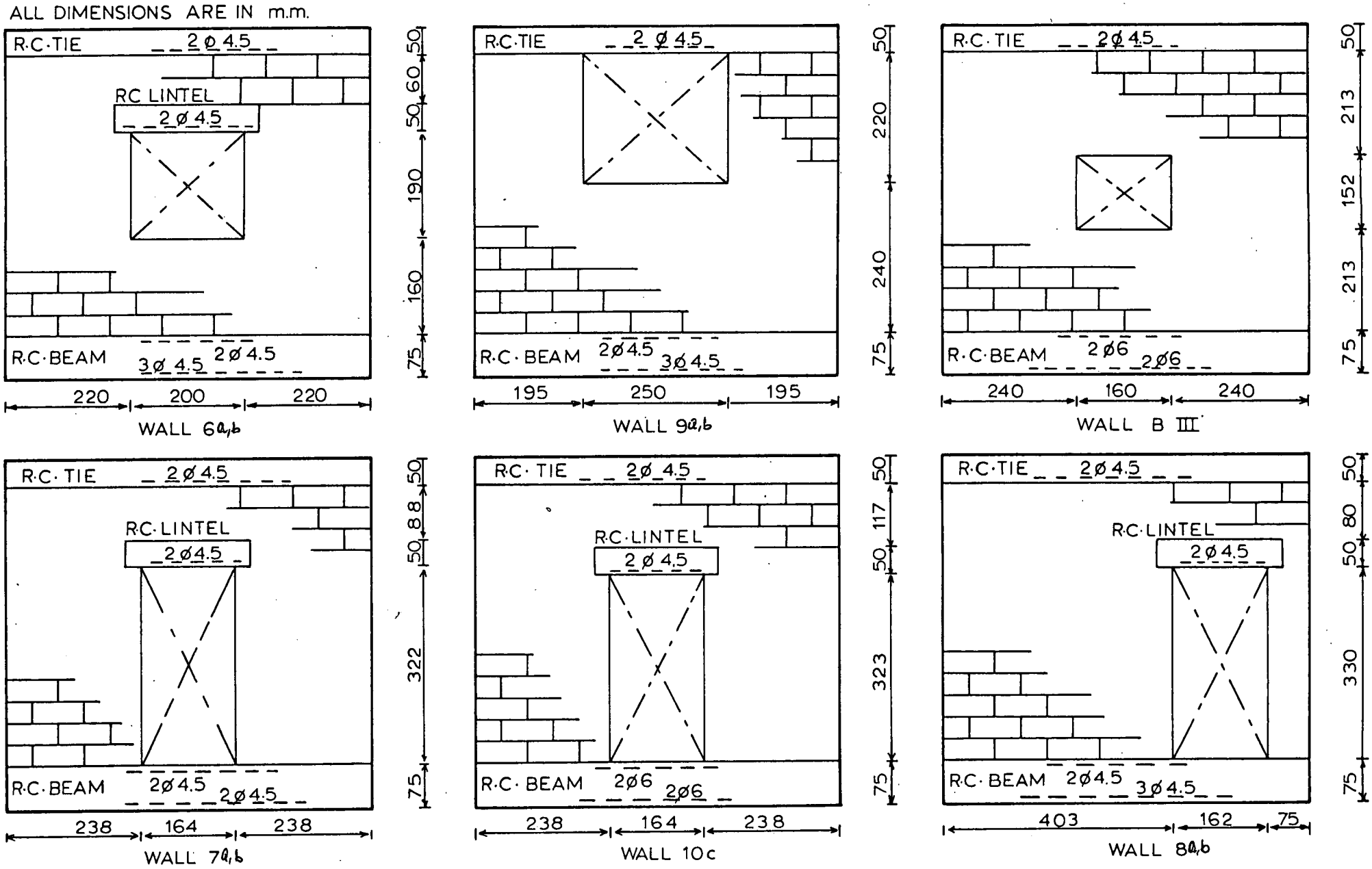

FIG. 3.23 DETAILS OF TEST WALLS.

TEST NO	WALL HEIGHT(h) mm	h/L	BEAM DIMENSIONS AND REINFORCEMENTS	LOAD AT APPEARANCE OF FIRST CRACK KN	SHAPE OF FIRST CRACK	FAILURE LOAD KN	MODE OF FAILURE
1a	279	0.48	76 x 36 mm 2 ϕ 4.5 2 ϕ 4.5	80	shear crack in the supporting beam	91	diagonal shear of the supporting beam and above support along the whole height of the wall
1b	279	0.48	76 x 36 mm 2 ϕ 4.5 2 ϕ 4.5	40	tension crack in the lower fibre of the supporting beam	90.5	diagonal shear of the supporting beam and along the whole height of the wall above support
1c	279	0.48	76 x 36 mm 2 ϕ 4.5 2 ϕ 4.5	30	shear crack in the supporting beam	100	shear of the supporting beam and diagonal shear above support along the whole height of the wall
2a	390	0.66	76 x 36 mm 2 ϕ 4.5 2 ϕ 4.5	60	shear crack in the supporting beam	105	shear of the supporting beam and vertical tensile splitting along the whole height of the wall
2b	390	0.66	76 x 36 mm 2 ϕ 4.5 2 ϕ 4.5	80	diagonal crack in the wall and shear crack in supporting beam	100	vertical tensile splitting of bricks above support and shear of the supporting beam
2c	390	0.66	76 x 36 mm 2 ϕ 4.5 2 ϕ 4.5	40	tension crack in supporting beam at midspan	109	vertical tensile splitting over the whole wall height
3A	444	0.76	76 x 36 mm 2 ϕ 4.5 2 ϕ 4.5	90	shear crack in the supporting beam	115	shear of the support beam and vertical tensile splitting above support along the whole height of wall
3b	444	0.76	76 x 36 mm 2 ϕ 4.5 2 ϕ 4.5	80	diagonal crack in wall ab above support	105	crushing of corner bricks above support
3c	444	0.76	76 x 36 mm 2 ϕ 4.5 2 ϕ 4.5	50	tension crack at midspan of supporting beam	110	vertical tensile splitting above support
4A	536	0.92	76 x 36 mm 2 ϕ 4.5 2 ϕ 4.5	50	tension crack at midspan of supporting beam	103.5	crushing and vertical tensile splitting of bricks above support
4B	536	0.92	76 x 36 mm 2 ϕ 4.5 2 ϕ 4.5	30	tension crack at midspan of supporting beam	104	vertical tensile splitting of bricks above support
5a	444	0.76	76 x 76 mm 2 ϕ 4.5 3 ϕ 4.5	50	tension crack in supporting beam at midspan	150	crushing and vertical tensile splitting of bricks above support and shear of the supporting beam
5b	444	0.76	76 x 76 mm 2 ϕ 4.5 3 ϕ 4.5	30	tension crack in supporting beam at midspan	181	crushing and vertical tensile splitting of bricks above support
5c	444	0.76	76 x 76 mm 2 ϕ 4.5 3 ϕ 4.5	50	tension crack in supporting beam at midspan	139	crushing of corner bricks above support
W1	381	0.50	76 x 38 mm 2 ϕ 6 2 ϕ 6	50	shear crack in supporting beam	100	crushing of corner bricks above support
10a	560	1.0	76 x 38 mm 2 ϕ 6 2 ϕ 6	80	shear crack in supporting beam	169	vertical shear over the whole height of wall above support

concentration in the wall as summarized in Table 3.9, and the intensity of loading on the supporting beam. Compared to solid panels, walls with either a central door or a window opening showed similar vertical stress distributions along the wall/beam interface, however, a small increase in the maximum vertical stress over the supports occurred in the latter.

The relationship between the applied load and the stress in the steel reinforcement of the supporting beam is shown in Figures 3.30-3.33. Table 3.10 summarizes the results of the axial force in the supporting beam calculated on the assumption that concrete being effective in tension before cracking and that an average stress was assumed to occur over the beam cross-section. The ratio (T/W) varies from 0.07 in the case of a central window opening to 0.255 in the case of a door opening near the support.

The load-deflection characteristics are given in Figures 3.34 to 3.38 and a comparative plot is given in Figure 3.39. The results indicate insignificant effect on the beam central deflection due to the central openings, however, a noticeable increase in the deflection is seen in the case of an offset door opening.

In Table 3.11, a summary is given of loads at the appearance of first crack, the ultimate loads and the modes of failure. It may be seen that the ultimate loads of walls with central openings are in the same order of magnitude and that

From Table 3.12 it can be seen that the central window opening did not have a marked effect on the wall strength. However, it is likely that the increase in the ultimate strength of walls 6 over that of the solid panels of series 5, may be due to any weakness in the solid panels (5a, 5c) resulting from defects of workmanship or variation in the strength of bricks or brickwork. The variation in the strength of brickwork may be due to insufficient filling of the mortar joints or varying joint thickness which gave rise to more flexural stresses in the bricks and hence the decrease in the ultimate strength. Similar comparison between wall BIII, which also contained a central window opening, and wall 10a indicates similarity in the behaviour of both walls.

It has now become evident that the location of a central window opening in the panel will have insignificant effect on the behaviour of a vertically loaded wall or on its ultimate strength. This is most likely attributable to the fact that with the opening being in such a position, the arching action could still take place in the panel through the lintel or any brickwork above the opening as illustrated in Figure 3.40, and therefore the wall behaved similarly to that without an opening.

they are comparable with those of solid panels, however, a reduction of more than 50 per cent in the ultimate load is indicated when a door opening occurred near to a support. Comparison of these loads with those predicted by the approximate method is given in Table 3.12.

3.9.2 Discussion of Results

The solid panels of series 5 described in Section A will be considered for correlation with those containing openings. Compared to walls of series 5, walls 6a and 6b, which contained a central window opening, showed a similar performance in the elastic stage and very near to the ultimate load. The vertical strain distribution in the bottom course of bricks, as shown in Figures 3.6 and 3.24, are very similar. It will also be noted from Tables 3.5 and 3.9 that the maximum vertical stress over the beam ends are nearly the same. Furthermore, with reference to Figure 3.39, it is clearly seen that the influence of the central window opening on the deflection characteristics of walls 6, is almost negligible. It is also to be noted that the first cracks occurred in walls 5 and 6 were observed at a load of 50 KN, and that the load-reinforcement characteristics follow the same pattern. Figures 3.13 and 3.30. Moreover, the walls behaved in a similar fashion near to failure and that their failure mechanisms involved the same cracking pattern followed by crushing of the corner bricks over the supports, Plate 5.

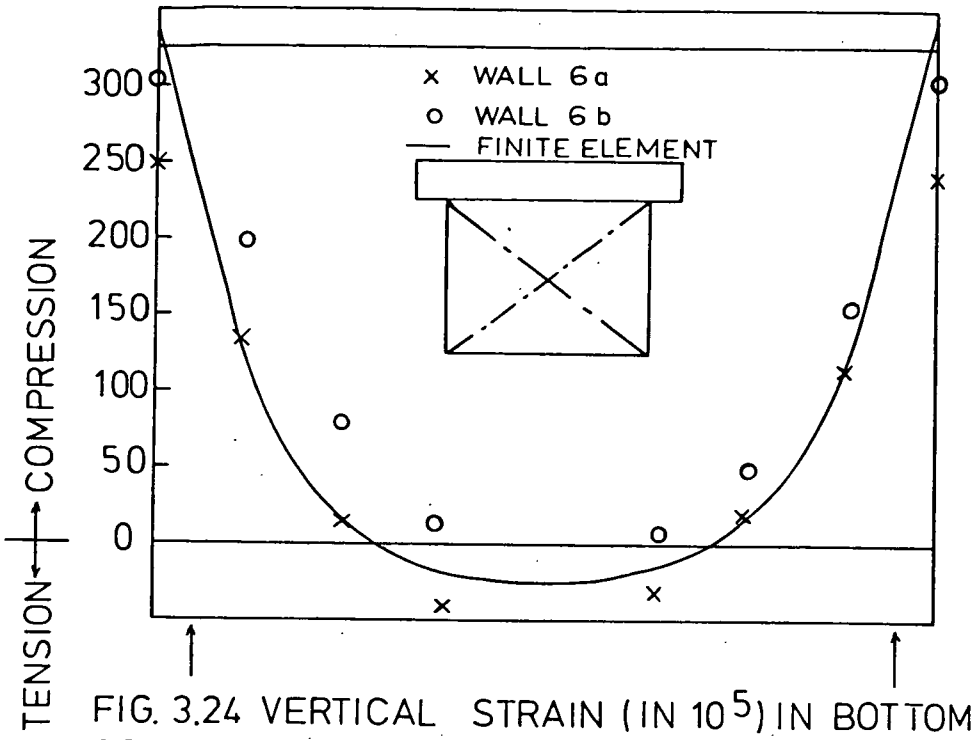

FIG. 3.24 VERTICAL STRAIN (IN 10^5) IN BOTTOM COURSE OF BRICKWORK IN WALLS 6 a, b AT W = 80 KN

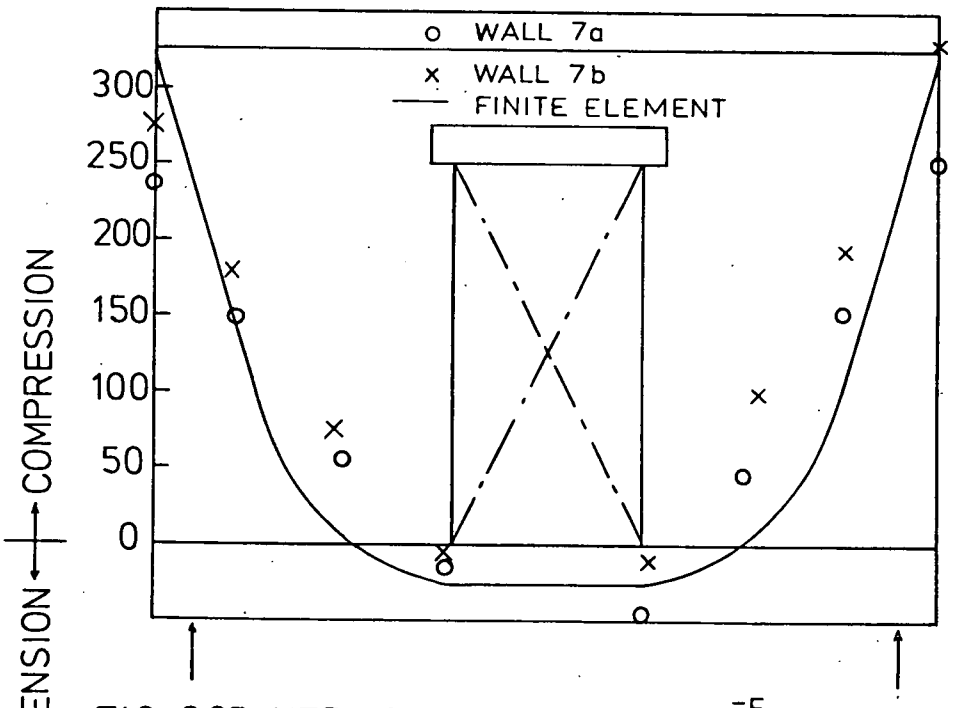

FIG. 3.25 VERTICAL STRAIN (IN 10^{-5}) IN BOTTOM COURSE OF BRICKWORK IN WALLS 7 a, b AT W = 70 KN

TABLE 3.9 COMPARISON OF VERTICAL STRESS CONCENTRATION

WALL NO	APPLIED STRESS f_p N/mm^2	MAXIMUM VERTICAL STRESS f_m N/mm^2			f_a/f_p	f_m/f_p		
		LEFT SUPPORT	RIGHT SUPPORT	AVERAGE f_a		EXPERIMENTAL	FINITE ELEMENT	APPROXIMATE
	2.60	9.77	7.29	8.53	3.27	3.76		
6a	4.33	16.80	15.37	16.08	3.71	3.88	5.10	6.49
	3.03	13.41	12.89	13.15	4.34	4.43		
6b	3.46	16.01	16.01	16.01	4.63	4.63	5.10	6.49
	2.60	11.98	15.75	13.87	5.33	6.06		
7a	3.03	14.58	17.58	16.08	5.52	5.80	5.55	6.41
	4.76	28.38	30.33	29.36	6.17	6.37		
7b	5.19	34.76	35.54	35.15	6.77	6.85	5.55	6.41
	2.16	8.33	23.24	-	-	10.76		
8a	2.60	11.33	33.62	-	-	12.92	9.80	10.37
	2.16	7.04	19.00	-	-	8.80		
8b	2.60	9.38	26.18	-	-	10.07	9.80	10.37
	4.33	23.18	29.56	26.37	6.09	6.83		
9a	4.76	26.56	36.59	31.57	6.63	7.69	6.30	6.63
	3.90	30.60	27.47	29.04	7.45	7.85		
9b	4.33	36.72	32.55	34.64	8.00	8.48	6.30	6.63
	2.46	10.68	17.81	14.24	5.79	7.24		
10c	4.10	19.14	29.95	24.55	5.99	7.30	7.00	6.93

TABLE 3.10 COMPARISON OF BEAM AXIAL FORCE

TEST NO	APPLIED LOAD KN	MAXIMUM AXIAL FORCE (T/W)		
		EXPERIMENTAL	FINITE ELEMENT	APPROXIMATE
6a	20	0.147	0.229	0.184
6a	50	0.139	0.229	0.184
6b	40	0.159	0.229	0.184
6b	50	0.138	0.229	0.184
7a	33	0.141	0.170	0.208
7b	65	0.185	0.170	0.208
8a	20	0.227	0.314	0.302
8b	20	0.255	0.314	0.302
9a	50	0.070	0.073	0.128
9a	60	0.082	0.073	0.128
9b	40	0.118	0.073	0.128
9b	50	0.159	0.073	0.128

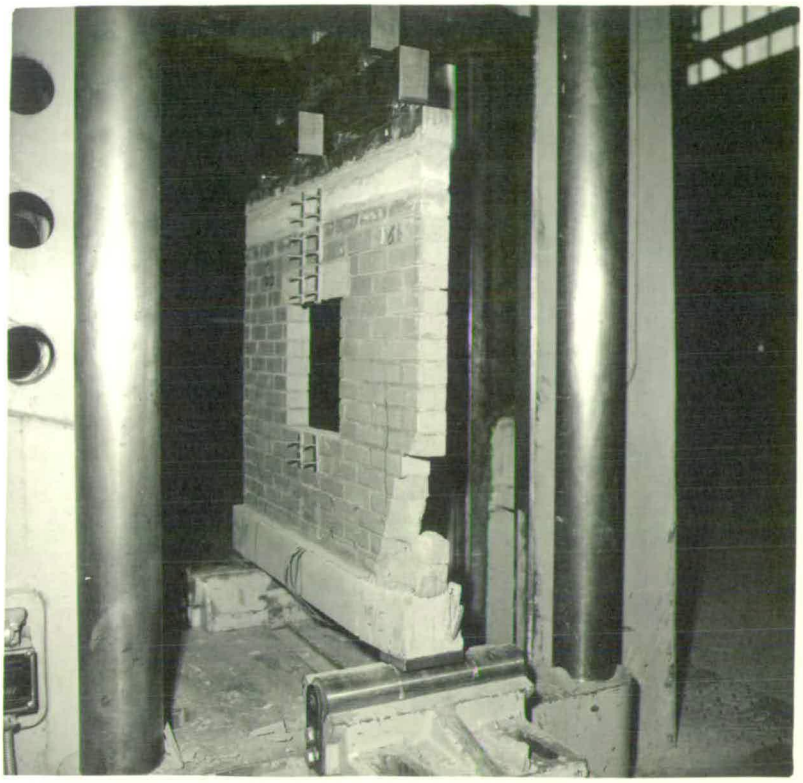

PLATE 5.1 WALL 6b AT FAILURE

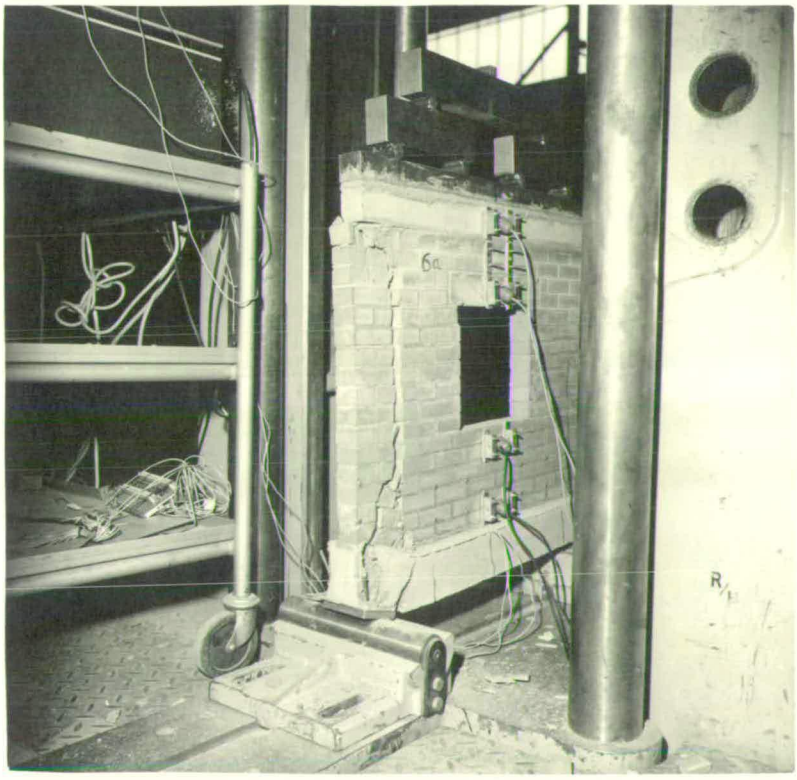

PLATE 5.2 WALL 6a AT FAILURE

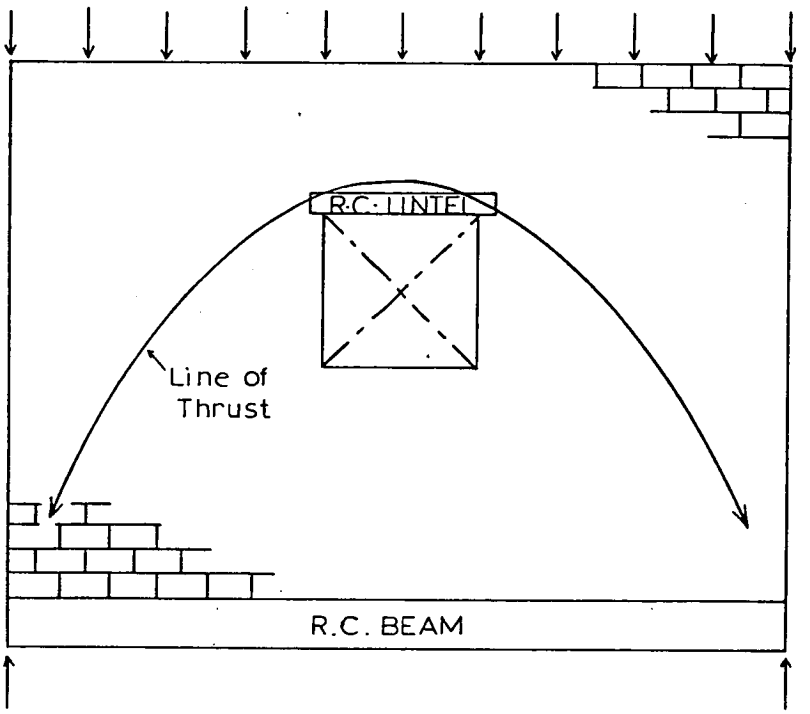

FIG. 3.40 Arching Action in Wall With Central Window Opening.

3.9.3 Effect of Large Opening Width

In walls 9a and 9b, the window opening was of a comparatively larger width and was located immediately below the upper tie. In this case, the upper tie completed the arch and thus due to the large width of opening, the arching effect spread outwards towards the edges of the wall as shown in Figure 3.41. As a consequence, a higher vertical stress concentration was induced in the wall over the supports and a relatively smaller axial force in the beam as indicated by Tables 3.9 and 3.10 respectively.

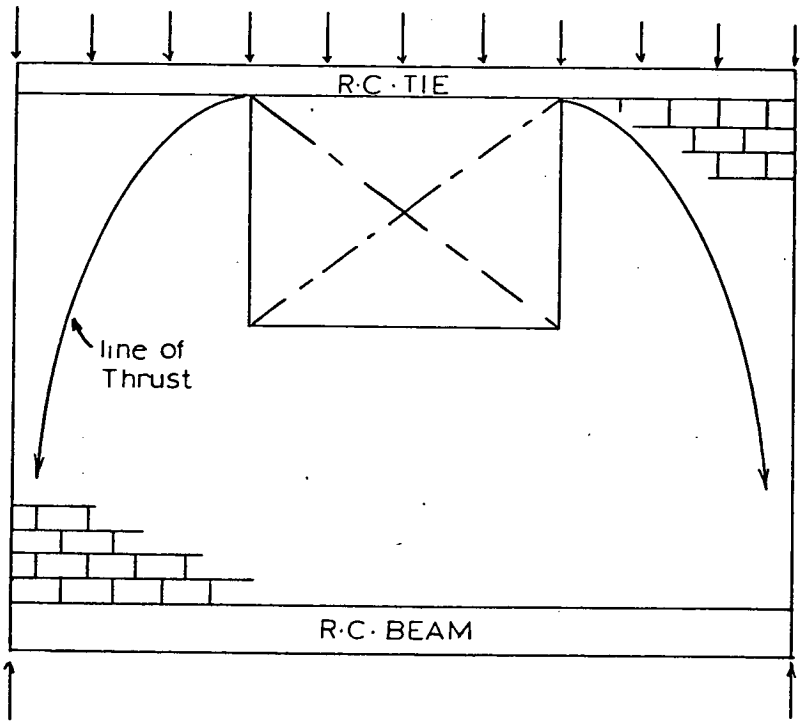

FIG. 3.41. ARCHING ACTION IN WALLS (9 a,b).

The first crack was observed as two symmetrical shear cracks in the supporting beam very near to the supports and at about 75 per cent of the ultimate load. Eventually, these were followed by crushing of the corner bricks over the supports and the appearance of horizontal separation cracks in the central region of the interface joints. Plate 6.1. The separation cracks may be caused by unequal bending of the wall and beam at the later stages of loading. Their appearance at midspan confirms that they were a result of vertical tension and not shear.

Compared to the solid panels of series 5, it is likely that the reduction in the ultimate strength of walls 9 was due to the increase in the vertical stress concentration in the panels over

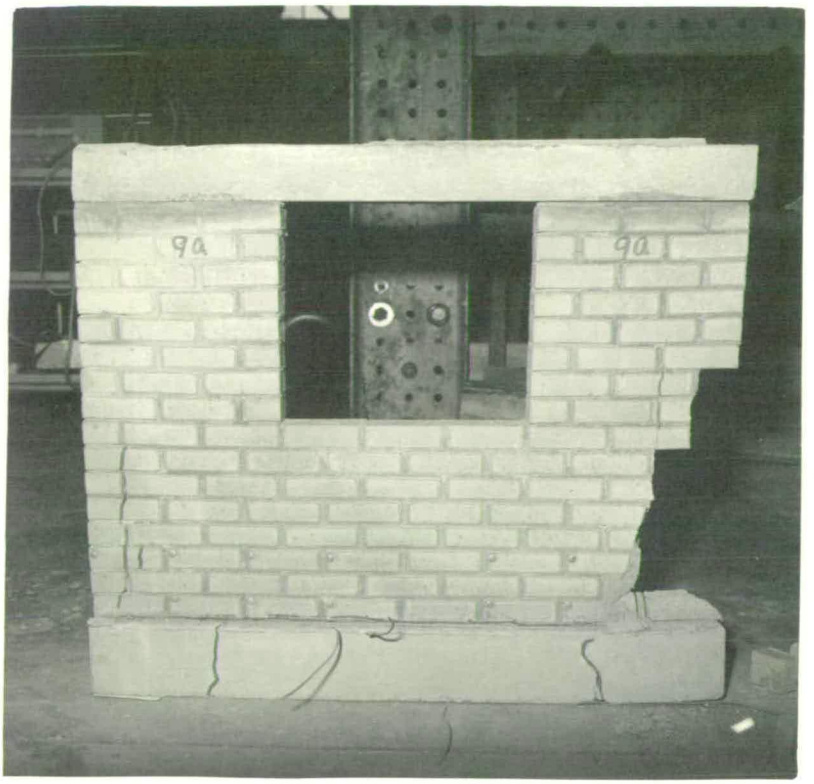

PLATE 6.1 WALL 9a AFTER FAILURE

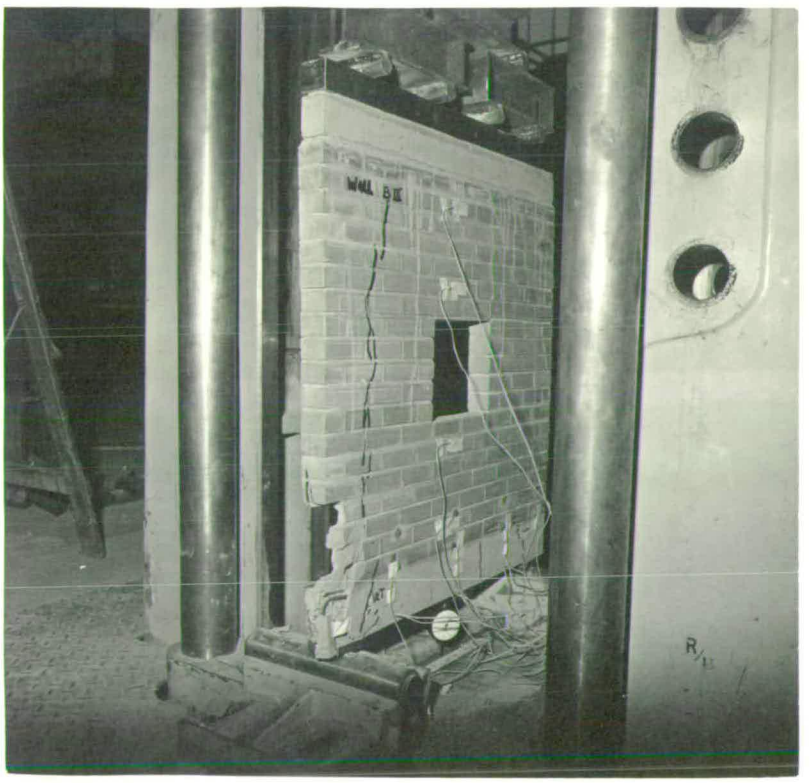

PLATE 6.2 WALL BIII AT FAILURE

the supports and to the crack pattern in the wall produced as a result of the relatively larger width of opening.

With reference to Figure 3.39, it can be seen that the larger width of opening had no appreciable effect on the load-deflection characteristics of the composite beam.

3.9.4 Effect of a Central Door Opening

In walls 7a, 7b and 10c, a doorway was located at midspan. Table 3.9 indicates an increase in the maximum vertical stress over that recorded in the solid walls of series 5.

Table 3.10 shows that the steel stresses and consequently the axial force in the supporting beam are slightly higher than those obtained in beams supporting solid panels. This is presumably because the depth of the composite beam at midspan was considerably smaller, which resulted in high bending stresses. For the same reason, the central deflection was found to be higher compared to that recorded for the beams of series 5, Figure 3.39.

The first crack was observed as a tension crack in the supporting beam immediately below the edge of opening at about 70-80 per cent of the ultimate load. At about the same load the crack pattern appeared in the wall as diagonal tension cracks extending between the lintel and the support points at both sides of the doorway. Upon further increase of load, the diagonal cracks widened and eventually lead to the wall failure by diagonal splitting and crushing of the corner bricks

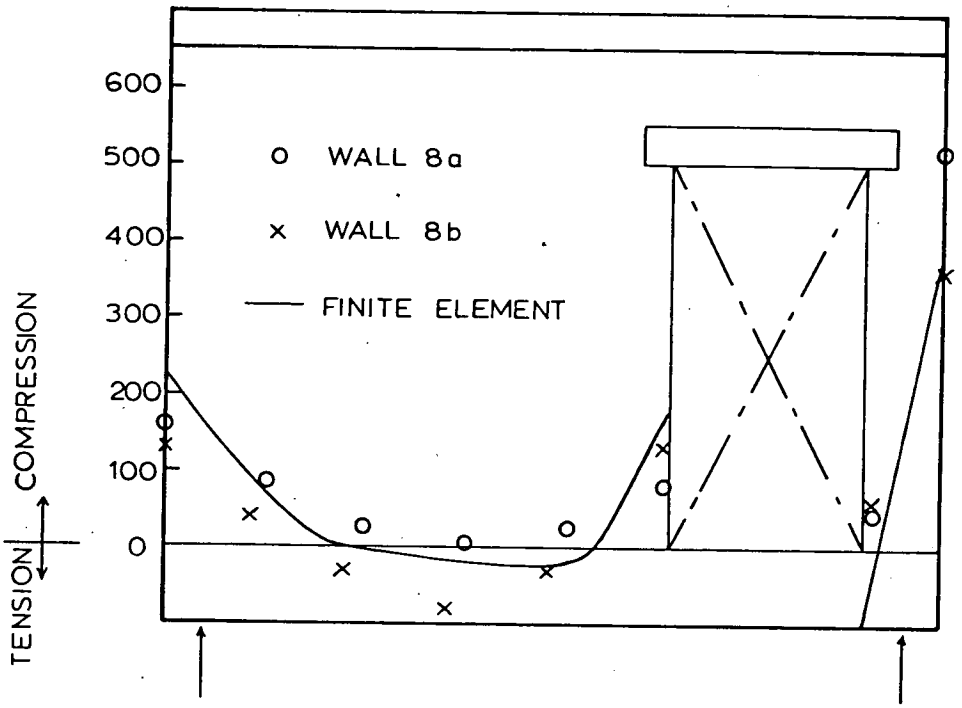

FIG. 3.26 VERTICAL STRAIN (IN 10^{-5}) IN BOTTOM COURSE OF BRICKWORK IN WALLS 8a,b AT W = 50 KN.

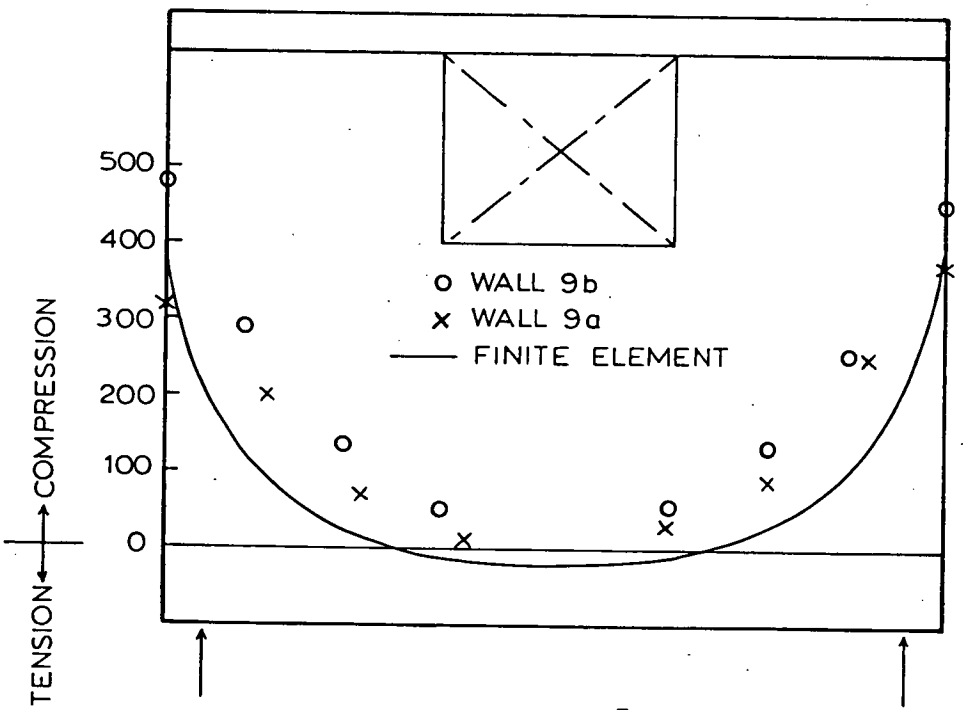

FIG. 3.27 VERTICAL STRAIN (IN 10^{-5}) IN BOTTOM COURSE OF BRICKWORK IN WALLS 9a,b. AT W = 80 KN.

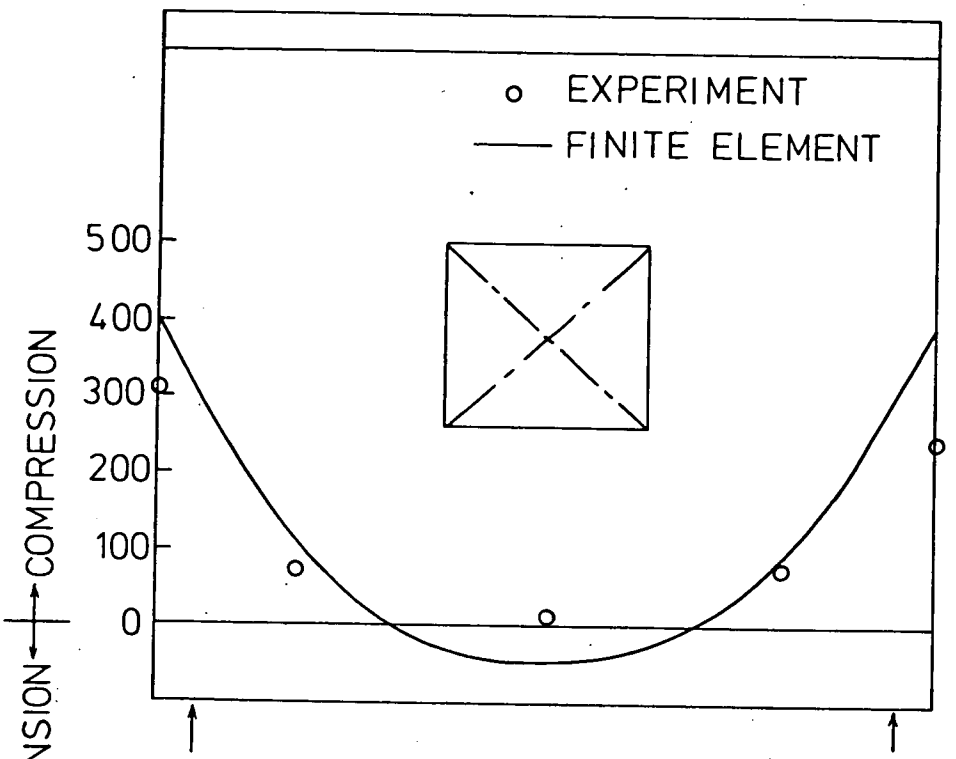

FIG. 3.28 VERTICAL STRAIN (IN 10^{-5}) IN BOTTOM COARSE OF BRICKWORK IN WALL BIII AT W = 100 KN.

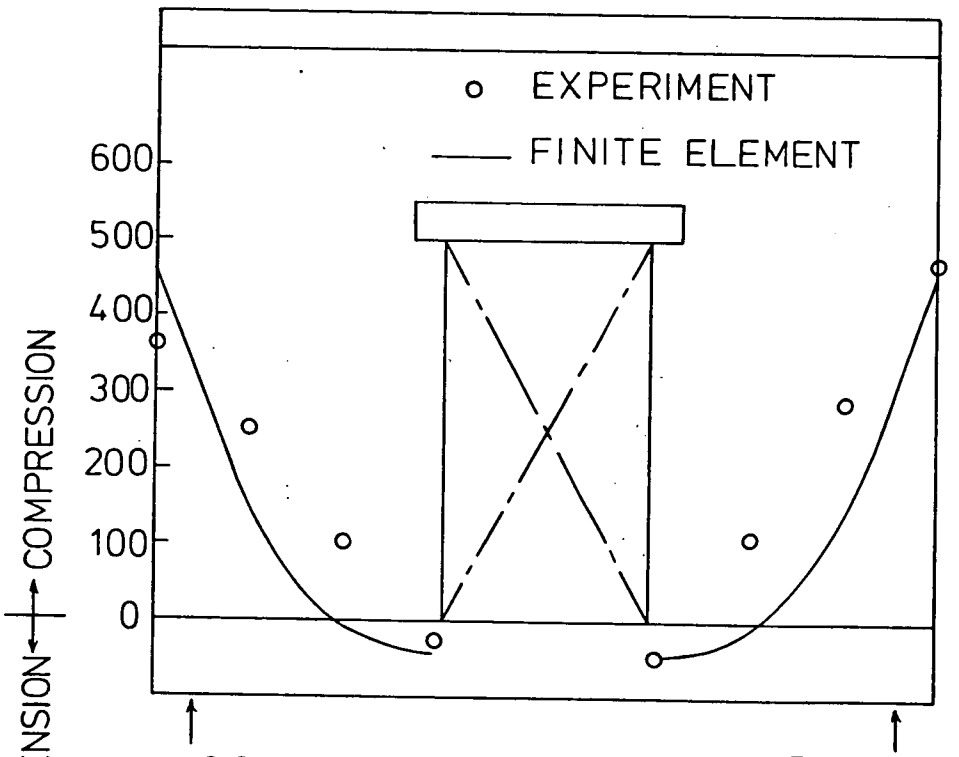

FIG. 3.29 VERTICAL STRAIN (IN 10^{-5}) IN BOTTOM COARSE OF BRICKWORK IN WALL 10C AT W = 100 KN.

over the supports. Plates 7 and 8.

The failure mode of these walls can reasonably be approximated to that of a square plate loaded along its diagonal. It is therefore possible to a great degree of approximation to predict the cracking as well as the ultimate load of walls with a central door opening using the formula proposed by Sen et al[33]. In this the splitting stress for a diagonally loaded square plate is given by :

$$\sigma = 0.3668 \frac{P}{S\,b}$$

in which σ is the splitting stress, P is the applied load, 2b is the diagonal length and S is the thickness.

In the case of walls 7a and 7b, the force P is the reaction resolved in the direction of the diagonal. If cracking is assumed to have occurred in the wall at 50 per cent of the ultimate load, it then follows from Figure 3.41 that P = 42.78 KN, b = 200 mm and S = 36 mm.

$$\text{Therefore, } \sigma = \frac{0.3668 \times 42.78}{36 \times 200}$$

$$= 2.18 \text{ N/mm}^2$$

This stress may be compared to 1.85 N/mm^2, the brick tensile strength, Table 3.1. It is apparent that an estimation of the failure load due to compression of the

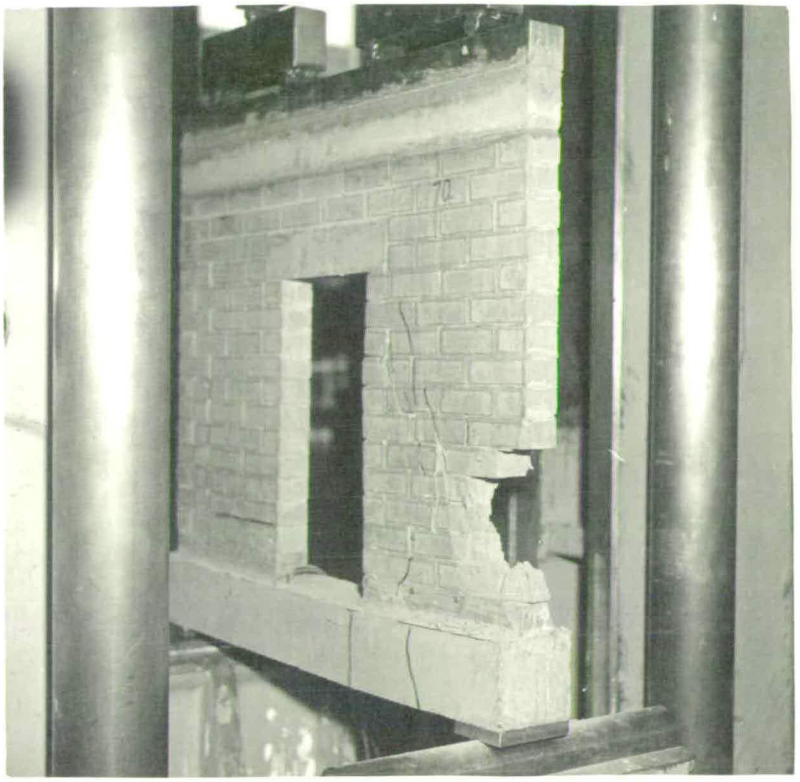

PLATE 7.1 WALL 7a AT FAILURE

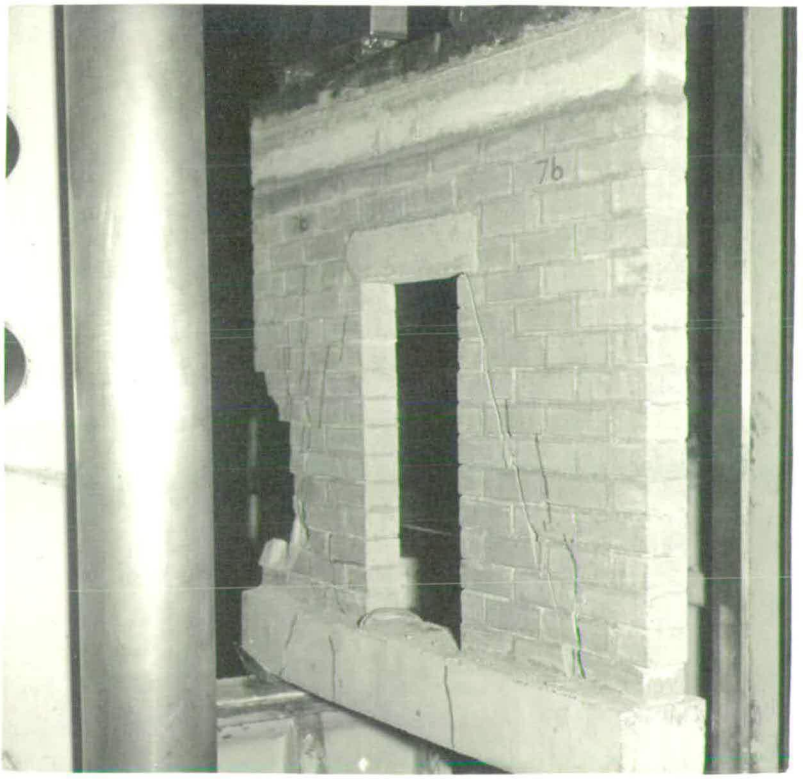

PLATE 7.2 CRACK PATTERN IN WALL 7b AT ULTIMATE LOAD

PLATE 8.1 WALL 10c AFTER FAILURE

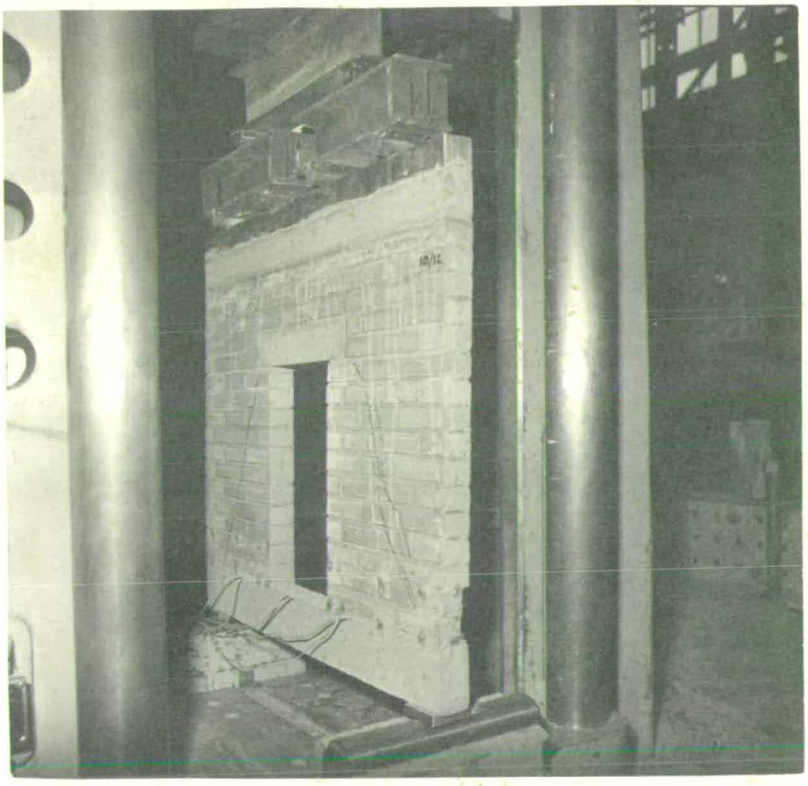

PLATE 8.2 CRACK PATTERN IN WALL 10c

brick panel may be obtained using the above formula, if the tensile strength of bricks is known.

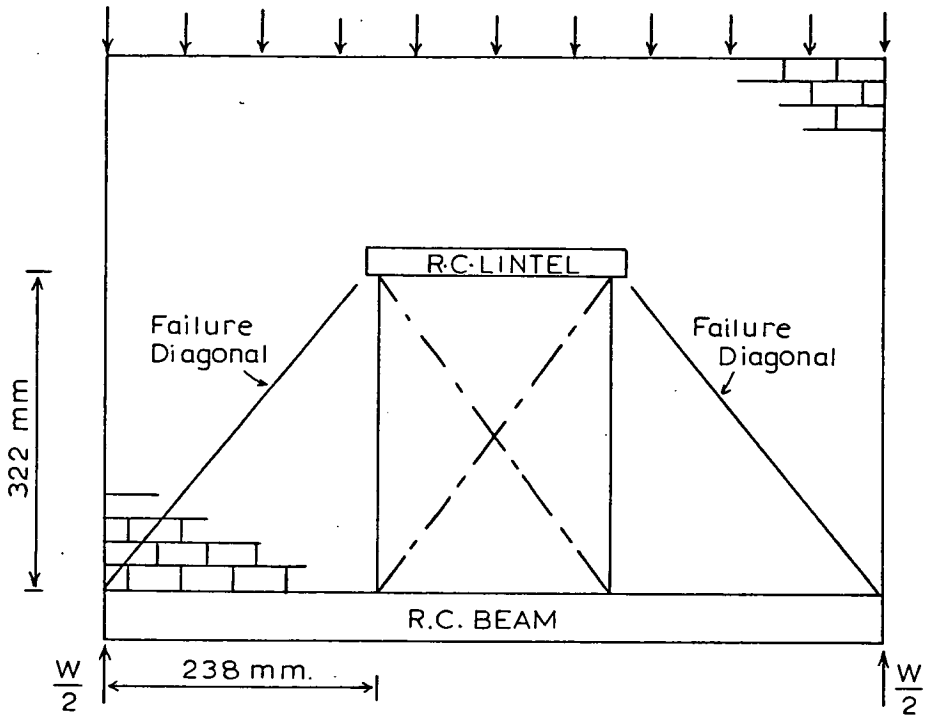

FIG. 3.41 FAILURE DIAGONAL IN WALLS (7a,b)

3.9.5 Effect of an Offset Door Opening

A doorway located in walls 8a and 8b at quarter span from the supports resulted in very significant changes in the stress distribution in the wall and beam and considerably influenced the interaction between them. This is clearly evident from the vertical strain distribution along the bottom course of bricks as shown in Figure 3.26. This indicates a remarkable increase in the maximum vertical stress over the supports. It will be also noted that the vertical stress concentration developed to the left-hand side of the opening indicates the formation of a

secondary arching system in the part of the panel to the left of opening as shown in Figure 3.42. The remaining portion of the load was transmitted down the pier of bricks to the right-hand support. Although the magnitude of this load was not measured experimentally, however, it has been calculated from the vertical stress diagram to be approximately half of the applied load.

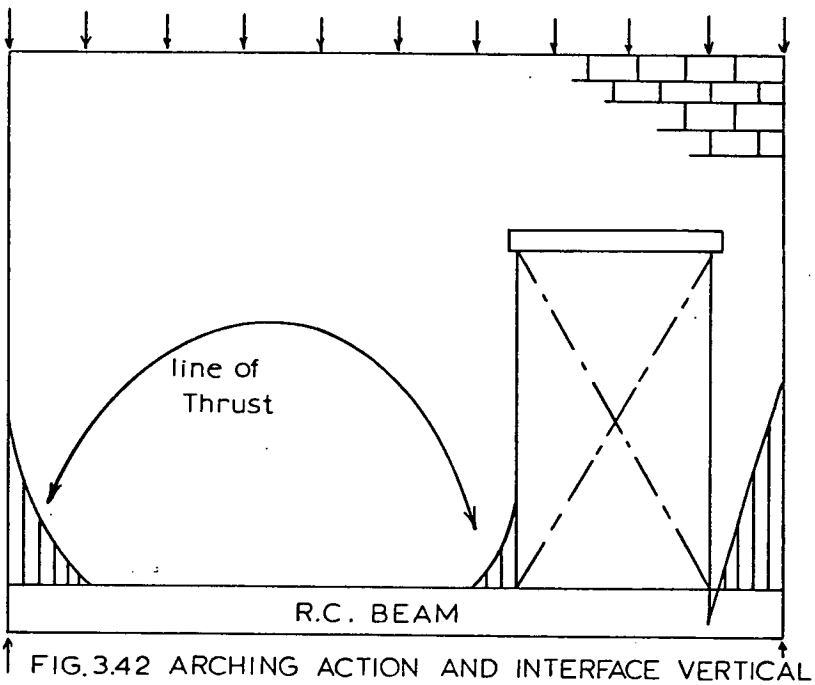

FIG. 3.42 ARCHING ACTION AND INTERFACE VERTICAL STRESS DISTRIBUTION IN WALLS (8a,b).

Figure 3.32 shows that the stress in the steel reinforcement of the supporting beam recorded in this case is the highest compared to all other cases. This may be attributable to the fact that the point-load effect produced part-way along the span gave rise to the high bending stresses. As a consequence also, the axial force in the beam was substantially increased as shown in Table 3.11. The influence on the

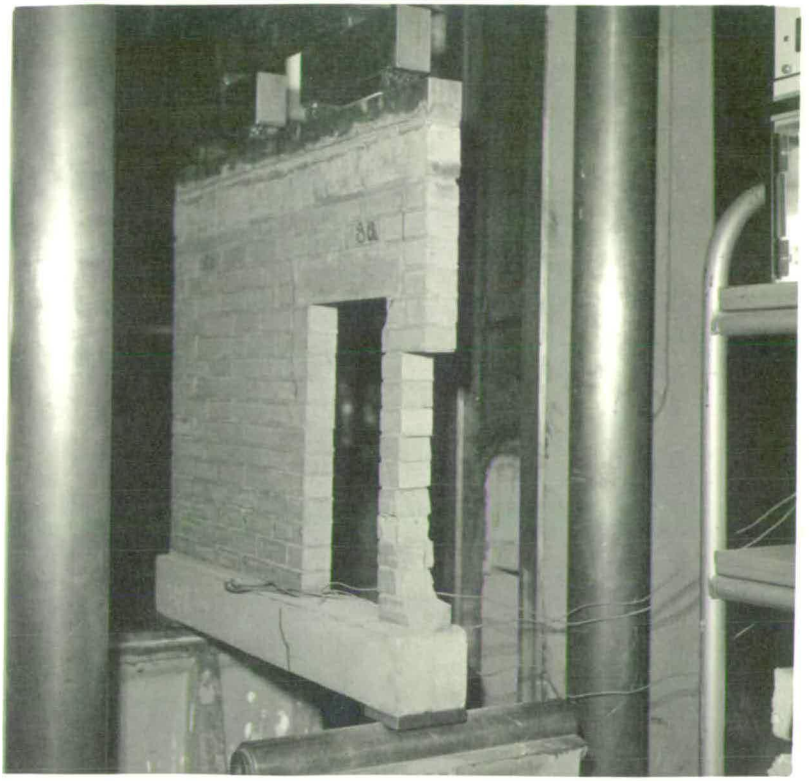

PLATE 9.1 WALL 8a AT FAILURE

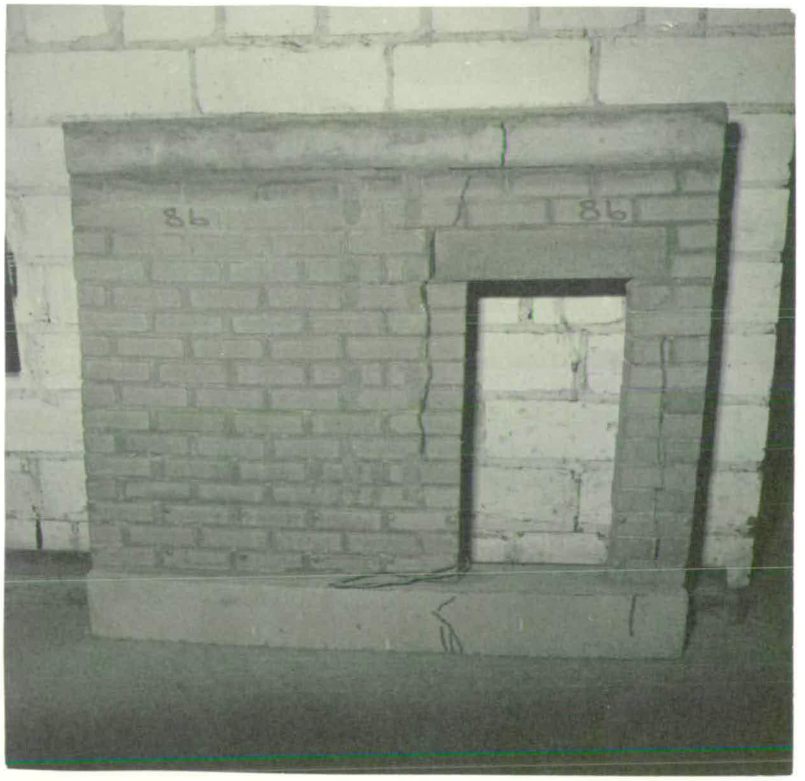

PLATE 9.2 CRACK PATTERN IN WALL 8b AFTER FAILURE

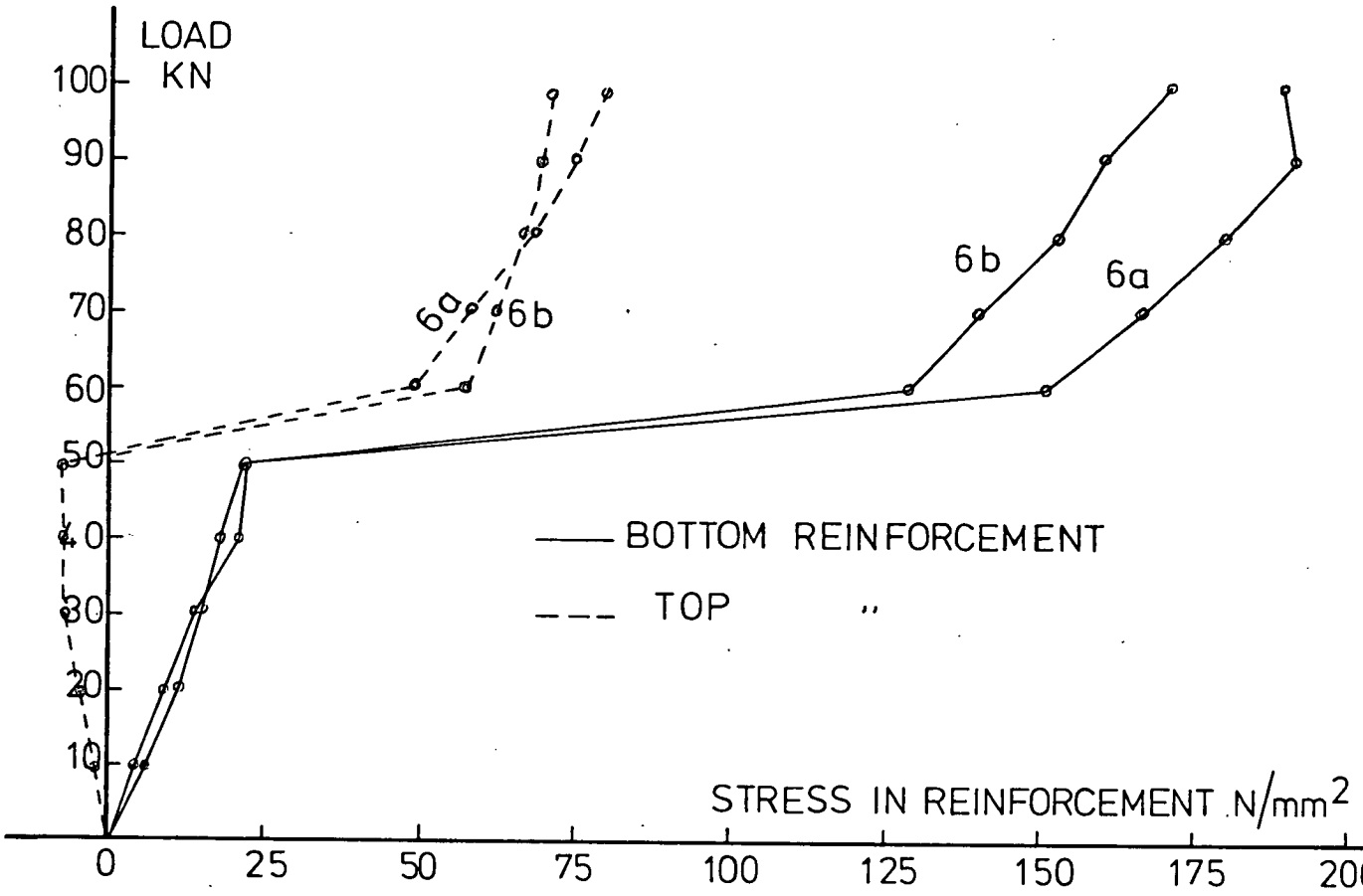

FIG. 3.30 RELATIONSHIP BETWEEN LOAD AND STRESS IN REINFORCEMENT IN BEAMS OF TESTS 6a AND 6b.

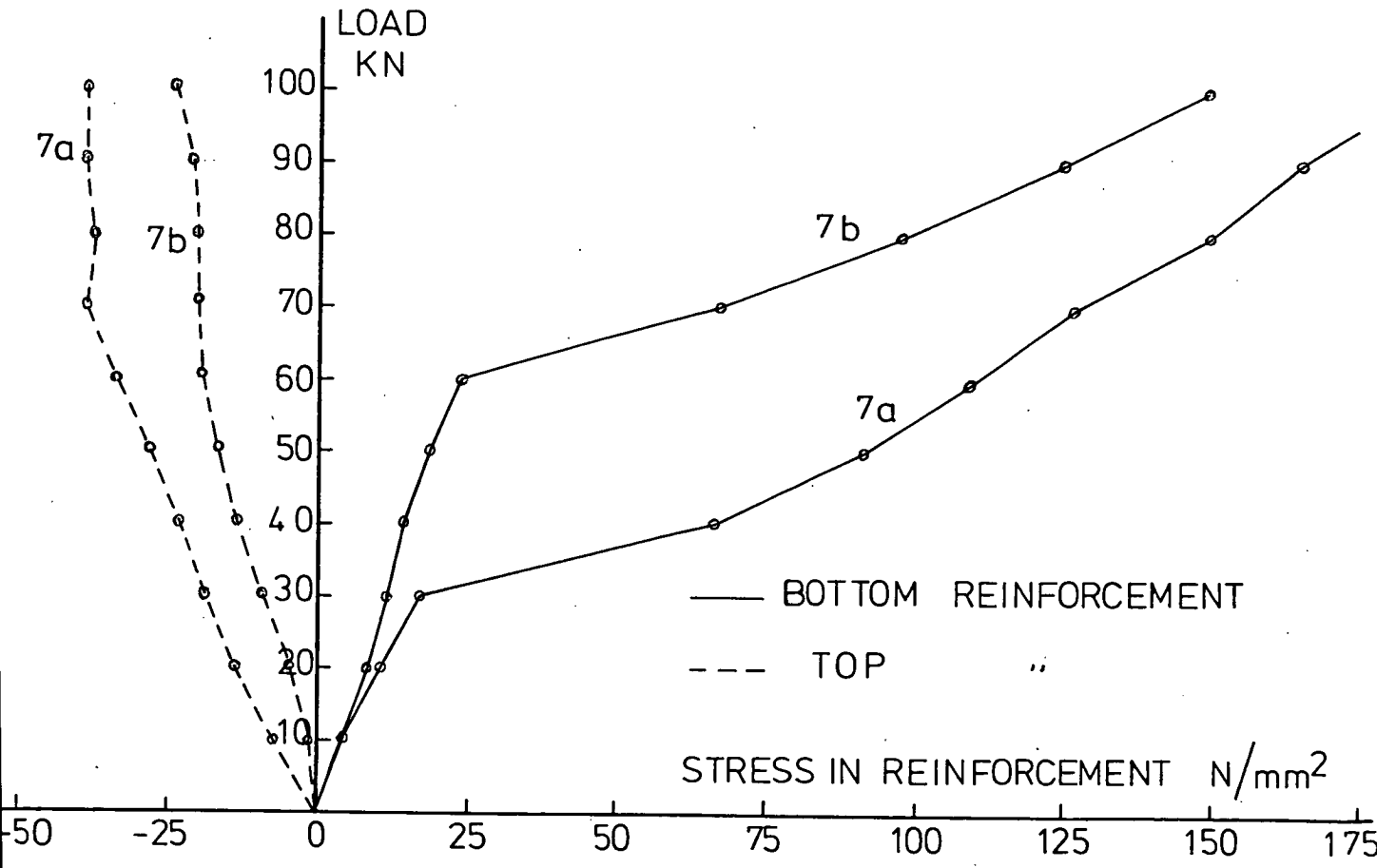

FIG. 3.31 RELATIONSHIP BETWEEN LOAD AND STRESS IN REINFORCEMENT IN BEAMS OF TESTS 7a AND 7b.

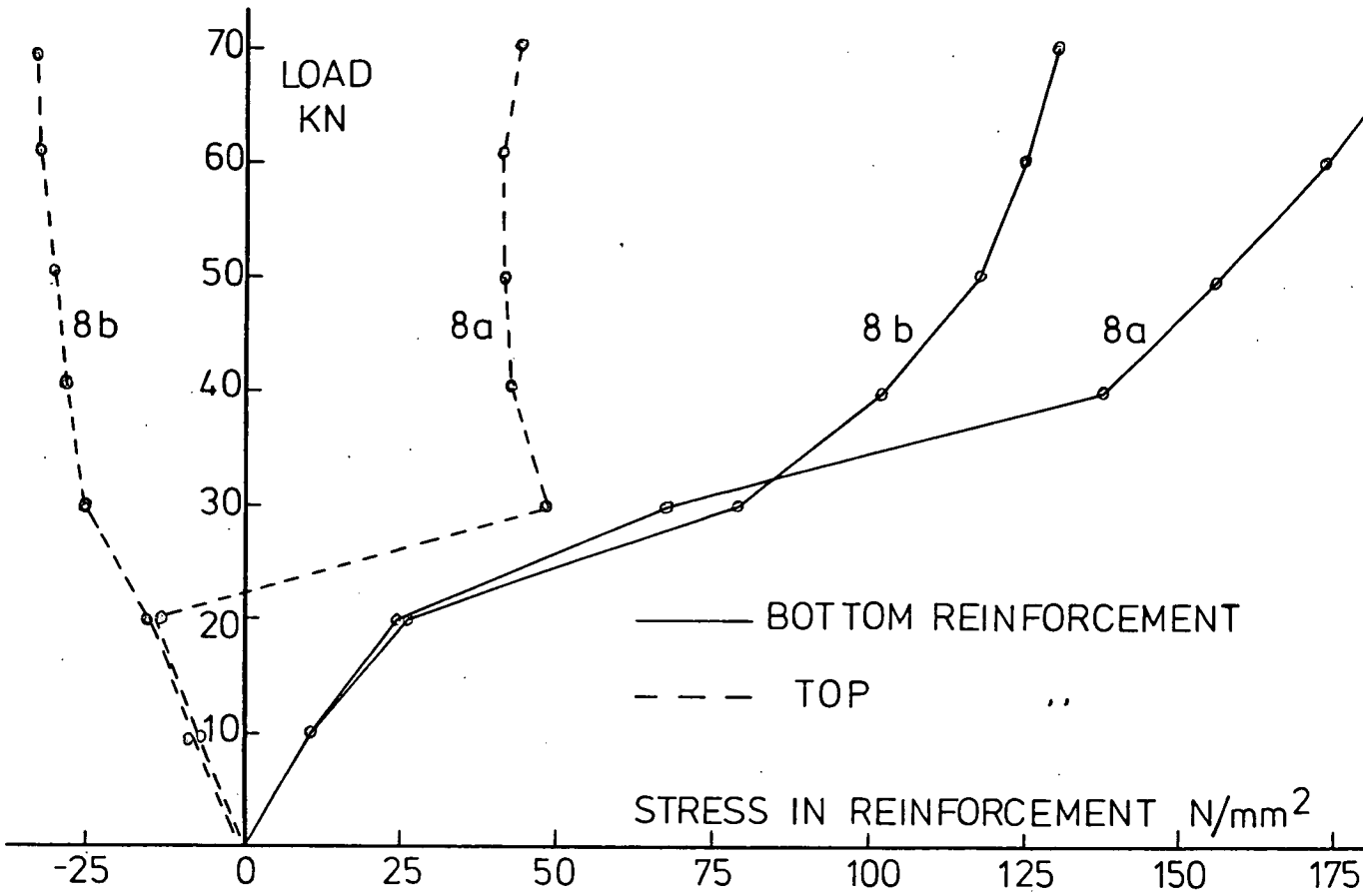

FIG. 3.32 RELATIONSHIP BETWEEN LOAD AND STRESS IN REINFORCEMENT IN BEAMS OF TESTS 8a AND 8b.

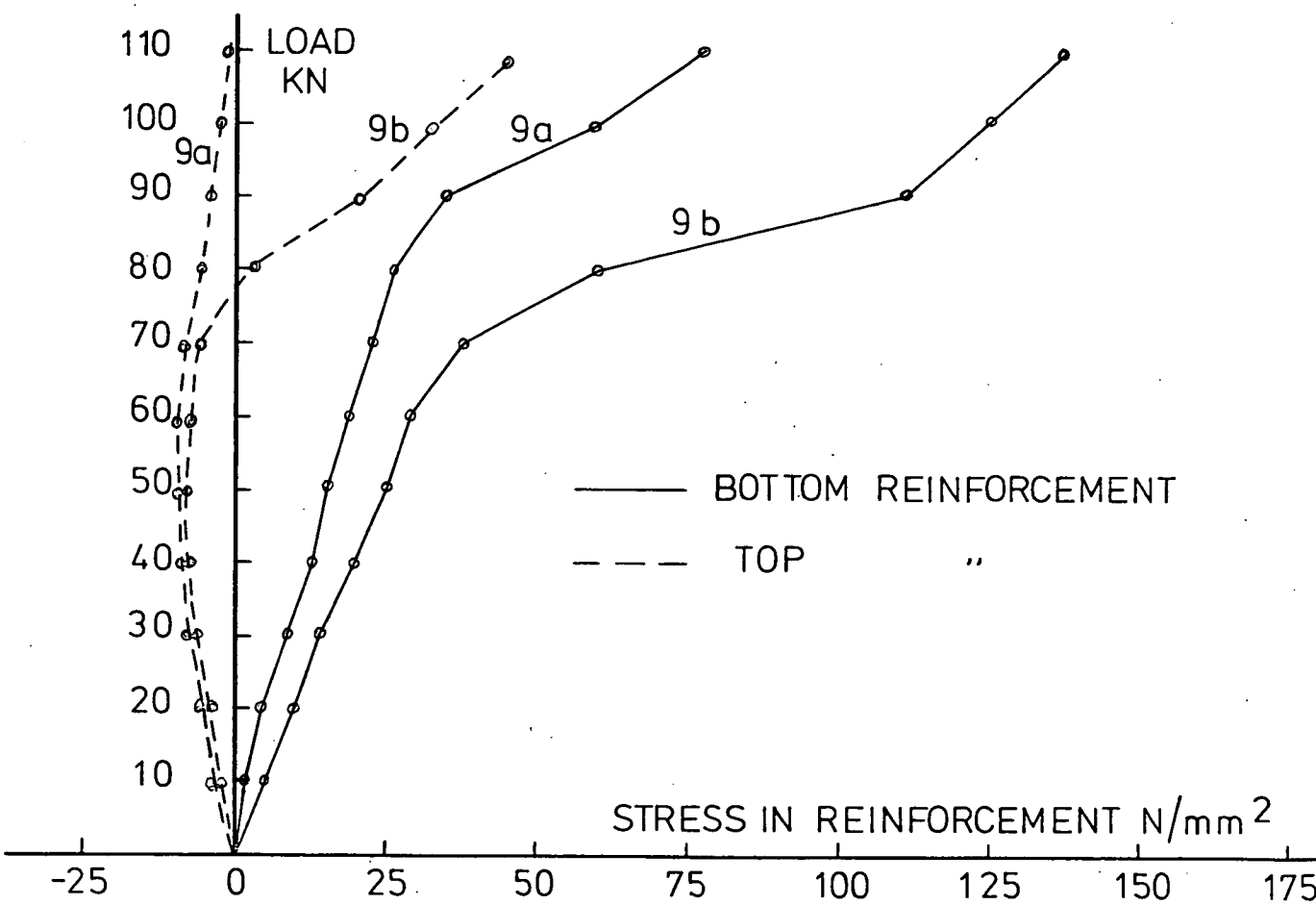

FIG. 3.33 RELATIONSHIP BETWEEN LOAD AND STRESS IN REINFORCEMENT IN BEAMS OF TESTS 9a AND 9b.

deflection characteristics is quite surprising. As seen from Figure 3.39, the magnitude of the central deflection recorded in walls 8a and 8b is 2.5 times that recorded in the case of solid walls.

Similar observations have been reported by Wood[2]. However, in his test the maximum vertical stress was observed to be at the bottom inner corner of the opening and not over the support.

The first crack was observed as a tension crack in the supporting beam immediately below the inner edge of the doorway at about 50 per cent of the ultimate load. On further increase of load, tensile cracks developed at the top corners of the opening and eventually the wall failed by vertical tensile splitting and crushing of the pier of bricks at a load approximately 50 per cent less than that recorded for solid walls. Plate 7. This substantial reduction in the strength capacity of the composite beam evidently indicates a significant reduction in the degree of the composite action of walls containing an offset door opening.

3.9.6 Comparison of Results

Table 3.9 shows a comparison of the experimental values of the vertical stress concentration in the wall and values predicted by the finite element analysis and the approximate formula. With the exception of walls of series 6, the finite

TABLE 3.11 SUMMARY OF TEST RESULTS

TEST NO	h/L	DIMENSIONS OF OPENING mm	SHAPE AND POSITION OF OPENING	LOAD AT APPEARANCE OF FIRST CRACK KN	SHAPE OF FIRST CRACK	FAILURE LOAD KN	MODE OF FAILURE
6a	0.76	200 x 190	Central Window Opening	50	Vertical tension crack in supporting beam at midspan	182.5	Crushing, vertical tensile splitting and shearing of bricks above support along the wall height. Shearing of the supporting beam.
6b	0.76	200 x 190	Central Window Opening	50	Tension crack at mid-span of supporting beam	174.5	Crushing of corner bricks above support and vertical tensile splitting along the wall height. Diagonal shearing of the supporting beam.
BIII	1.0	159 x 152	Central Window Opening Without Lintel	120	Diagonal shear crack in supporting beam	165	Crushing of corner bricks above support and vertical tensile splitting along the entire wall height. Shearing of the supporting beam.
7a	0.76	322 x 164	Central Door Opening	110	Tension crack in supporting beam between support and edge of opening	136	Crushing of corner bricks above supports and diagonal splitting between top corners of the opening and the supports.
7b	0.76	322 x 164	Central Door Opening	100	Tension crack in supporting beam between edge of opening and support	141.5	Crushing of corner bricks above supports and diagonal splitting between top corners of the opening and the supports.
10c	0.84	323 x 163	Central Door Opening	120	Diagonal tension crack in bricks over support	154	Crushing of corner bricks above supports and diagonal splitting between top corners of the opening and the supports.
8a	0.76	330 x 162	Door Opening at Quarter Span	50	Vertical tension crack in beam below inner edge of opening	75	Crushing and vertical tensile splitting of bricks above support adjacent to opening. Vertical tensile splitting at top corners of opening.
8b	0.76	330 x 162	Door Opening at Quarter Span	40	Vertical tension crack in beam below inner edge of opening	83	Vertical tensile splitting of bricks on both sides of the opening.
9a	0.76	250 x 220	Central Window Opening with Upper Tie as Lintel	100	Two symmetrical diagonal shear cracks in beam near supports	150	Crushing and vertical tensile splitting of corner bricks above supports and separation of wall from beam along common boundary.
9b	0.76	250 x 220	Central Window Opening with Upper Tie as Lintel	110	Two symmetrical diagonal shear cracks in beam near supports	131	Crushing of corner bricks above support and separation of wall from beam along the central region of the interface joint.

element method has underestimated the magnitude of the maximum vertical stress. However, in general, the results are in close agreement with the experimental average stress. The approximate results on the other hand compare favourably with the experimental values. The discrepancy between the theoretical and experimental results is mainly attributable to the assumption that brickwork is homogeneous and elastic material.

Comparison of the axial force at midspan of the supporting beam is given in Table 3.10. This indicates that results predicted by the finite element and the approximate methods are higher than those computed from the reinforcement strain. This may be due to the fact that the axial force has been computed from the average reinforcement strain assumed acting over the whole beam cross-section. This will underestimate the axial force, since the average of the fibre strains should be considered for the calculation of the force in the concrete.

Table 3.12 gives a comparison between the ultimate loads predicted by the approximate formula and the actual loads. Satisfactory agreement is obtained and the results are seen to be differing within the limits of between -18.8 and 13.1 per cent. This is as expected for the reason that the approximate formula is based on elasticity assumptions.

Figures 3.34 to 3.38 show comparative plots of the beam central deflection. It can be seen that the approximate method is in reasonable agreement with the experimental results

FIG. 3.34 LOAD DEFLECTION CURVE OF BEAM SOFFIT AT MIDSPAN.

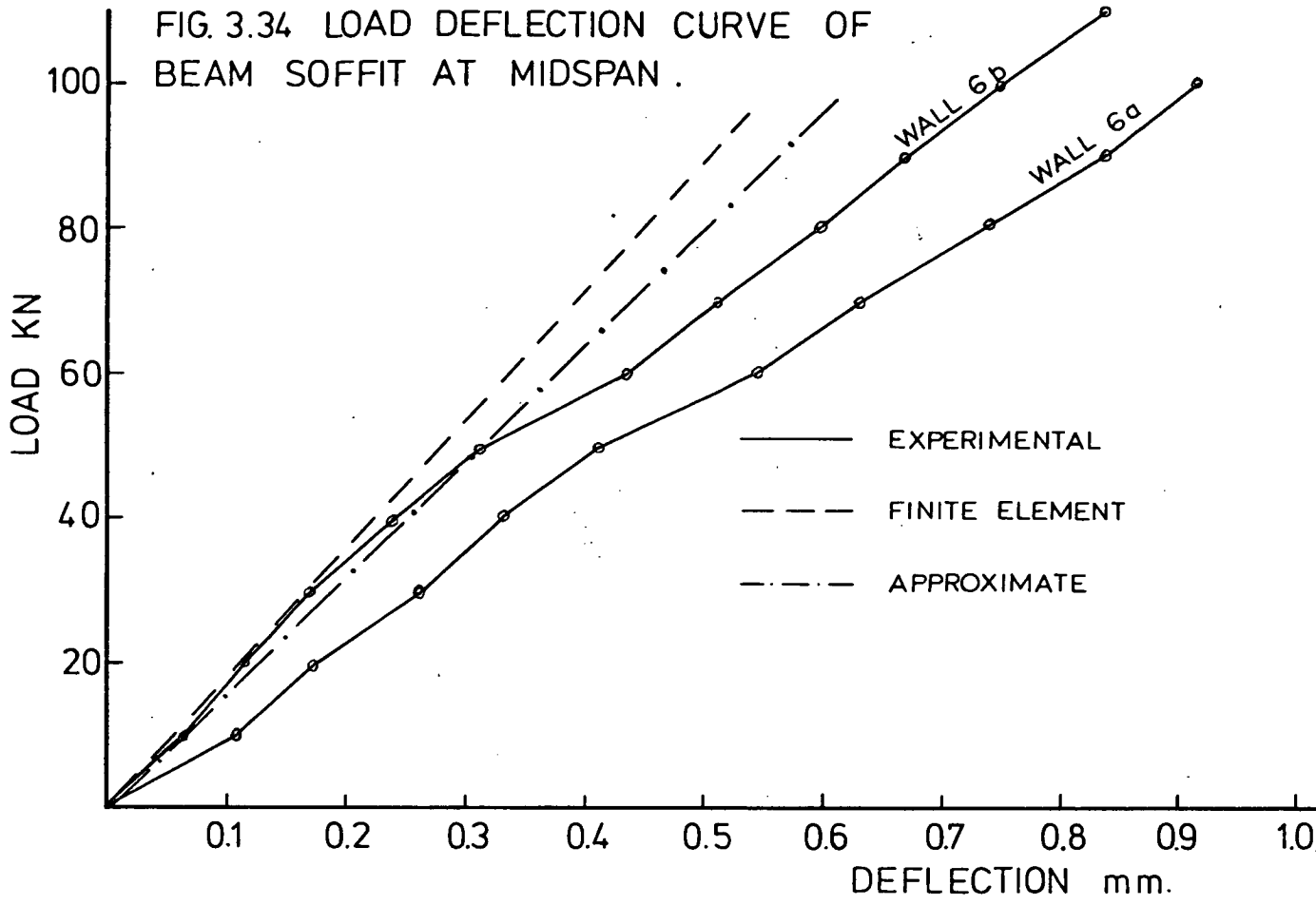

FIG. 3.35 LOAD DEFLECTION CURVE OF BEAM SOFFIT AT MIDSPAN.

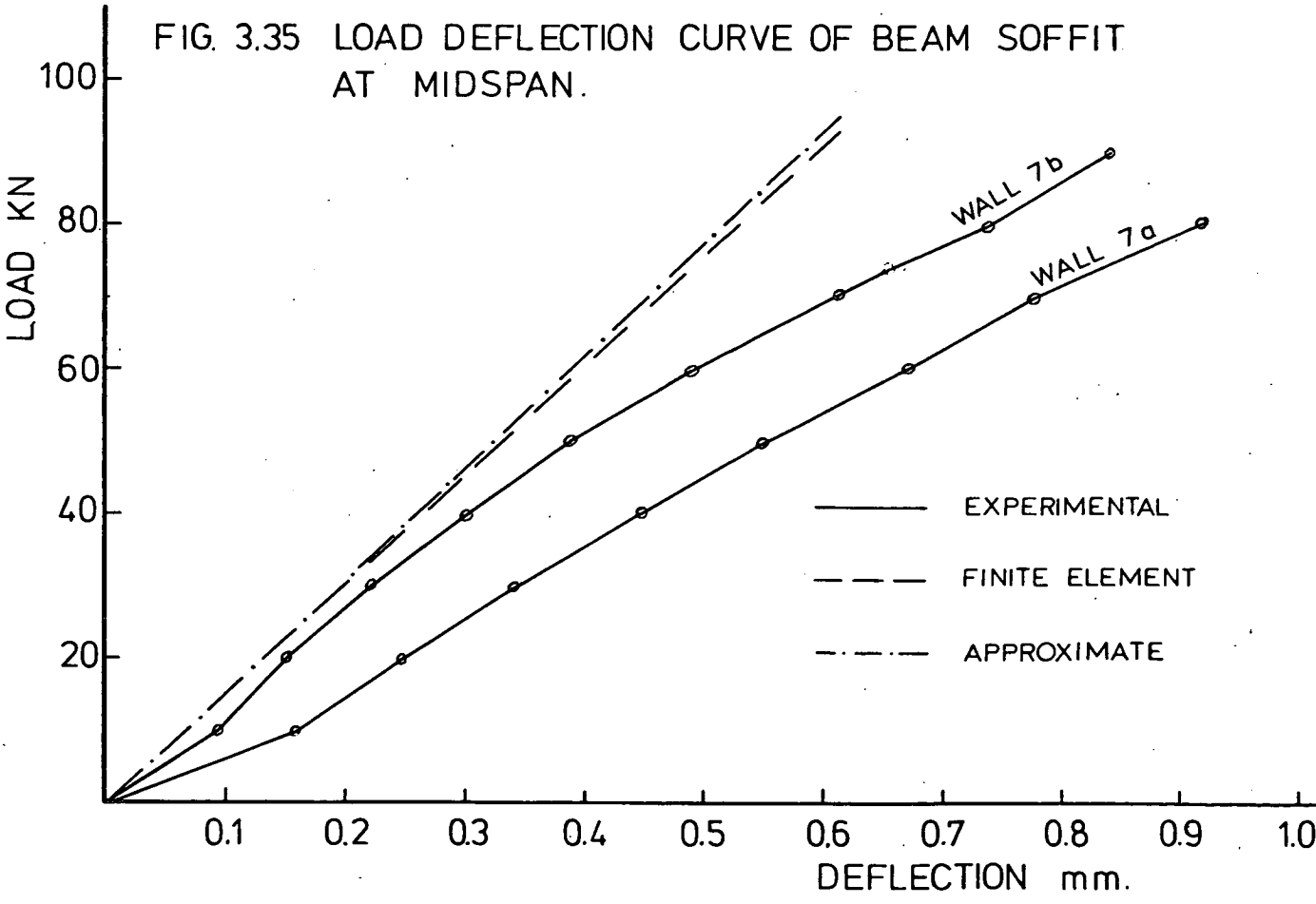

FIG. 3.36 LOAD DEFLECTION OF BEAM SOFFIT AT MIDSPAN.

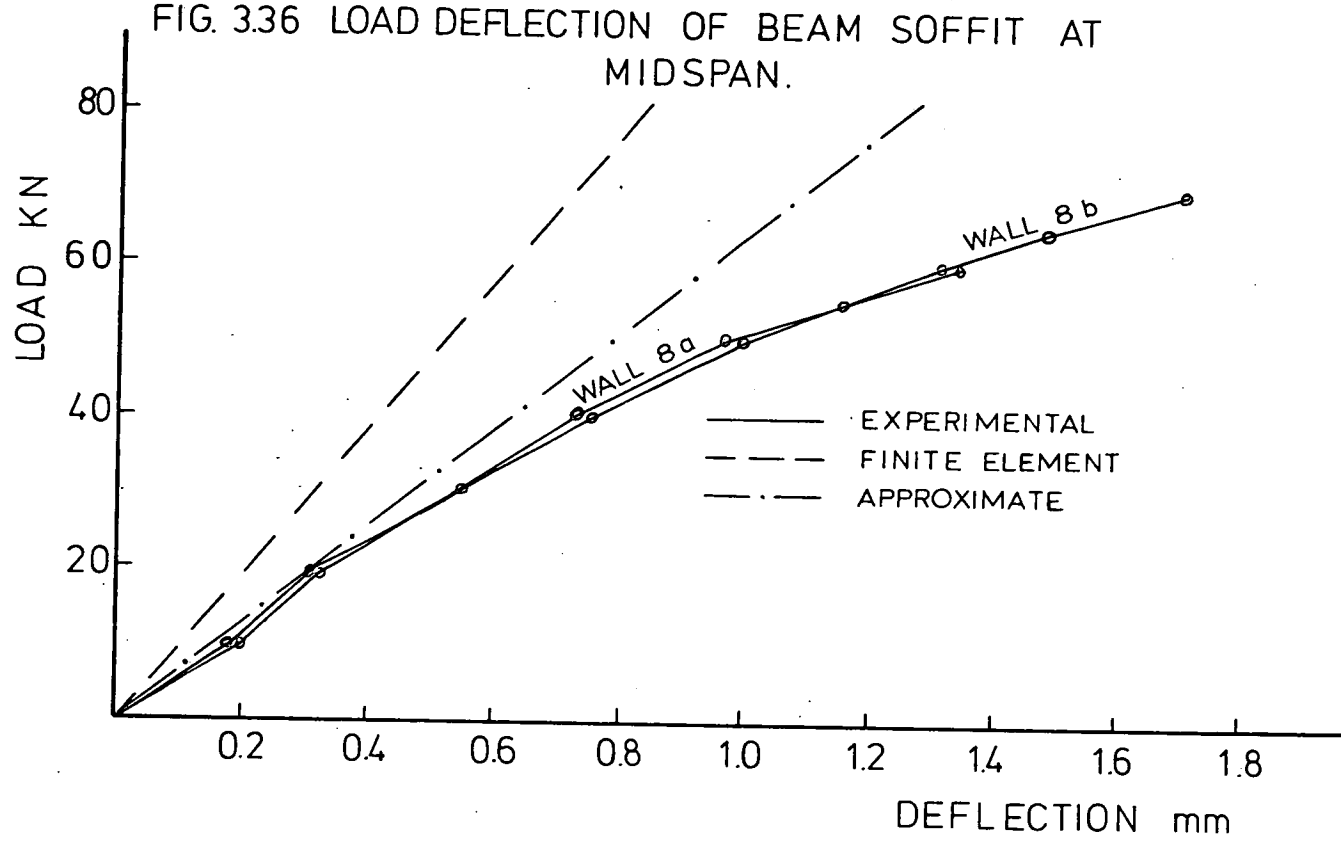

FIG. 3.37 LOAD DEFLECTION CURVE OF BEAM SOFFIT AT MIDSPAN.

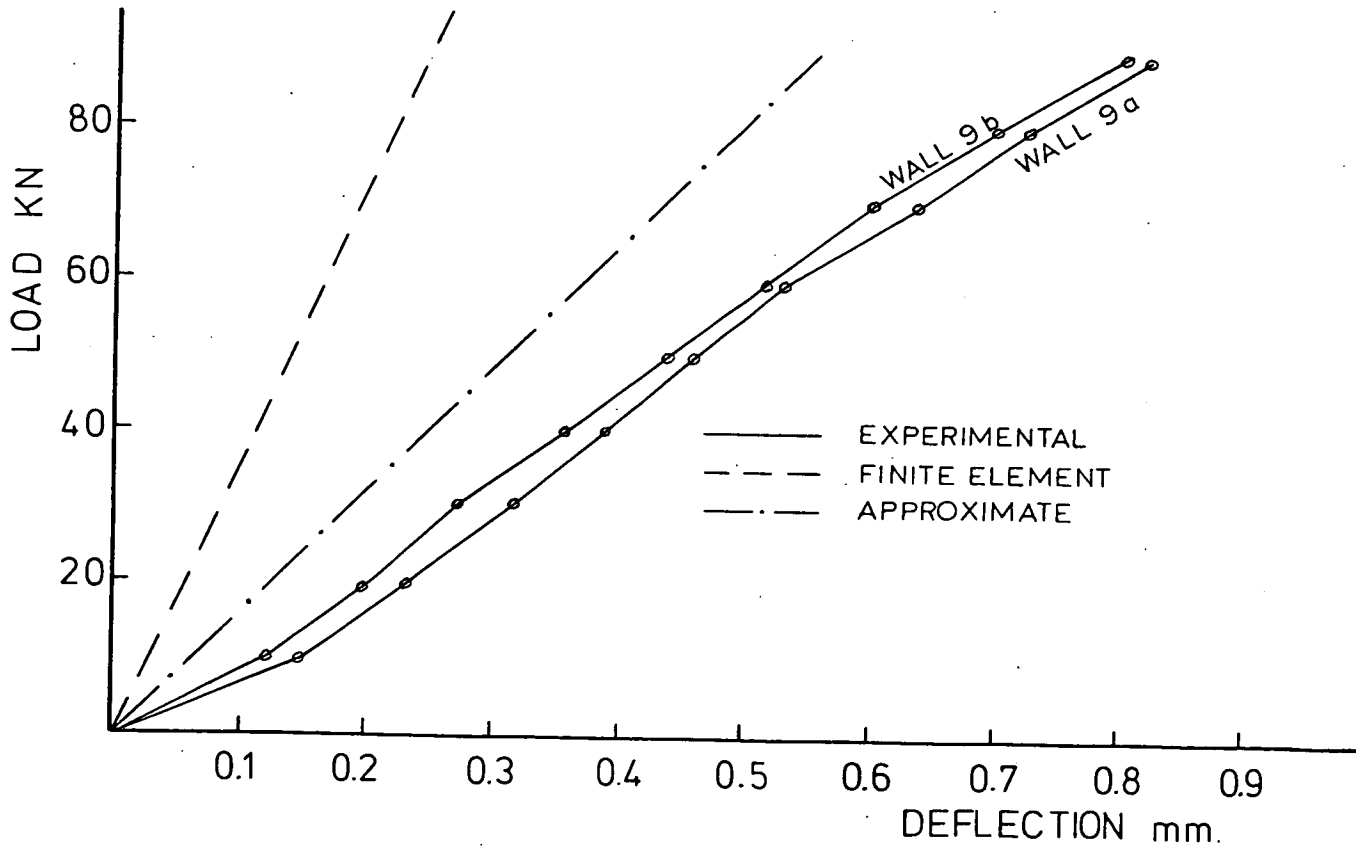

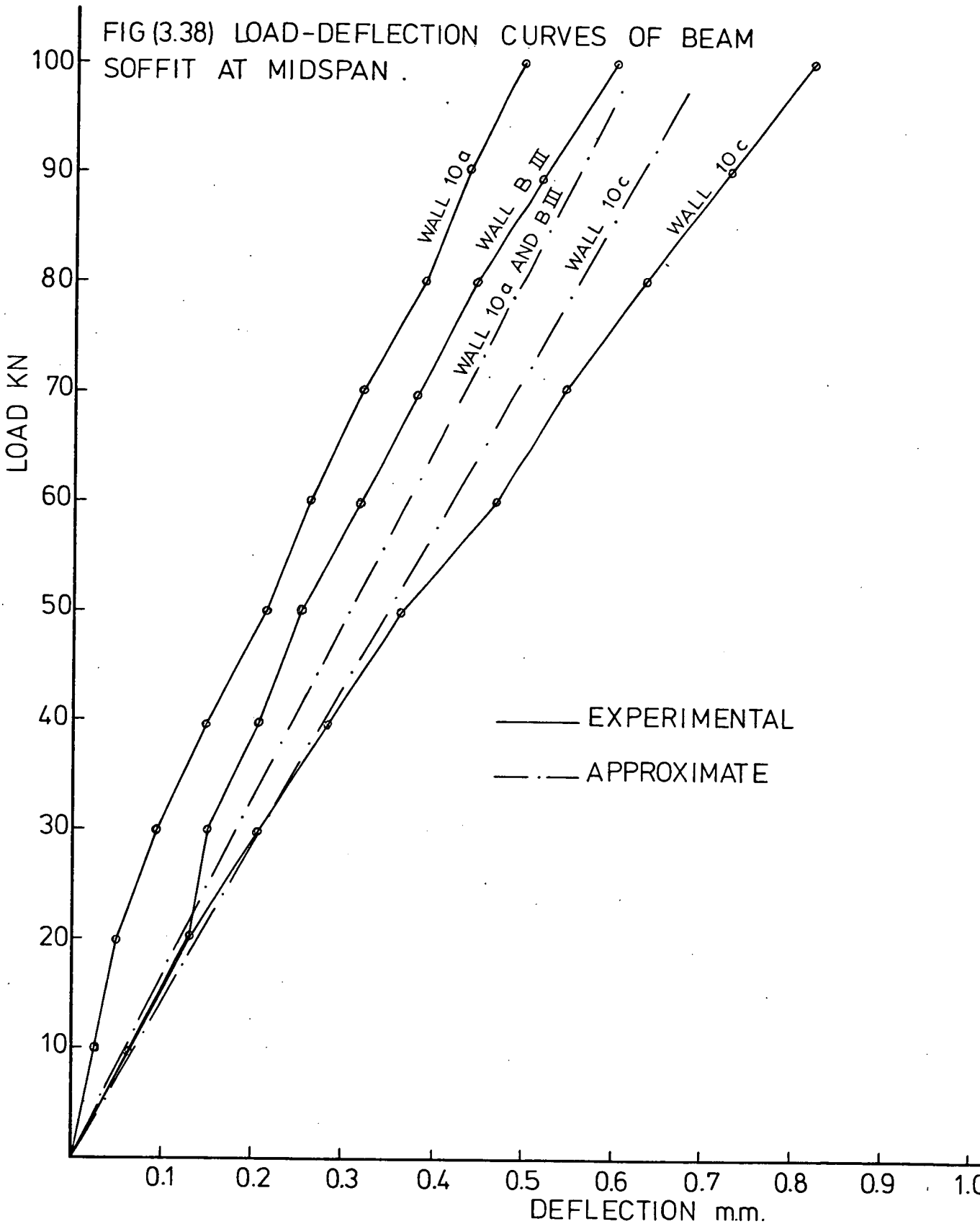
FIG (3.38) LOAD-DEFLECTION CURVES OF BEAM SOFFIT AT MIDSPAN .
LOAD KN
100
90
80
70
60
50
40
30
20
10
0.1
0.2
0.3
0.4
0.5
0.6
0.7
0.8
0.9
1.0
DEFLECTION m.m.
WALL 10a
WALL B III
WALL 10a AND B III
WALL 10c
WALL 10c
EXPERIMENTAL
APPROXIMATE

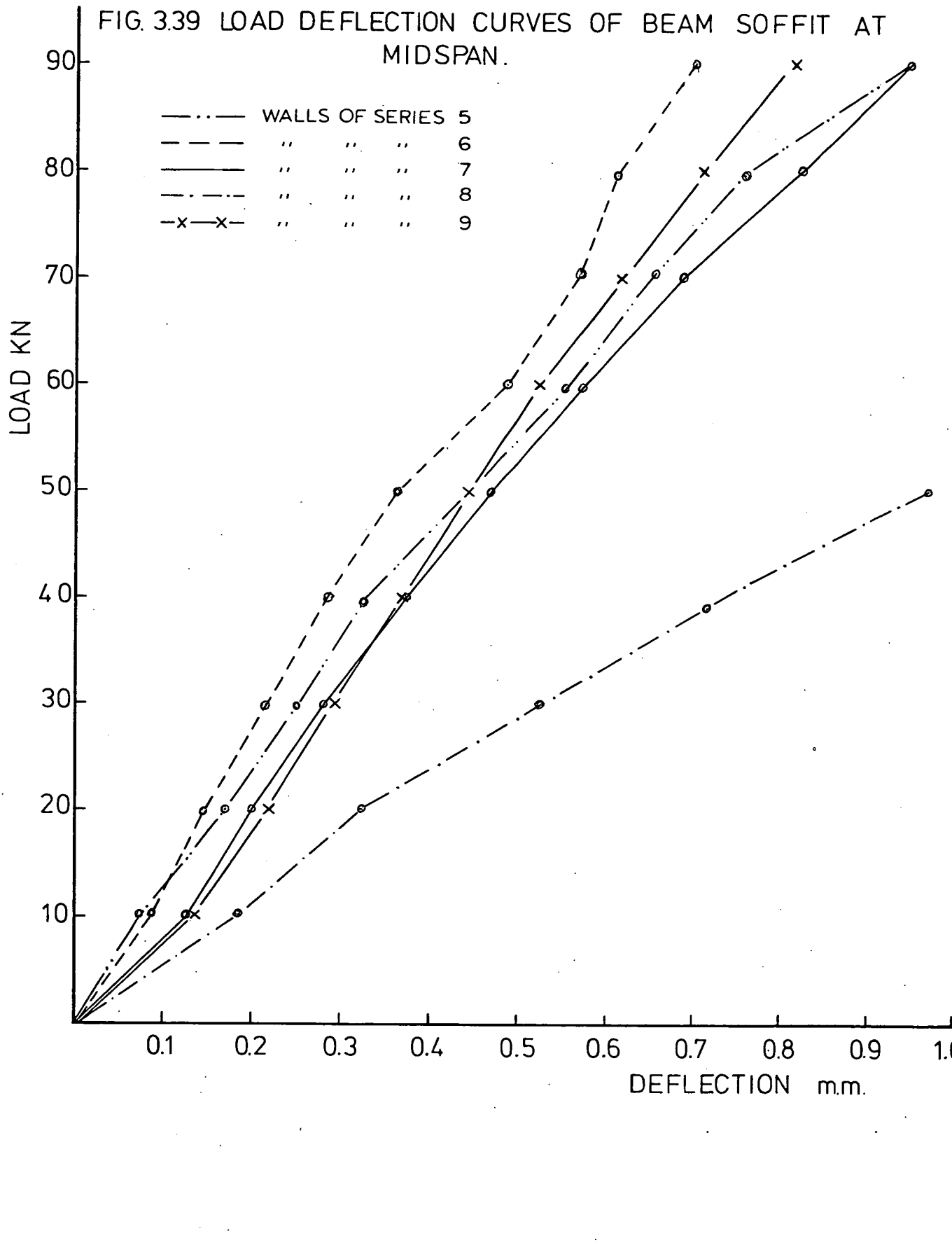
FIG. 3.39 LOAD DEFLECTION CURVES OF BEAM SOFFIT AT MIDSPAN.
WALLS OF SERIES 5
" " " 6
" " " 7
" " " 8
" " " 9
LOAD KN
90
80
70
60
50
40
30
20
10
0.1
0.2
0.3
0.4
0.5
0.6
0.7
0.8
0.9
DEFLECTION m.m.

TABLE 3.12 COMPARISON OF ULTIMATE LOAD

TEST NO	FAILURE LOAD KN		% DIFFERENCE
	EXPERIMENTAL	APPROXIMATE	
6a	182.5	148.1	-18.8
6b	174.5	148.1	-15.1
7a	136.0	148.1	8.9
7b	141.5	148.1	4.7
8a	75.0	73.0	-2.7
8b	83.0	73.0	-12.0
9a	150.0	148.1	-1.3
9b	131.0	148.1	13.1

particularly in the elastic range. The finite element, however, has underestimated the actual deflection.

3.9.7 Conclusion

In conclusion to this Section, the following may be noted :

1. Apart from a small increase in the maximum vertical stress over the supports, the location of a central door or window opening in a wall insignificantly affects the composite action between the wall and its supporting beam.

2. When a doorway is located near to a support, the maximum vertical stress in the wall is substantially increased and tensile stresses develop round the top corners of the opening. Compared to solid walls with a central opening, the reduction of up to 50 per cent in the ultimate load indicates a considerable loss in the composite action. Vertical and horizontal prestressing around the opening could prevent tensile cracks from occurring at these points and could well increase the wall carrying capacity.

3. The results indicate that the approximate method of analysis can also provide a basis for a simple design procedure for composite beams with openings.

CHAPTER 4 : ANALYTICAL STUDY OF THE COMPOSITE ACTION OF WALLS ON SIMPLE SUPPORTED BEAMS

4.1 INTRODUCTION

It has long been recognised that the bending produced in a beam supporting a vertically loaded wall is far less than would be expected if the total load was uniformly distributed over the span. When the wall acts as an infill, it contributes in stiffening the structure, reduces the deformation under load, and increases the strength beyond what can be expected in the elastic design of the framework. This stiffening effect is of economic importance since if it is taken into account in the design, permits reduced dimensioning and saving in material for the members of the structure. A study of the composite action is thus of importance for economy as well as for closer approximation of the actual behaviour of the structure. The analytical work in this field includes the Airy stress function of Rosenhaupt[4], the variational approach of Coull[8], the lattic analogy of Colbourne[10], and the shear lag method of Yettram and Hirst[12]. Various analytical solutions based on the finite element method have also appeared in the last decade. All of these investigations indicate stress concentration in the wall over the supports, due to the arching of the vertical load between the supports, and also high tensile force in the supporting beam as a result of the tied arch action.

In this Chapter, a similar finite element study of the interaction between walls and their supporting beams is presented. Approximate practical methods of calculation have been developed on the basis of the results obtained by the accurate theoretical solution of practical cases. Comparison of the approximate results with the theoretical and experimental results is included.

4.2 THE FINITE ELEMENT METHOD

Since the late fifties, the finite element method has been developed simultaneously with the increasing use of high speed digital computers and with the growing emphasis on numerical methods for engineering analysis. Problems involving complex material properties and boundary conditions, necessitate the employment of the numerical methods, among which the finite element method has proved to be the most versatile.

The method is based on the replacement of the actual physical problem by an analysis model consisting of an assemblage of a finite number of discrete elements. These elements are considered to be connected at their corners or nodal points. The properties of the assemblage follow a similar behaviour to that of the real continuous structure. Simple functions are chosen to approximate the distribution or variation of the actual displacements over each finite element in terms of its nodal displacements. Essentially, the displacement function must be continuous within the elements, and the displacements must be

compatible between adjacent elements. The principle of minimum potential energy is then employed to obtain for each element a set of equilibrium equations from its material and geometric properties. The coefficients of these equilibrium equations constitute the element stiffness matrix. The stiffness matrix relates the displacements at the nodal points to the applied forces at these nodes. The equilibrium equations for the entire body are then obtained by combining the equations for the individual elements in such a way that continuity of displacements is present at the interconnecting nodes. These equations are then modified for the given displacement boundary conditions and solved to give the unknown displacements. From the known displacements, strains and stresses can be determined using the basic principles of elasticity.

The reduction of the infinite number of degrees of freedom of the actual problem to a discrete managable number, introduces some simplifying assumptions in the element formulation and consequently, the accuracy of the results depends on the number of elements used in the model. This, however, must be chosen to give sufficiently accurate results while being reasonably economical on computer time and storage. The finite element method has been described in detail in reference (34).

It is apparent that a masonry system being non-homogeneous, creates some difficulty in its analysis by the finite element method. For a more realistic representation of the masonry system, the finite element model should consist of an assemblage

of elements representing the individual masonry units and the adjacent mortar joints. However, such representation requires considerable amount of effort for the preparation of the input data, as well as an enormous computer storage capacity. Smith et al[35,36] used this type of idealisation for the analysis of small brickwork segments under axial compression. They showed that any analysis based on the assumption of a homogeneous material may lead to a substantial underestimation of the maximum stress. Male and Arbon[15], and Riddington[19], however, applied the method successfully on masonry systems on the basis of a homogeneous material. This later approach has been adopted in the present work.

Of the main advantages of the finite element method, is its capability to combine plane stress and beam elements to deal with typical structures encountered in practice. The main criterion of the assembly is that the same number of degrees of freedom is available from the wall and the beam elements at the nodes of the common boundary[37]. Male and Arbon[15] idealised the wall and the beam by similar triangular elements and therefore the compatibility condition was automatically satisfied. The horizontal stress distribution in the supporting beam produced by this configuration was shown to be non-linear, whereas Saw[18], using the photoelastic analysis showed that the distribution of these stresses is linear across the beam depth. Green[16] and Saw[18] represented the wall and the supporting beam by combining rectangular elements and line

elements in bending. This type of idealisation seems to be more realistic than the use of a large number of plane elements for the beam, and therefore it has been adopted in this analysis.

In most formulations of plane stress elements, two degrees of freedom are assigned at each node. These degrees of freedom are represented by translations in the coordinate directions. As the line element in bending has an extra rotational degree of freedom per node, its connection with a quadrilateral element having two degrees of freedom at each node will result in violation of compatibility at the interconnecting nodes. This difficulty can be overcome by either the addition of a rotational degree of freedom at the interconnecting nodes of the quadrilateral element, an approach used by MacLeod[38] and Pole[39] for the derivation of rectangular element and by Fellipa[39] for the derivation of the quadrilateral element, or the expression of the rotational degree of freedom of the flexural element in terms of the equivalent translations as described by Green[16], Figure 4.1(a).

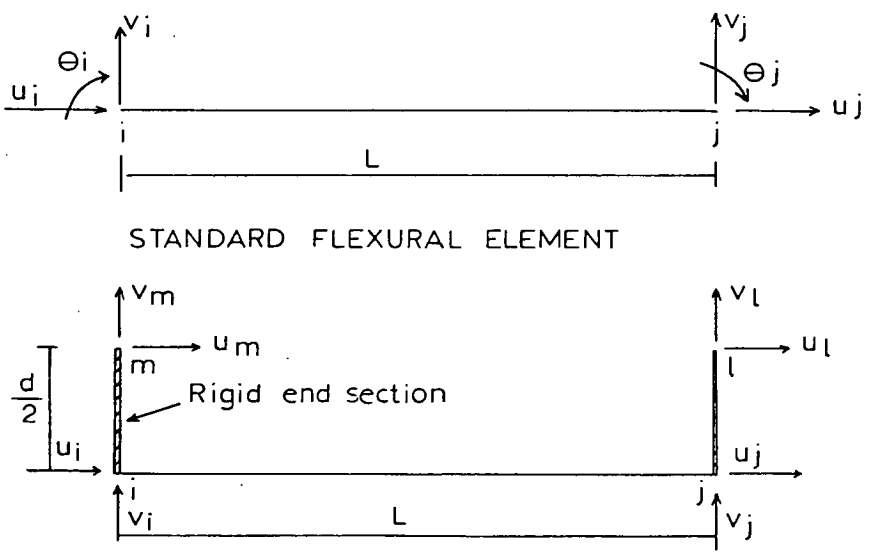

FIG. 4.1(a) ECCENTRIC BENDING ELEMENT

The finite element solution is also affected by the element aspect ratio. The aspect ratio describes the shape of the element in the assemblage and is defined as the ratio of the largest dimension of the element to the smallest dimension. The optimum aspect ratio at any location within the grid depends largely upon the difference in rate of change of displacements in different directions. If the displacements vary at about the same rate in each direction, the closer the aspect ratio to unity, the better the accuracy of the results[34]. Typical analysis has been carried on a cantilever with five different meshes as shown in Figure 4.1(b). The rectangular element 'PSRCSH' "Plane Stress Rectangle with Constant Shear", with four nodal points at the corners has been used. In order to isolate the effect of the changing aspect ratio, the number of elements is kept constant in each case, and the number of nodes is also kept nearly the same. The results are summarised in Table 4.1. From the results it can be concluded that the closer the aspect ratio to unity, the closer is the solution to the exact one.

In the following section, the application of the finite element to the wall on beam problem is described. The computer program used was STRUDL[40] which is part of the standard I.C.E.S. package. The program has been developed at the M.I.T. and implemented on the I.B.M. system/360 at Edinburgh Regional Computing Centre. Solution times have proved to be very fast, for a typical problem using 81 rectangular elements and 9 beam

TABLE 4.1 EFFECT OF THE ELEMENT ASPECT RATIO

CASE	ASPECT RATIO	NUMBER OF NODES	NUMER OF ELEMENTS	C.P.U.TIME SEC.	DEFLECTION UNITS	% DIFFERENCE
1	3	26	12	3.15	261.84	1.42
2	1.33	21	12	2.94	262.15	1.30
3	3	20	12	2.76	261.83	1.42
4	5.3	20	12	2.80	258.9	2.52
5	12	21	12	2.65	249.63	6

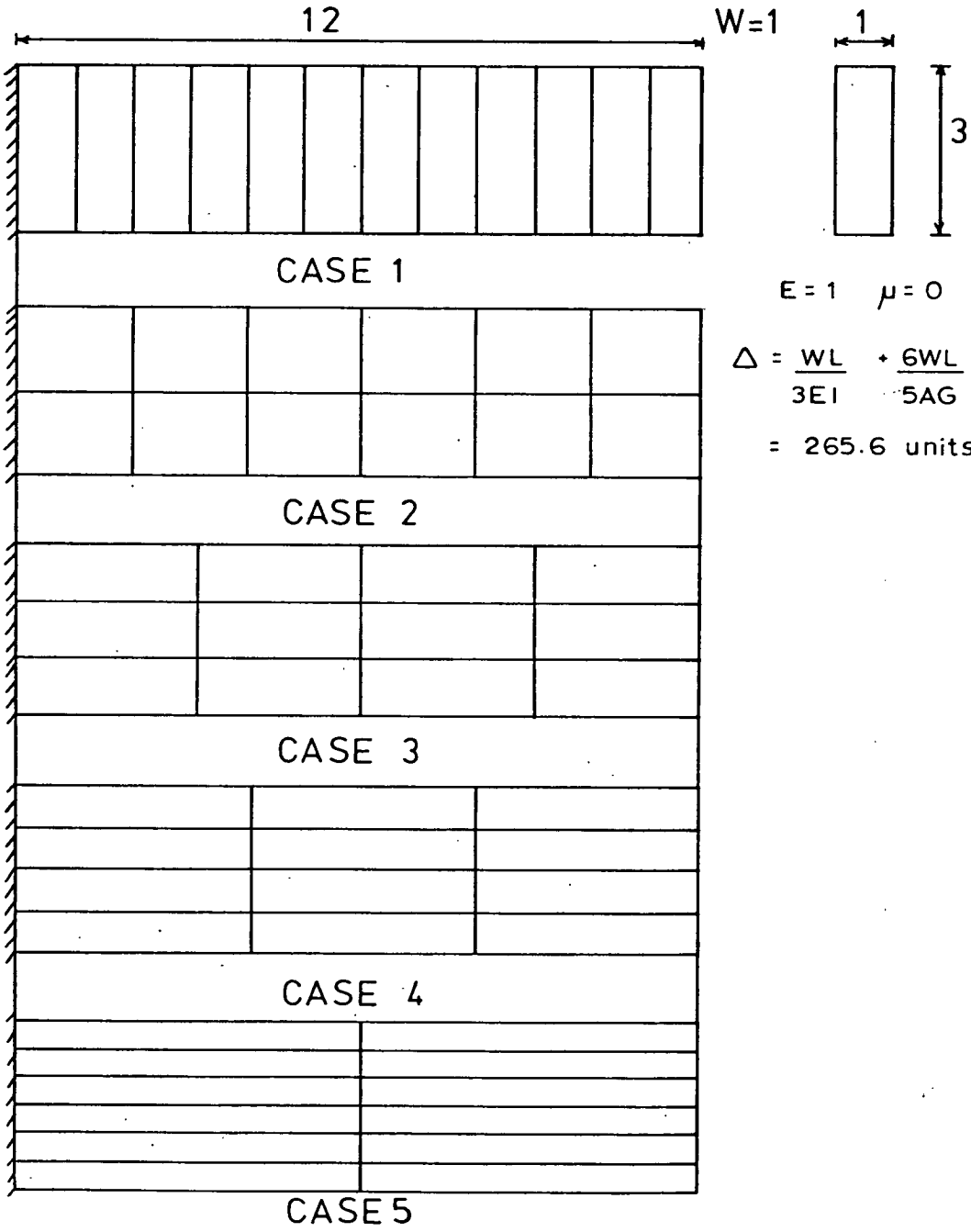

FIG. 4.16 EFFECT OF ASPECT RATIO

elements with 8 different beam stiffnesses, the central processing unit (C.P.U.) time was 71 seconds.

4.3 ANALYSIS PROCEDURE

The problem is analysed as a plane stress problem on the assumption that the brickwork material is homogeneous. The STRUDL program permits the combination of members and elements of different types in the solution of the problem. At first a rectangular element type 'PSROT' with four corner nodes and three degrees of freedom per node, was used. These degrees of freedom are represented by two translations in the coordinate directions, and the third corresponds to in-plane rotation. Unfortunately, this element did not perform satisfactorily. The displacements and strains seemed to be correct, but the stresses were not treated properly. The error was discovered later to be within the element program itself[41]. Another type of rectangular element the 'PSRCSH' has then been used for idealization of the wall. This has four corner nodes with only two translational degrees of freedom per node. The element is used only for plane stress or plane strain problems and is assumed to have constant or average shear acting across the face. The element stiffness matrix is computed based on the following displacement function :

$$U = \alpha_1 + \alpha_2 x + \alpha_3 y + \alpha_4 xy$$

$$V = \alpha_5 + \alpha_6 x + \alpha_7 y + \alpha_8 xy$$

This function produces a quadratic displacement field over the element, but a linear displacement variation along the edges. The element results are the displacements, strains, stresses, and principal stresses at the centroid of the element.

Line elements in bending are used to represent the supporting beam. As the centroidal axes of the bending elements do not actually lie along the boundary of the wall elements, an eccentricity equal to half the beam depth has been introduced, Figure 4.1(c). Violation of the compatibility requirement at the interconnecting nodes has not much affected the accuracy of the results. The explanation for this may be that the displacement field assumed for the rectangular element yields an approximate structure that is stiffer than the actual structure, but the lack of compatibility may have resulted in a decrease in the stiffness of the approximate structure. These compensating effects may thus cause the results to be close to the exact solution[45].

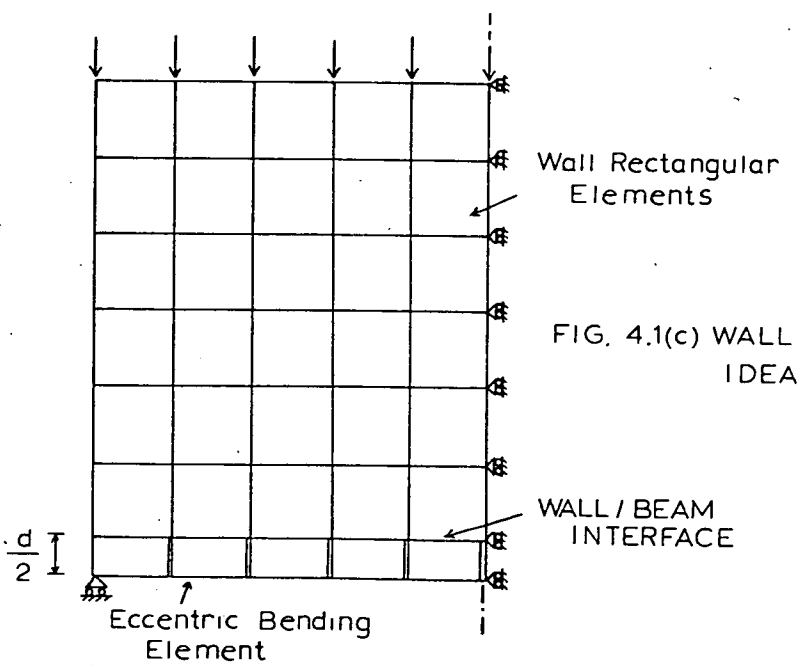

FIG. 4.1(c) WALL / BEAM IDEALIZATION

4.4 COMPARISON OF THE FINITE ELEMENT SOLUTION WITH THE EXISTING SOLUTIONS

As a test of the accuracy of the finite element program, it was decided to investigate initially a wall on beam problem which has already been solved previously. Solutions of the problem have been proposed by a number of authors, the most detailed results being those of Rosenhaupt[4], Coull[8], Colbourne[10], Yettram and Hirst[12] and Green[16]. The dimensions and properties of the wall and beam are shown in Figure 4.2. The modular ratio of 30 represents the case of a lightweight concrete block wall on a reinforced concrete beam. The wall is represented by 200 mm square mesh using the rectangular element type 'PSRCSH', and the supporting beam by a series of bending elements with and without eccentricity. The results obtained are shown in Figures 4.2 to 4.6 together with results predicted by alternative methods where available.

The horizontal stress in the wall predicted by Colbourne and Green solutions is not in good agreement with that predicted by the finite element using bending elements without eccentricity, Figure 4.3. In the upper half of the wall, the compression is overestimated whereas tensile stresses are produced at the bottom of the wall. The explanation for this may be due to the fact that when the axis of the bending elements is assumed to lie along the wall boundary, the moment arm is raised as a result of which the centre of compression in the wall also rises, and consequently higher compressive stresses will be produced in the upper part of the wall and tensile stresses in the bottom part.

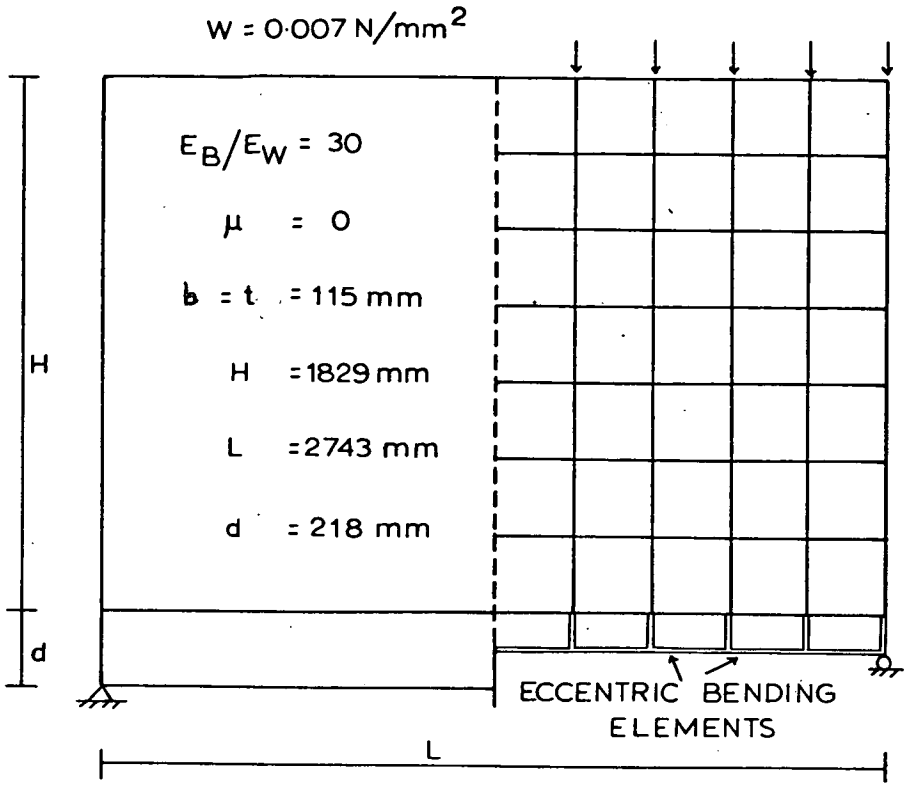

FIG. 4.2 DIMENSIONS AND PROPERTIES OF TEST EXAMPLE

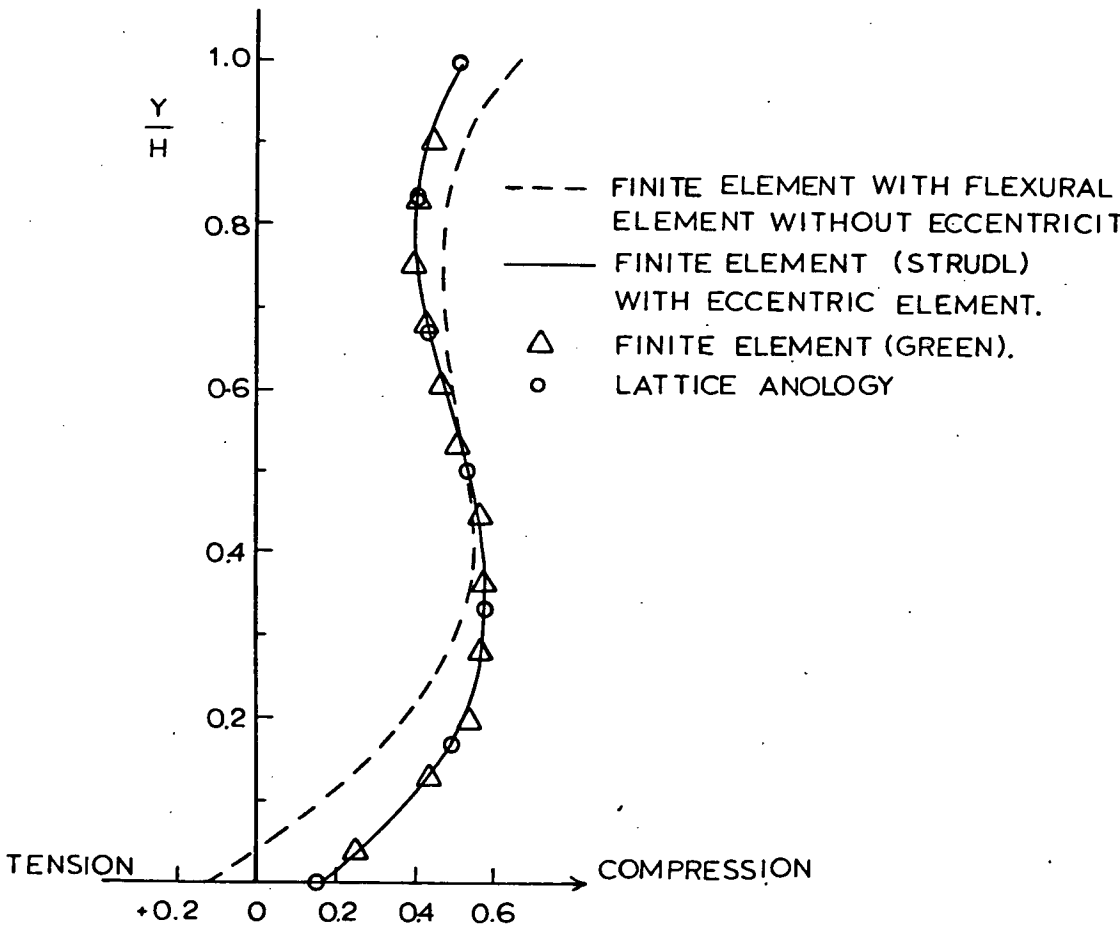

FIG. 4.3 HORIZONTAL STRESS DISTRIBUTION AT MIDSPAN.

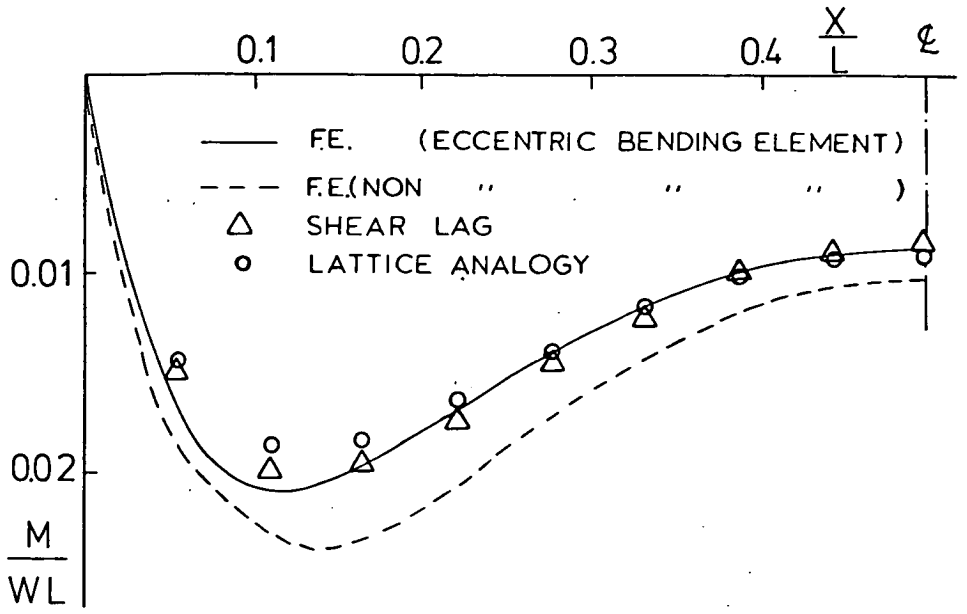

FIG. 4.4 VARIATION OF BENDING MOMENT ALONG SUPPORTING BEAM.

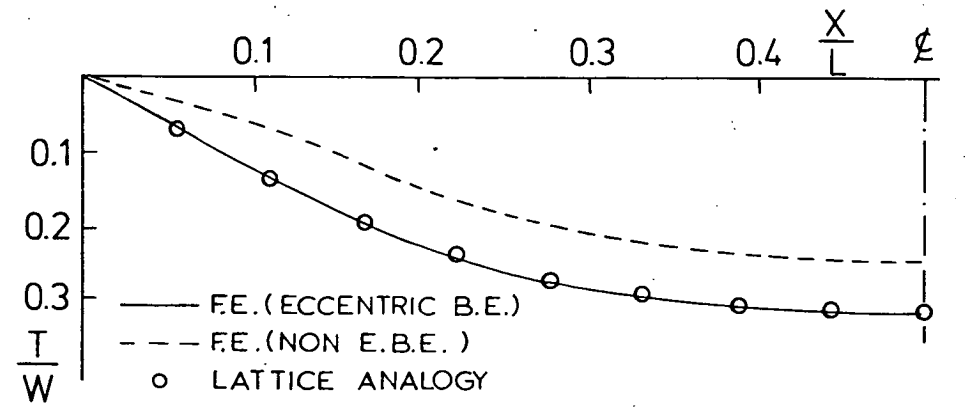

FIG. 4.5 a VARIATION OF AXIAL FORCE IN SUPPORTING BEAM.

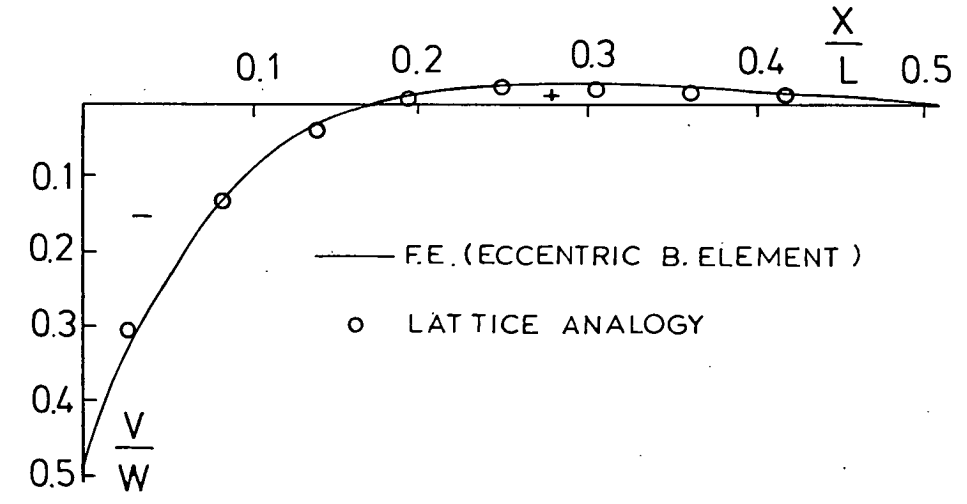

FIG. 4.5 b VARIATION OF BEAM SHEAR FORCE.

The results, however, are in very good agreement with both solutions when the finite eccentricity has been introduced. Regarding the axial and shear forces in the supporting beam, Figures 4.5(a), (b) indicate that a striking similarity exists between the finite element results and those predicted by the lattice analogy of Colbourne. In the absence of the beam eccentricity, however, the axial force is substantially smaller and this is presumably due to the contribution of the wall in taking some of the tensile forces.

In Figure 4.4, the results of the bending moments predicted by the lattice analogy, the shear lag, and the finite element methods are shown to be of the same order of magnitude along the central region of the supporting beam. However, the bending moment produced by the non-eccentric bending element, is shown to be much higher due to the elimination of the counter bending effect produced by the horizontal force at the wall-beam interface.

For the vertical stress distribution at the wall-beam interface, Figure 4.6 indicates that the lattice analogy solution is in very good agreement with the finite element results, whereas the shear lag method predicts high tensile stresses in the central region and high compressive stresses at the wall edges. Coull's variational method, however, predicts the highest tensile stresses over the central region and the lowest compressive stresses over the supports. Perhaps this is due to the insufficient terms being considered by Coull in

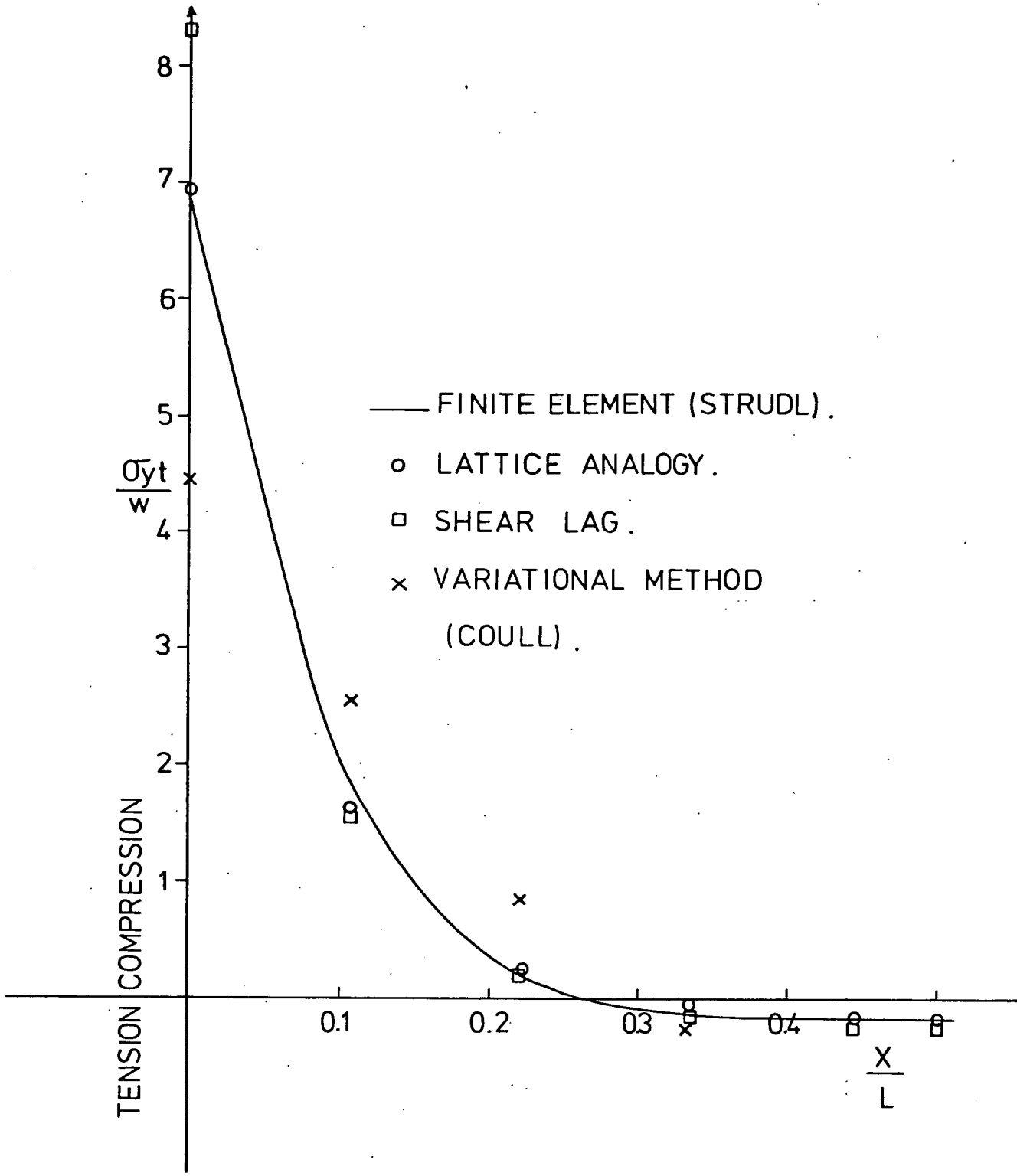

FIG. 4.6 DISTRIBUTION OF THE VERTICAL STRESS AT THE WALL / BEAM INTERFACE.

the assumed stress series, thus resulting in the approximate parabolic distribution shown in Figure 4.6. The highest vertical stress concentration over the supports is predicted by the finite difference of Rosenhaupt, not shown in Figure 4.6. This is because Rosenhaupt neglects the bending rigidity of the supporting beam and this has the effect, as Coull points out,of eliminating the normal stresses between the wall and the beam and therefore the load is entirely carried at the bottom corners of the wall.

From the foregoing discussion, it has been shown that the finite element solution predicted by the STRUDL program compares favourably with Colbourne and Green solutions and on the whole in good agreement with the solution of Yettram and Hirst. The program has thus proved to be sufficiently accurate in predicting the composite behaviour of wall on beam structure, and therefore, it has been used for the complete analysis of the problem as will be described in the following sections.

4.5 PARAMETERS AFFECTING THE COMPOSITE BEHAVIOUR OF WALLS ON BEAMS

The significant parameters which may have influence on the interacting behaviour between walls and their supporting beams are as listed below :

1. The wall height/span ratio.

2. The thickness of the wall.

3. The modular ratio.

4. The beam depth/span ratio.

5. The beam cross-sectional area and its second moment of area.

6. The beam support width.

With the exception of the beam support width, the above variables have been combined into two non-dimensional parameters. These are defined as the wall-beam relative flexural stiffness parameter :

$$R = \sqrt[4]{\frac{h^3 t E_w}{I E_b}}$$

and the axial stiffness parameter :

$$K = \frac{h t E_w}{A E_b}$$

For the study of the wall height effect, seven height/span ratios ranging from 0.33 to 1.5 have been considered in the analyses. The effect of the beam depth/span ratio is investigated by analysing five different cases in conjunction with each wall height. Modular ratios of 3, 4, 5 and 30 are assumed in the analysis of four walls. The first three represent the case of brickwork wall on reinforced concrete beam and the fourth the same wall on a steel beam.

The finite element representation of a typical wall on beam is shown in Figure 4.7. The modulus of elasticity of the wall material, which is assumed to be homogeneous, is 7 KN/mm^2, and its Poisson's ratio is 0.1. For all analyses, the span of the wall and its thickness are respectively, 3.66 M and 114 mm. The beam width is 150 mm. The wall is subjected to uniformly distributed load applied along its upper edge.

4.6 DISCUSSION OF THE RESULTS

All results are summarized in Tables 4.2 to 4.6. Typical stress distributions in a wall of 0.66 height/span ratio are shown in non-dimensionalized forms in Figures 4.8 to 4.11.

4.6.1 Wall Stresses

The distribution of the vertical stress in the wall is shown in Figure 4.8. This indicates concentration of the vertical stress over the supports and for a short distance along the wall-beam interface. This concentration occurs as a result of the arching action taking place in the wall. This phenomenon is clearly demonstrated by the principal stresses distribution shown in Figure 4.11. Comparative plots of the vertical stress distribution at the wall-beam interface with varying beam span/depth ratio and modular ratio are given in Figures 4.12 and 4.13 respectively. In Table 4.2, the maximum vertical stress is expressed as a ratio of the average applied stress. This ratio is defined as the stress concentration factor.

TABLE 4.2 VERTICAL STRESS CONCENTRATION IN THE WALL

H/L		0.33		0.5		0.66		0.75		1.0		1.25		1.5	
L/d	E_b/E_w	R	MAX STRESS / AV STRESS	R	MAX STRESS / AV STRESS	R	MAX STRESS / AV STRESS	R	MAX STRESS / AV STRESS	R	MAX STRESS / AV STRESS	R	MAX STRESS / AV STRESS	R	MAX STRESS / AV STRESS
8	4	2.56	6.6	3.46	7	4.30	7.4	4.7	7.8	5.83	8.2	6.89	8.2	7.90	8.2
12	4	3.46	9	4.70	9.7	5.83	10	6.36	10.8	7.90	11.7	9.33	11.7	10.70	11.7
15	4	4.10	11.0	5.55	11.6	6.89	11.9	7.52	12.2	9.33	12.8	11.04	12.8	12.65	12.8
20	4	5.08	12	6.89	13	8.55	13.6	9.34	14.2	11.58	15	13.69	15	15.70	15
24	4	5.83	14	7.90	14.8	9.80	15.6	10.7	16.4	13.28	17.8	15.7	17.8	18	17.8
12	3	3.72	10.6	5.05	10.8	6.26	11.1	6.84	11.5	-	-	-	-	-	-
12	5	3.28	9	4.44	9.4	5.51	9.46	6.02	9.4	-	-	-	-	-	-
12	30	2.09	6	2.84	6.3	3.52	6.4	3.85	6.6	-	-	-	-	-	-

TABLE 4.3 AXIAL FORCE AT THE BEAM MIDSPAN

H/L		0.33		0.5		0.66		0.75		1.0		1.25		1.5	
L/d	E_b/E_w	K	T/W	K	T/W	K	T/W	K	T/W	K	T/W	K	T/W	K	T/W
8	4	0.50	0.417	0.75	0.324	1.0	0.296	1.13	0.290	1.5	0.267	1.88	0.265	2.25	0.265
12	4	0.75	0.398	1.13	0.287	1.5	0.252	1.69	0.244	2.25	0.218	2.81	0.216	3.38	0.216
15	4	0.94	0.369	1.41	0.252	1.88	0.218	2.11	0.211	2.81	0.185	3.52	0.184	4.22	0.184
20	4	1.25	0.319	1.88	0.207	2.5	0.174	2.81	0.168	3.75	0.147	4.69	0.144	5.63	0.144
24	4	1.50	0.285	2.25	0.179	3.0	0.148	3.38	0.142	4.5	0.123	5.63	0.122	6.75	0.122
12	3	1.00	0.370	1.50	0.259	2.0	0.225	2.25	0.219	-	-	-	-	-	-
12	5	0.60	0.417	0.90	0.285	1.2	0.269	1.35	0.261	-	-	-	-	-	-
12	30	0.10	0.426	0.15	0.343	0.2	0.315	0.23	0.310	-	-	-	-	-	-

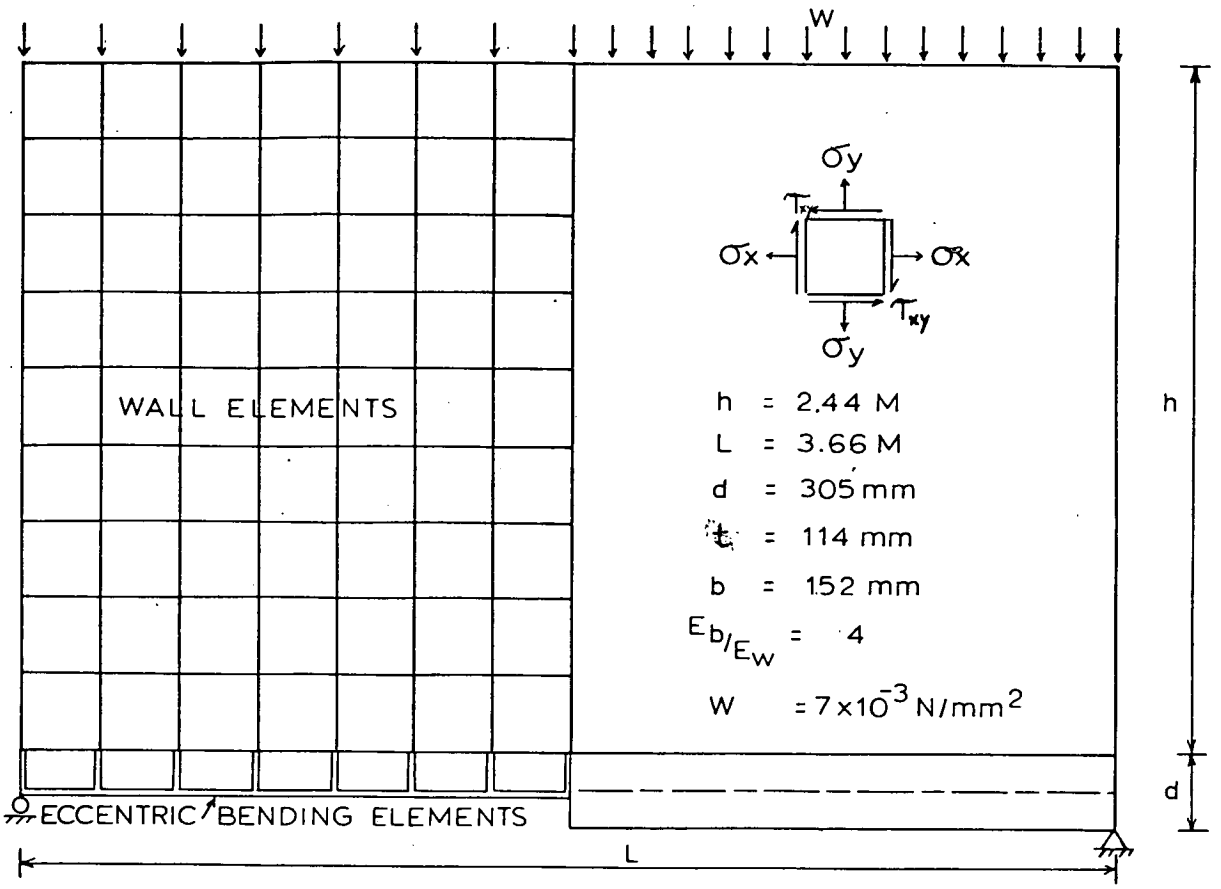

FIG. 4.7 FINITE ELEMENT IDEALIZATION

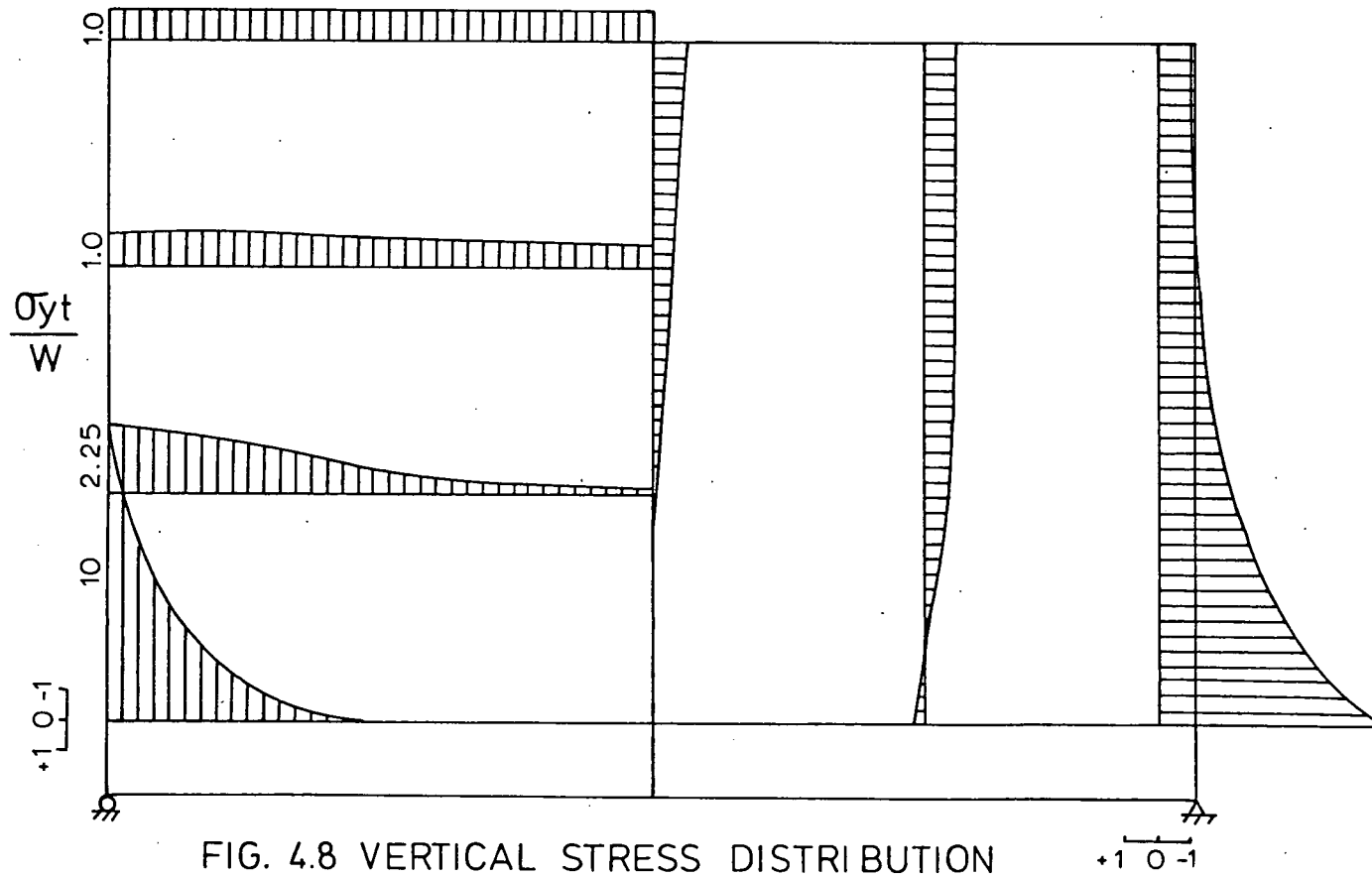

FIG. 4.8 VERTICAL STRESS DISTRIBUTION

The results indicate that the contact stresses and consequently the stress concentration are mainly affected by the relative stiffness parameter R. A slight increase in the value of R by a decrease in either the beam depth or the modular ratio, results in a substantial increase in the stress concentration and a decrease in the contact length. The concentration factor is much more affected by the beam span/depth ratio than by the modular ratio. The influence of the wall height on the magnitude of the vertical stresses is observed in Table 4.2. For walls with height/span ratio more than unity, the wall height has no effect on the stress distribution. Burhouse[11], using the lattice analogy of Colbourne[10], has also shown that the vertical stress concentration in the wall is not influenced by the wall height once this exceeds a value of unity. It has also been suggested by Coull[8], that for walls whose height is greater than the span, practically no diffusion of stress occurs in the section above the unit height/span position.

The horizontal stress distribution along vertical sections in the wall is shown in Figure 4.9. It shows horizontal compressive stresses over the entire height of the wall. The beam acting as a tie to the arch formed in the wall, as mentioned earlier, takes the tensile forces. The horizontal compression stresses are higher in the lower section of the wall. Based on the assumption that the resultant tensile force is acting at the centre of the supporting beam, an internal moment arm has been found. From the value of the moment, the tensile force at the beam midspan has been calculated. Table 4.7 shows the moment

TABLE 4.4 MAXIMUM AND MINIMUM BENDING MOMENTS ($\times 10^{-4}$) IN THE SUPPORTING BEAM

H/L		0.33		0.5		0.66		0.75		1.0		1.25		1.5	
L/d	E_b/E_w	$\frac{M_{max}}{WL}$	$\frac{M_{min}}{WL}$	$\frac{M_{max}}{WL}$	$\frac{M_{min}}{WL}$	$\frac{M_{max}}{WL}$	$\frac{M_{min}}{WL}$	$\frac{M_{max}}{WL}$	$\frac{M_{min}}{WL}$	$\frac{M_{max}}{WL}$	$\frac{M_{min}}{WL}$	$\frac{M_{max}}{WL}$	$\frac{M_{min}}{WL}$	$\frac{M_{max}}{WL}$	$\frac{M_{min}}{WL}$
8	4	153	106	153	68	154	60	155	59	179	57	179	57	179	57
12	4	115	39	115	20	118	16	120	15	129	14	129	14	129	14
15	4	97	22	99	11	100	8	100	8	101	7	101	7	101	7
20	4	72	11	75	5	75	3	76	3	68	3	68	3	68	3
24	4	57	6	60	3	60	2	60	2	50	2	50	2	50	2
12	3	104	31	106	15	111	12	112	11	-	-	-	-	-	-
12	5	120	46	118	20	128	20	129	19	-	-	-	-	-	-
12	30	247	228	232	159	233	145	233	143	-	-	-	-	-	-

TABLE 4.5 MAXIMUM SHEAR STRESS AT WALL/BEAM INTERFACE

H/L		0.33	0.5	0.66	0.75	1.0	1.25	1.5
L/d	E_b/E_w	MAXIMUM SHEAR STRESS ($\frac{\tau.t}{\omega}$)						
8	4	2.05	1.80	1.75	1.68	1.65	1.55	1.55
12	4	2.40	2.25	2.20	2.15	1.90	1.90	1.90
15	4	2.90	2.65	2.60	2.55	2.5	2.5	2.5
20	4	3.65	3.40	3.30	3.20	3.00	3.00	3.00
24	4	4.30	4.00	3.90	3.80	3.50	3.50	3.50
12	3	2.75	2.40	2.35	2.35	-	-	-
12	5	2.30	2.20	2.15	2.10	-	-	-
12	30	1.90	1.65	1.60	1.50	-	-	-

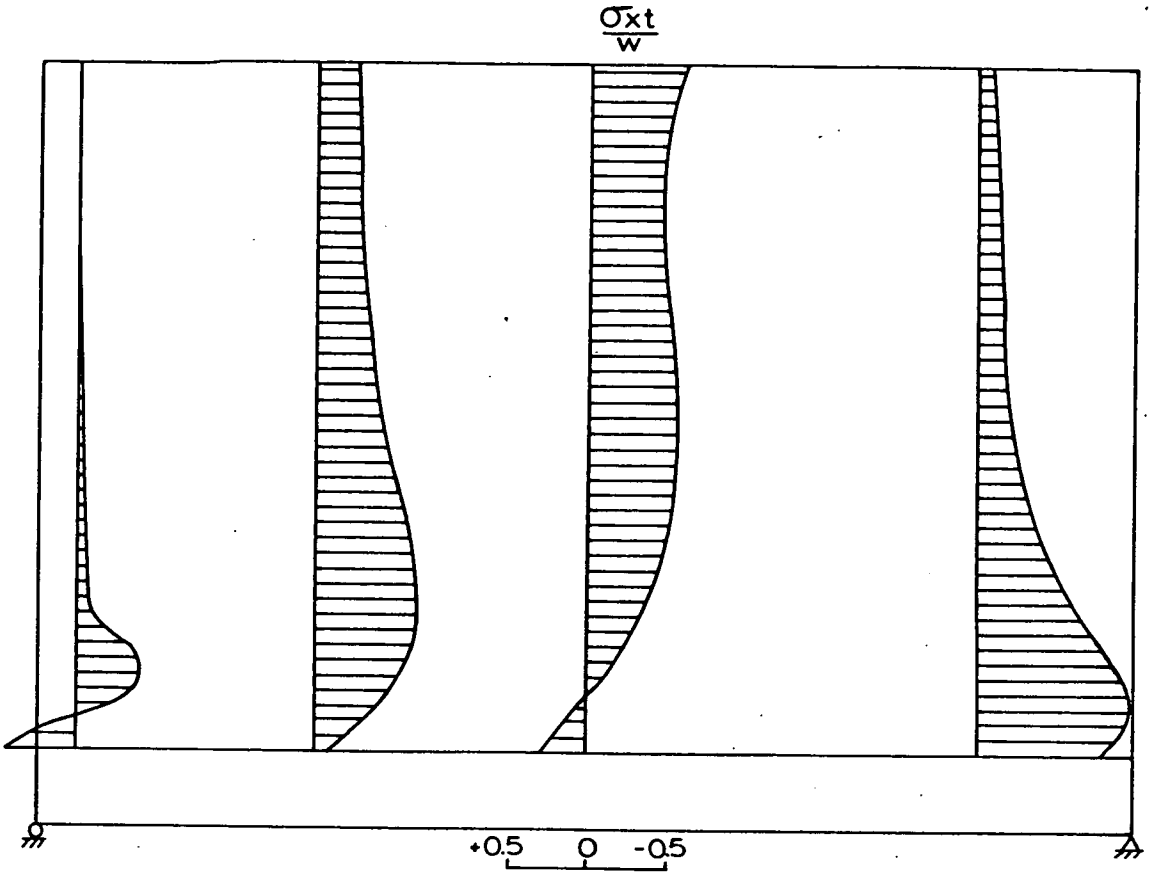

FIG 4.9 HORIZONTAL STRESS DISTRIBUTION.

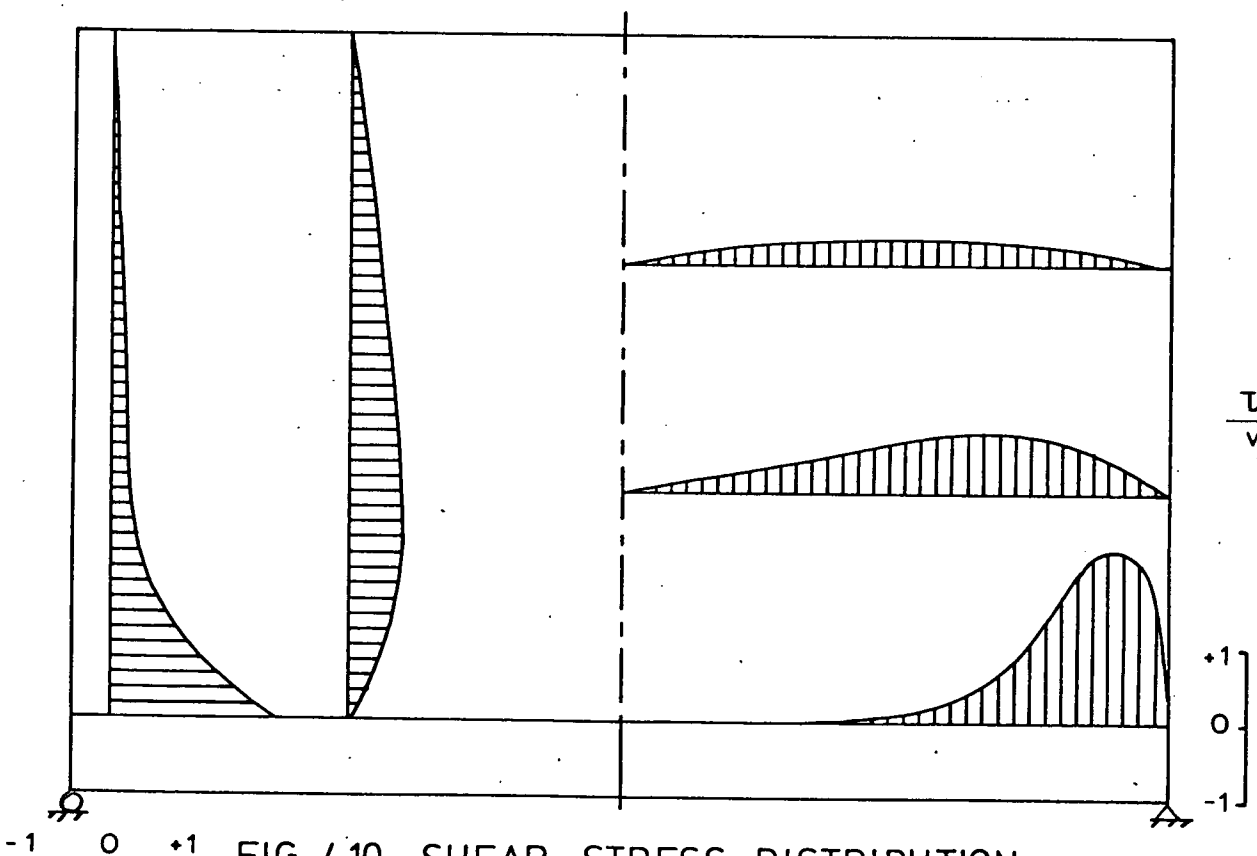

FIG 4.10 SHEAR STRESS DISTRIBUTION.

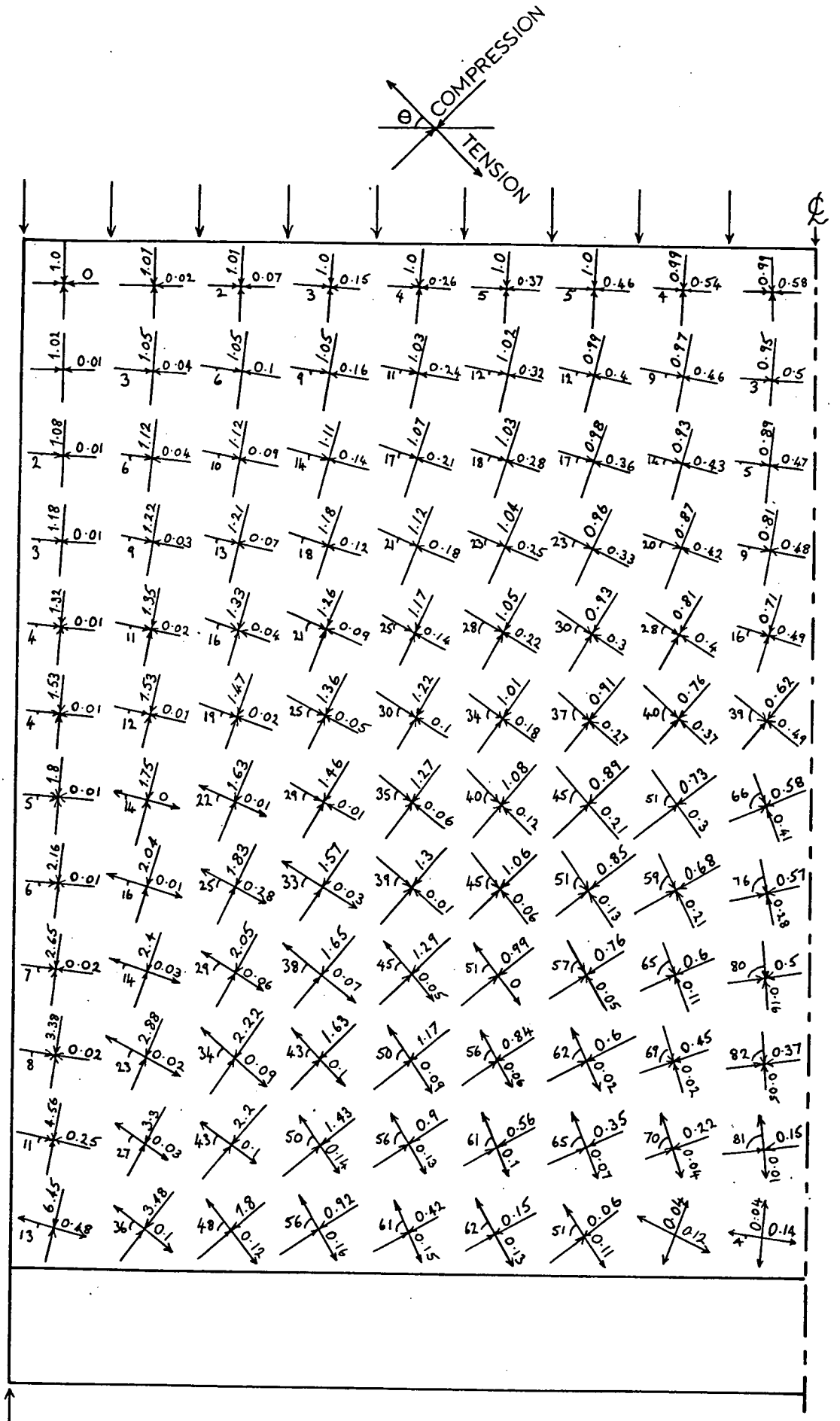

FIG.(4.11) PRINCIPAL STRESSES

TABLE 4.6 BEAM CENTRAL DEFLECTION AT ($W = 7\ KN/mm^2$)

H/L		0.33	0.5	0.66	0.75	1.0	1.25	1.5
L/d	E_b/E_w	DEFLECTION (IN 10^{-4} mm)						
8	4	62	48	46	45	45	45	45
12	4	84	63	59	58	58	58	58
15	4	95	70	65	65	65	65	65
20	4	108	79	73	72	70	70	70
24	4	115	83	77	77	73	73	73
12	3	89	66	62	61	-	-	-
12	5	80	63	57	56	-	-	-
12	30	55	44	42	42	-	-	-

TABLE 4.7 VARIATION OF THE INTERNAL MOMENT ARM AND BEAM AXIAL FORCE WITH (L/d)

L/d	a/L	T/W	
		EXACT	APPROXIMATE
8	0.41	0.296	0.300
12	0.43	0.252	0.290
15	0.44	0.218	0.278
20	0.46	0.174	0.272
24	0.48	0.148	0.260

TABLE 4.8 FLEXURAL STIFFNESS PARAMETER

AUTHOR	STIFFNESS PARAMETER
COULL	$\left(\frac{L}{2d}\right)^3\left(\frac{t}{b}\right)\frac{E_w}{E_b}$
GREEN	$\frac{L^3 t E_w}{I E_b}$
SMITH AND RIDDINGTON	$\left(\frac{L^3 t E_w}{I E_b}\right)^{0.25}$
LEVY AND SPIRA	$2\left(\frac{E_b I}{E_w t}\right)^{0.33}$
PRESENT AUTHOR	$\left(\frac{h^3 t E_w}{I E_b}\right)^{0.25}$

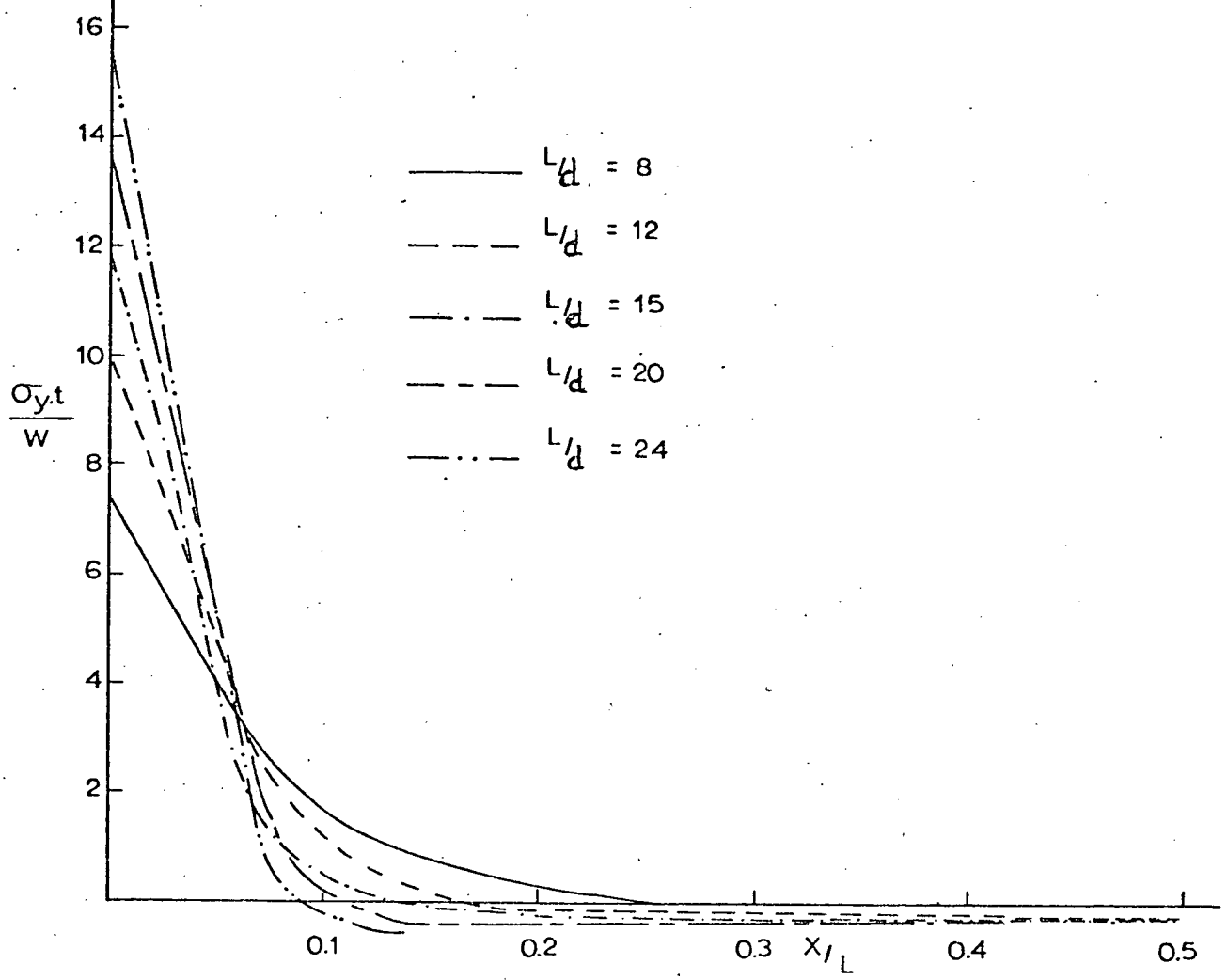

FIG 4.12 VARIATION OF THE VERTICAL STRESS AT THE WALL/BEAM INTERFACE WITH L/d FOR $E_b/E_w = 4$

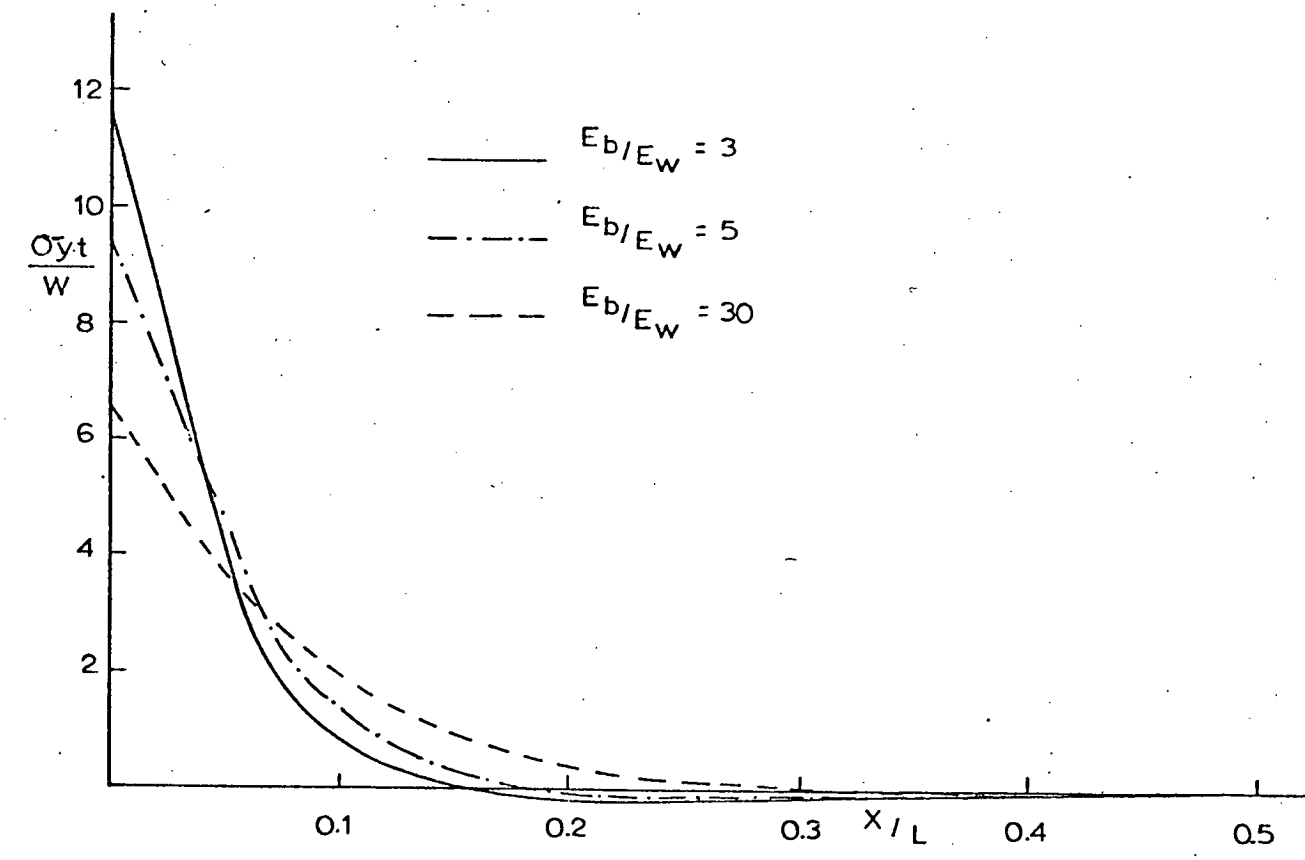

FIG. 4.13 VARIATION OF THE VERTICAL STRESS AT THE WALL/BEAM INTERFACE WITH E_b/E_w FOR L/d = 12

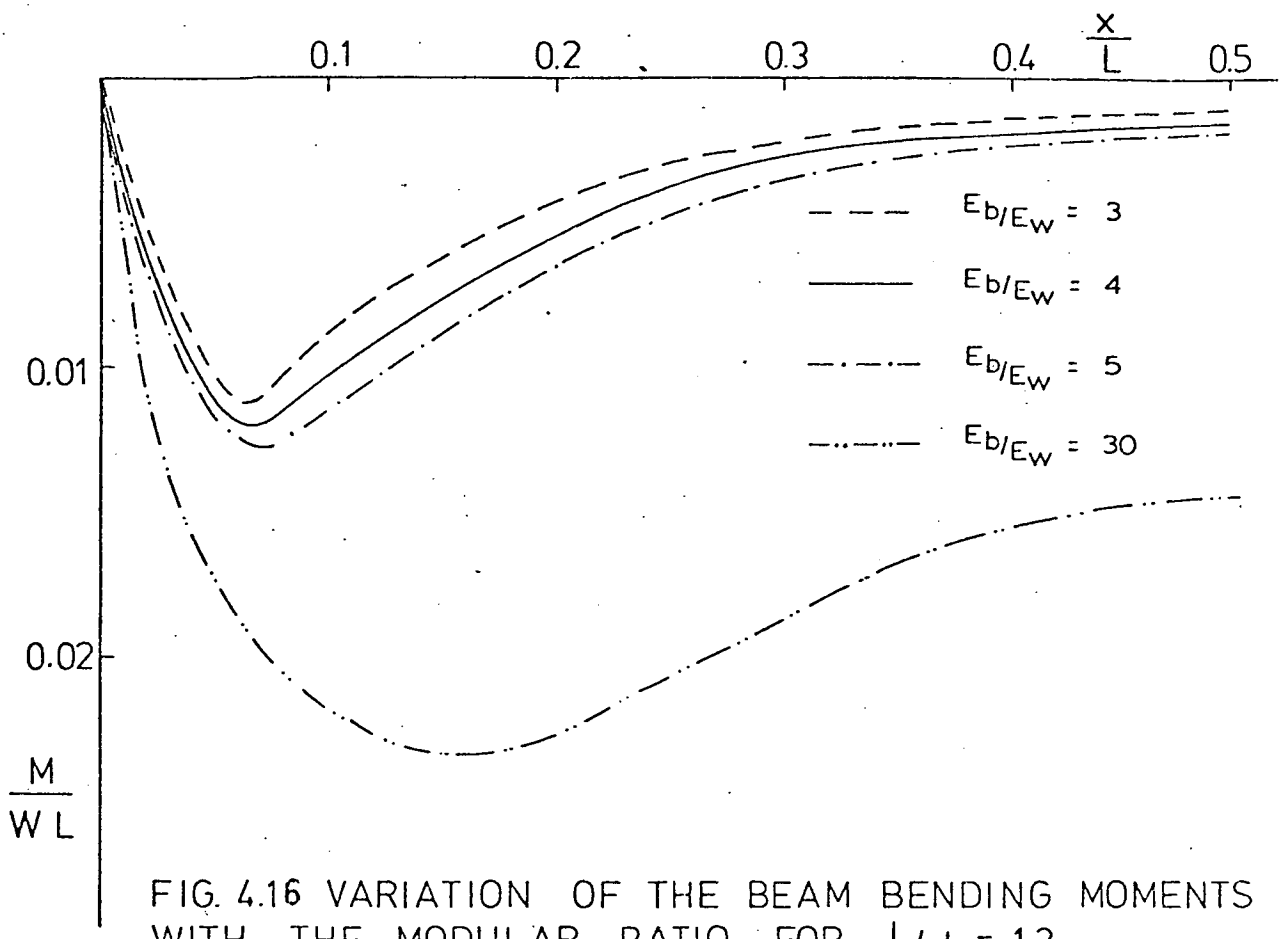

FIG. 4.16 VARIATION OF THE BEAM BENDING MOMENTS WITH THE MODULAR RATIO FOR $L/d = 12$

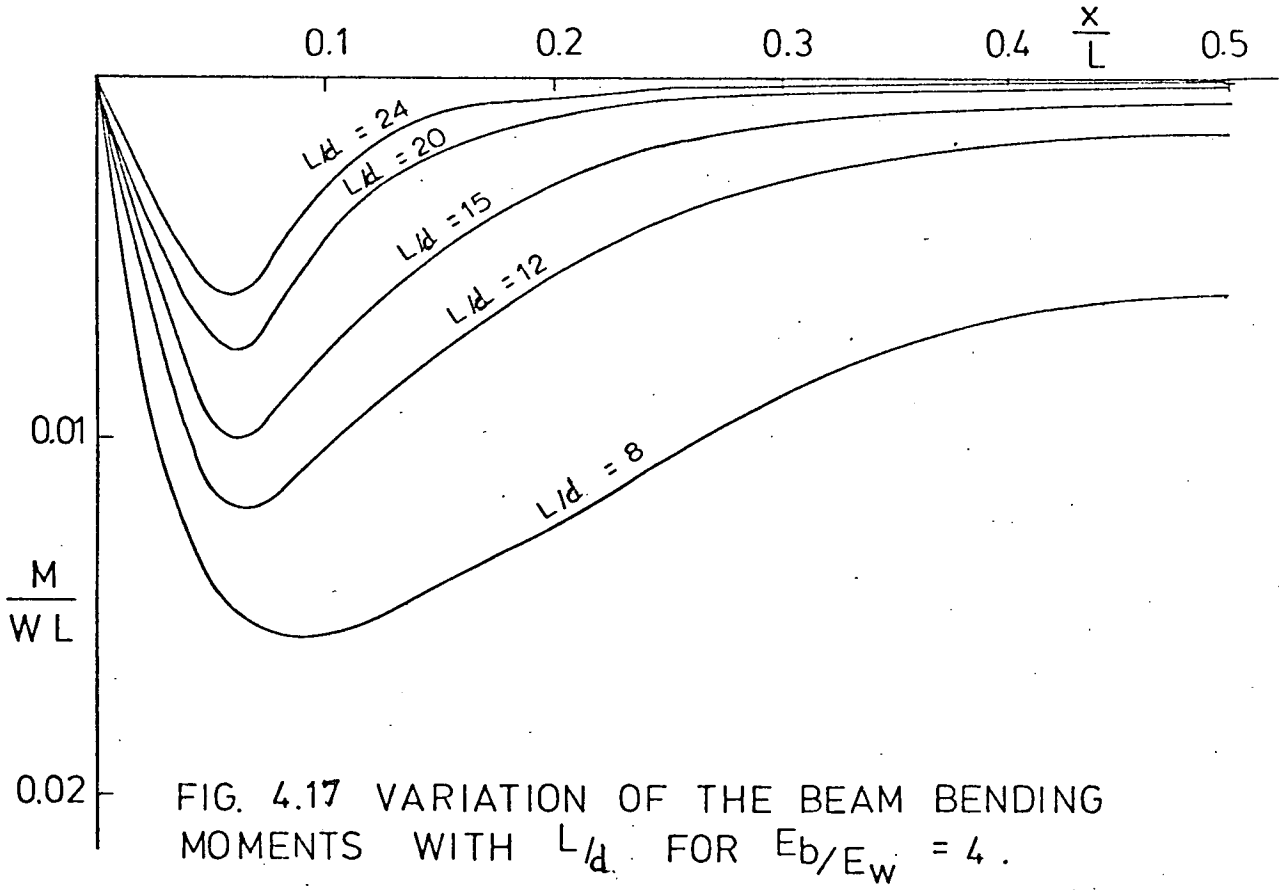

FIG. 4.17 VARIATION OF THE BEAM BENDING MOMENTS WITH L/d FOR $E_{b/E_w} = 4$.

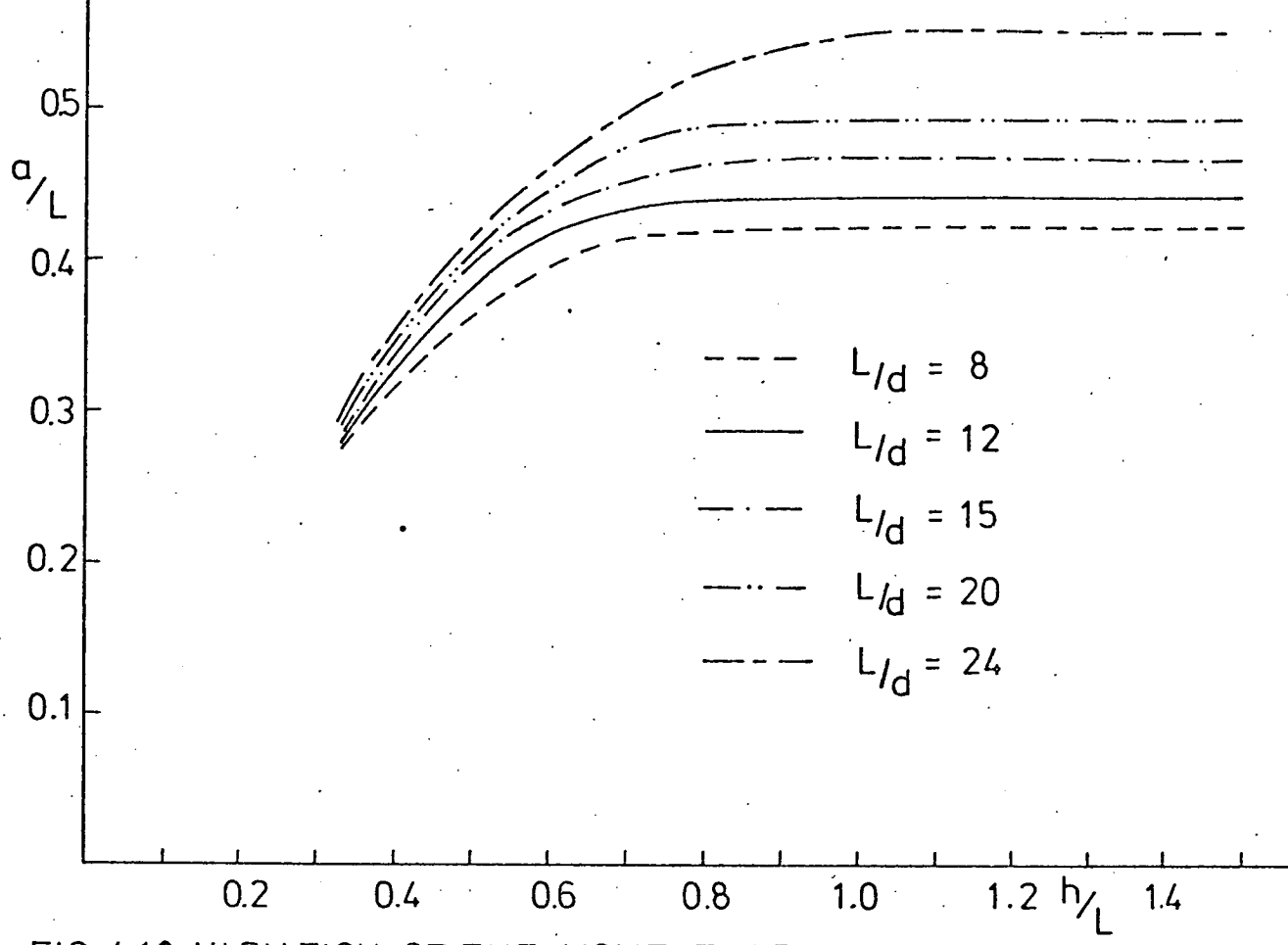

FIG. 4.18 VARIATION OF THE MOMENT ARM WITH h/L FOR $E_b/E_w = 4$.

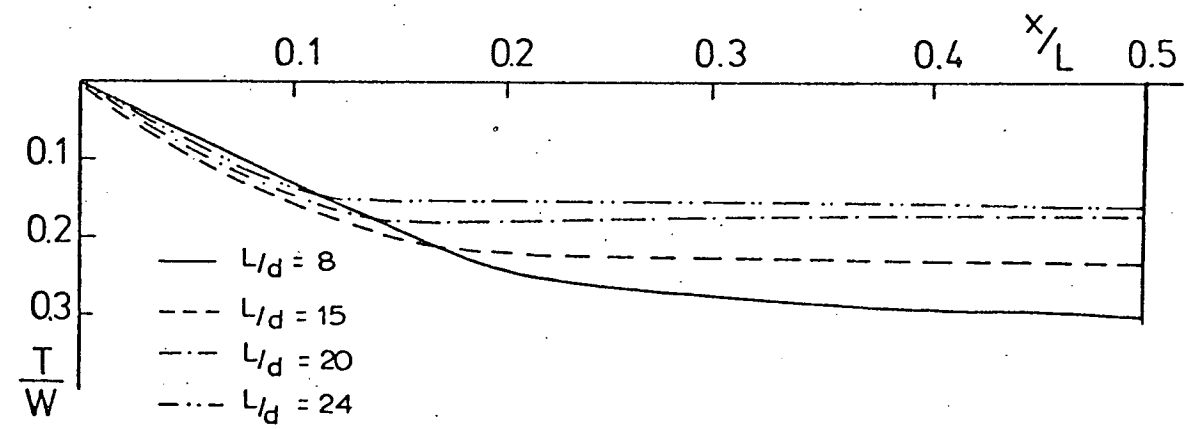

FIG. 4.19 VARIATION OF THE BEAM AXIAL FORCE WITH L/d FOR $E_b/E_w = 4$.

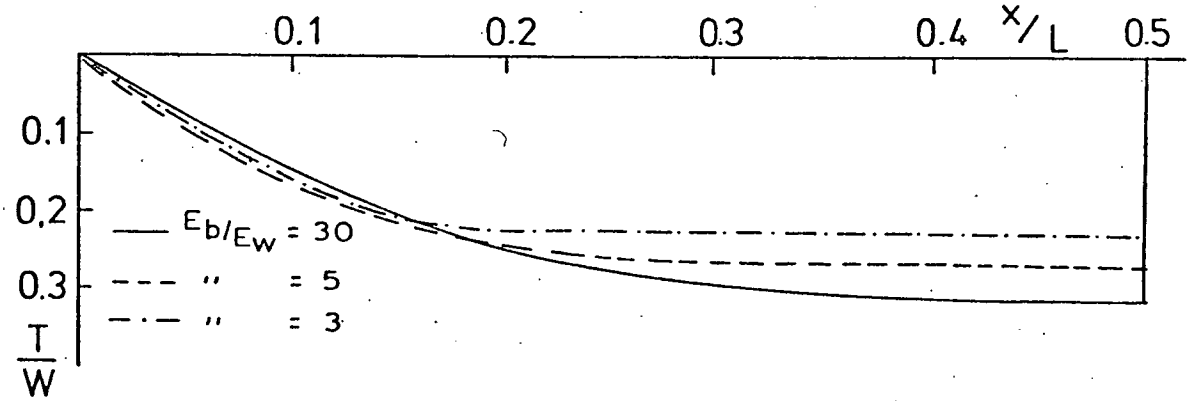

FIG. 4.20 VARIATION OF THE BEAM AXIAL FORCE WITH THE MODULAR RATIO FOR $L/d = 12$

arm expressed as a ratio of the span and also compares the calculated values of the axial force with that obtained by the exact analysis. Figure 4.18 shows the variation of the moment arm with the beam depth and the wall height/span ratio. It will be noted that for walls whose height is greater than the span, there is no change in the moment arm and that the limiting value of the moment arm/span ratio is 0.55. It is also seen from Table 4.7 that the calculated axial force is significantly higher than the exactly predicted. Practically speaking, any cracking which occurs and the consequent transference of resistance against tensile forces to the reinforcement, would lead to an increase in the actual value of the moment arm over that determined theoretically. Accordingly, this method will be conservative and uneconomical in calculating the beam reinforcement.

Figure 4.10 shows the distribution of the shear stress in the wall. This shows concentration of the contact shear stress near the supports. Comparative plots of the shear stress along the contact surface with varying beam span/depth ratio and modular ratio are shown in Figures 4.14 and 4.15 respectively. The results indicate that the contact shear stress is substantially affected by the beam span/depth ratio than by the modular ratio. For the composite action to develop this shear stress must be transmitted efficiently across the boundary between the wall and beam. Shear failure at the interface has been shown by Male and Arbon[15] to result in high tensile stresses developing in the wall

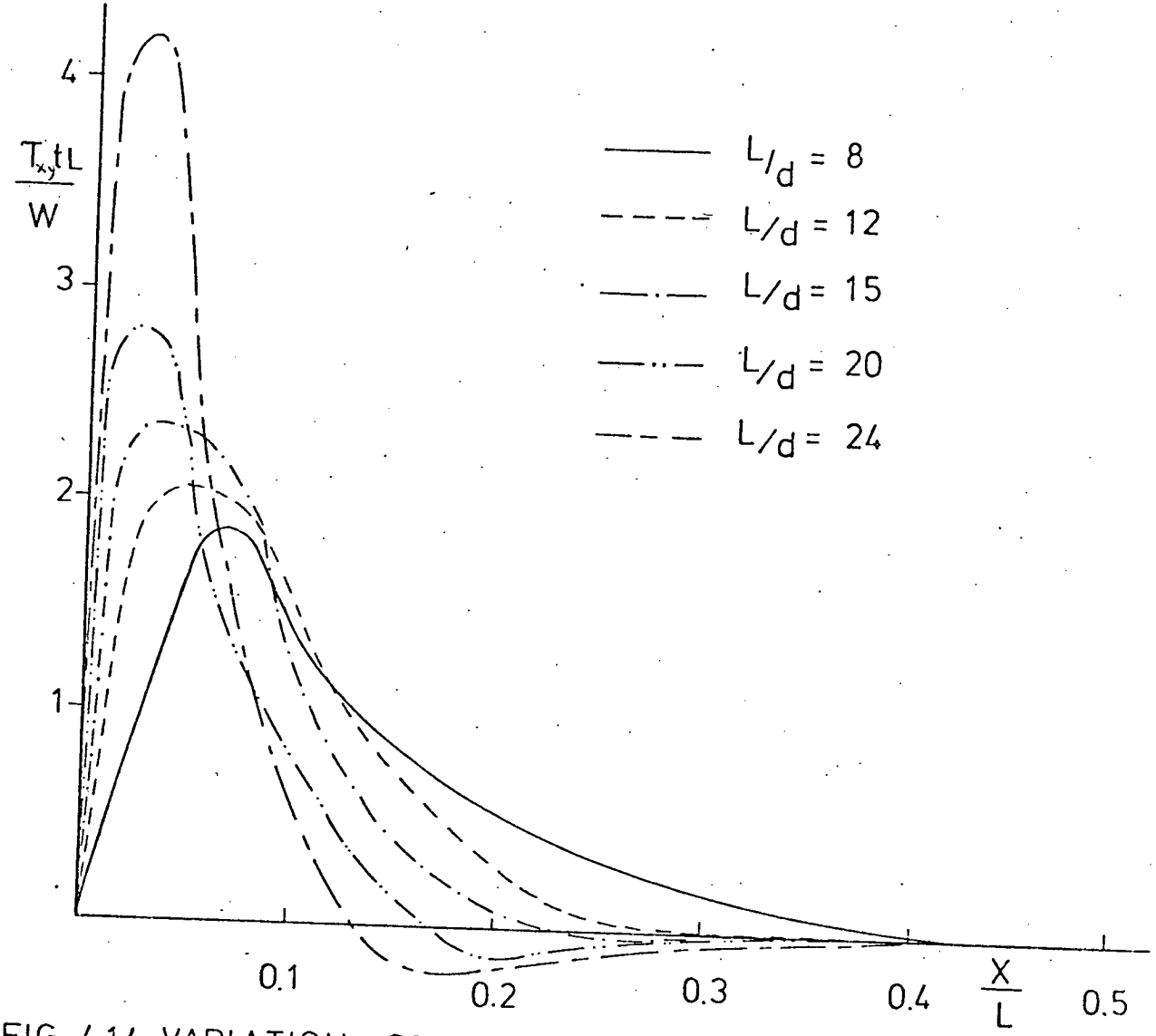

FIG. 4.14 VARIATION OF THE HORIZONTAL SHEAR STRESS AT THE WALL/BEAM INTERFACE WITH L/d FOR $E_{b/E_w} = 4$.

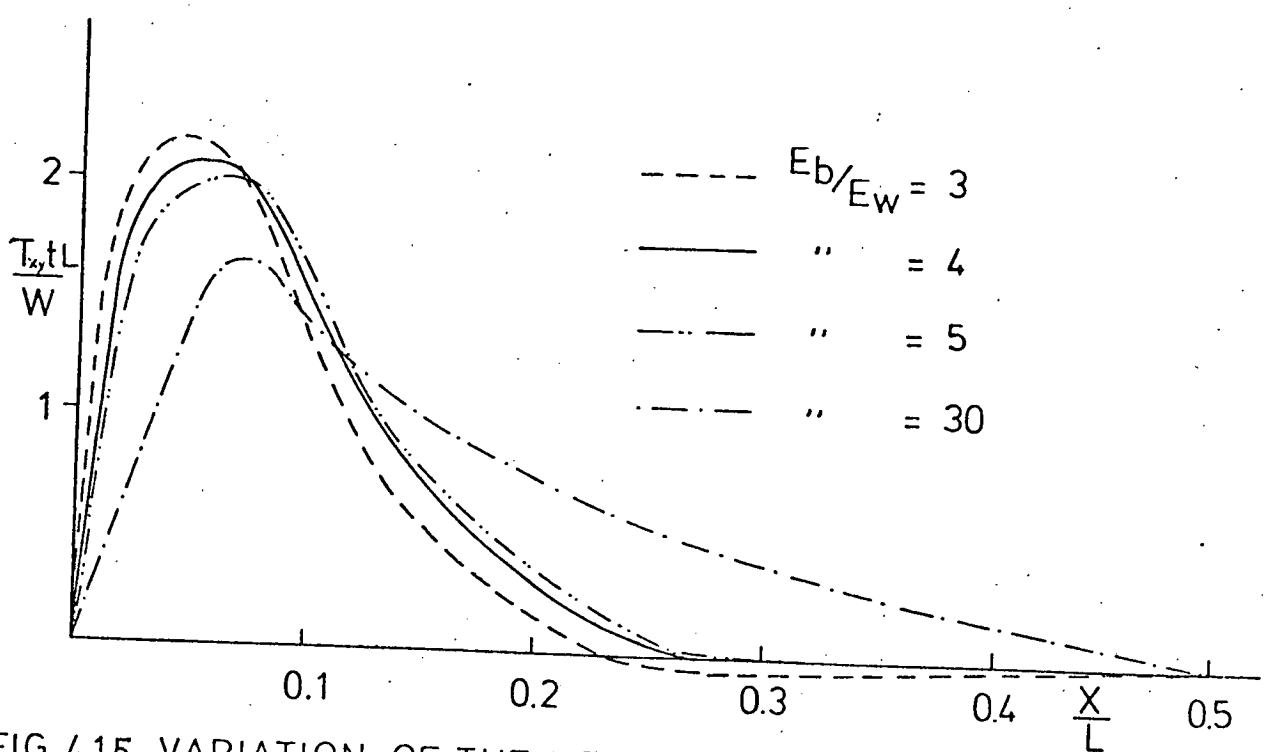

FIG. 4.15. VARIATION OF THE HORIZONTAL SHEAR STRESS AT THE WALL/BEAM INTERFACE WITH E_{b/E_w} FOR $L/d = 12$.

with the probability of cracking. This type of failure is not anticipated in high walls, since the maximum shear stress decreases with the increase in the wall height as shown in Table 4.5.

4.6.2 Beam Forces

The variation of the beam bending moment with the modular ratio and the beam span/depth ratio, are shown in Figures 4.16 and 4.17, respectively. The maximum value of the bending moment occurs very near to the supports whereas the minimum moment occurs at midspan. The results of the maximum and minimum bending moments are summarized in Table 4.4. It can be seen that the influence of the modular ratio on the beam bending moment is substantial. The effect of increasing either the modular ratio or the beam depth is to increase the bending moment across the span of the beam. Theoretically, an infinitely stiff beam would cause the applied load to be transmitted down the wall unchanged for which the value of the bending moment would be WL/8. Furthermore, the results indicate that the wall height does not significantly affect the beam bending moments.

Figures 4.19 and 4.20 illustrate the effect on the beam axial force of varying the beam span/depth ratio and the modular ratio respectively. This shows that the effect of varying the beam span/depth ratio is more noticeable than the effect of the modular ratio. However, the combined effect of both parameters

is reflected by the relative axial stiffness parameter K, illustrated in Table 4.3. This indicates that the axial force at midspan is proportional to the stiffness parameter K. For a relatively flexible beam the results indicate that the axial force in the beam is almost uniform along the span except for a short length near the supports where it increases from zero to a constant value.

The distributions of the beam shear force with varying span/depth and modular ratios have been plotted respectively in Figures 4.20(a) and (b). It can be seen that these follow the same trend as that of the interface vertical stress shown in Figures 4.12 and 4.13.

An examination of these results indicates that for a relatively stiff beam the shear force extends along a distance from the supports equal to one-fifth of the span. For a relatively flexible beam, however, the shear force acts along a distance not more than one-tenth of the span.

Typical results of the supporting beam central deflection at an applied load of 7 KN/M^2, are shown in Table 4.6. Graphical comparison of the influence of the beam span/depth ratio and the modular ratio on the beam deflection are shown in Figures 4.21 and 4.22 respectively. It should be pointed out that the actual deflection in the plastic range is very much under-estimated by the elastic analysis. It is therefore not recommended that any firm conclusion should be drawn in this respect.

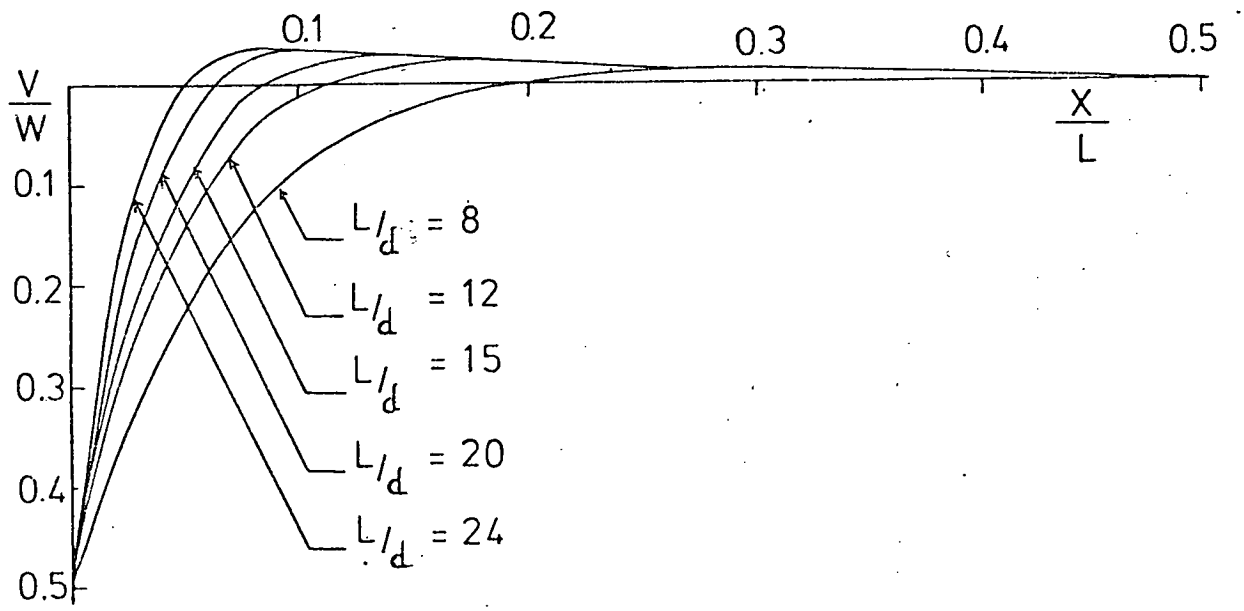

FIG. 4.20a VARIATION OF BEAM SHEAR FORCE WITH (L/d).

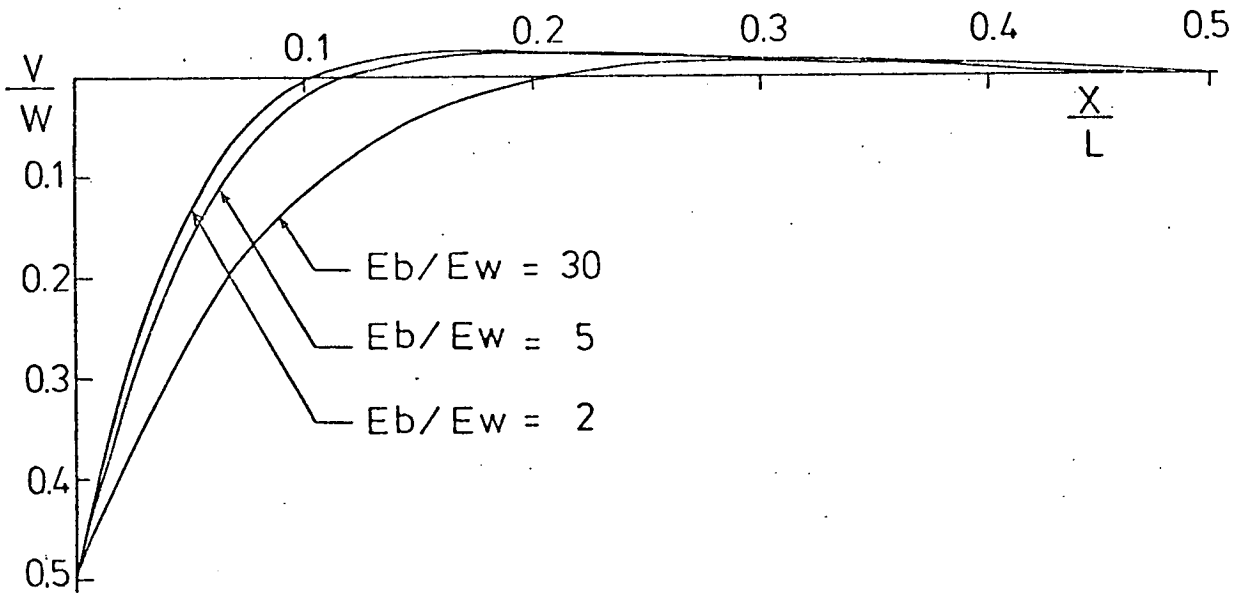

FIG. 4.20b VARIATION OF BEAM SHEAR FORCE WITH (E_b/E_w).

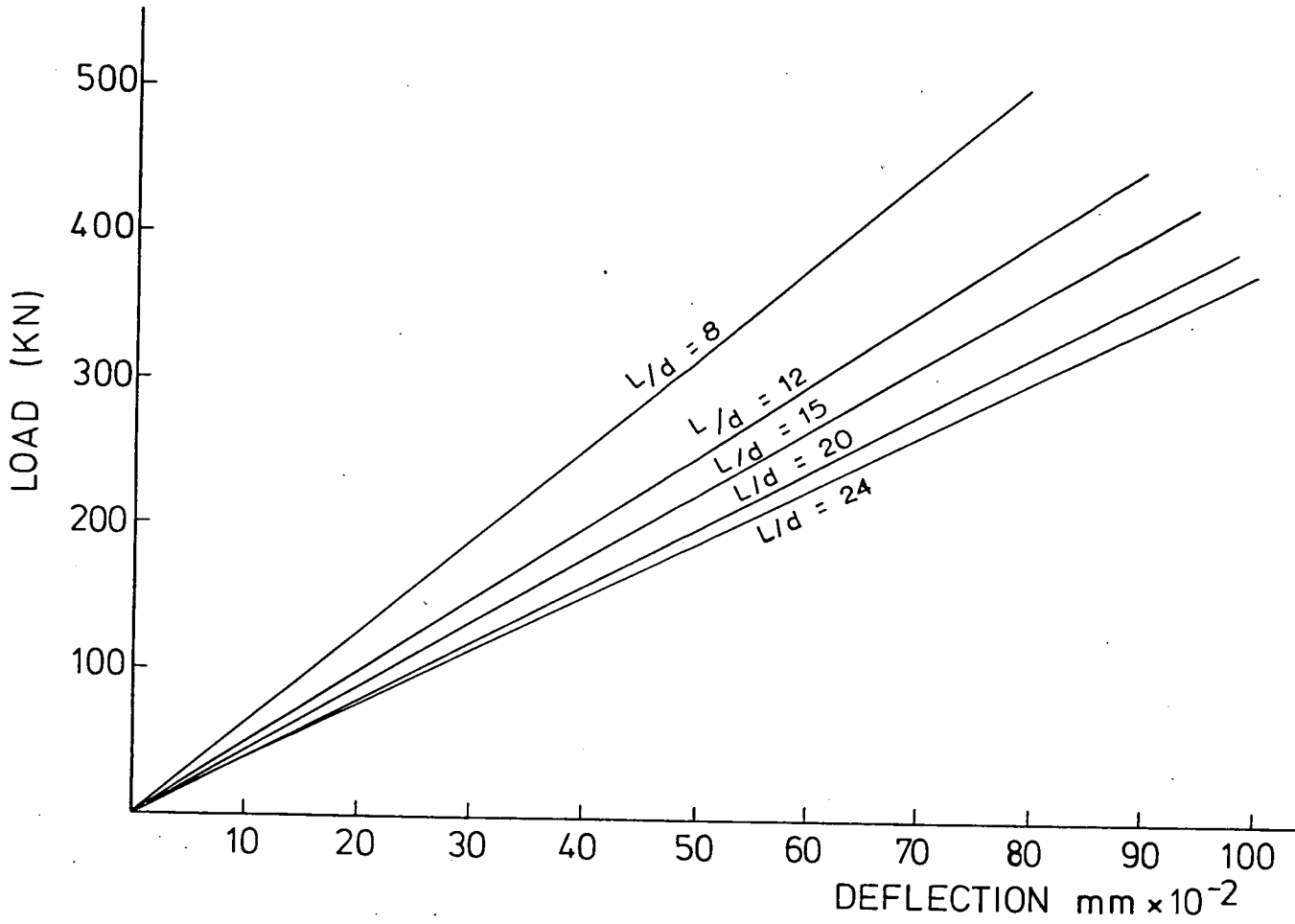

FIG. 4.21 BEAM CENTRAL DEFLECTION AT $E_b/E_w = 4$.

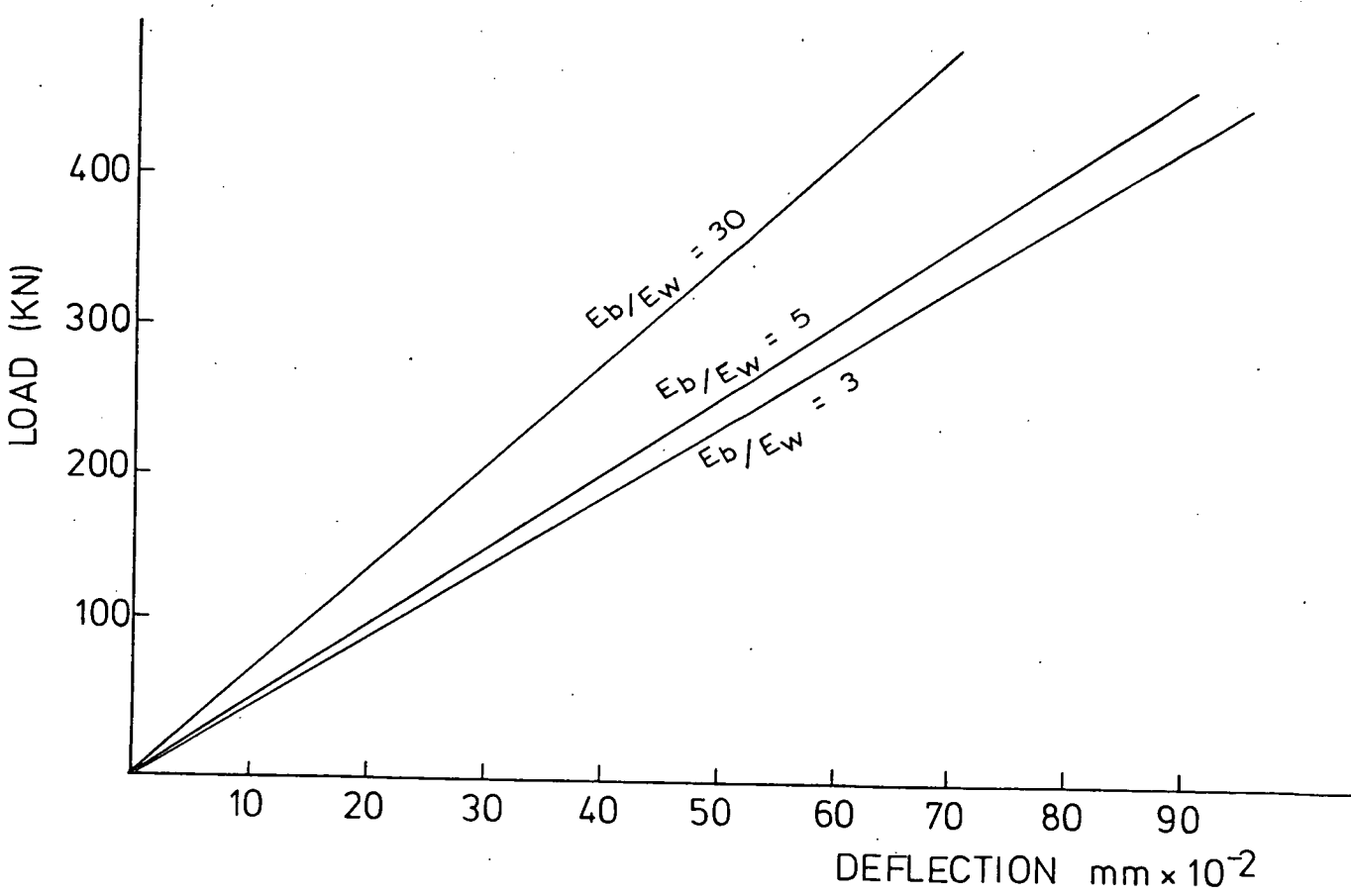

FIG. 4.22 BEAM CENTRAL DEFLECTION AT $L/d = 12$.

4.7 APPROXIMATE ANALYSIS

On the basis of the results obtained by the finite element analysis formulae for approximate design analysis are suggested in the following sections. The proposed approximations are concerned with solid walls on simply supported beams.

4.7.1 Vertical Stress Concentration in the Wall

The composite action between a wall and its supporting beam significantly affects the distribution of load transmitted through the wall to the beam. The composite action is similar to that of a tied arch, the arch forming in the wall with the beam acting as a tie. As a result of the arching action, the vertical stresses in the wall concentrate over the support points as described in Section 4.6. The extent of the influence of different parameters on the degree of the stress concentration has also been discussed. It is noteworthy that in the majority of cases, the vertical stress concentration in the wall is a major failure criterion. The effect of the stress concentration on the beam, however, is to produce a bending moment which is substantially less than would be expected if the load was uniformly distributed over the full span. It has now been established by many researchers[8,13,14,16] that the great differences in flexural stiffness between the wall and the supporting beam is the predominant factor influencing the degree of the stress concentration in the wall and consequently the loading on the beam. Various expressions of the flexural stiffness parameter have been

proposed by different researchers. Table 4.8 shows some of these expressions.

In this approximate analysis, the relative stiffness parameter is denoted by R and is defined as below :

$$R = \left(\frac{h^3 t E_w}{I E_b} \right)^{0.25} \quad \ldots (4.7.1)$$

This parameter, selected on the basis of results obtained by the finite element analysis, is similar to that proposed by Smith and Riddington[14], with the beam span being replaced by the wall height. The term $(h^3 E_w)$ also replaces the modulus of foundation in the parameter used in the analysis of beam on elastic foundation[42]. From the author's point of view, it seems more logical to include the wall height rather than the span, since the parameter describes relative bending rigidities of the wall and the beam. An expression approximating the relation between the stiffness parameter, R, and the stress concentration factor, C, has been derived from the linear relationship shown in Figure 4.23. This is given by :

$$C = (1 + \beta R) \quad \ldots (4.7.2)$$

The stress concentration factor has been defined in Section 4.6 as the ratio of the maximum vertical stress to the average applied stress. According to this definition, the approximate maximum value of the contact stress, f_m, will be :

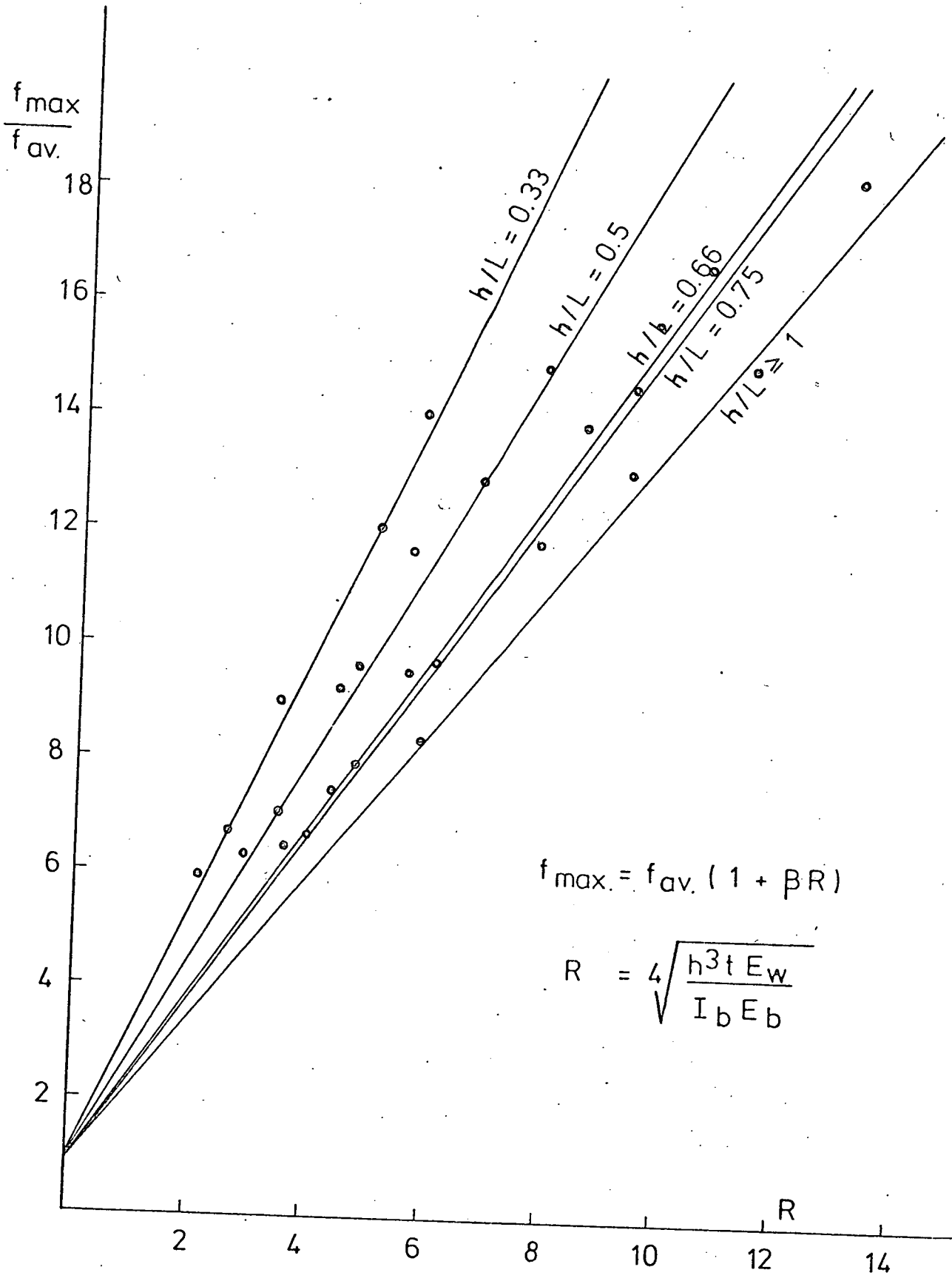

FIG. 4.23 VARIATION OF THE VERTICAL STRESS CONCENTRATION WITH R.

$$f_m = \frac{W}{Lt}(1 + \beta R) \qquad \ldots (4.7.3)$$

The value of the coefficient β is obtained from Figures 4.24 in which β is shown to vary inversely with the wall height/span ratio. This apparently indicates that the value of the maximum vertical stress is inversely proportional to the wall height. However, the opposite is true. It is because with an increasing wall height, the increase in the parameter R in Equation (4.7.3) is much more pronounced than the decreasing effect of the coefficient β.

As described earlier, the stiffness parameter, R, has the most predominant influence on the vertical stress distribution along the contact surface. For a very slender supporting beam, ie, with very high value of R, the distribution of the vertical stress is triangular. This produces the highest stress concentration and the shortest length of contact and is due to the outspread of the arch in the wall. In walls supported on relatively stiff beams with low values of R, the contact vertical stress spreads towards the centre of the span giving rise to the lowest stress concentration over the supports due to the low arch induced in the wall. The distribution of the contact stress in this case is closely approximated to that of a third degree parabola. For beams with intermediate values of R, the corresponding stress distribution along the contact surface is approximated as a simple parabola. The three cases of the beam

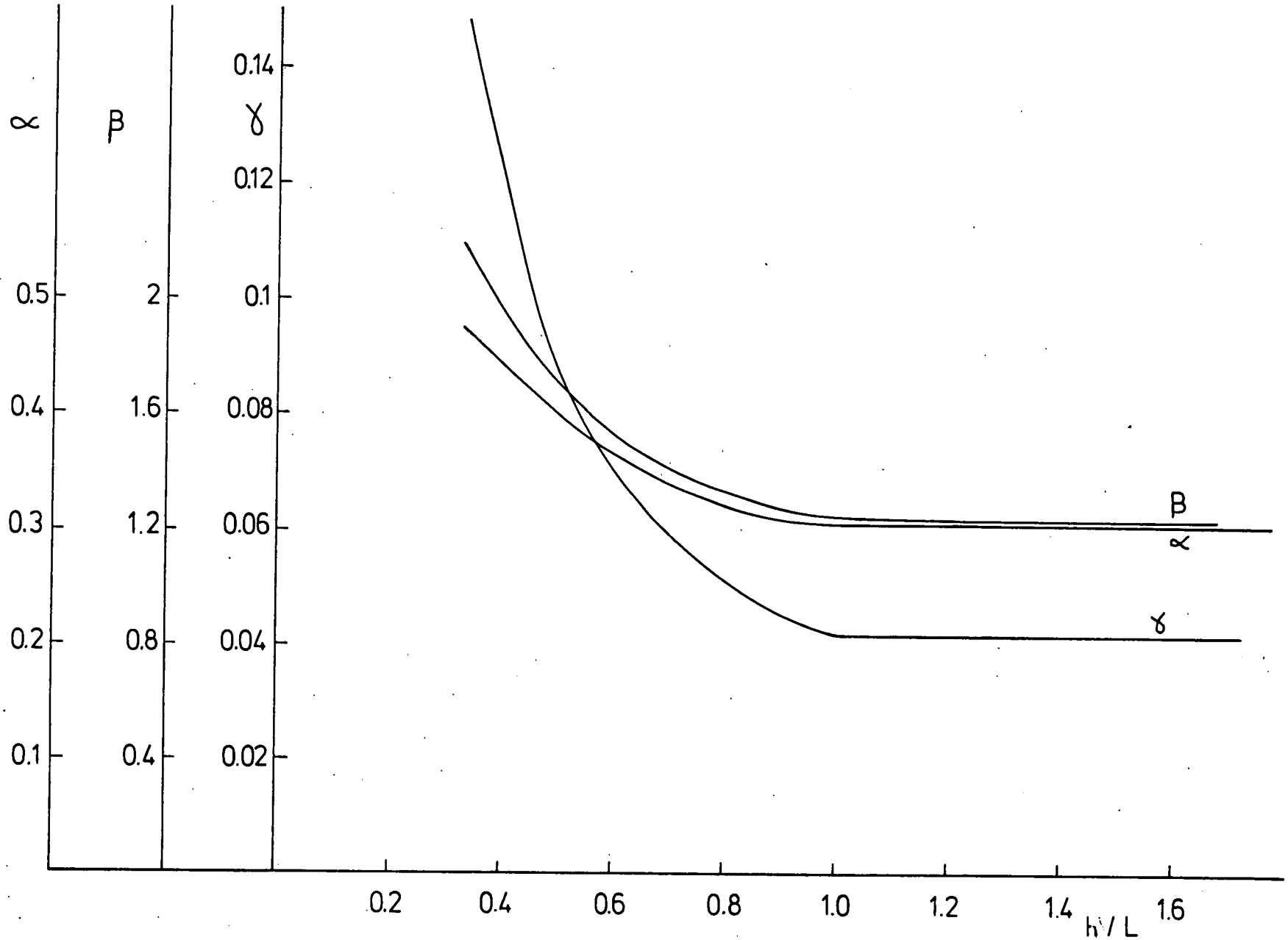

FIG 4.24 VARIATION OF α, β & γ WITH h/L

stiffness and thus the stress distribution have been defined by the following limits of the parameter R :

$R \geqslant 7$ Triangular stress distribution.

$5 < R < 7$ Parabolic distribution (quadratic).

$R \leqslant 5$ Parabolic distribution (cubic).

The distributions are shown diagramatically in Figure 4.25.

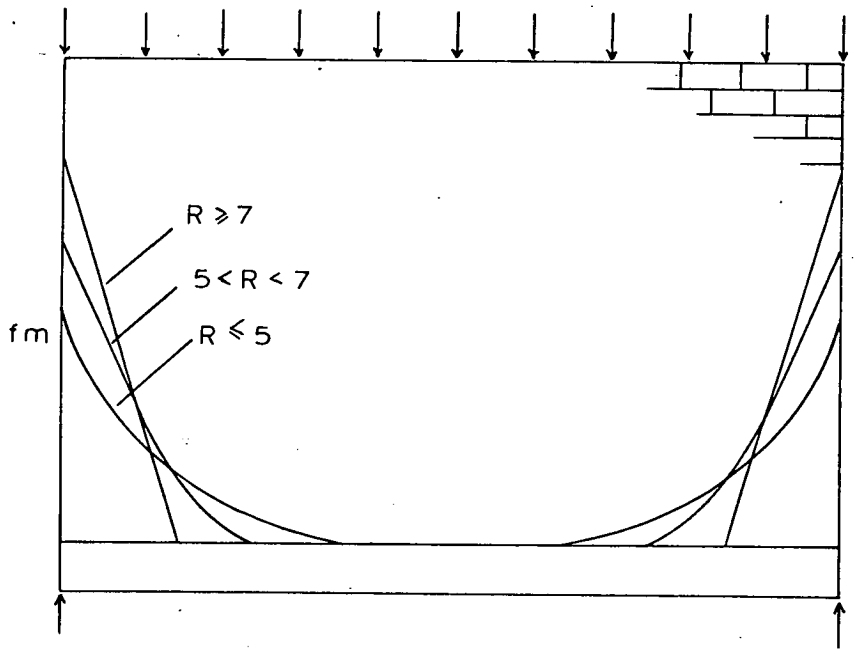

Figure 4.25 Vertical Stress Distribution along the Wall/Beam Interface

By virtue of equilibrium of vertical forces, the area under any of the stress curves in Figure 4.25 should correspond to the applied load. In view of this, the applied load has been calculated for various values of R, using the assumed stress

distributions. The results are summarized in Table 4.9.

The agreement between the exact and the approximately calculated loads is very good for the case of $R \leqslant 5$. For the remaining cases, the discrepancy varies within the limits of between -2.4 to 22 percent indicating an over-estimation of the applied load. This is probably attributable to the tensile loads in the central region of the span, being ignored in the calculation. However, practical values of the parameter, R, as will be seen later, lie within the range of 5 for which the proposed stress distribution appears to be satisfactory.

4.7.2 Beam Axial Force

It may be assumed that the axial force in the supporting beam depends mainly on a relative axial stiffness parameter, K which expresses the relative axial rigidity as :

$$K = \frac{h\ t\ E_w}{A\ E_b} \qquad \ldots (4.7.4)$$

Variation of the axial force at the beam midspan with the stiffness parameter, K, is summarised in Table 4.3. The axial force at midspan has been found to vary linearly with K as shown in Figure 4.26. The relationship can be expressed in the form :

$$T = W(\alpha - \gamma K) \qquad \ldots (4.7.5)$$

α and γ are coefficients whose values depend on the height/span ratio

TABLE 4.9 VARIATION OF THE VERTICAL STRESS CONCENTRATION WITH R

H/L	L/d	E_b/E_w	R	C	LENGTH OF CONTACT $\frac{\ell}{L}$	% DIFFERENCE IN CALCULATED LOAD
0.5	12	30	2.84	6.3	0.31	-3.8
0.5	8	4	3.46	7	0.28	-2.7
0.66	12	30	3.52	6.4	0.30	-4
0.66	8	4	4.30	7.4	0.26	3.4
0.5	12	5	4.44	9.3	0.22	3.3
0.5	12	4	4.70	9.7	0.21	2.4
0.5	12	3	5.05	10.8	0.16	15
0.66	12	5	5.51	9.46	0.19	22
0.5	15	4	5.55	11.6	0.14	7.4
0.66	12	4	5.83	10.0	0.18	22
1.0	8	4	5.83	8.2	0.22	17
0.66	12	3	6.26	11.1	0.15	11
0.75	12	4	6.36	10.8	0.17	20
0.75	12	3	6.84	11.5	0.15	17
0.66	15	4	6.89	11.9	0.13	-2.4
0.50	24	4	7.9	14.8	0.08	15
0.66	20	4	8.55	13.6	0.08	12
0.66	24	4	9.8	14.8	0.07	3

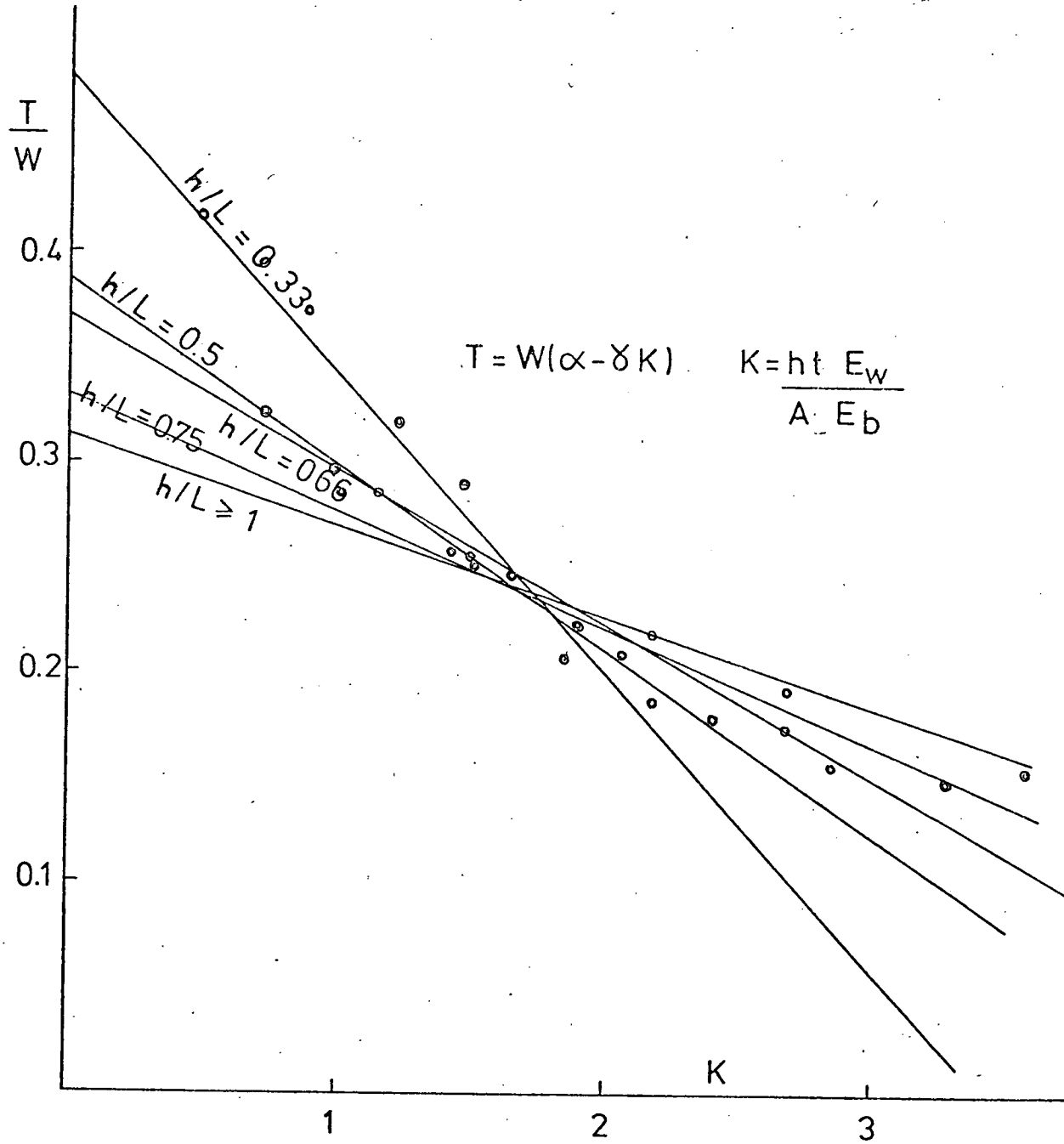

FIG. 4.26 VARIATION OF THE BEAM AXIAL FORCE (T) WITH THE AXIAL STIFFNESS (K).

and can be obtained from Figure 4.24.

For a typical case of brickwork wall whose height/span ratio equals 0.66, supported on a reinforced concrete beam whose span/depth ratio and width are respectively 17.5 and 1.5 times the wall thickness, the approximately predicted axial force at midspan is W/4.34. A corresponding value of W/4 has been estimated by Wood and Simms[3], by assuming a parabolic line of thrust inside the wall. Green[16], using a moment arm of 0.55 times the span, has estimated the force to be W/4.4. In both cases Wood and Green did not consider the effect of the modular ratio and the relative beam stiffness.

An interesting observation drawn from Figure 4.26 is that for a value of the stiffness parameter K equals 1.75, the corresponding axial force is always W/4.32, irrespective of the wall height/span ratio. This value is almost equal to that derived for the above general case.

4.7.3 Peak Shear Stress on the Wall/Beam Interface

For full composite action to develop between the wall and its supporting beam, the shear strength at the wall/beam boundary should be adequate to transfer the horizontal shear stress induced across the interface as a result of the arching action. Figure 4.27 shows the forces acting on a beam and wall elements.

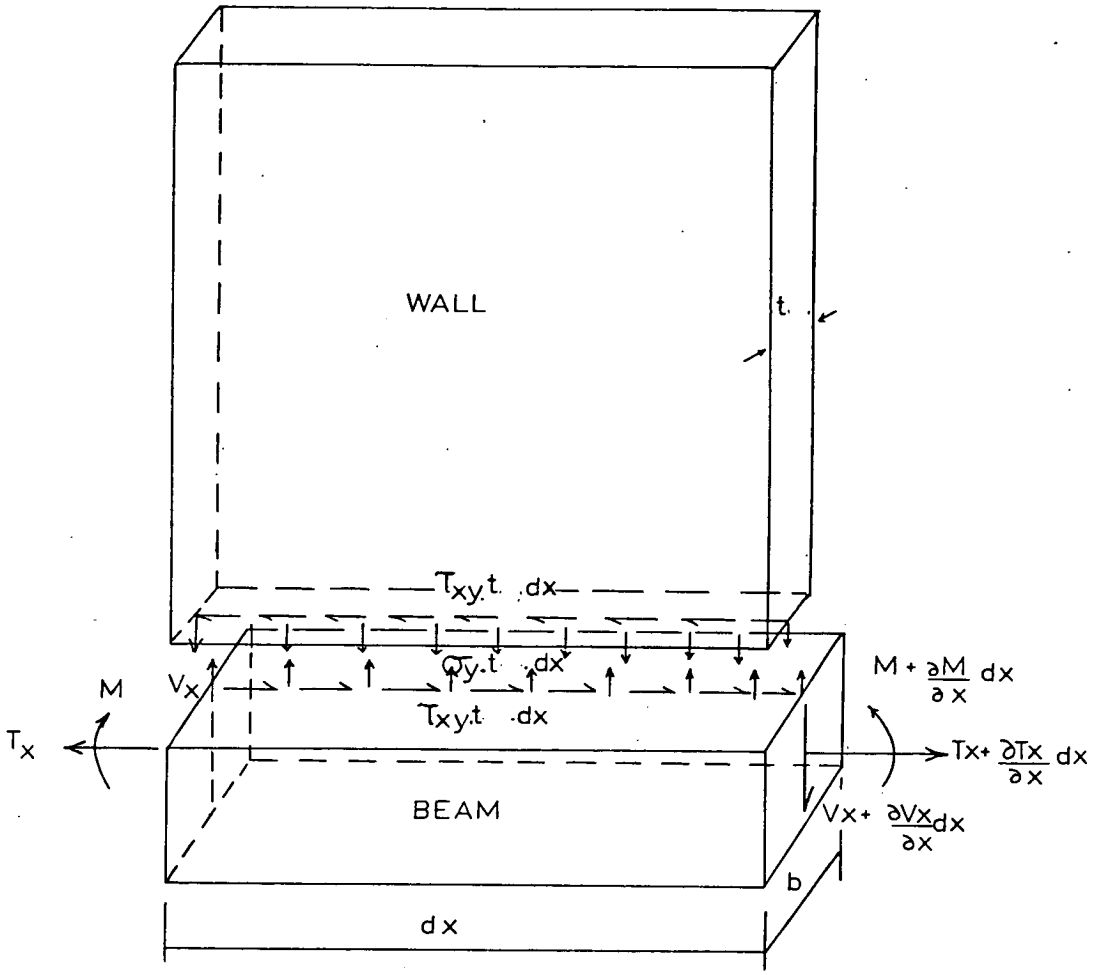

Figure 4.27 Forces on a Wall/Beam Element

Resolving horizontally, we obtain :

$$\tau_{xy} t \, dx = \frac{\partial T_x}{\partial x} dx \qquad \ldots (4.7.6)$$

Integration of both sides between the limits of zero and L/2 yields :

$$\int_0^{L/2} \tau_{xy} t \, dx = T \qquad \ldots (4.7.7)$$

As T is the axial force in the supporting beam, this relation tends to indicate that for the composite action to develop, the interface shear force must be resisted by the supporting beam.

For the approximate estimation of the maximum shear stress at the wall/beam interface, it will be assumed that the distributions of the vertical and shear stresses along the interface are both triangular as shown in Figure 4.28.

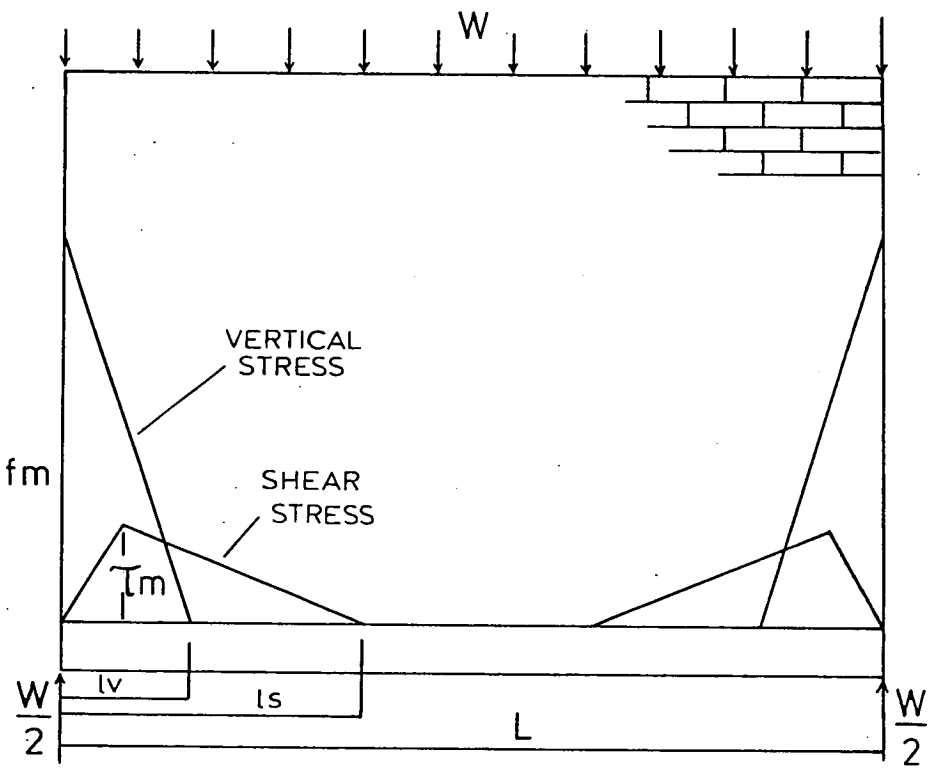

Figure 4.28 Vertical and Shear Stress Distributions at Wall/Beam Interface

From the finite element analysis it has been found that the length of contact of the horizontal shear stress varies from two to three times that of the vertical stress. A conservative value of two will be assumed.

By equilibrium of vertical forces :

$$f_m \ell_v t = W \qquad \ldots (4.7.8)$$

Substitution of f_m from (4.6.3) yields :

$$\ell_v = \frac{L}{(1 + \beta R)} \qquad \ldots (4.7.9)$$

$$\therefore \ell_s = \frac{2L}{(1 + \beta R)} \qquad \ldots (4.7.10)$$

Evaluation of the integral in (4.7.7) by assuming triangular stress distribution gives :

$$\frac{\tau_m \ell_s t}{2} = T \qquad \ldots (4.7.11)$$

Noting that,

$$T = W(\alpha - \gamma K)$$

$$\therefore \tau_m = \frac{W(\alpha - \gamma K)(1 + \beta R)}{Lt} \qquad \ldots (4.7.12)$$

As mentioned earlier, the shear strength of the interface joint should be capable of resisting this maximum shear stress. Tests on 'three brick' specimens carried out by Burhouse[11] showed that there are two components contributing to the shear strength of the joint. These are the bond strength of the

mortar and a frictional component given by the following relationship :

$$\tau_j = \tau_b + \mu f \qquad \ldots (4.7.13)$$

in which τ_b is the bond shear strength, μ is the coefficient of friction, and f is the compressive stress normal to the shearing plane. A conservative estimate of the coefficient of friction between the brickwork and concrete is 0.5[14]. The ultimate shear strength of the joint is thus given by :

$$\tau_{ult} = \tau_b + 0.5\ f_m \qquad \ldots (4.7.14)$$

As the peak shear stress occurs close to the supports, f_m is taken as that given by equation (4.6.3) :

$$\therefore\ \tau_{ult} = \tau_b + \frac{0.5\ W}{Lt}\ (1 + \beta R) \qquad \ldots (4.7.15)$$

It would be unwise to depend on the mortar bond strength which may be destroyed by loads applied directly to the beam. Moreover, in the presence of a damp-proof course, the resistance to sliding would have to be provided by friction. In view of this, comparison of equations (4.7.12) and (4.7.15) reveals that the horizontal shear stress will be adequately transmitted through the interface joint provided that :

$$W\left(\alpha - \frac{\gamma h\ t\ E_w}{A\ E_b}\right) \leqslant 0.5 \qquad \ldots (4.7.16)$$

This condition, however, is satisfied in all wall/beams for which the value of α is less than 0.5, Figure 4.24. Since this corresponds to a height/span ratio of 0.3, it follows that the interface peak shear stress will not be considered as a failure criterion. In this regard, Rosenhaupt[6] achieved satisfactory behaviour of walls at height/span ratio as low as 0.29 but his results do not agreee with tests carried out by Burhouse[11]. Further research is required to establish a lower bound on this value.

4.7.4 Beam Bending Moment

The supporting beam is subjected to the action of vertical forces and horizontal shear at the wall/beam interface. The horizontal shear force is thus eccentric with respect to the centroid of the beam. This has the effect of causing a substantial reduction in the bending moments produced by the vertical forces. This effect is much more pronounced at midspan where the bending moment is found to be minimum. The maximum bending moment occurs very near to the supports where the effect of the force is insignificant.

It has been established in Section 4.7.1 that the vertical stress distribution is governed by three limits defined for the parameter R. Accordingly, moment expressions corresponding to each limit will be derived.

The bending moment due to the vertical loading is maximum

over the central region of the span and is obtained with reference to Figure 4.29 by :

$$M_v = \frac{Wr\ell_v}{2} \qquad \ldots (4.7.17)$$

in which $r\ell_v$ is the distance from the support reaction to the centroid of the stress diagram.

By equilibrium of forces :

$$\frac{W}{2} = \lambda f_m \ell_v t \qquad \ldots (4.7.18)$$

where λ is a coefficient which depends on the shape of the stress diagram. Substitution of ℓ_v from (4.7.18) to (4.7.17) gives :

$$M_v = \frac{W^2 r}{4 f_m \lambda t} \qquad \ldots (4.7.19)$$

f_m is given by Equation (4.7.3) as :

$$f_m = \frac{W}{Lt}(1 + \beta R)$$

$$\therefore \quad M_v = \frac{WLr}{4\lambda(1 + \beta R)} \qquad \ldots (4.7.20)$$

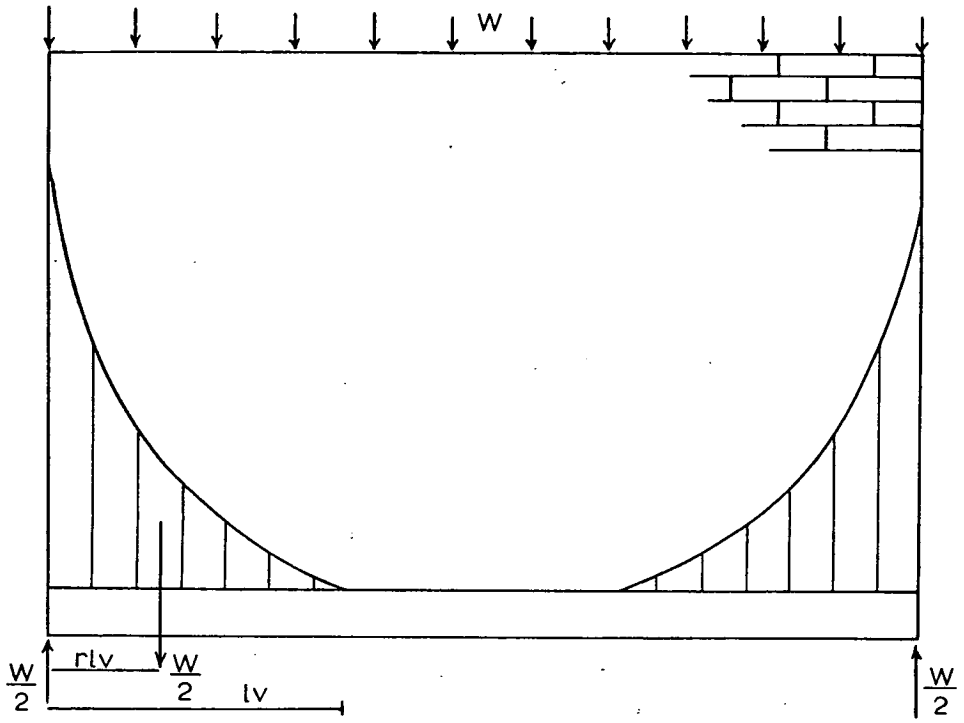

FIG. 4.29 VERTICAL LOADING ON SUPPORTING BEAM.

The bending moment produced by the horizontal shear force at any distance x from the support is given by :

$$M_H = -\frac{d}{2} \int_0^x \tau_x \cdot t \cdot dx \qquad \ldots (4.7.21)$$

The value of the integral can be shown, with the aid of Figure 4.27, to be equal to the axial force T_x at the distance x.

$$\therefore \quad M_H = -\frac{d}{2} \cdot T_x \qquad \ldots (4.7.22)$$

The force T_x can be related to the axial force T at mid-span by the approximate linear relationship shown in Figure 4.30 and given by :

$$T_x = \frac{2\,T\,x}{L} \qquad \ldots (4.7.23)$$

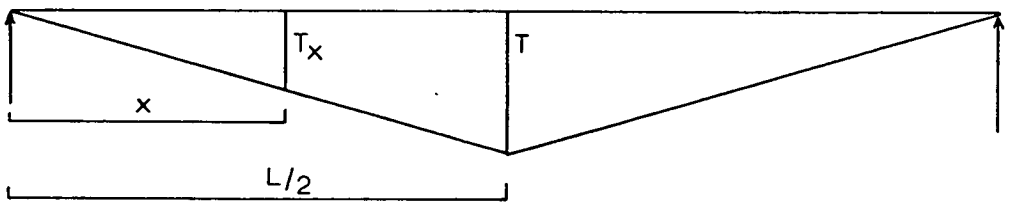

FIG. 4.30 APPROXIMATE DISTRIBUTION OF AXIAL FORCE IN SUPPORTING BEAM.

Substituting for T from (4.7.5) gives :

$$M_H = -\frac{dWx}{L}(\alpha - \gamma K) \qquad \ldots (4.7.24)$$

The resultant bending moment produced by the combined effect of the vertical and horizontal forces is therefore :

$$M_R = M_V + M_H = \frac{WL^2 r - 4\lambda dWx(\alpha - \gamma K)(1 + \beta R)}{4\lambda L(1 + \beta R)} \qquad \ldots (4.7.25)$$

The maximum bending moment is assumed to occur at a distance from the support reaction equal to the contact length. This assumption, however, is approximate since the point of maximum bending moment should be obtained by differentiating the moment

expression with respect to x.

The maximum bending moment is thus given by :

$$M_m = \frac{WLr - 2Wd(\alpha - \gamma K)}{4\lambda(1 + \beta R)} \qquad \ldots (4.7.26)$$

The value of the central bending moment obtained at x = L/2 is as follows :

$$M_c = \frac{WLr - 2Wd(\alpha - \gamma K)(1 + \beta R)}{4\lambda(1 + \beta R)} \qquad \ldots (4.7.27)$$

The three cases considered according to the magnitude of the relative stiffness parameter R, are as follows :

Case (a)

$R \leqslant 5$ stiff beam

$r = 0.2$ and $\lambda = 0.25$

The maximum bending moment occurs at a distance ℓ_v from the supports given by :

$$\ell_v = \frac{2L}{(1 + \beta R)}$$

and its magnitude is given by :

$$M_m = \frac{WL - 10\ Wd(\alpha - \gamma K)}{5(1 + \beta R)} \qquad \ldots (4.7.28)$$

and the midspan moment is obtained by :

$$M_c = \frac{WL - 2.5\ Wd(\alpha - \gamma K)(1 + \beta R)}{5(1 + \beta R)} \qquad \ldots (4.7.29)$$

Case (b)

$5 < R < 7$ flexible beam

$r = 0.25$ and $\lambda = 0.33$

The maximum moment occurs at a distance from the supports equal to

$$\ell_v = \frac{3L}{2(1 + \beta R)}$$

Its magnitude is therefore :

$$M_m = \frac{WL - 8\ Wd(\alpha - \gamma K)}{5.33(1 + \beta R)} \qquad \ldots (4.7.30)$$

and the corresponding central moment :

$$M_c = \frac{WL - 2.66\ Wd(\alpha - \gamma K)(1 + \beta R)}{5.33(1 + \beta R)} \qquad \ldots (4.7.31)$$

Case (c)

$R \geqslant 7$ very flexible beam

$r = 0.33$ and $\lambda = 0.5$

The maximum bending moment occurs at $\ell_v = L/(1 + \beta R)$, and is approximated as :

$$M_m = \frac{WL - 6\,Wd(\alpha - \gamma K)}{6(1 + \beta R)} \qquad \ldots (4.7.32)$$

and the midspan moment as :

$$M_c = \frac{WL - 3\,Wd(\alpha - \gamma K)(1 + \beta R)}{6(1 + \beta R)} \qquad \ldots (4.7.33)$$

4.7.5 Beam Central Deflection

The beam central deflection is computed based on the assumption that the vertical stress distribution along the wall/beam interface is triangular, ie, for the case of a very flexible beam in which the deflection is the most excessive.

The vertical deflection due to the triangular loadings is given by :

$$\delta_v = \frac{WL^3(3 + 10\,\beta R + 5\,\beta^2 R^2)}{240\,E_b I(1 + \beta R)^3} \qquad \ldots (4.7.34)$$

The horizontal shear force at the wall/beam interface causes an upward vertical deflection estimated by :

$$\delta_H = \frac{WL^2 d(\alpha - \gamma K)}{24\,E_b I} \qquad \ldots (4.7.35)$$

The central deflection of the panel due to the shear effect is obtained from the theory of elasticity[43] on the assumption of zero Poisson ratio :

$$\delta_s = \frac{3\,WL}{10\,E_w ht} \qquad \ldots (4.7.36)$$

The resultant central deflection is thus :

$$\delta_R = \frac{WL^3(3 + 10\,\beta R + 5\,\beta^2 R^2)}{240\,E_b I(1 + \beta R)^3} + \frac{3\,WL}{10\,E_w ht} - \frac{WL^2 d(\alpha - \gamma K)}{24\,E_b I} +$$

$$\frac{1}{384} \cdot \frac{W_b L^3}{E_b I} \qquad \ldots (4.7.37)$$

where the last term accounts for beam self weight.

4.7.6 Ultimate Load

For a more accurate assessment of the ultimate strength, the behaviour of the composite structure at the plastic stage should be investigated. However, in the present study, only elastic analysis has been considered and therefore any prediction of the ultimate strength will be grossly approximate.

As described earlier in Chapter 3, the test walls exhibited two distinct types of failures. These are either by tensile splitting of bricks over the supports, usualling accompanied by crushing of corner bricks, or by shear failure across the wall height near the supports. In all walls that failed in shear, diagonal shear cracking was first observed in the supporting beam. Considering this, it has been mentioned before that the shear strength of the wall is mainly affected by the shear strength of the supporting beam and that failure

of the supporting beam in shear, will eventually lead to the wall failure.

The common type of failure observed in most of the test panels occurred by tensile splitting and crushing of corner bricks over the supports. Provided that the supporting beam is of sufficient strength to avoid failure in axial tension before the wall failure, the ultimate strength of the composite structure is thus defined by crushing of the wall material at points where the maximum compressive strength of the material has been exceeded. These are usually the support points over which the vertical stress concentrates as a result of the induced arching action. In this locality the bricks are in a state of axial compression and lateral tension due to the lateral differential strain resulting from the difference in the elastic properties of bricks and mortar. The mortar, however, is in a state of triaxial compression.

When the maximum tensile stress exceeds the brick tensile strength, tensile splitting occurs. The horizontal bending stresses over the support region are sufficiently small to be neglected, Figure 4.9. It is also assumed that the maximum shear stress at the wall/beam interface occurs at the point at which tensile cracking occurs. Assuming the maximum vertical stress to be occurring at that point, the tensile stress in the wall is given by :

$$f_t = \frac{W(1 + \beta R)}{2\ Lt} \left(\sqrt{1 + 4(\alpha - \gamma K)^2} - 1\right) \qquad \ldots (4.7.38)$$

and the load at which the tensile cracks appear is then :

$$W_c = \frac{2f'_t Lt}{(1 + \beta R)(\sqrt{1 + 4(\alpha - \gamma K)^2} - 1)} \quad \ldots (4.7.39)$$

where f'_t is the brick maximum tensile strength.

At the occurrance of these tensile cracks, the panel, however, will not be assumed to have failed. Upon the further increase of load, failure of bricks over the supports will take place in compression, typically by tensile splitting and crushing. At this stage the maximum compressive stress f_c has exceeded the maximum compressive strength of the bricks f'_c. It follows that :

$$f'_c = \frac{W_u}{2Lt}(1 + \beta R)[1 + \sqrt{1 + 4(\alpha - \gamma K)^2}] \quad \ldots (4.7.40)$$

and the ultimate load W_u is thus given by :

$$W_u = \frac{2 f'_c Lt}{(1 + \beta R)\ [1 + \sqrt{1 + 4(\alpha - \gamma K)^2}]} \quad \ldots (4.7.41)$$

4.8 COMPARISON OF RESULTS

4.8.1 Vertical Stress Concentration

Table 4.10 shows comparison between the vertical stress

TABLE 4.10 COMPARISON OF THE VERTICAL STRESS CONCENTRATION

L (m)	H/L	AUTHOR	SMITH AND RIDDINGTON	BURHOUSE	YETTRAN AND HIRST	COULL	COLBOURNE	LEVY AND SPIRA
2.74	0.66	5.26	7.51	-	6.02	-	-	-
2.74	0.66	5.88	8.75	-	7.07	-	-	-
2.74	0.66	6.77	10.55	-	8.36	4.53	6.96	-
2.74	0.66	8.17	13.46	-	10.10	-	-	-
2.74	0.66	10.72	18.93	-	12.68	-	-	-
1.8	0.58	4.21	5.68	3.22	-	-	-	-
1.8	0.58	6.70	10.82	5.66	-	-	-	-
1.8	0.58	10.6	19.37	8.34	-	-	-	-
1.8	0.83	11.33	19.37	8.34	-	-	-	-
2	0.64	10.5	19.1	-	-	-	-	9.36
3.6	0.50	8.61	15.44	8.33*	-	-	-	-
3.6	0.73	9.22	15.44	10.89*	-	-	-	-
3.6	0.75	9.55	15.44	8.72*	-	-	-	-

The authors results based on equation (4.6.2) given by $C = [1 + \beta(\frac{h^3 t\, E_w}{I\, E_b})^{0.25}]$

Smith and Riddington formula expressing the stress concentration is given by

$$\sigma = 1.63 \frac{W}{Lt} (E_w t L^3/EI)^{0.28} \qquad (46)$$

.

The results predicted by Burhouse[11] are obtained using the lattic analogy of Colbourne. The three last values* are from the experimental results on full scale tests.

The method used by Yettram and Hirst[12] was the shear lag method. Coull[18] used the variational method and Levy and Spira[13] used the stress function and the finite difference technique.

concentration in the wall predicted by the approximate method and other existing methods. The results compare favourably with those predicted by the lattice analogy of Colbourne and the stress function of Levy and Spira. The results are also in good agreement with the experimental results from full scale tests carried out by Burhouse. The shear lag method slightly overestimates the vertical stress which may be due to the effect of the stringers width. The variational method of Coull, on the other hand, tends to underestimate the vertical stress concentration and this as explained earlier, may be due to the very few terms considered in the assumed stress series. The results predicted by the approximate method of Smith and Riddington appear to be very high in comparison with most of other results. In their analyses, the relative stiffness parameter assumed in the calculation of the peak vertical stress contains the span of the wall as a variable and no account has been made for the varying wall height. In this regard, they proposed a limit for the wall height of not less than 0.6 times the span. It follows that all walls supported on identical beams will acquire the same stress concentration irrespective of their heights. The present approximate expression for the maximum stress in the wall, takes into account the effect of varying both the wall height and span. The results are thus shown to be in a reasonable agreement with most other solutions.

4.8.2 Contact Shear Stress

In Table 4.10 comparison is made between the exact peak

shear stress at the wall/beam interface predicted by the finite element, the approximate results predicted by equation (4.7.13), and the results predicted by the approximate formula of Smith and Riddington. The agreement between the exactly calculated shear stress and the author approximating expression is reasonably good. The results predicted by Smith and Riddington appear to be very high. The reason for this may be due to the over-estimation of the axial force in the supporting beam and to the assumption that this force is constant for all beams which seems not to be true as described earlier in Section 4.7.2.

4.8.3 Beam Bending Moment

Comparison between the approximately calculated and the exact bending moment is shown in Table 4.12. The agreement is seen to be satisfactory particularly for the range of $R \leqslant 5$. In the case of $R > 5$, the bending moment is slightly overestimated. This is presumably due to the underestimation of the axial force resulting from the assumed linear distribution. Parabolic distribution would have been more accurate but at the expence of more computational difficulty. It is, however, worth mentioning that values of the stiffness parameter R in cases of either brickwork wall on a steel beam or light-weight concrete block wall on reinforced concrete beam, are within the range of 5. For a brickwork wall on reinforced concrete beam the corresponding values of R are within the range of 7. Consequently it can be concluded that the approximate expressions are more accurate in

TABLE 4.11 COMPARISON OF THE MAXIMUM SHEAR STRESS AT THE WALL/BEAM INTERFACE

H/L	K	R	EXACT $(\frac{\tau_m . t}{\omega})$ F.E.	AUTHOR •	SMITH AND RIDDINGTON *
0.33	0.5	2.56	2.05	2.67	2.91
0.33	0.94	4.10	2.90	3.39	4.67
0.33	1.25	5.08	3.65	3.57	5.79
0.5	1.41	5.55	2.65	2.93	4.67
0.5	1.88	6.89	3.40	3.04	5.80
0.5	1.50	5.04	2.40	2.60	4.24
0.66	1	4.30	1.75	2.14	2.91
0.66	1.50	5.51	2.20	2.36	3.73
0.66	1.88	6.89	2.60	2.63	4.67
0.75	1.69	6.36	2.15	2.36	3.95
0.75	2.11	7.52	2.55	2.71	4.67
0.75	1.35	6.02	2.20	2.43	3.73
1.0	1.5	5.83	1.65	1.99	2.91
1.0	2.25	7.9	1.90	2.31	3.95

• Predicted by equation (4.7.3) $\tau_m = \frac{W(\alpha - \gamma K)(1 + \beta R)}{Lt}$

* Predicted by [14] : $\tau_m = \frac{W/L^3 t\ E_w/I\ E_b)^{0.25}}{2\ tL}$

TABLE 4.12 COMPARISON OF THE EXACT AND APPROXIMATE BENDING MOMENTS

H/L	R	EXACT $\frac{M}{WL} \times 10^{-4}$	APPROXIMATE $\frac{M}{WL} \times 10^{-4}$	% DIFFERENCE
0.5	2.83	232	229	-1.4
0.5	3.46	153	166	8
0.66	3.52	233	231	-0.2
0.66*	3.92	214	216	1.2
0.66	4.30	154	174	12.6
0.66	6.26	111	155	31
0.75	3.85	233	233	0
0.75	4.70	155	178	15
0.75	6.36	120	161	34
1.0	5.83	179	171	-4.9
0.5	2.83	159	176 •	10
0.5	3.46	68	75 •	11
0.66	3.52	145	180 •	24
0.66	4.30	60	90 •	50

• Central Bending Moment

* Span = 2.74 m

predicting bending moments for the first two cases. The central moment is also overestimated, nevertheless, the predicted values have never exceeded W/100.

4.8.4 Ultimate Load

Comparison between the ultimate load predicted by the approximate formula and the experimental results has been referred to in Section 3.6 of Chapter 3.

4.9 CONCLUSIONS

From the foregoing analyses the following conclusions may be drawn :

1. The finite element method has provided a complete solution to the wall/beam interaction problem. The lattice analogy represents an alternative approach.

2. On the basis of the analyses of a considerable number of cases, the influence of some significant parameters was investigated with the aim of formulating simple design procedures.

3. The approximate method of analysis proposed is based on two non-dimensional relative stiffness parameters on which the distributions of stresses in the wall and beam are found to depend. These are the flexural stiffness parameter R and the axial stiffness parameter K.

4. The analyses has confirmed the basic assumption of the composite action that the composite beam behaves as a tied arch; the wall taking the compression and the beam acting as a tie.

5. The maximum bending moment in the beam occurs very near to the supports and the vertical shear extends from the support sections to about one-tenth to one-fifth of the span.

CHAPTER 5 : FINITE ELEMENT ANALYSIS OF WALLS WITH OPENINGS

5.1 INTRODUCTION

When an opening in the form of a door or a window is located in a wall supported on a beam, the stress distribution in the wall and beam and hence the composite action between them will depend not only on their relative stiffness but also on the position and size of that opening.

In so far as the position of the opening is concerned, centrally located openings have no marked influence on the stress flow in the wall so long as the arching action can still form through the brickwork or lintel above the opening. However, with a door opening being located near a support, a secondary arch tends to form and there is a reduction in the degree of the composite action. In this case, a point-load effect is produced partway along the span, thus resulting in a very high vertical stress concentration in the wall and consequently high bending moment in the supporting beam.

The effect of the size of opening, however, is not much pronounced. It will be shown in this Chapter that the height of the arching thrust in the wall is governed by the dimensions of the opening and it will be seen that it is the magnitude of the maximum vertical stress in the wall which is mainly influenced by this parameter.

The present Chapter extends the study to include the composite behaviour of walls with openings. The STRUDL finite element program was used for the analysis and the significant parameters considered in the analysis are the size and position of the opening. Based on the results obtained, an approximate method of analysis has been proposed, comparison with which is referred to in Section B of Chapter 3.

5.2 ANALYSIS PROCEDURE

The analysis is based on the results obtained using the STRUDL finite element program. The rectangular finite element 'PSRCSH', described in Chapter 4, was used for the wall in conjunction with eccentric line elements for the beam. The dimensions and properties of the walls are shown in Figures 5.1 and 5.2.

The effect of varying the size of opening, has been studied through variation of the opening width and depth, respectively. In series B, the depth of a central window opening is kept constant, while the width is varied from 0.16 to 0.5 times the span. The dimensions of the walls analysed, are summarized in Table 5.1(a).

In series C, the width of the opening is fixed and the depth is varied between 0.28 to 1.0 times the wall height. Six different walls containing either a central window or door opening have been analysed. The dimensions of the walls are

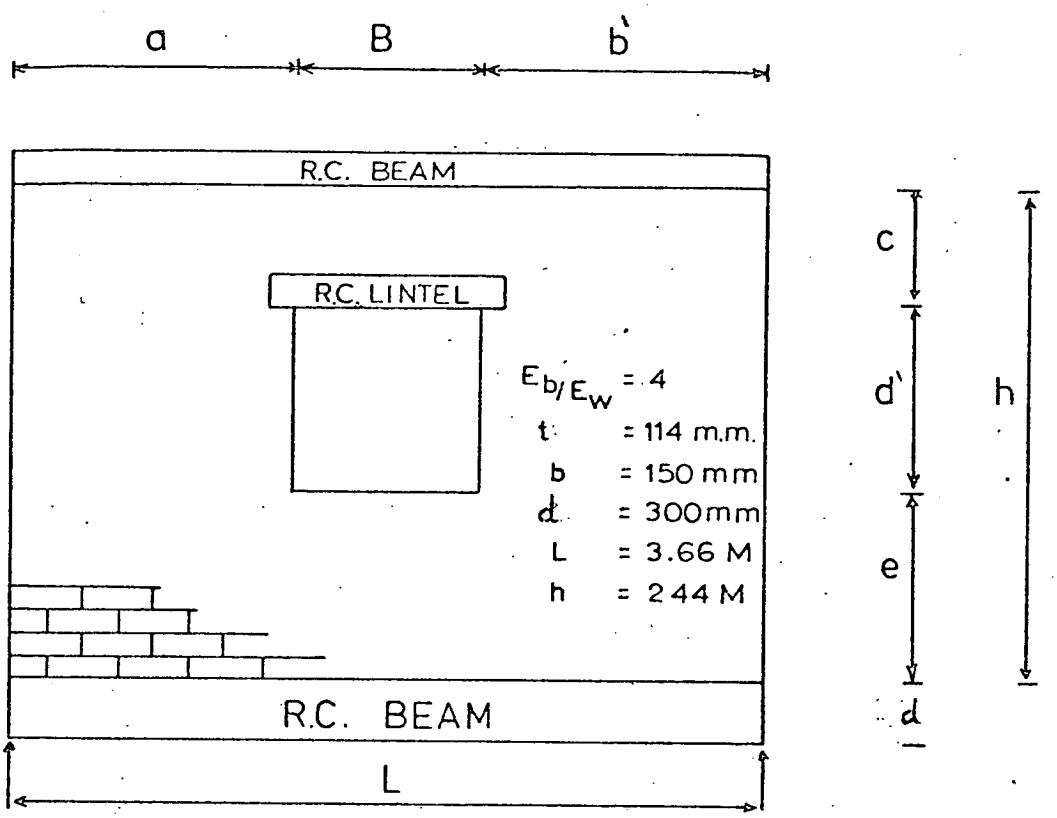

FIG. 5.1 DIMENSIONS AND PROPERTIES OF WALLS OF SERIES B AND C.

WALL No.	TYPE OF OPENING	B/L	d'/h	a/L	b'/L	c/h	e/h
B1	Window	0.16	0.375	0.416	0.416	0.25	0.375
B2	,,	0.25	0.375	0.375	0.375	0.25	0.375
B3	,,	0.33	0.375	0.330	0.330	0.25	0.375
B4	,,	0.50	0.375	0.25	0.25	0.25	0.375
C1	,,	0.25	0.375	0.375	0.375	0.0	0.625
C2	,,	0.25	0.375	0.375	0.375	0.25	0.375
C3	Door	0.25	1.0	0.375	0.375	0.0	0.0
C4	,,	0.25	0.75	0.375	0.375	0.25	0.0
C5	Window	0.25	0.375	0.375	0.375	0.34	0.28
C6	Window	0.16	0.281	0.416	0.416	0.44	0.28

TABLE 5.1a DIMENSIONS OF WALLS OF SERIES B & C.

also shown in Table 5.1(a).

To study the effect of the position of the opening, a window opening is located in three different positions near a support. The effect of a doorway situated near a support has also been investigated. The dimensions of the walls in this series (D), are shown in Figure 5.2 and summarized in Table 5.1(b).

5.3 DISCUSSION OF THE RESULTS

5.3.1 Effect of Size of Opening

The effects of the size of opening on the wall stresses and beam forces, are discussed with reference to walls of series B and C.

5.3.1.1 *Effect of the Opening Width*

5.3.1.1.1 *Wall Stresses* : The distribution of the vertical stress in the walls of series B, is shown in Figure 5.4. The interface vertical stress is shown in Figure 5.5. It will be noted that the stress pattern is similar to that in an identical wall without an opening. The magnitudes, however, being slightly higher. An increase in the opening width, results in an increase in the magnitude of the maximum vertical stress over the supports as shown in Table 5.2. With reference to Figure 5.13, it is clearly evident that the amount of

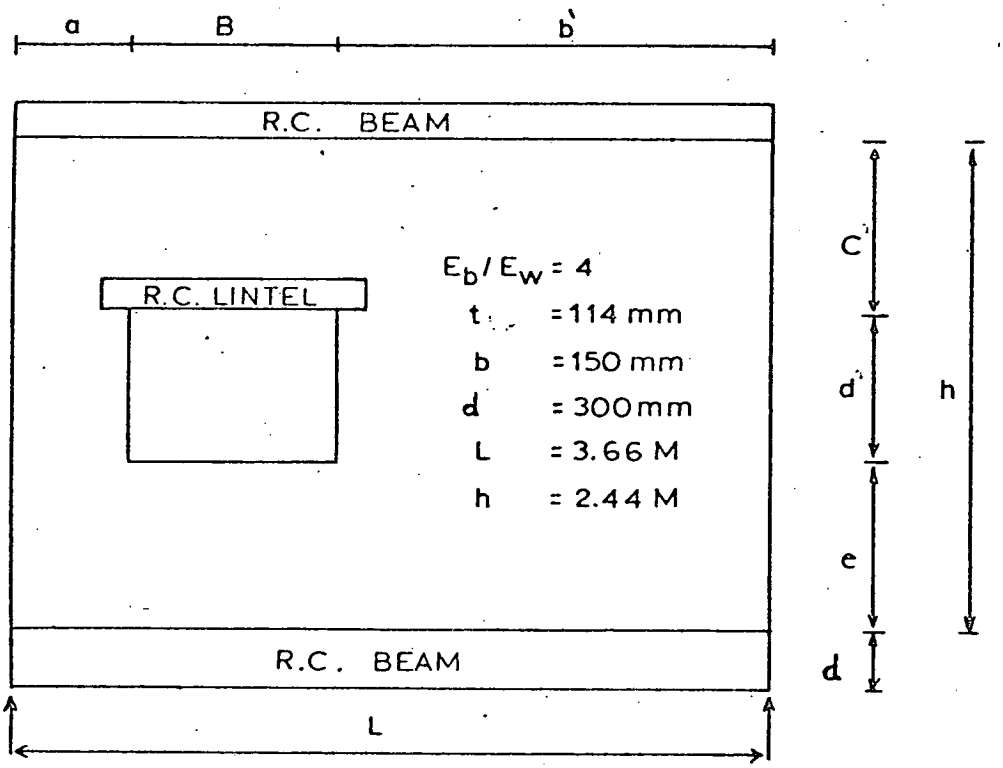

FIG. 5.2 DIMENSIONS AND PROPERTIES OF SERIES D.

WALL No.	TYPE OF OPENING	B/L	d'/h	a/L	b'/L	C'/h
D1	WINDOW	0.25	0.375	0.125	0.625	0.25
D2	"	"	"	0.187	0.563	"
D3	"	"	"	0.25	0.500	"
D4	DOOR	"	0.75	0.125	0.625	"
D5	"	"	"	0.187	0.563	"
D6	"	"	"	0.250	0.500	"

TABLE 5.1 b DIMENSIONS OF SERIES D.

TABLE 5.2 VERTICAL STRESS CONCENTRATION IN THE WALL

WALL NO	TYPE OF OPENING	POSITION OF OPENING	B/L	D/h	MAXIMUM STRESS / AVERAGE STRESS
B1	Window	Central	0.16	0.375	10.8
B2	Window	Central	0.25	0.375	11.0
B3	Window	Central	0.33	0.375	11.4
B4	Window	Central	0.50	0.375	11.8
SOLID WALL	-	-	-	-	10.0

compression, in addition to the usual bending stresses, in the lintel over the opening, is mostly due to the formation of the arch through the lintel. It therefore follows that the opening width governs the spread of the arch in the wall and, as will be seen later, the vertical stress concentration over the supports.

Figure 5.3 shows the horizontal stress distribution in the walls of series B. The stress distribution along a vertical line through the opening, indicates that the brickwork above and below the opening, behave as if they are two separate fixed ended beams. The amount of compression in the lintel is decreased with increasing opening width. This may be attributable to the increase in the tensile bending stress, associated with the increase in the opening width. Away from the periphery of the opening, the effect of the varying opening width is insignificant, however, the amount of compression at the bottom of the wall is slightly increased due to the out-spread of the arching effect.

The patterns of the interface shearing stresses depicted in Figure 5.6 are similar to those in the case of a wall without an opening. The magnitude of the peak stress however is decreasing with increasing opening width which indicates a corresponding decrease in the degree of the composite action. The significance of this stress in the composite action between the wall and the beam, has been discussed in Chapter 4.

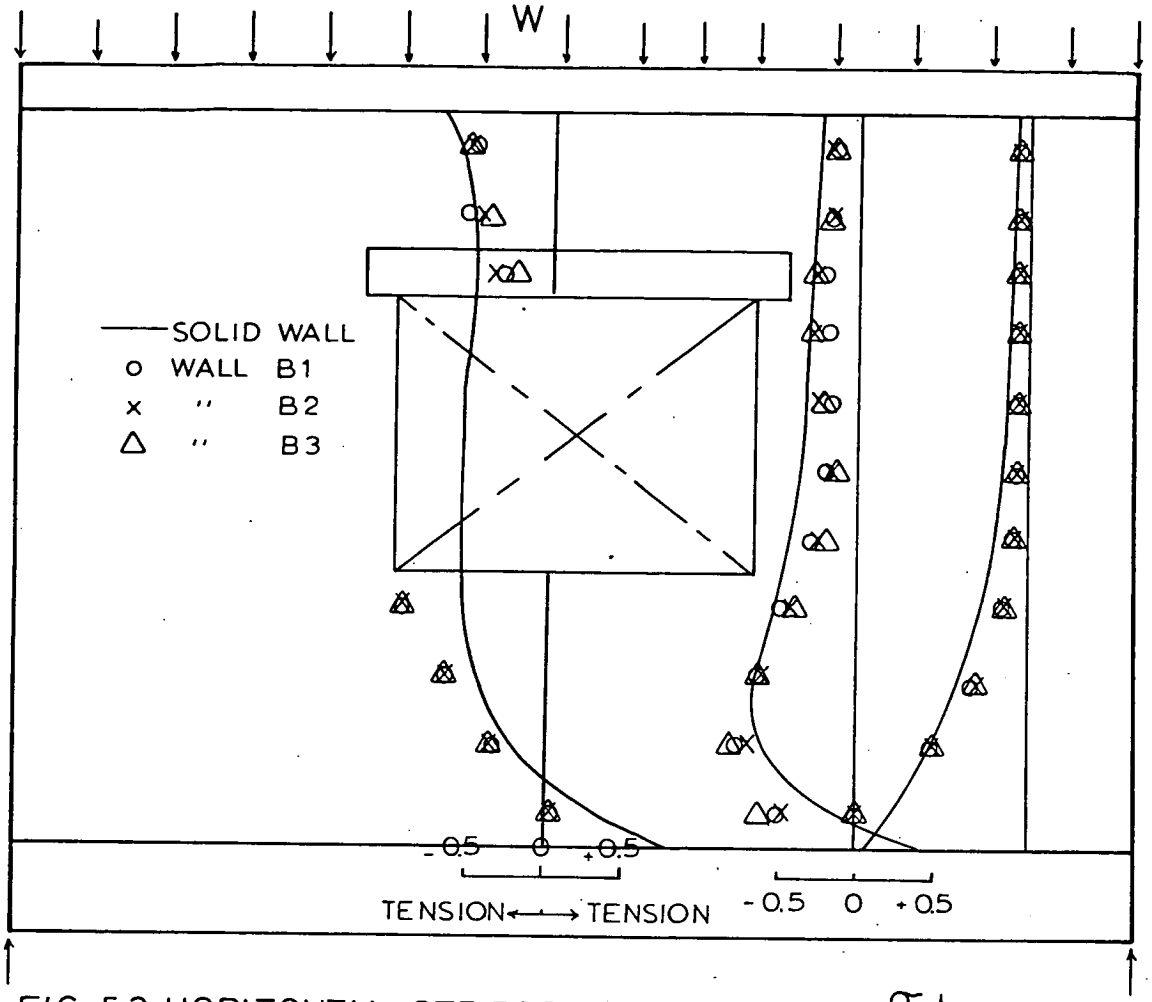

FIG. 5.3 HORIZONTAL STRESS DISTRIBUTION σ_{xt}/W IN WALL SERIES 8.

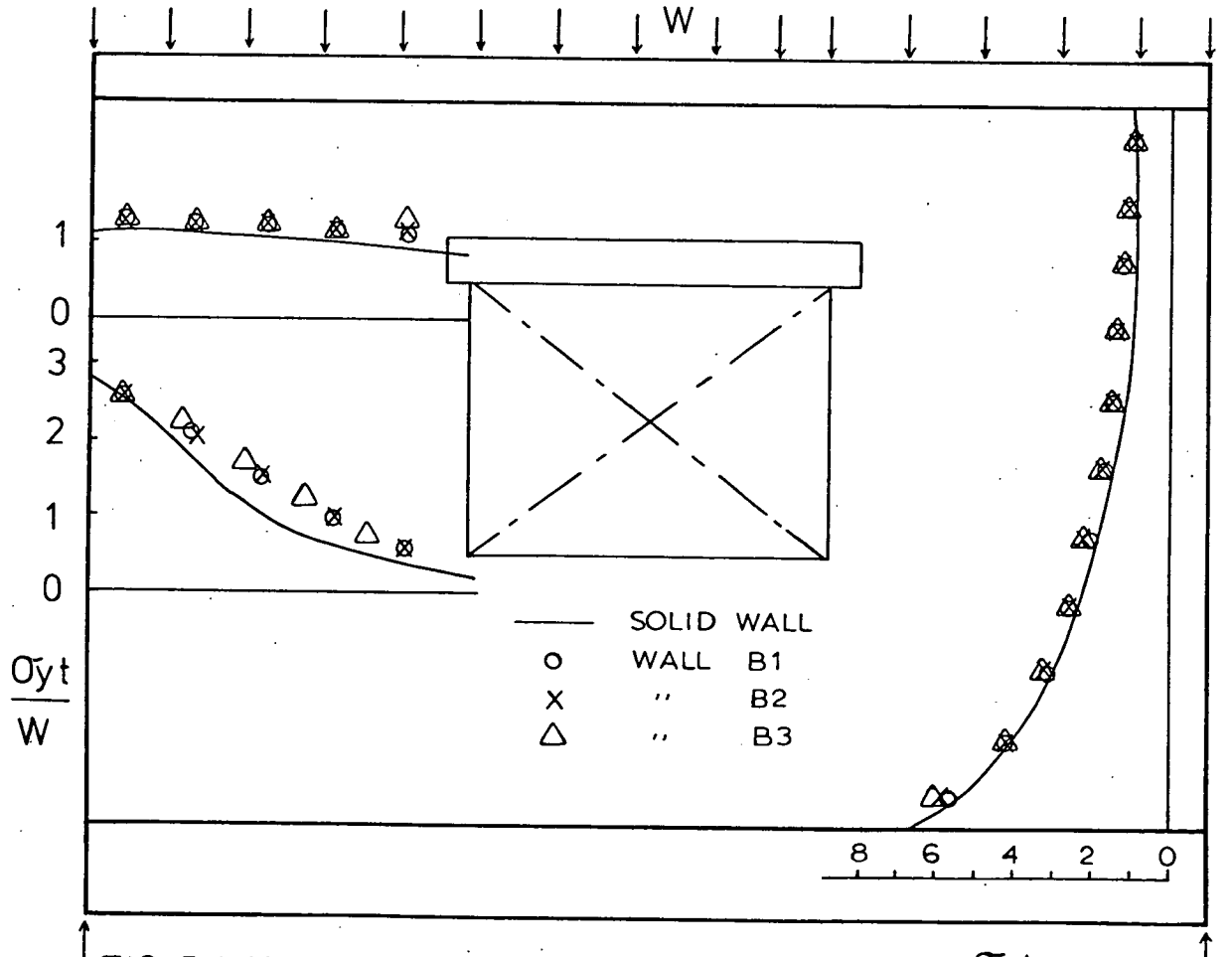

FIG. 5.4 VERTICAL STRESS DISTRIBUTION IN σ_{yt}/W IN WALLS OF SERIES B.

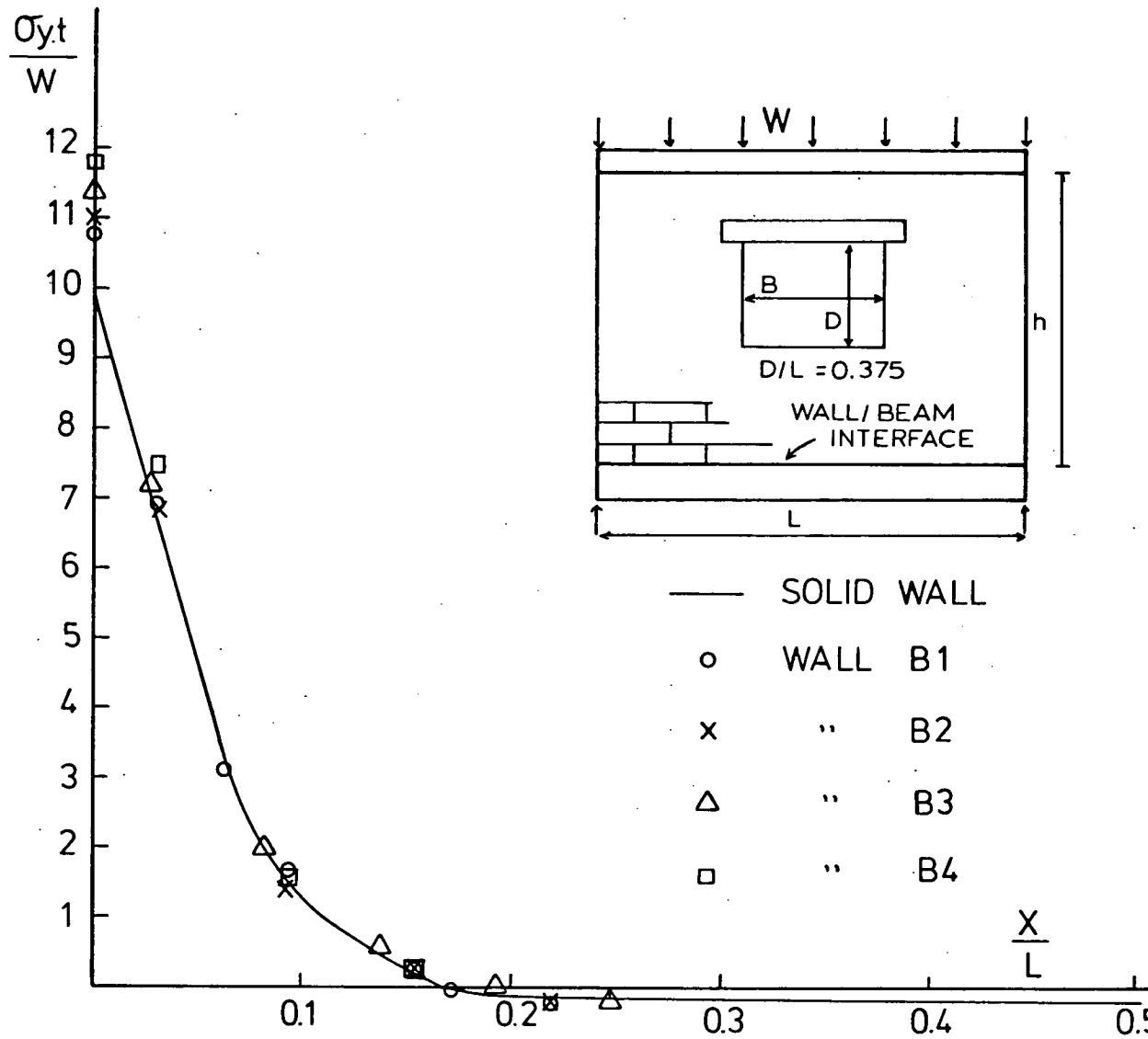

FIG. 5.5 VARIATION OF THE VERTICAL STRESS AT THE WALL /BEAM INERFACE WITH THE OPENING WIDTH.

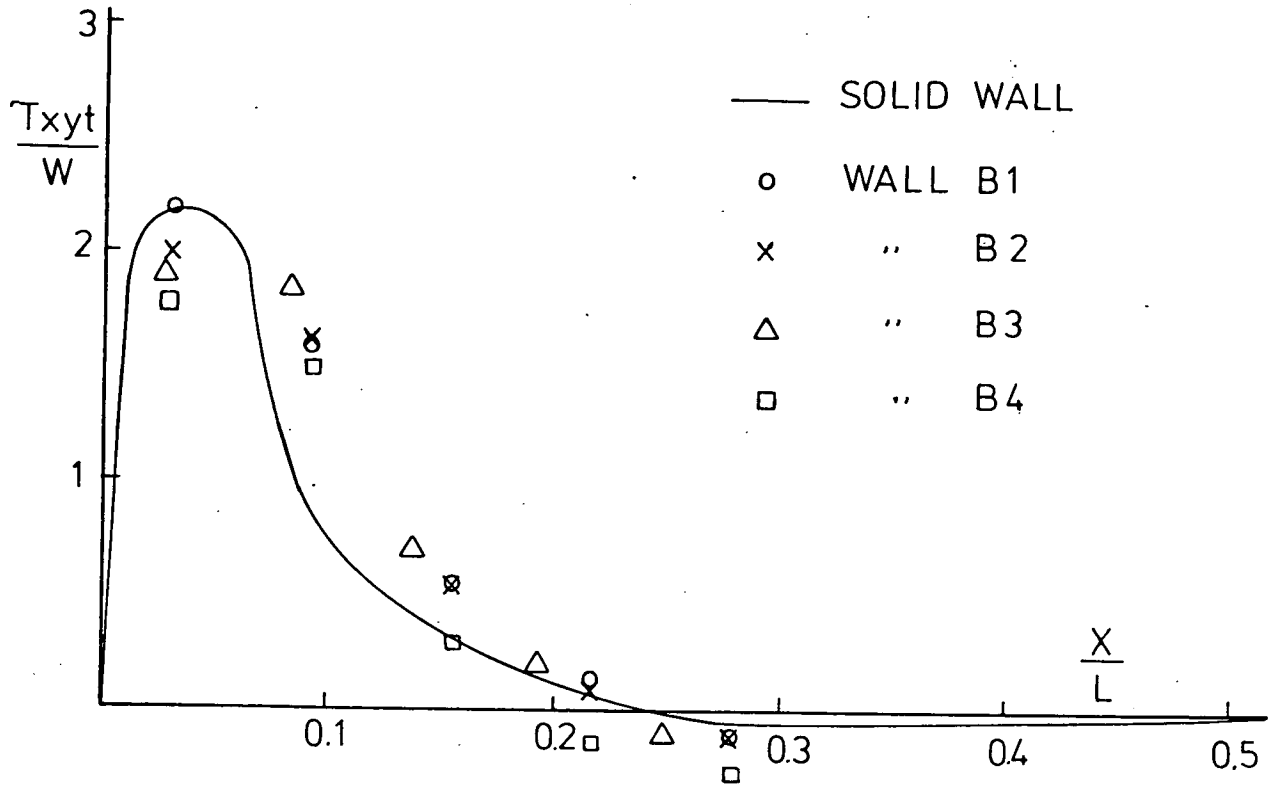

FIG. 5.6 VARIATION OF THE HORIZONTAL SHEAR STRESS AT THE WALL/BEAM INTERFACE WITH THE OPENING WIDTH.

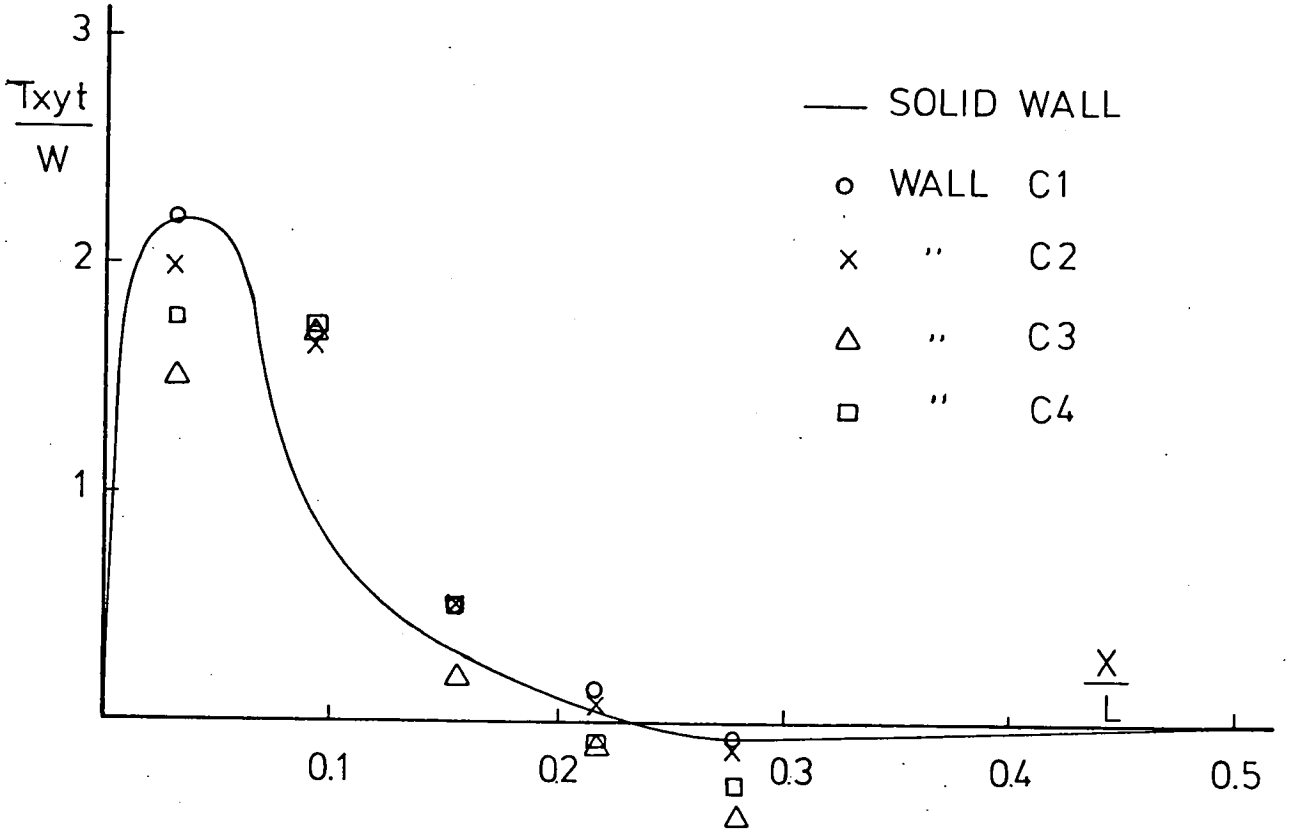

FIG. 5.7 VARIATION OF THE HORIZONTAL SHEAR STRESS AT THE WALL/BEAM INTERFACE WITH THE OPENING DEPTH.

5.3.1.1.2 *Beam Forces* : Figure 5.8 illustrates the bending moments in the supporting beam for walls of series B. An examination of the results indicated that they coincide with the results obtained in the case of a plain wall. It will also be noted that the effect of the opening width is insignificant.

Table 5.3 shows the axial force in the supporting beam expressed as a ratio of the applied load. The reduction in the axial force associated with the increase in the opening width, is mainly due to the corresponding reduction in the interface horizontal shear stress.

The deflection at midspan is summarized in a non-dimensionalized form in Table 5.4. The results indicate that the part of wall above the opening has deflected substantially compared to the deflection of the supporting beam. This is because of the difference in the flexural rigidities of the sections above and below the opening. It is also realised that the deflection of the lintel increases with the increase in the opening width. The central opening and the variation in its width, however, have negligible effect on the beam central deflection.

5.3.1.2 *Effect of the Opening Depth*

5.3.1.2.1 *Wall Stresses* : In order to give an overall view of the variation of the stresses in the wall with the openings depth, the principal stresses have been plotted for various

TABLE 5.3 BEAM BENDING MOMENTS AND AXIAL FORCE

WALL NO	BENDING MOMENT $\frac{M}{WL} \times 10^{-4}$		AXIAL FORCE T/W	
	MAXIMUM	MIDSPAN	MAXIMUM	MIDSPAN
B1	121	16	0.233	0.231
B2	122	15	0.227	0.222
B3	120	14	0.228	0.217
B4	123	10	0.200	0.178
SOLID WALL	118	16	0.251	0.251

TABLE 5.4 DEFLECTION AT MIDSPAN AT APPLIED LOAD OF 7 KN/M^2

WALL NO	DEFLECTION OF LINTEL $(\frac{\delta}{L} \times 10^{-6})$	DEFLECTION OF BEAM $(\frac{\delta}{L} \times 10^{-6})$
B1	1.88	1.62
B2	1.96	1.58
B3	2.02	1.56
B4	2.82	1.42
SOLID WALL	-	1.60

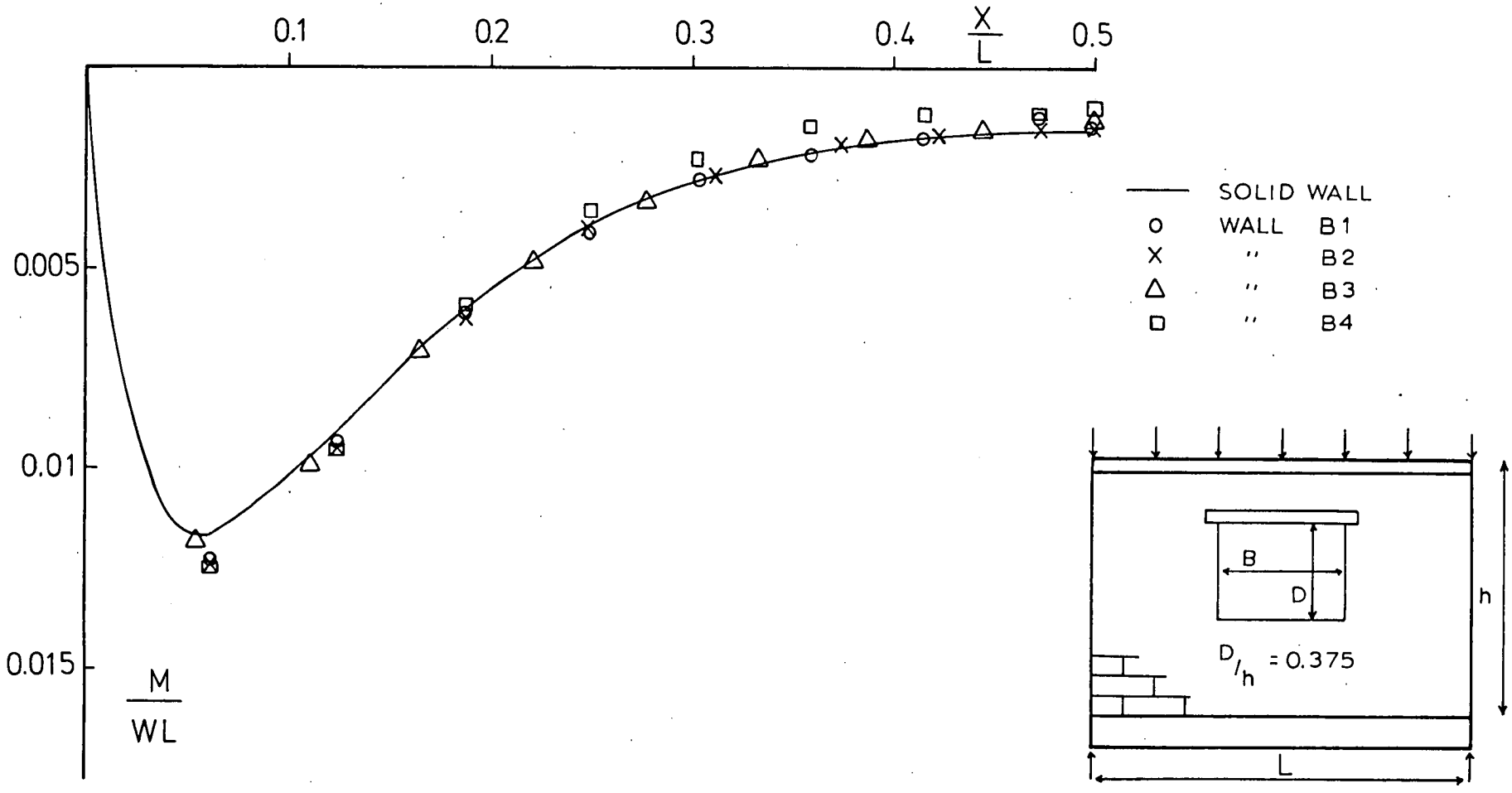

FIG. 5.8 VARIATION OF BENDING MOMENTS WITH OPENING WIDTH.

central door or window openings (see Figures 5.12 to 5.15). The variation of the vertical stress for various sections in the wall and along the wall/beam interface are given in Figures 5.10 and 5.11 respectively. It can be seen in these figures that the stress pattern at points away from the opening is similar to that predicted in a wall without an opening. At the bottom of the wall, however, the magnitude of the stress is slightly higher. At the top corners of the opening, small stress concentration occurs. It is interesting to note that a central door or window opening of the same width at the same height, will produce nearly the same vertical stress concentration over the supports. (Walls C2 and C4). Openings at higher levels in the wall, will produce higher stress concentration over the supports. (Walls C1 and C3). This is mainly due to the fact that the arching action takes place through the lintel and the part of wall above the opening. Hence, the height of opening, controls the outspread of the arch, and consequently the concentration of the stress over the supports. This is clearly illustrated by the principal stress distributions shown in Figures 5.12 to 5.15.

Figure 5.9 shows that in walls containing a central door or window opening, horizontal compressive stresses dominate over the entire wall height, with increased stress concentration in the lintel of up to twice that in the solid wall, as in wall C4. Again this confirms that the arching thrust has formed through the lintel. In the case of wall C1,

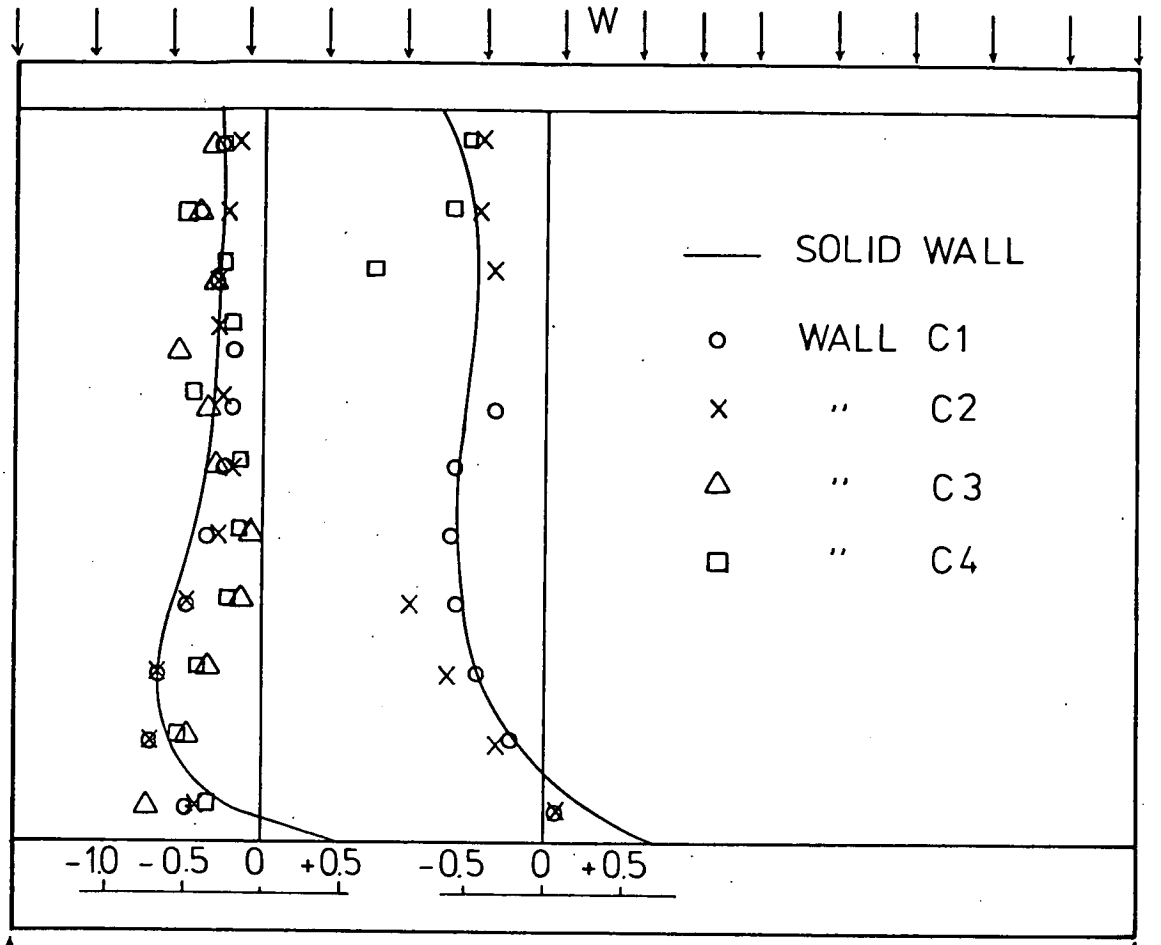

FIG. 5.9 HORIZONTAL STRESS DISTRIBUTION IN $\sigma_{xt}/_{w}$ IN WALLS OF SERIES C.

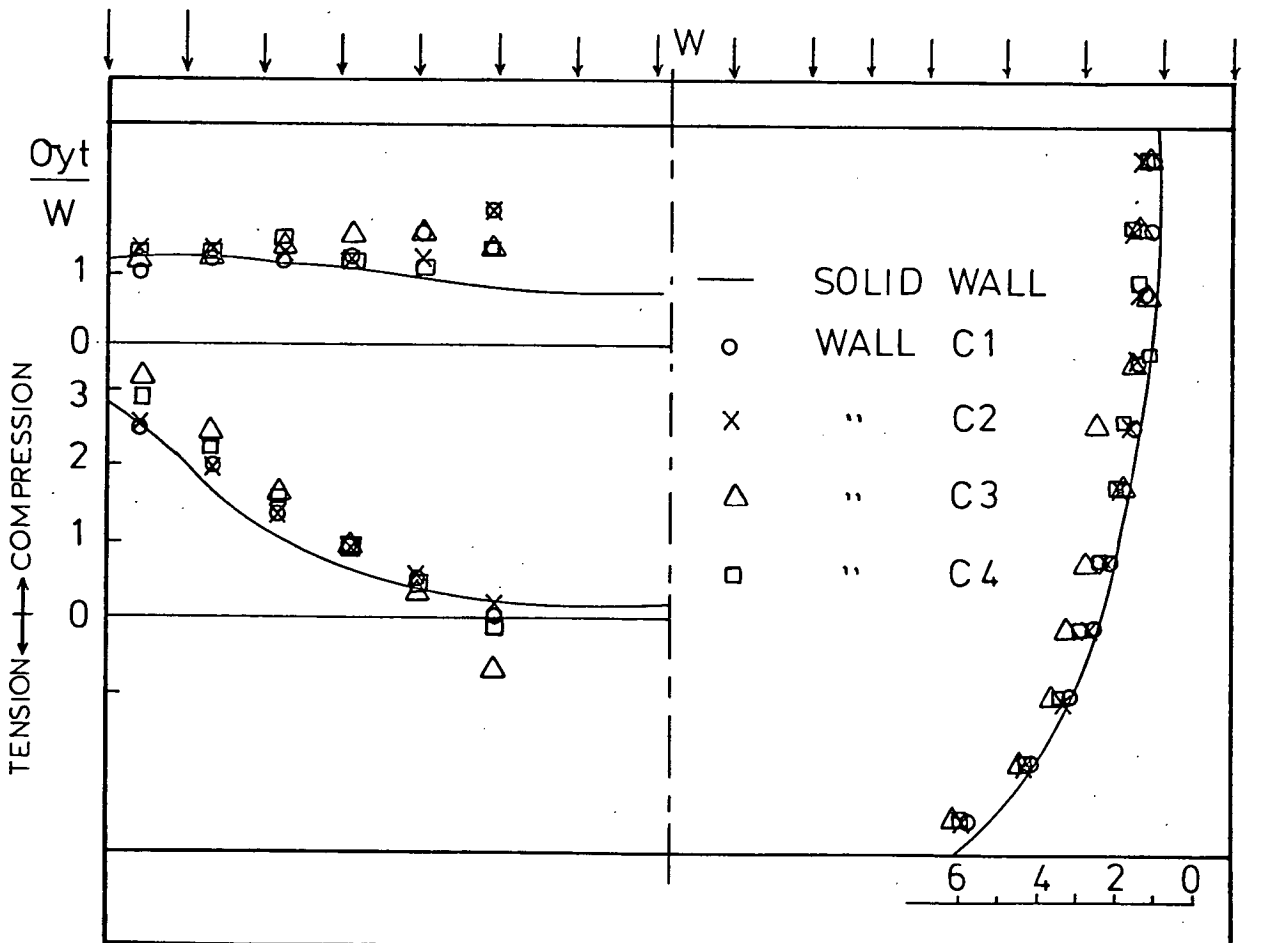

FIG. 5.10 VERTICAL STRESS DISTRIBUTION IN $\sigma_{yt}/_{w}$ IN WALLS OF SERIES C.

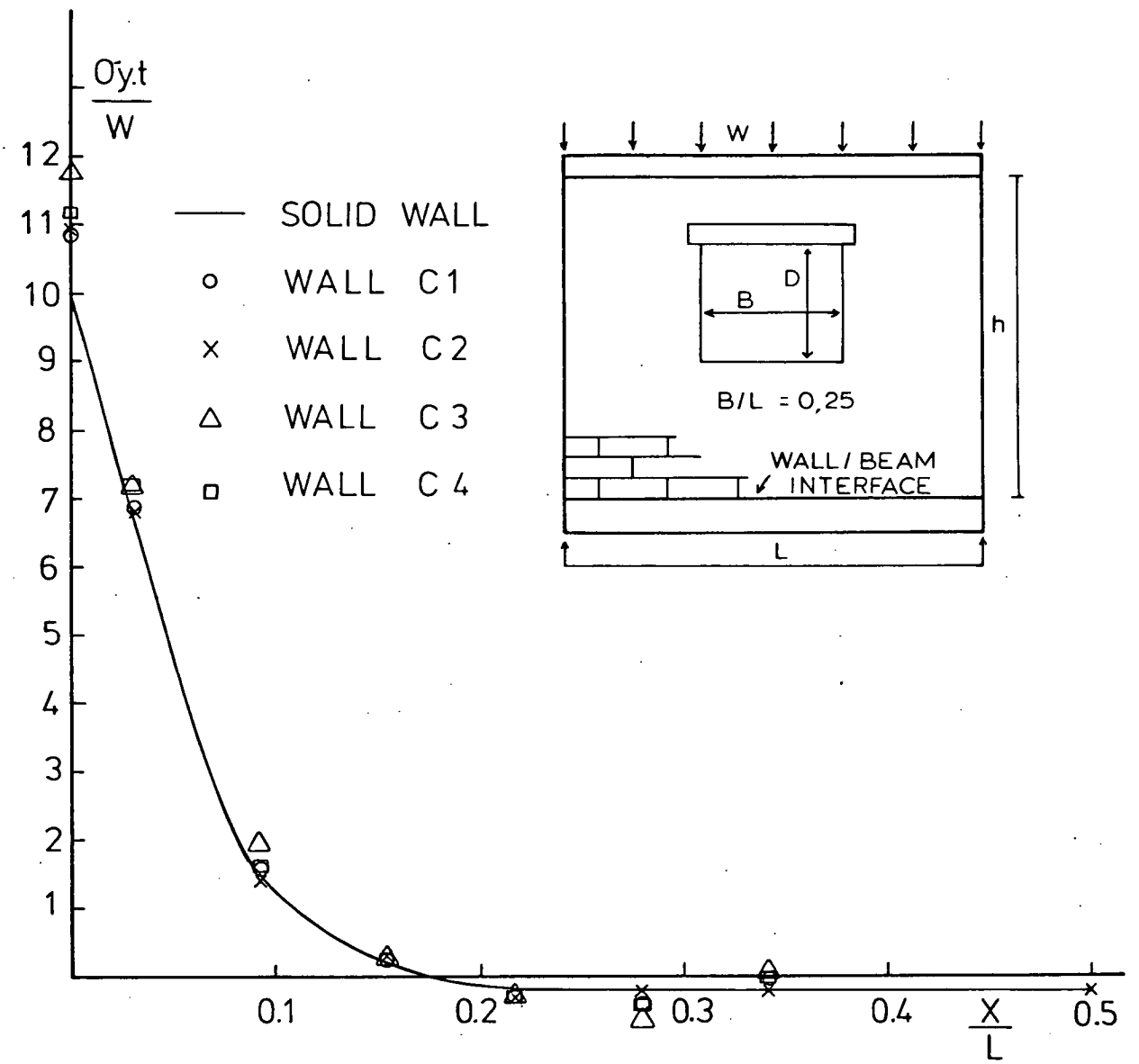

FIG. 5.11 VARIATION OF THE VERTICAL STRESS AT THE WALL/BEAM INTERFACE WITH THE OPENING DEPTH.

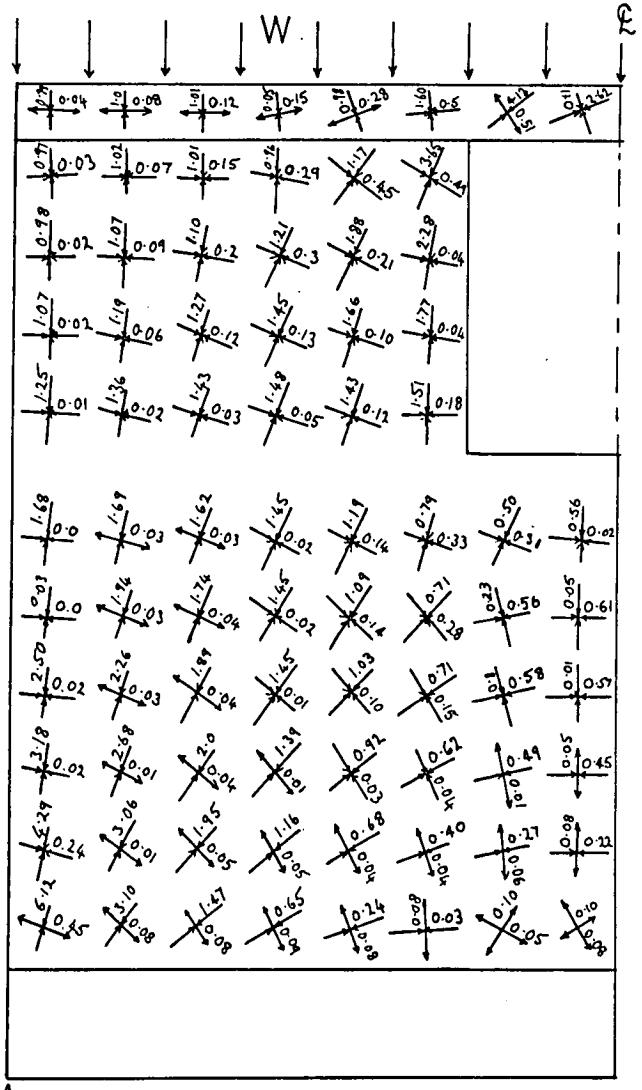

FIG. 5.12 PRINCIPAL STRESSES (IN $\frac{\sigma t l}{W}$) IN WALL C1.

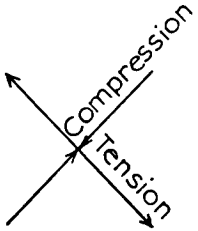

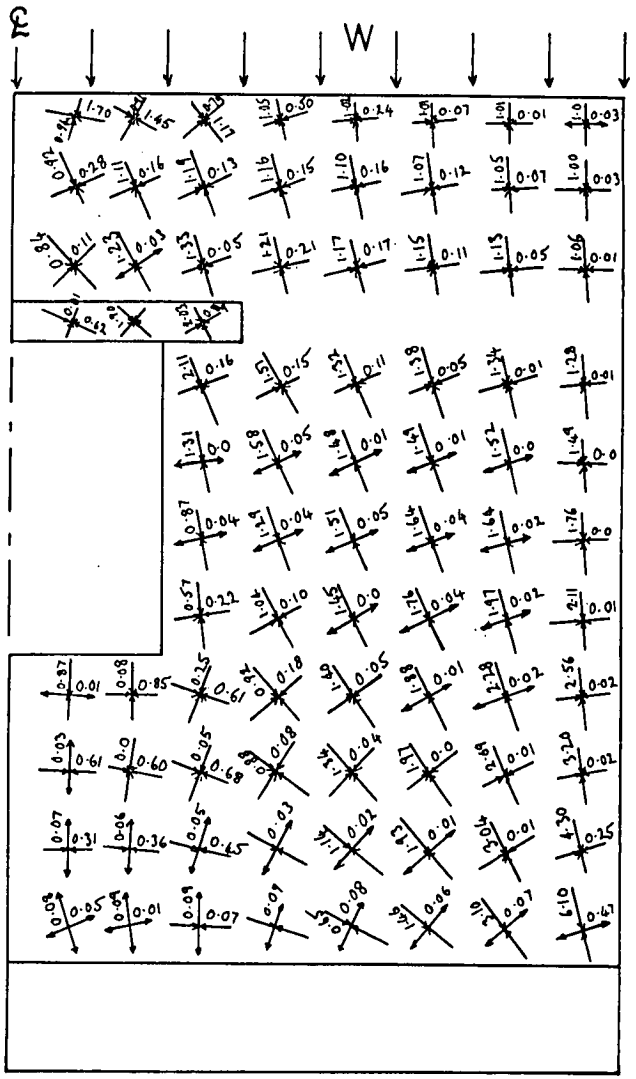

FIG. 5.13 PRINCIPAL STRESSES (IN $\frac{\sigma t l}{W}$) IN WALL B2.

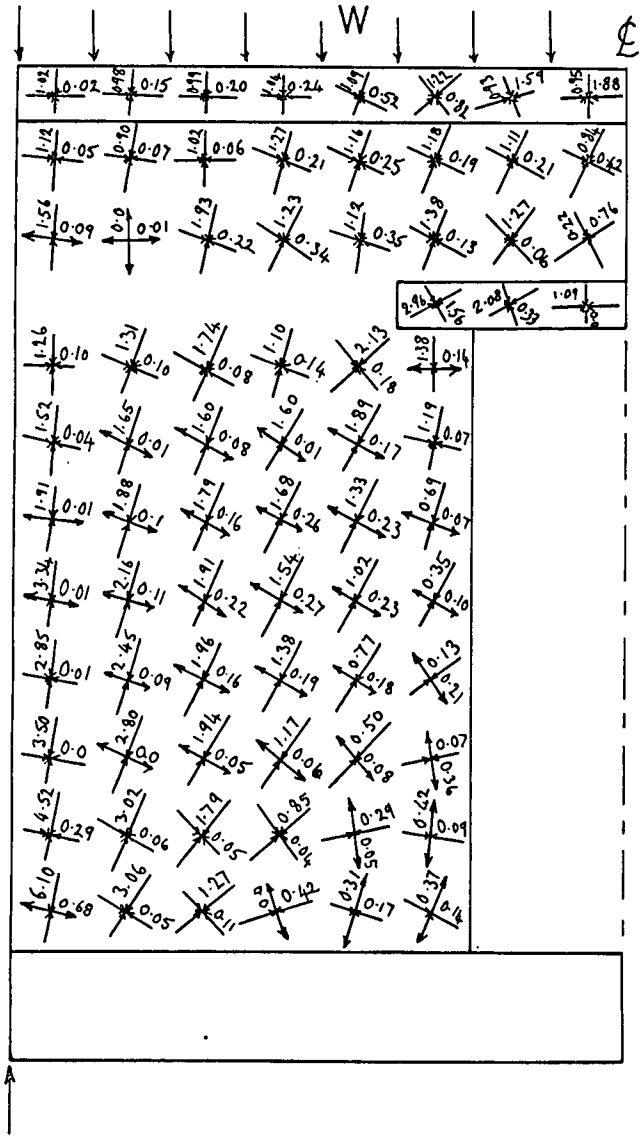

FIG. 5.14 PRINCIPAL STRESSES (IN $\frac{\sigma t L}{W}$) IN C4.

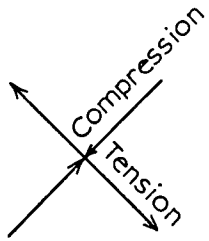

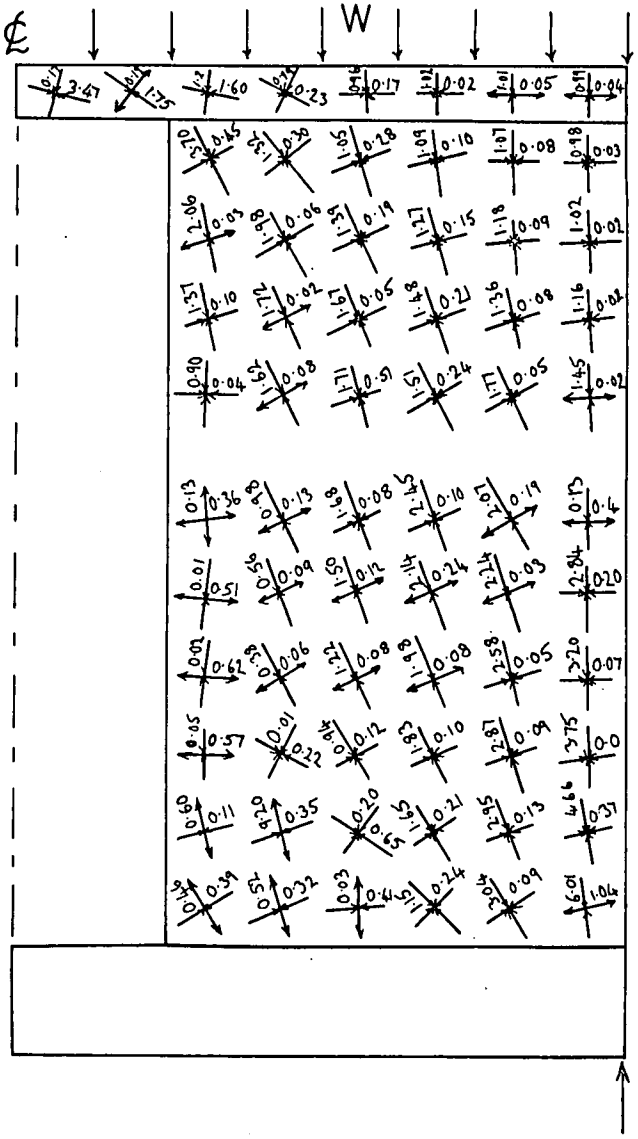

FIG. 5.15 PRINCIPAL STRESSES (IN $\frac{\sigma t L}{W}$) IN WALL C3.

where a window opening has been located just below the upper tie, the arch has formed through the tie and the stresses in the part of the wall below the opening are identical to those in the solid wall.

The distribution of the shear stress at the wall/beam interface for walls of series C, is given in Figure 5.7. It can be seen that the overall shear stress along the interface of a solid wall is slightly higher than that developed in walls with openings. The effect of varying opening depth is noted in the variation of the peak stress. The maximum stress produced when a doorway occurs through the entire wall height (wall C3) is 15 per cent less than that produced when a window opening is situated at the same level (wall C1). Comparison of results for walls C1 and C2, reveals that identical window openings, at different heights, will produce nearly the same shear stress along the wall/beam interface.

5.3.1.2.2 *Beam Forces* : The influence of the depth of a central opening on the bending moments in the supporting beam, is illustrated in Figure 5.16. It is obvious from the Figure that a door opening produces a substantial increase in the bending moment along the central region of the span. This is mainly attributable to the reduced section of the composite beam in this region. In the remaining part of the span, the effect of the central door or window opening is seen to be insignificant.

The variation of the beam axial force with the opening depth may be seen with reference to Table 5.6. The axial force is seen to decrease with increasing opening depth. This is as expected since the interface shear stress, has been shown to decrease with the increase in the opening depth.

It can also be seen from Table 5.6 that a central doorway gives rise to a central deflection 40 per cent more than that in a solid wall or a wall with a window opening. It is obvious that this is due to the reduced flexural rigidity of the composite beam at the region of the opening.

5.3.2 Effect of Position of Opening

5.3.2.1 *Wall Stresses*

In the case where a window opening occurs near a support, significant changes occurs in the stress flow. Figure 5.22 shows the principal stresses in wall D1, in which it may be seen that significant tensile stresses have developed in the lintel and at the top right-hand corner of the opening whereas vertical stress concentration occurs around the bottom right-hand corner. Due to the occurrance of an opening near the support, the arching effect has set itself below the opening increasing the compression in that part of the panel as seen from Figure 5.22. Although the vertical stress concentration over the supports is not very much increased, however, it will be noted from Table 5.7 that the closer the opening to a support,

TABLE 5.5 VERTICAL STRESS CONCENTRATION IN WALLS OF SERIES C

WALL NO	TYPE OF OPENING	POSITION OF OPENING	B/L	D/h	$\frac{\text{MAXIMUM STRESS}}{\text{AVERAGE STRESS}}$
C1	Window	Central	0.25	0.375	11.0
C2	Window	Central	0.25	0.375	11.0
C3	Door	Central	0.25	1.000	11.8
C4	Door	Central	0.25	0.750	11.2
C5	Window	Central	0.25	0.375	10.6
C6	Window	Central	0.16	0.281	10.4
SOLID WALL	-	-	-	-	10.0

TABLE 5.6 BEAM BENDING MOMENT, AXIAL FORCE AND CENTRAL DEFLECTION IN WALLS IN SERIES C

WALL NO	BENDING MOMENT $\frac{M}{WL} \times 10^{-4}$		AXIAL FORCE T/W		CENTRAL DEFLECTION $(\frac{\delta}{L} \times 10^{-6})$
	MAXIMUM	MIDSPAN	MAXIMUM	MIDSPAN	
C1	121	13	0.229	0.222	1.54
C2	122	15	0.227	0.222	1.58
C3	126	46	0.203	0.149	2.33
C4	123	28	0.206	0.179	1.80
C5	117	16	0.209	0.198	1.57
C6	122	16	0.220	0.215	1.58
SOLID WALL	118	16	0.251	0.251	1.60

TABLE 5.7 VERTICAL STRESS CONCENTRATION IN WALLS OF SERIES D

WALL NO	TYPE OF OPENING	CENTRE OF OPENING FROM SUPPORT	B/L	D/h	STRESS CONCENTRATION	
					LEFT SUPPORT	RIGHT SUPPORT
D1	Window	0.25 L	0.25	0.375	11.8	10.5
D2	Window	0.31 L	0.25	0.375	11.6	10.8
D3	Window	0.375 L	0.25	0.375	11.4	11.0
D4	Door	0.25 L	0.25	0.750	13.5	10.6
D5	Door	0.31 L	0.25	0.750	11.8	11.2
D6	Door	0.375 L	0.25	0.750	11.5	11.0
SOLID WALL	-	-	-	-	10.0	10.0

TABLE 5.8 BEAM BENDING MOMENT, AXIAL FORCE AND CENTRAL DEFLECTION IN WALLS OF SERIES D

WALL NO	BENDING MOMENT $\frac{M}{WL} \times 10^{-4}$		AXIAL FORCE T/W		CENTRAL DEFLECTION ($\frac{\delta}{L} \times 10^{-6}$)
	MAXIMUM	MIDSPAN	MAXIMUM	MIDSPAN	
D1	117	26	0.279	0.279	1.78
D2	117	22	0.254	0.252	1.66
D3	122	20	0.251	0.251	1.73
D4	164	51	0.269	0.259	3.52
D5	125	68	0.244	0.211	2.70
D6	124	68	0.230	0.177	2.20
SOLID WALL	118	16	0.251	0.251	1.60

the higher is the stress concentration.

The horizontal stress distribution at midspan shown in Figure 5.17, indicates a substantial increase in the compression in the lower part and a decrease in the upper part of the panel respectively. At sections away from the opening, however, the stress distribution is near to that of a plain wall.

Figure 5.24 shows the variation of the interface shear stress with the position of opening. For the case of an offset window opening, the distribution of the stress is more or less similar to that in a wall without an opening. The peak stress approaches that in a solid wall as the opening is located closer to midspan.

5.3.2.2 *Beam Forces*

Figure 5.20 shows that the effect of an offset window opening on the beam bending moment is insignificant. Apart from the small increase in the moment in the central region of the span, the distribution of the bending moments is similar to that in a beam supporting a solid wall. This can be attributed to the fact that the interface vertical stresses shown in Figure 5.19 have not been very much affected.

Table 5.8 shows that the axial force in the supporting beam has not been appreciably affected. For a window opening at quarter span (wall D1), the axial force is 11 per cent more than that in a beam supporting a solid wall. The axial

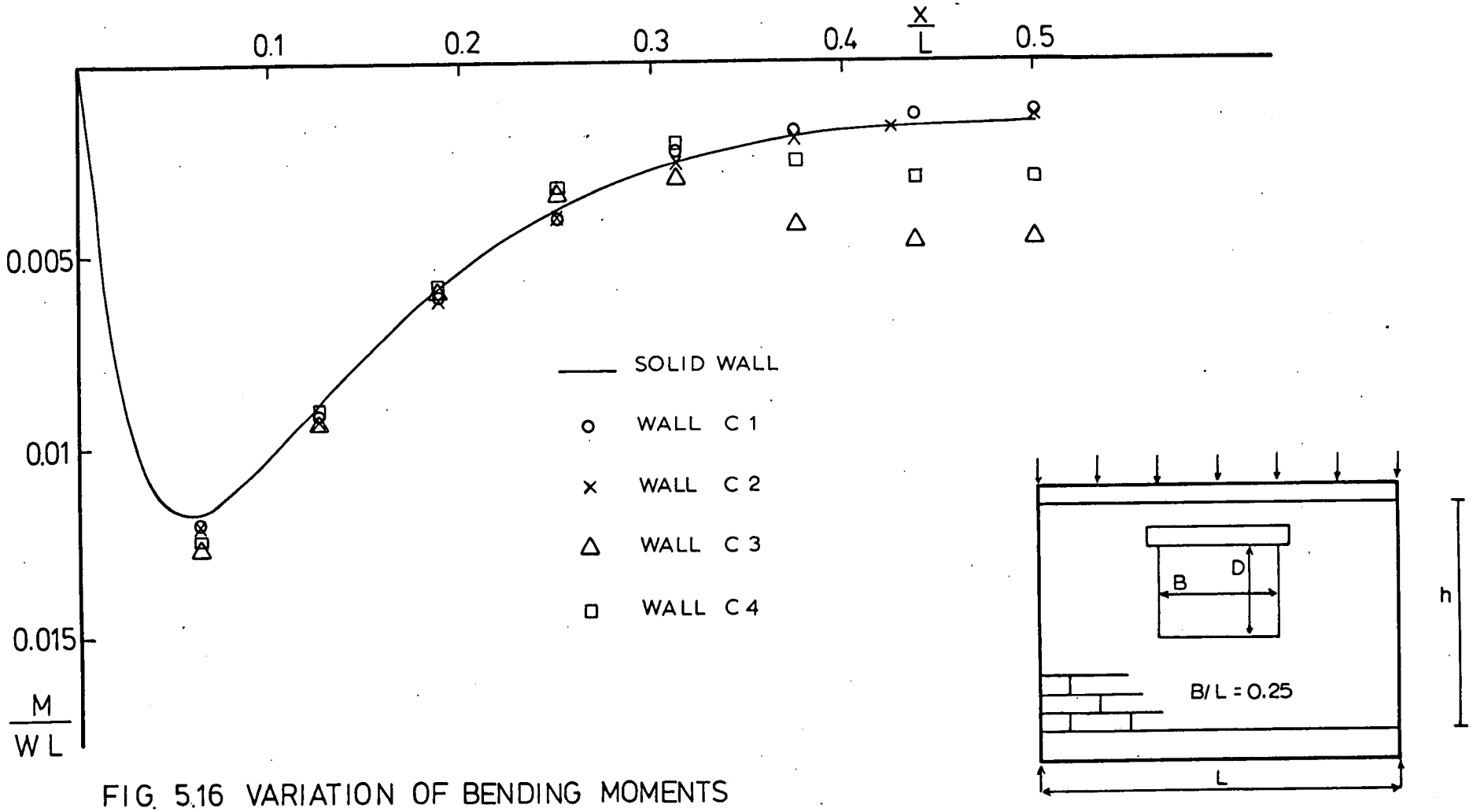

FIG. 5.16 VARIATION OF BENDING MOMENTS WITH OPENING DEPTH.

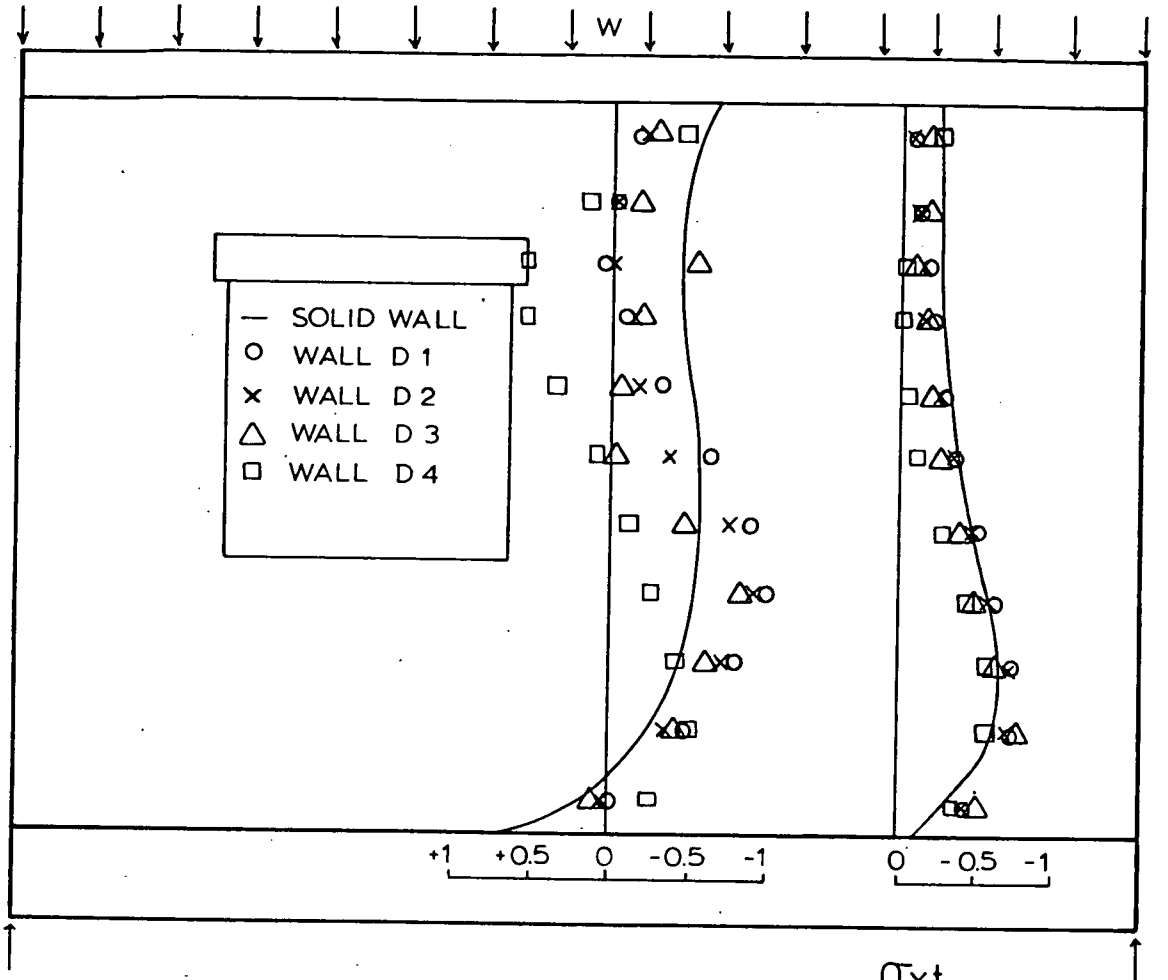

FIG. 5.17 HORIZONTAL STRESS DISTRIBUTION $\frac{\sigma_{xt}}{w}$ IN WALLS OF SERIES D.

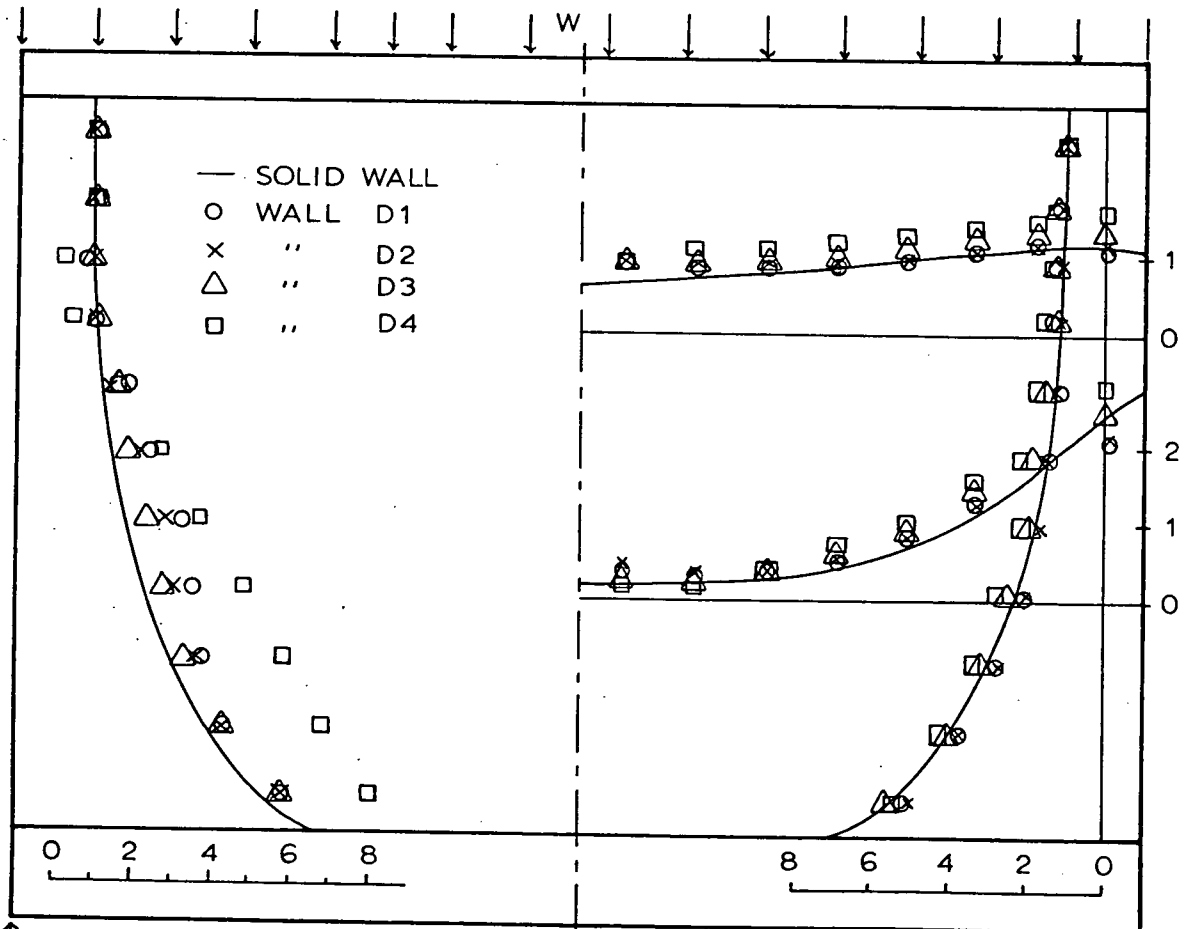

FIG. 5.18 VERTICAL STRESS DISTRIBUTION ($\frac{\sigma_{yt}}{w}$) IN WALLS OF SERIES D.

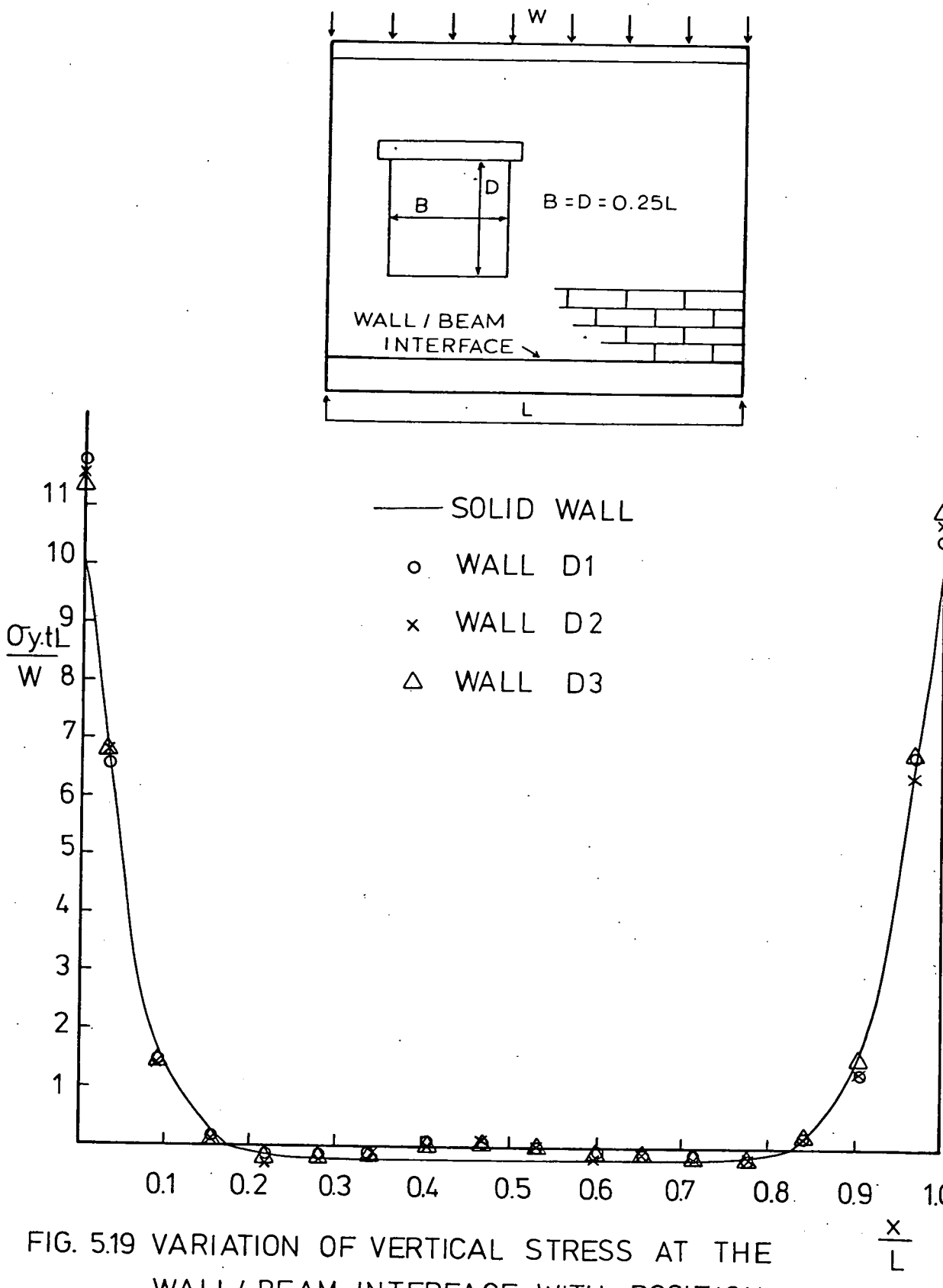

FIG. 5.19 VARIATION OF VERTICAL STRESS AT THE WALL/ BEAM INTERFACE WITH POSITION OF OPENING.

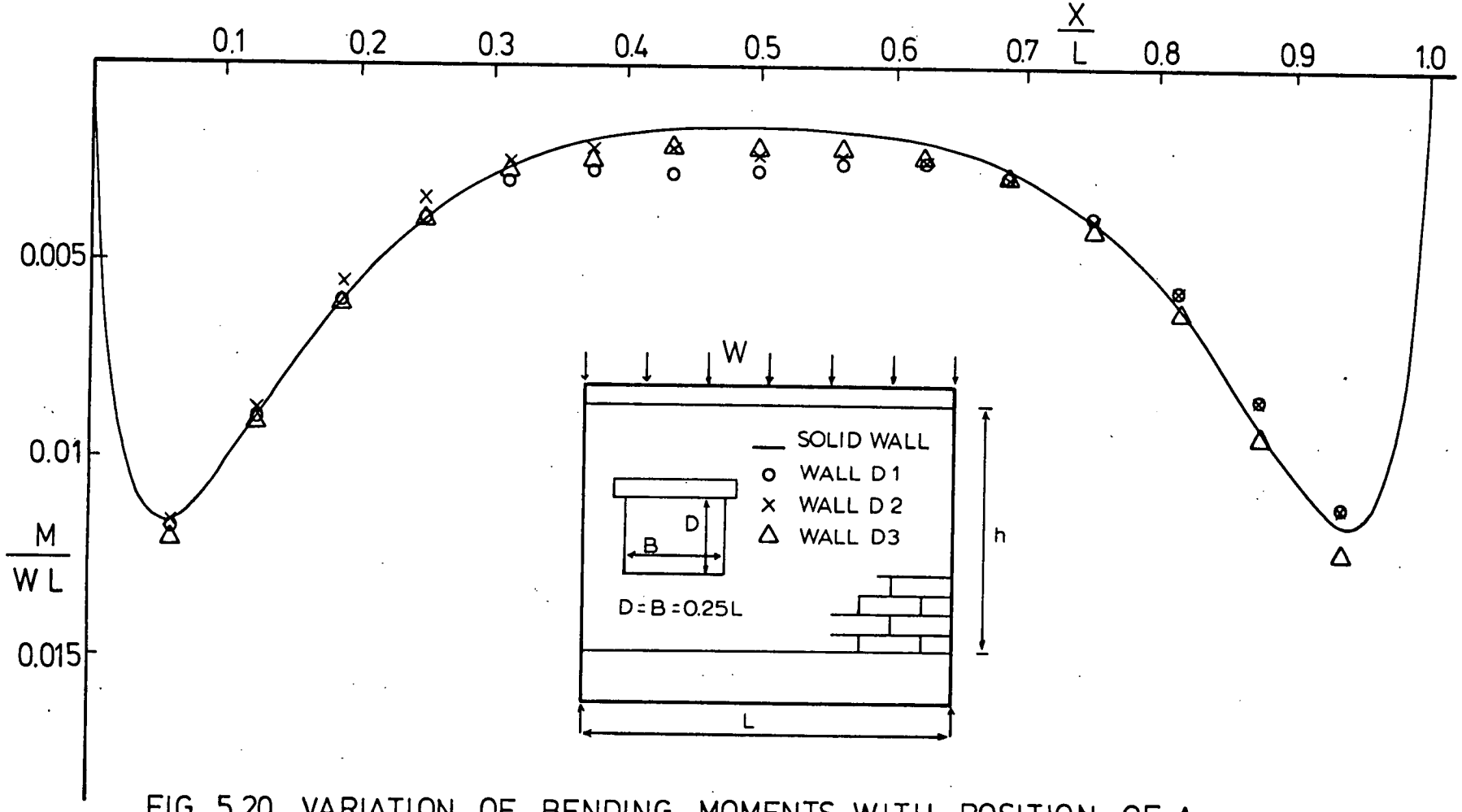

FIG. 5.20 VARIATION OF BENDING MOMENTS WITH POSITION OF A WINDOW OPENING.

force increases as the opening is located nearer to the support because of the increased bending stresses.

5.3.3 Effect of an Offset Door Opening

An offset door has a much more pronounced effect on the wall stresses and the beam forces. The stress flow has completely altered as shown by the principal stress distribution in Figure 5.23. It may be seen that significant tensile stresses have developed around the top right-hand corner of the opening, in the lintel over the opening, as well as at the bottom left-hand corner of the opening. It is obvious that the arching between the supports could not be completed because of the doorway. A secondary arching system, therefore, appears to have set itself in the part of the panel to the right of the opening. This results in a vertical stress concentration at the bottom right-hand corner of the opening as illustrated in Figure 5.21. The part of the load transmitted down to the left-hand support has given rise to a substantial increase in the vertical stress concentration of nearly 32 per cent over that in a solid wall. Over the other support an increase of 20 per cent is realized (Table 5.7).

The horizontal stress distribution at midspan plotted in Figure 5.17 indicates a noticeable deviation from that in a wall without opening. Tensile stresses have developed in the upper part of the panel, while an increase in the

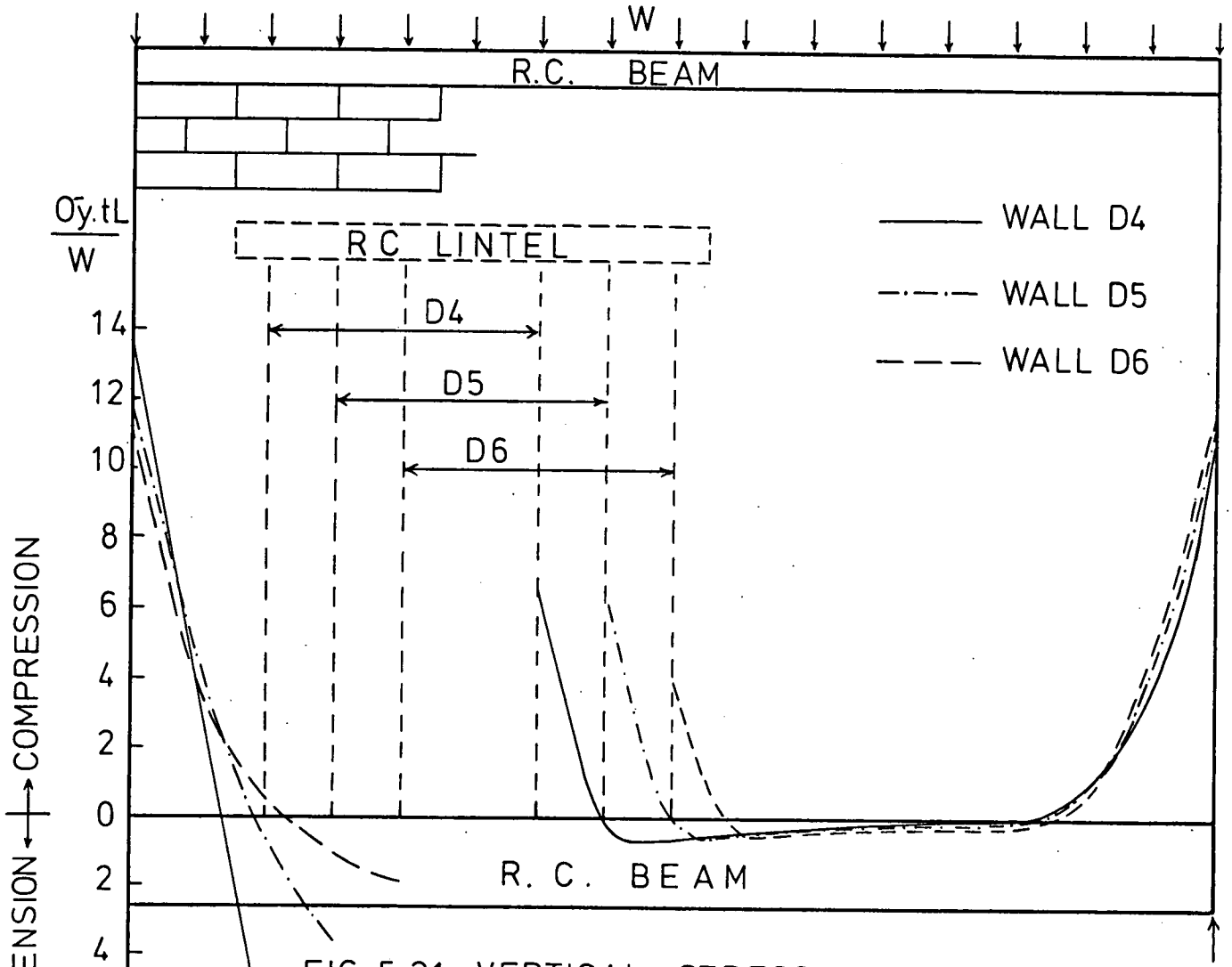

FIG 5 21 VERTICAL STRESS DISTRIBUTION ALONG WALL/BEAM INTERFACE IN WALLS D4 TO D6.

compression appears to have occurred at the bottom of the wall. This may be attributable to the fact that the centre of compression is displaced downwards as a result of the arch being formed over a shorter span, as indicated in Figure 5.25.

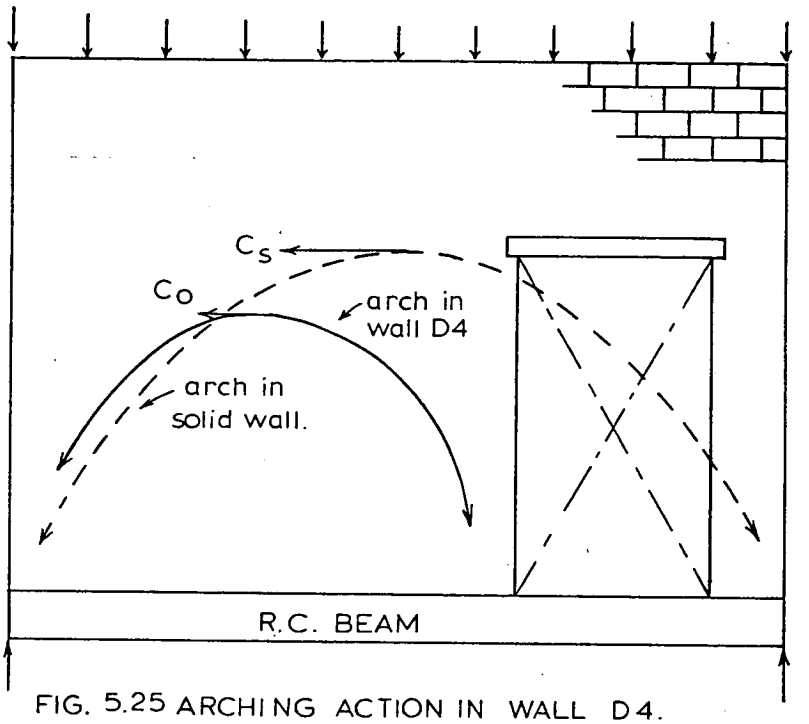

FIG. 5.25 ARCHING ACTION IN WALL D4.

The influence of these tensile stresses has been shown in Chapter 3, to cause vertical splitting at the top corners of the opening and eventually lead to the wall failure, Plate 7.

It is most likely that the significant changes in the stress flow in the wall have affected the interacting behaviour between the wall and beam.

A noticeable reduction in the composite action is clearly

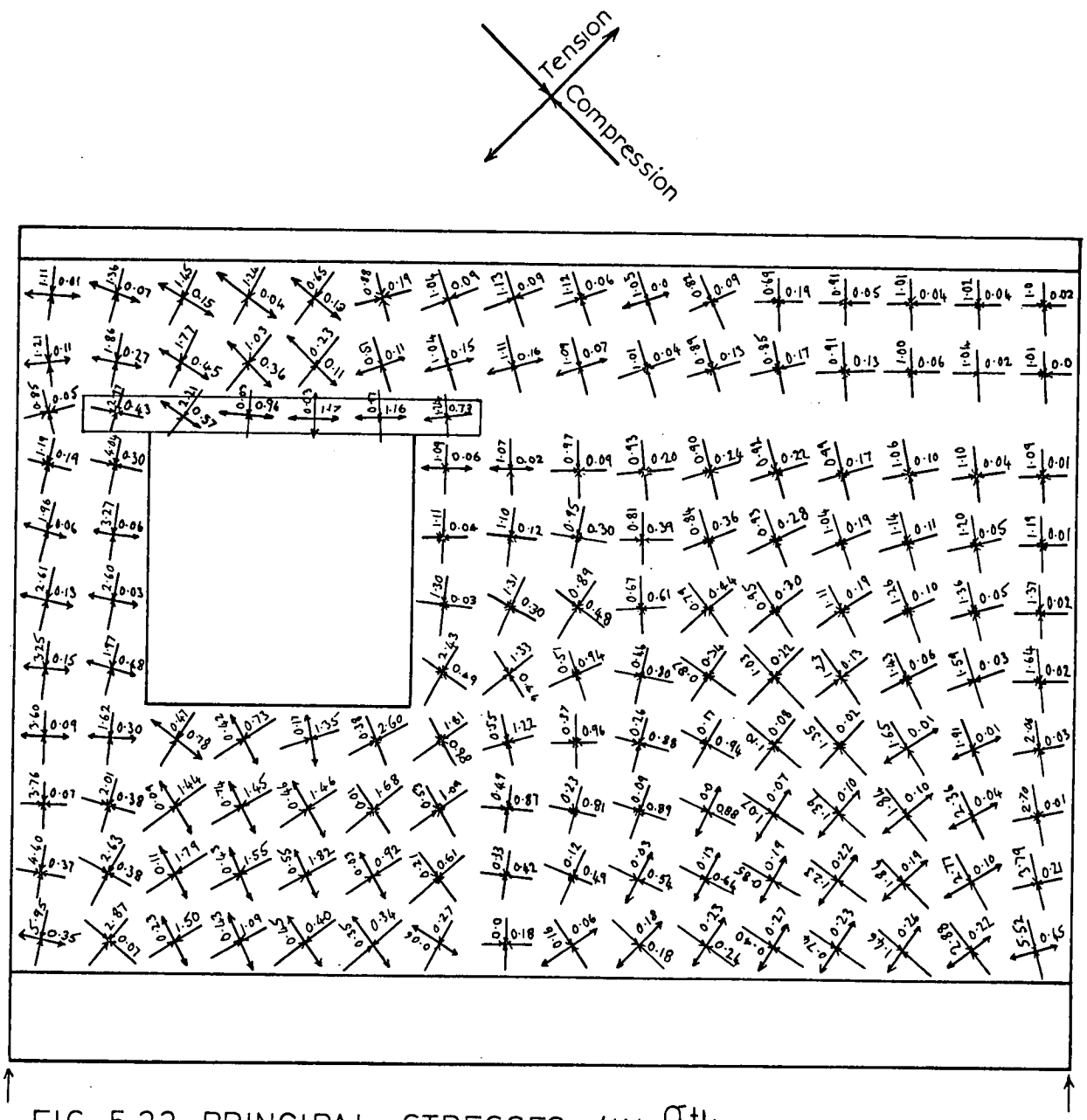

FIG. 5.22 PRINCIPAL STRESSES (IN $\frac{\sigma.t_1}{W}$) IN WALL D1.

indicated by the reduction in the interface shear stress shown in Figure 5.24. It is seen that in the region of the doorway the peak shear stress is reduced by almost 50 per cent compared to that in the case of a solid wall, whereas away from the periphery of the opening, it is reduced by about 15 per cent.

The vertical loading on the beam, as denoted by the interface vertical stress distribution shown in Figure 5.21, gives rise to a point-load effect along the span. The high bending moment induced in the beam undoubtedly results from this point-load effect. The magnitude of this moment is noted from Figure 5.26 to be 40 per cent more compared to that in a beam supporting a solid wall. The midspan bending moment however is substantially increased.

An examination of the results in Table 5.8 reveals that the axial force in a beam supporting a wall containing an offset window opening (wall D1), is slightly higher than that induced in a similar beam when a door opening occurs at the same position (wall D4). This is perhaps attributable to the fact that in the case of wall D4 the axial force results mainly from the bending stresses, the contribution from the tied-arch action being very small, whereas in the case of wall D1 because of the relatively increased degree of composite action, the axial force is due to the combined effect of the tied-arch action and the bending stresses.

From Table 5.12, it is also evident that the doorway opening has a marked influence on the deflection characteristics

TABLE 5.10 COMPARISON OF BEAM AXIAL FORCE

L/d	K	MAXIMUM AXIAL FORCE T/W			APPROXIMATE
		a/L = 0.125	a/L = 0.187	a/L = 0.250	
8	1.0	0.333	0.290	0.261	0.292
12	1.5	0.269	0.242	0.230	0.268
15	1.88	0.242	0.218	0.267	0.248
20	2.5	0.213	0.190	0.181	0.218
24	3.0	0.190	0.168	0.160	0.190

TABLE 5.11 BEAM BENDING MOMENT IN WALLS D4 TO D6

R	MAXIMUM BENDING MOMENT $(\frac{M}{WL})\times10^{-4}$				% DIFFERENCE		
	SOLID WALL	WALL D4	WALL D5	WALL D6	WALL D4	WALL D5	WALL D6
5.83	117	164	125	124	40	7	6
6.89	98	108	105	104	10	7	6
8.55	75	81	78	77	8	4	3
9.80	60	64	62	61	7	3	2

TABLE 5.12 DEFLECTION OF BEAM SUPPORTING WALLS WITH OFFSET DOOR OPENING

WALL NO	L/d	DEFLECTION $\frac{\delta}{L}\times10^{-6}$			$\frac{\delta_{av}}{\delta_s}$ *
		MAXIMUM	CENTRAL	AVERAGE	
SOLID WALL	8	1.25	1.25	1.25	
	12	1.60	1.60	1.60	
	15	1.78	1.78	1.78	
	20	2.00	2.00	2.00	
	24	2.12	2.12	2.12	
D4	8	2.66	2.60	2.63	2.10
	12	3.67	3.52	3.60	2.25
	15	4.13	3.88	4.01	2.25
	20	4.59	4.25	4.42	2.21
	24	4.81	4.37	4.59	2.17
D5	8	2.08	2.08	2.08	1.66
	12	2.71	2.70	2.71	1.69
	15	2.99	2.97	2.98	1.67
	20	3.31	3.26	3.29	1.65
	24	3.49	3.42	3.46	1.63
D6	8	1.73	1.73	1.73	1.38
	12	2.20	2.20	2.20	1.38
	15	2.42	2.42	2.42	1.36
	20	2.68	2.68	2.68	1.34
	24	2.84	2.84	2.84	1.34

* $\frac{\delta_{av}}{\delta_s}$ *denotes the average deflection in walls D4 to D6 as a ratio of the deflection in a similar solid wall.*

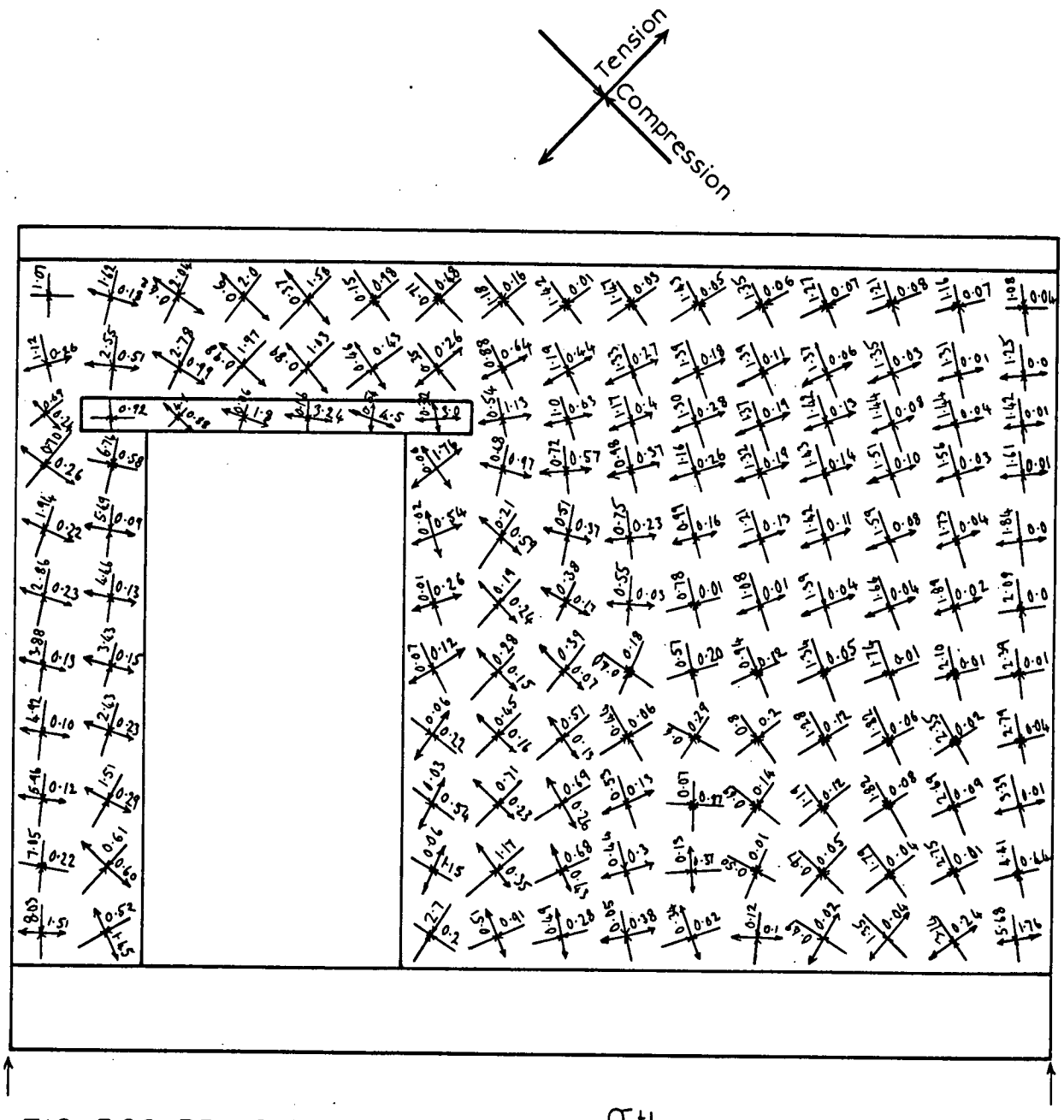

FIG. 5.23 PRINCIPAL STRESSES (IN $\frac{\sigma.tL}{W}$) IN WALL D4.

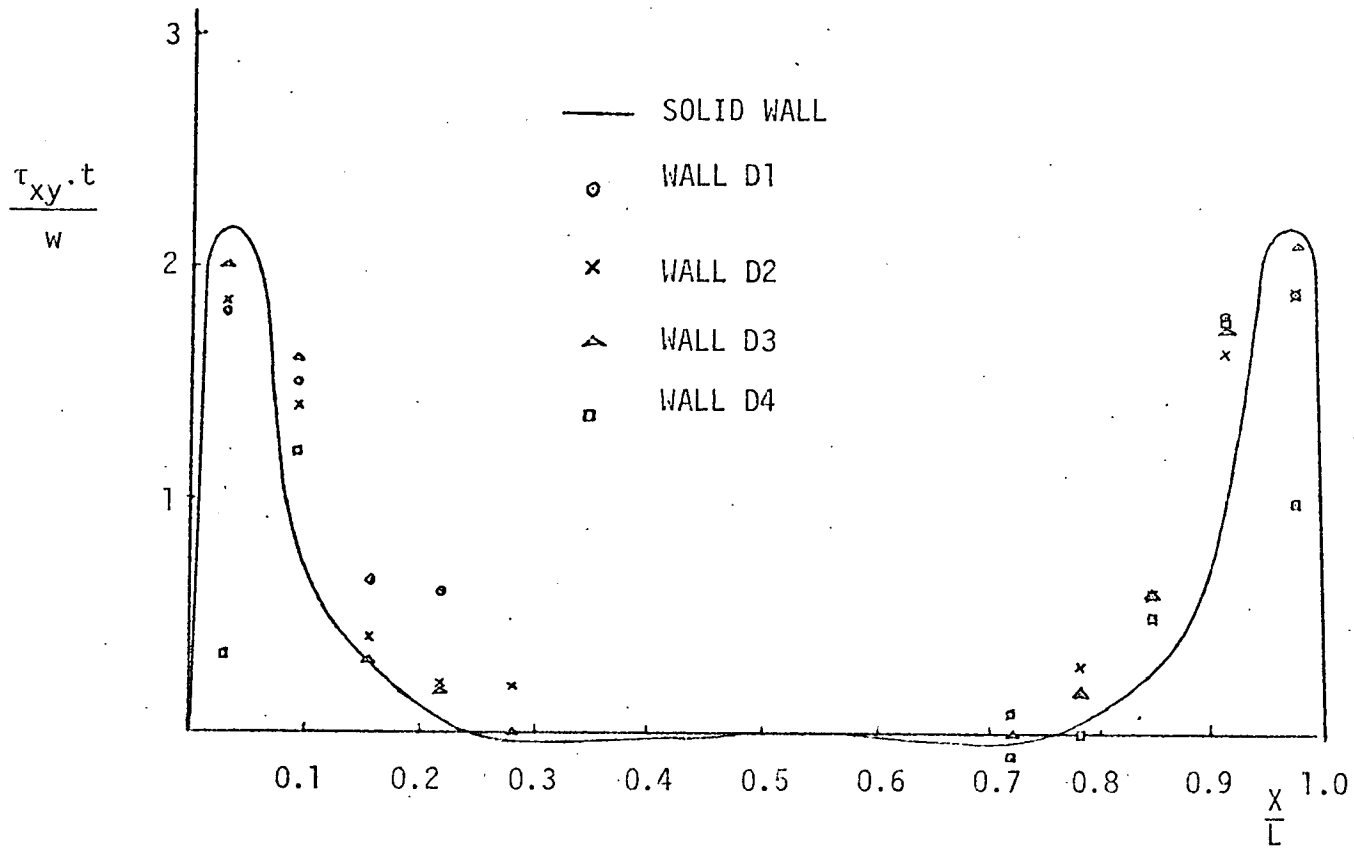

Figure 5.24 Interface Horizontal Shear Stress Distribution in Walls of Series D

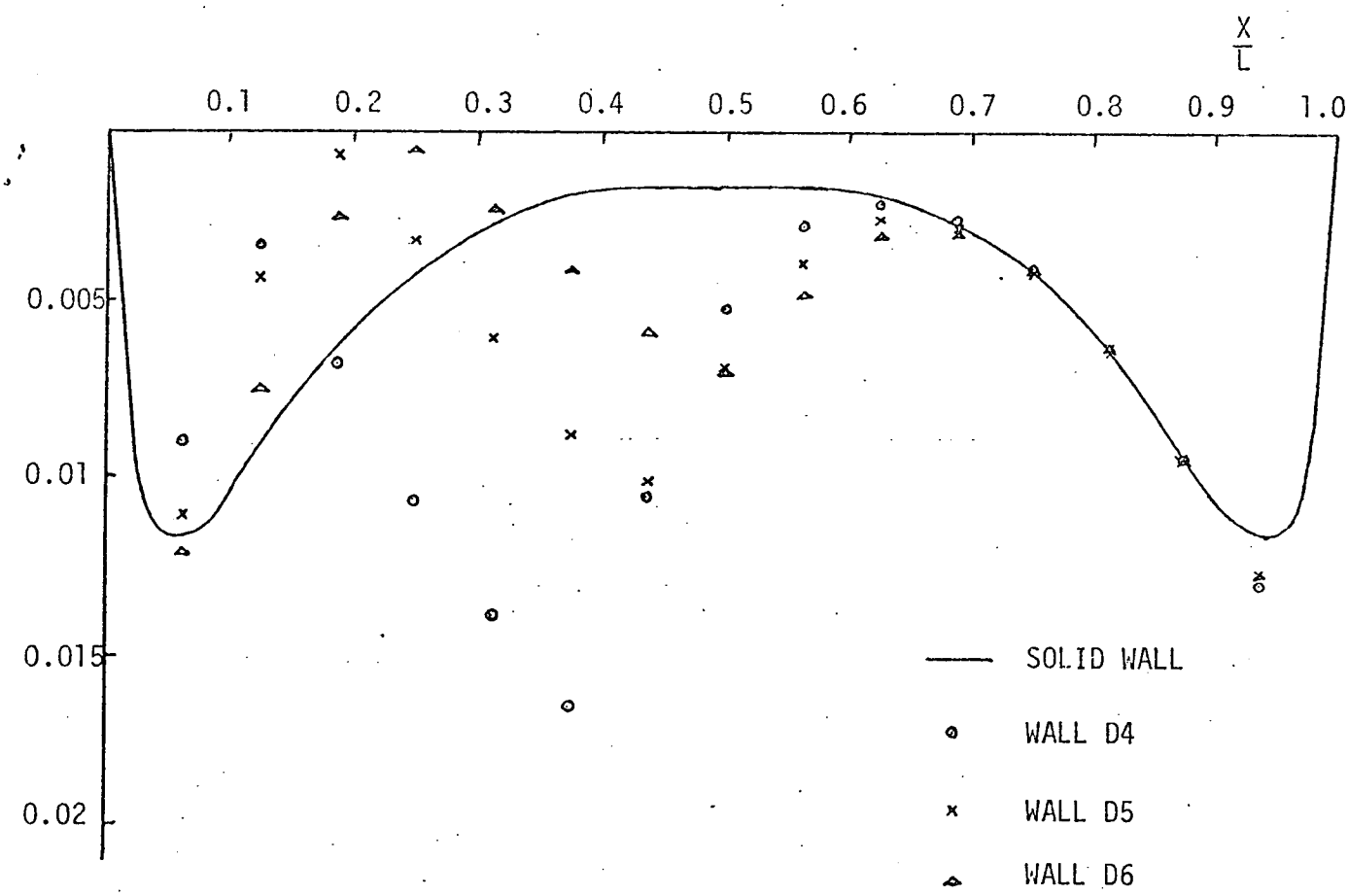

Figure 5.26 Distribution of Beam Bending Moments in Walls D4 to D6

of the composite beam. It is clear from the results that the inclusion of a doorway opening near to a support has the effect of increasing the deflection by a large amount namely up to more than twice that which occurs in a solid wall.

From the foregoing discussion, it may be concluded that apart from the increase in the vertical stress concentration over the supports, the influence of a central door or window opening on the interaction between the wall and beam is insignificant. For an opening near a support, however, the stress flow is influenced by the geometry of that opening. An offset door opening gives rise to a point-load effect part-way along the span and hence induces very high vertical stress concentration in the wall and substantial bending moment and deflection in the supporting beam.

5.4 APPROXIMATE ANALYSIS

5.4.1 Walls with Central Opening

In Section 5.3, it has been shown that apart from the small increase in the maximum vertical stress in the bottom corners of the wall, the effect of a central door or window opening on the behaviour of the composite beam is insignificant. The approximate formulae proposed in Chapter 4 for the analysis of walls without openings should therefore be applicable to a great extent to the analysis of walls containing central openings. Comparison with the experimental results is referred

to in Section B of Chapter 3.

As regards the maximum vertical stress in the wall and axial force in the beam, the following approximate analysis is proposed.

5.4.1.1 *Maximum Vertical Stress*

A wall on beam behaves, as described earlier, in a similar way to a tied arch, with the wall arching across the span and the beam acting as a tie. The arching thrust in the wall is assumed to follow a parabolic distribution as shown in Figure 5.27.

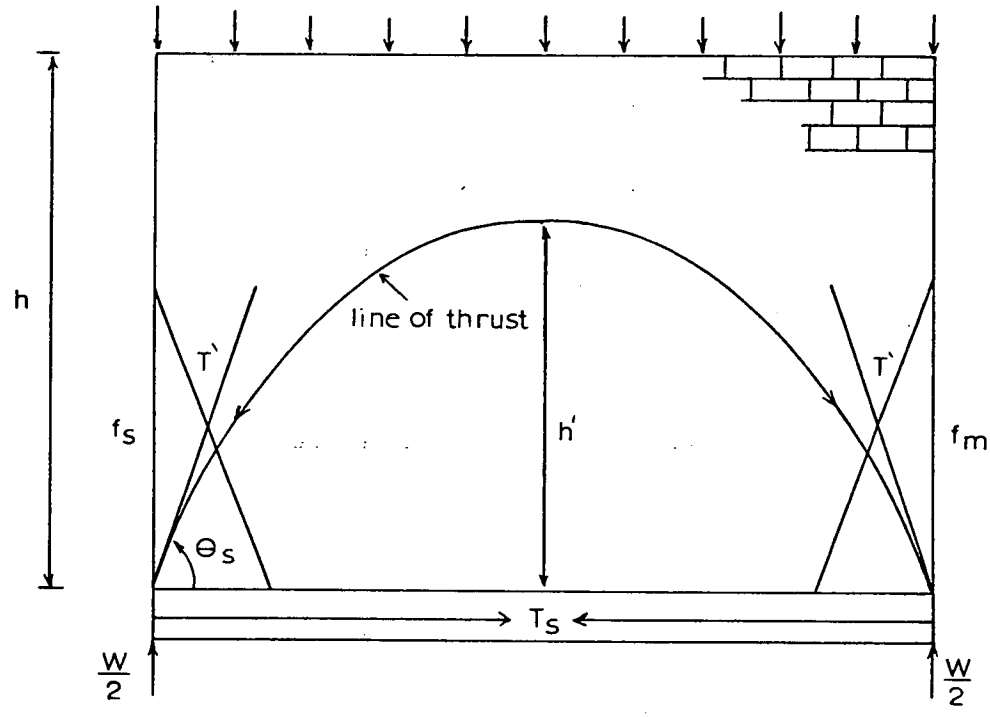

FIG. 5.27 Tied Arch Action In A Solid Wall.

It is apparent from the principal stress distribution shown in Figure 4.11 that the height of the parabola (h') is

approximately 0.6 h. Wood and Simms[3] suggested that the maximum allowed value of h' is 0.7 L, whereas the minimum value is 0.66 h. It has been shown in Chapter 4 that for walls of height-to-span ratio greater than 1, the stress distribution remains unchanged. A limiting h/L ratio of 1 will thus be considered for which the value of h' will be 0.7 h according to the upper limit proposed by Wood and Simms. However, to avoid the complication arising in assuming different h/L ratios, a mean value of 0.65 h will be assumed.

At the support points the arching thrust is resolved into a vertical and a horizontal component. The vertical component equals the reaction and the horizontal component gives rise to the interface shear stress. The slope of the parabola at these points determines the intensity of the maximum vertical stress. An outspread of the arch, as induced in a wall supported on a flexible beam, will result in a high vertical stress concentration, whereas the vertical loading on the beam spreads towards the centre of span when the arch flattens, as in the case of a relatively stiff supporting beam.

When a central opening occurs in the wall, the arching thrust is formed through the lintel whenever this occurs at 0.65 h or above. This is illustrated by the principal stress distributions shown in Figures 5.12 to 5.15.

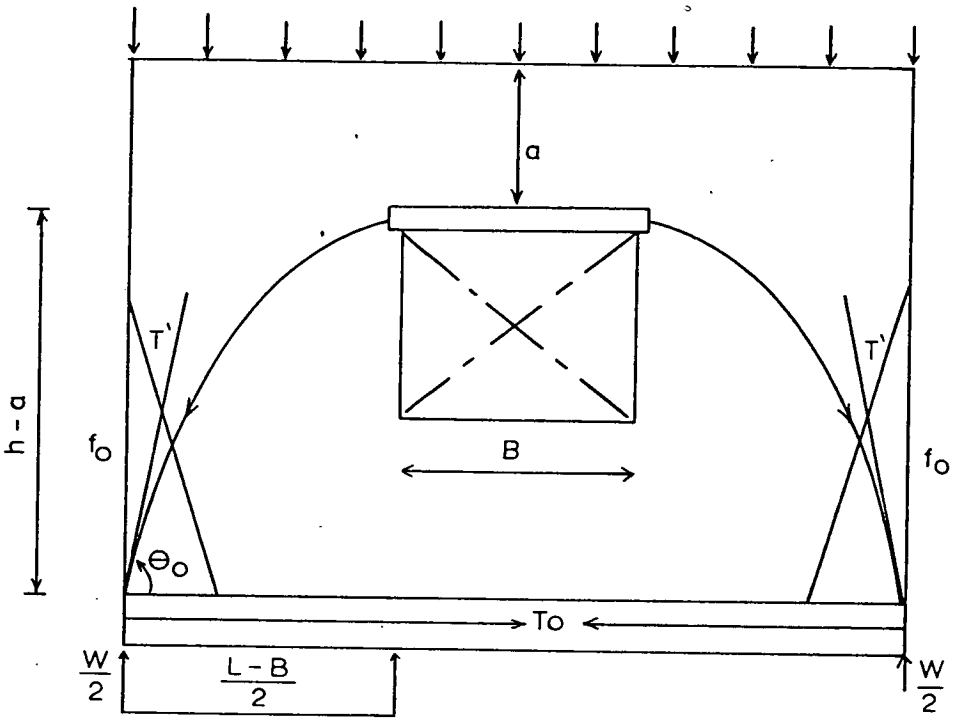

FIG. 5.28 Arching Action In A Wall With A Central Opening

The magnitudes of the arching thrust (T') in a solid wall and that in a similar wall containing a central opening are equal. However, its inclination at the support points in the latter is governed not only by the relative stiffness parameter R but also by the geometry of the opening.

If the magnitude of the maximum vertical stress and the inclination of the thrust at the support in a solid wall are denoted by f_s and θ_s respectively, and if the corresponding values in a wall with an opening are denoted by f_o and θ_o respectively, then by comparison :

$$\frac{f_s}{f_o} = \frac{\sin \theta_s}{\sin \theta_o} \qquad \ldots (5.1)$$

$$\therefore \quad f_o = f_s \frac{\sin \theta_o}{\sin \theta_s} \qquad \ldots (5.2)$$

From the parabolic distributions of the resultant thrust, it follows that

$$\theta_s = \tan^{-1} \frac{4h'}{L} \qquad \ldots (5.3)$$

and

$$\theta_o = \tan^{-1} \frac{4(h - a)}{L - B} \qquad \ldots (5.4)$$

$$\therefore \quad f_o = f_s \frac{\sin[\tan^{-1} \frac{4(h - a)}{L - B}]}{\sin[\tan^{-1} \frac{4h'}{L}]} \qquad \ldots (5.5)$$

but $h' = 0.65\ h$ and by substituting for f_s from equation (4.7.3)

$$f_o = \frac{W}{Lt} (1 + \beta R) \frac{\sin[\tan^{-1} \frac{4(h - a)}{L - B}]}{\sin[\tan^{-1} \frac{2.6\ h}{L}]} \qquad \ldots (5.6)$$

5.4.1.2 *Beam and Axial Force*

It has been shown in Chapter 4, that the horizontal shear stress at the wall/beam interface is resisted by the axial force in the beam. As the magnitude of the shear stress is governed by the slope of the resultant thrust over the supports, it is possible that the axial force in a beam supporting a wall with

a central opening could also be derived using the same procedure adopted in the evaluation of the maximum vertical stress.

If the axial force in the beam supporting a solid wall is denoted by T_s and that in an identical beam supporting a similar wall with a central opening is T_o, then by comparison :

$$\frac{T_o}{T_s} = \frac{\cos \theta_o}{\cos \theta_s} \qquad \ldots (5.7)$$

From which,

$$T_o = T_s \frac{\cos \theta_o}{\cos \theta_s} \qquad \ldots (5.8)$$

Substituting for T_s from equation (4.7.5) and for θ_s and θ_o from (5.3) and (5.4) respectively, gives :

$$T_o = W(\alpha - \gamma K) \frac{\cos[\tan^{-1} \frac{4(h - a)}{L - B}]}{\cos[\tan^{-1} \frac{2.6\ h}{L}]} \qquad \ldots (5.9)$$

5.4.2 Walls with Offset Opening

5.4.2.1 *Maximum Vertical Stress*

In order to study the influence of the relative beam stiffness on the magnitude of the maximum vertical stress over the support near to a doorway, the beam stiffness was varied in the case of walls D4 to D6.

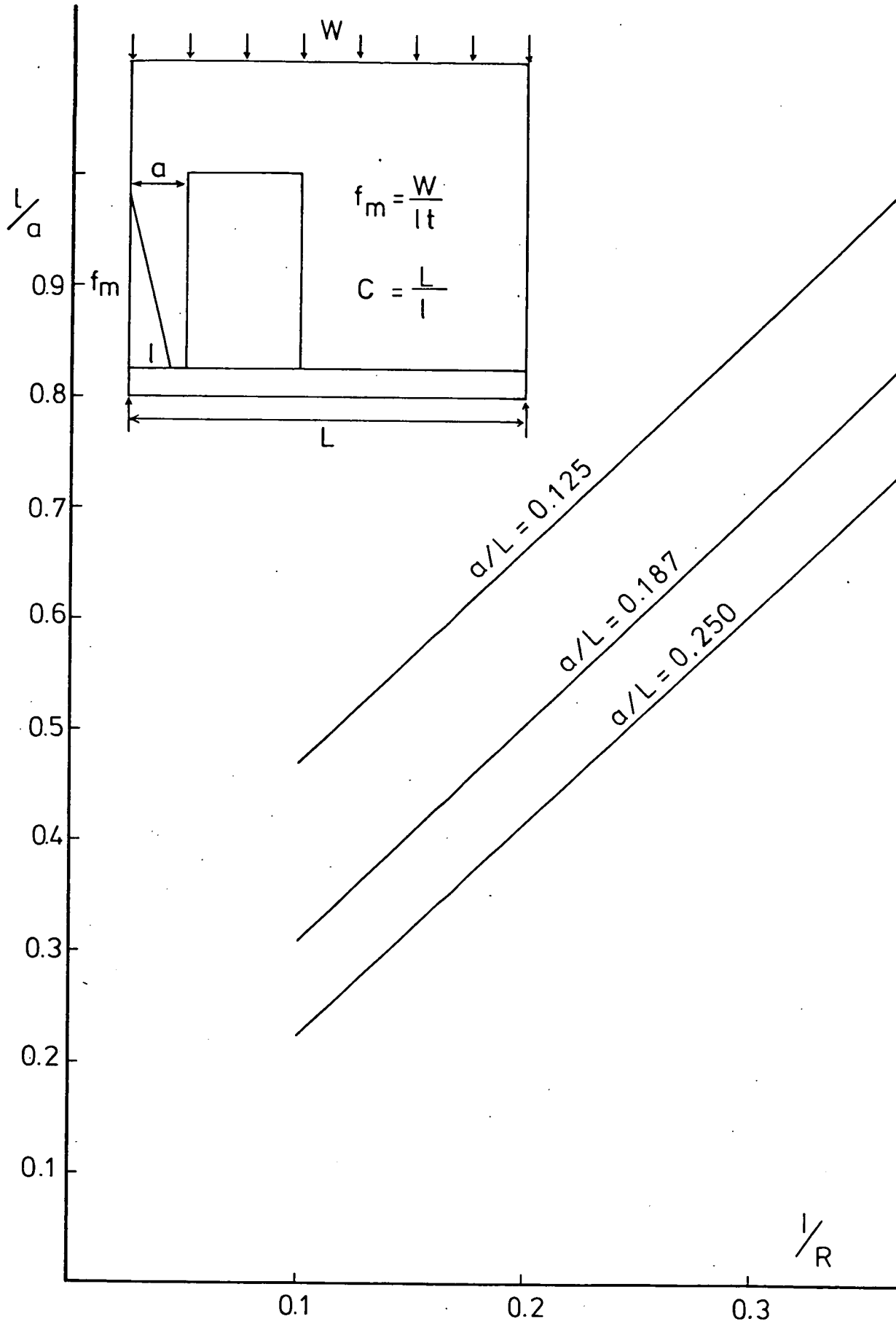

FIG. 5.29 VARIATION OF CONTACT LENGTH (l) WITH ($\frac{l}{R}$).

The results indicated that the maximum vertical stress is influenced by the relative beam stiffness as well as by the width (a) of the wall section to the left-hand side of the opening, Figure 5.29.

The effect of the relative beam stiffness on the magnitude of the maximum vertical stress has been discussed in Chapter 4. It is also obvious that with increasing section width the stress concentration decreases. The results are summarized in Table 5.9. In all cases the distribution of the interface vertical stress along the length a is approximately triangular, with tensile stresses developing at the bottom corner of the doorway.

The portion of the load transmitted down to the support near the opening is not constant, but actually varying within a range of 0.367 W to approximately 0.5 W, depending on the relative beam stiffness and the width a. Conservatively, half of the total load will be assumed to be carried by that section of the wall.

Assuming a triangular stress distribution and neglecting the tensile stresses at the bottom corner of the opening, a contact length (ℓ) has been derived using the values of the maximum vertical stress obtained from the finite element results. This has been plotted in Figure 5.29 in a non-dimensionalized form as (ℓ/a) against the reciprocal of the stiffness parameter R. A linear relationship for each

section width is seen to exist.

From Figure 5.29 by resolving vertically

$$\frac{f_m \cdot \ell \cdot t}{2} = \frac{W}{2} \qquad \ldots (5.10)$$

$$\therefore \quad f_m = \frac{W}{\ell t} \qquad \ldots (5.11)$$

ℓ can be obtained from Figure 5.29.

Since the average stress is given by $\frac{W}{\ell t}$, it follows that the stress concentration factor (C) is given by :

$$C = \frac{f_m}{f_{av}} = \frac{L}{\ell} \qquad \ldots (5.12)$$

TABLE 5.9 MAXIMUM VERTICAL STRESS IN WALLS D4 TO D6

		Maximum Vertical Stress ($\frac{f.t}{\omega}$)		
L/d	R	a/L = 0.125	a/L = 0.187	a/L = 0.250
8	4.29	10.8	8.8	8.4
12	5.83	13.5	11.8	11.4
15	6.89	14.6	13.8	13.0
20	8.55	15.8	15.0	14.8
24	9.80	16.4	16.0	15.6

5.4.2.2 *Beam Axial Force*

As in the case of solid walls, the axial force in a beam supporting a wall with offset opening is mainly influenced by the wall/beam relative axial stiffness. The effect of distance (a) of opening from the support, as indicated by Table 5.10, is not much pronounced. This is also shown diagramatically in Figure 5.30.

As seen from Figure 5.30, an approximate linear relationship exists between the axial force, non-dimensionalized as (T/W), and the axial stiffness parameter K for each value of a/L. Figure 5.30 also indicates that T/W varies insignificantly with a/L. It will therefore be assumed that T/W is constant for $a/L \geq 0.125$, which yields the following approximate expression for the axial force in a beam supporting a wall with an offset opening :

$$T = W(0.325 - 0.048\ K) \qquad \ldots (5.13)$$

5.4.2.3 *Beam Bending Moment*

The distribution of the bending moment in a beam supporting a wall with an offset door opening is illustrated in Figure 5.26. It is clearly evident that the opening has markedly affected the moment distribution particularly along the central region of the span. A noticeable effect is the development of a peak moment immediately below the inner edge of the opening.

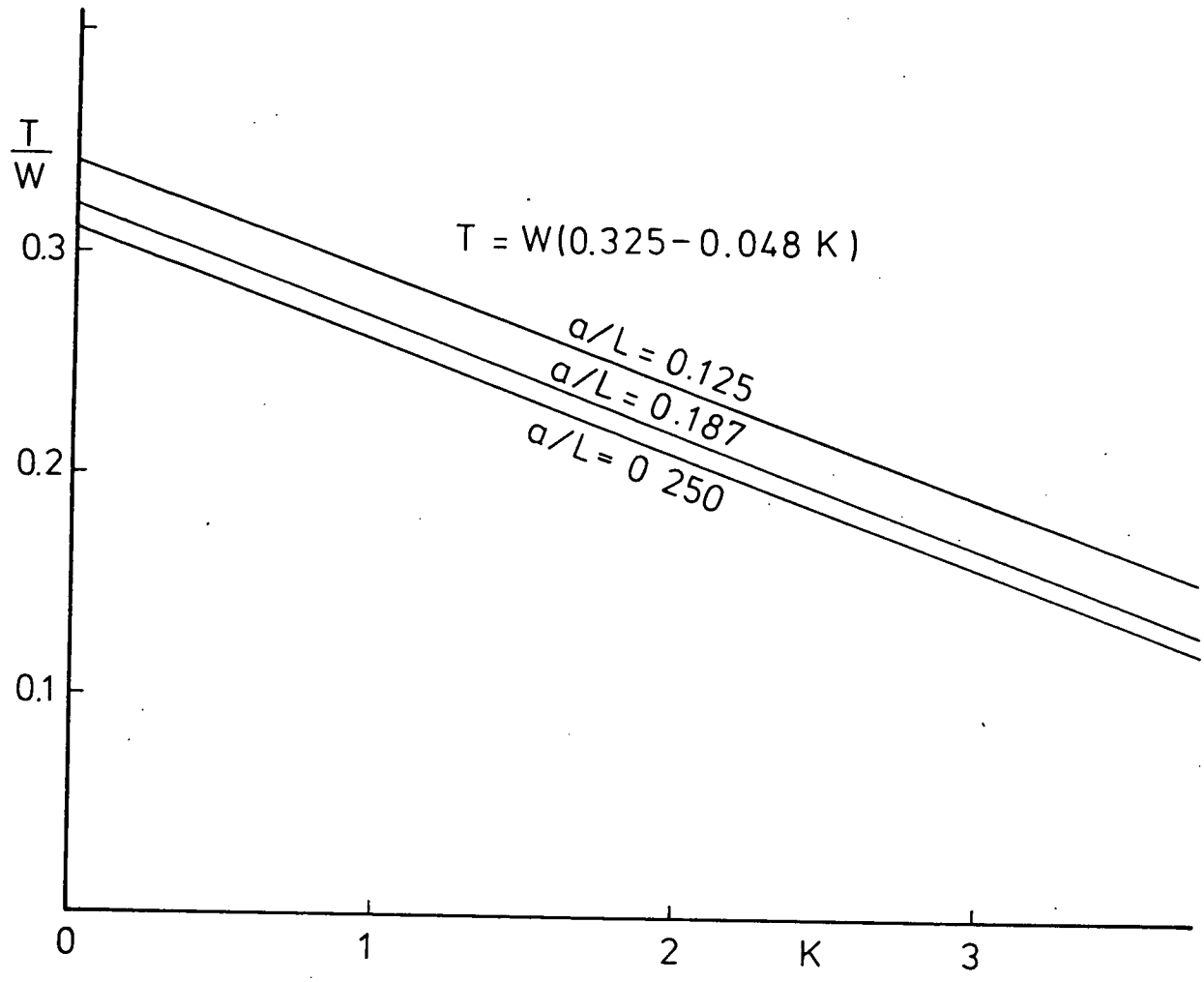

FIG. 5.30 VARIATION OF BEAM AXIAL FORCE WITH K.

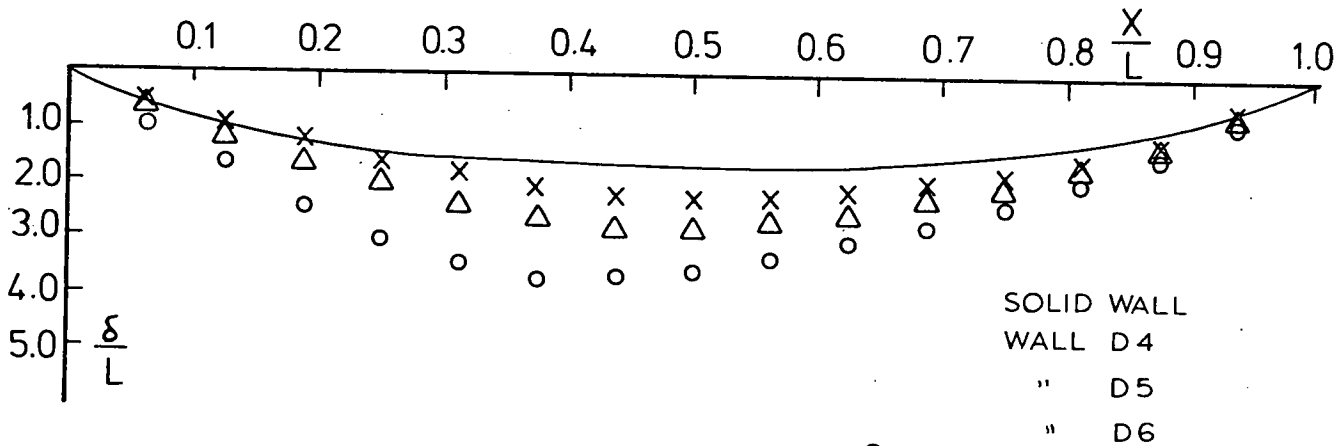

FIG. 5.31 DEFLECTION DISTRIBUTION (IN 10^6) ALONG SPAN OF SUPPORTING BEAM.

The bending moments at approximately one-third of the span from the right-hand support are of the same order of megnitude compared to that in a beam supporting a solid wall. However, the peak moment has increased by 10 per cent for the three locations of the doorway. The central bending moment is increased by 200 to 300 per cent.

Table 5.11 shows the magnitude of the maximum bending moments in the beam expressed in a non-dimensionalized form as (M/WL). The percentage difference between these values and the corresponding values in a beam supporting a similar solid wall vary between 2 to 40 per cent in accordance with variation in the stiffness parameter R.

Although it was not found possible to drive a suitable approximate expression for the moments, nevertheless, it is suggested that the maximum bending moment in the beam for $R \leqslant 6$ and $a/L \leqslant 0.125$ is increased by 40 per cent over the value for solid walls as given in Chapter 4. Otherwise, it is 10 percent more for all values of R and a/L.

5.4.2.5 *Ultimate Load*

It has been shown in Chapter 3 that walls with offset door opening failed by tensile splitting and crushing of the pier of bricks at the side of the opening. From experiments and the finite element analysis it has been found that the portion of the load transmitted down the section of width (a), Figure 5.29,

is approximately half the applied load. It therefore follows that the average stress (f'_{av}) in the section is given by :

$$f'_{av} = \frac{W}{2} \cdot \frac{1}{at} \qquad \ldots (5.14)$$

Failure will occur when the average stress exceeds the brickwork crushing strength,

$$\therefore \qquad W_{ult} = 2f_c \cdot at \qquad \ldots (5.15)$$

5.4.2.6 *Beam Deflection*

Figure 5.31 shows the deflection along the beam span for an applied load of 7 KN/M^2. The results for different L/d ratios are summarized in Table 5.12, from which it can be seen that the average deflection varies between 1.34 to 2.25 times that encountered in solid walls. It is to be noted that the maximum deflection is slightly displaced from midspan towards the inner edge of opening, however, the maximum values and those at midspan are almost identical.

From Figure 5.30, it may be seen that the measured central deflection in walls 8a and 8b is nearly 2.5 times that recorded in walls of series 5. The approximate maximum or central deflection in a beam supporting a wall with an offset door opening will thus be assumed to be 2.5 times that in the

case of a solid wall and is given by :

$$\delta_o = \frac{WL^3(3 + 10\,\beta R + 5\,\beta^2 R^2)}{96\,E_b I(1 + \beta R)^3} + \frac{0.75\,WL}{E_w\,h\,t_w} - \frac{WL^3 d(\alpha - \gamma K)}{9.6\,E_b I} + \frac{W_b L^3}{154\,E_b I}$$

Comparisons with the experimental results are referred to in Section B of Chapter 3.

CHAPTER 6 : ANALYSIS OF THE COMPOSITE ACTION OF WALLS AND THEIR SUPPORTING STRUCTURES

6.1 INTRODUCTION

In the previous chapters the analysis of the interaction of composite beams has been confined to the case of point supported beams. The point-support condition is unlikely to occur in practice, although it represents the most severe boundary condition.

The influence of different boundary conditions has been investigated and the results are given in this chapter. The boundary conditions considered were :

1. The effect of beam support width.
2. The effect of vertical edge ties or stanchions.
3. The behaviour of walls on continuous beams.
4. The effect of loading at the beam level.
5. The influence of fixity of the supports.

The method adopted for numerical solution was the finite element method using the same STRUDL computer program as explained earlier in Chapter 4. This permits expression of the boundary conditions in all directions, with the degree of accuracy of the same order as that of the fundamental data of the problem.

A number of particular cases illustrating the above five boundary conditions was studied on the same wall/beam structure for the purpose of comparison. Fig. 4.7.

6.2 EFFECT OF BEAM SUPPORT WIDTH

In many shear wall buildings, the shear walls are supported on a frame-type of a structure to provide a large open space at the ground floor. Load-bearing walls of houses and light buildings are usually built on short bored piles in expansive soils. In these cases, the beam supports have a finite width which as will be seen, affects the stress distribution in the wall and beam specifically in the region of the supports.

In this analysis, a support width of 0.055 times the full span or 0.063 times the clear span was considered and was idealized as zero vertical and horizontal displacements and zero rotation over the support points.

The distribution of the interface vertical stress is shown in Figure 6.1. The characteristic of this stress distribution is that the magnitude of the vertical stress decreases towards the edges of the wall and that the maximum stress occurs over the inner side of the support. This indicates that the arching effect is taking place over the clear span rather than over the full length of the wall as in the case of a point-supported beam.

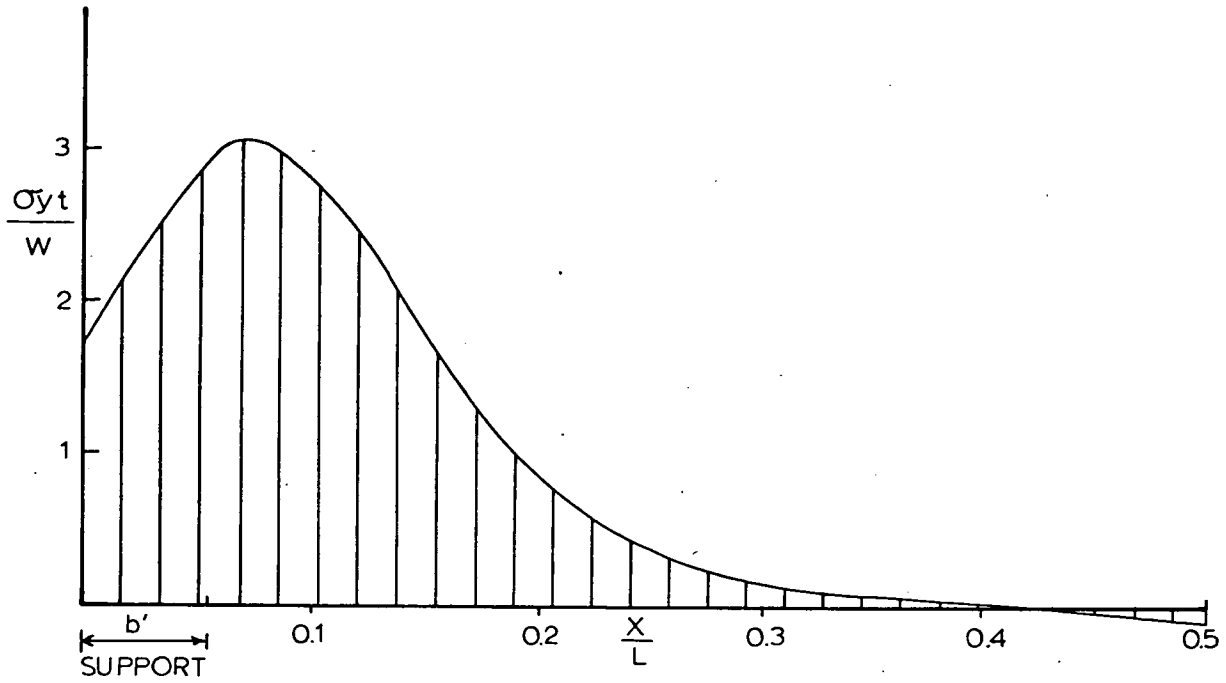

FIG. 6.1 VERTICAL STRESS DISTRIBUTION AT THE WALL/BEAM INTERFACE

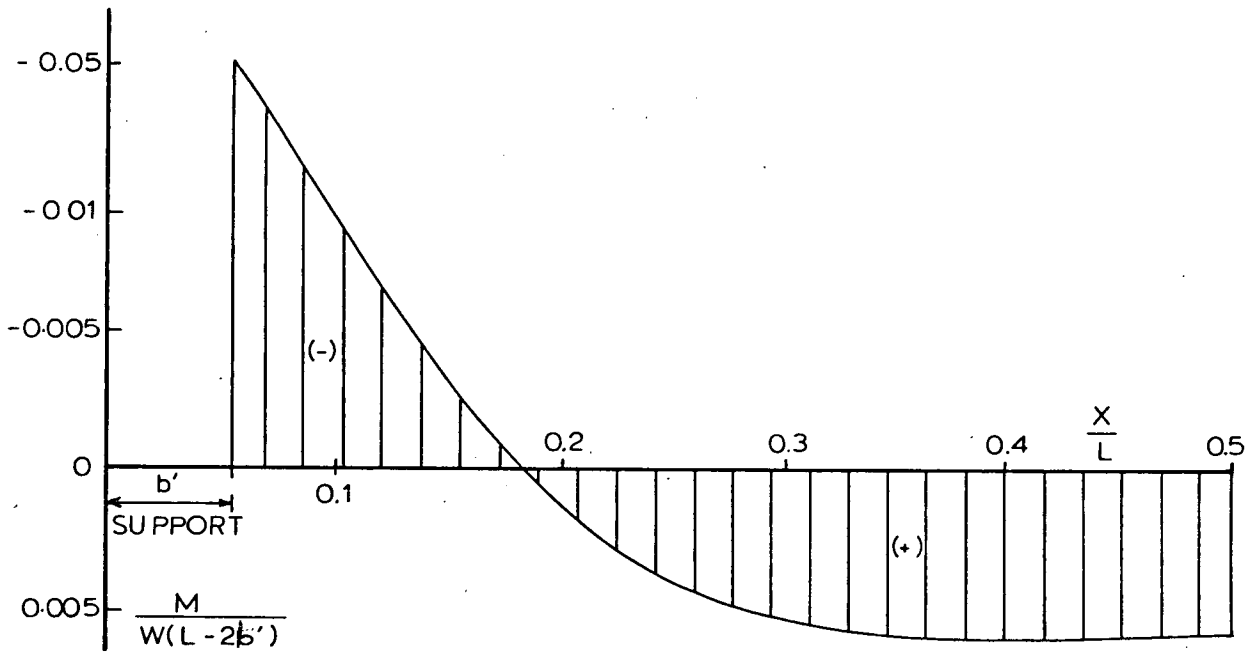

FIG. 6.2 BEAM BENDING MOMENTS

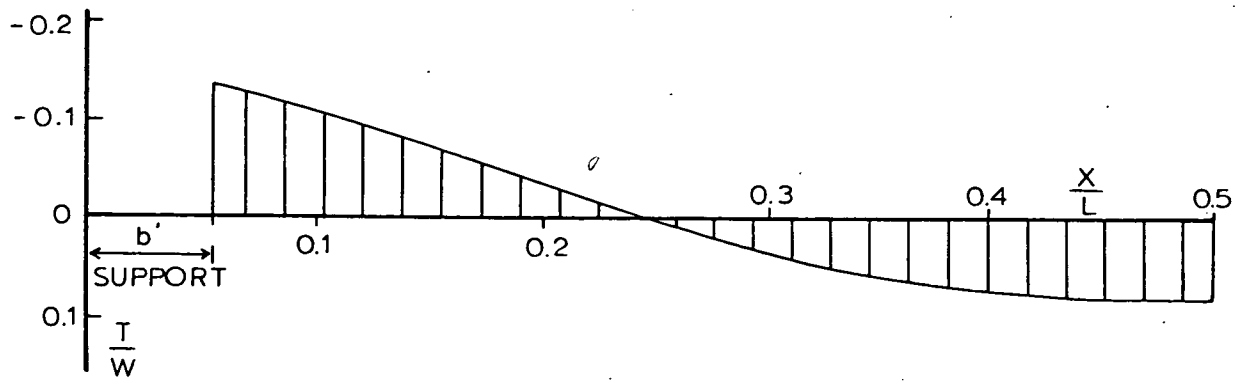

FIG. 6.3 BEAM AXIAL FORCE.

A remarkable effect of the finite support width is the substantial reduction in the magnitude of the vertical stress concentration over the supports. In the region above the support the wall has been relieved from the stress concentration to almost less than one-third the magnitude of that obtained in the case of a point-supported beam. As has been shown in Chapters 3 and 4 that the maximum vertical stress over the supports is the dominant failure criterion, it appears that the ultimate carrying capacity of composite beams of finite support width will be more than that of a similar wall on a point-supported identical beam.

The bending moment distribution in the supporting beam is shown in Figure 6.2. This indicates sagging moments in the central region of the span and appreciable amount of hogging moment at the supports. The hogging moment is mainly due to the fixity at the ends of the beam. The absolute maximum value of this moment is about three times the sagging moment at midspan.

Figure 6.3 shows the distribution of the axial force in the supporting beam. This is shown to be tensile along the central region of the span and compressive near the supports. The absolute maximum of the axial force occurs at the inner side of the support and it is twice the maximum tensile force at midspan. Compared to a point-supported beam, the maximum tensile force at midspan has been reduced by more than 60 per cent.

Experimental investigation carried out by Green[16] on shear wall perspex models, vertically loaded by two-point loads, has shown that high tensile forces exist in the supporting beam over a greater portion of the span than predicted by the finite element analysis. He therefore suggested that the reinforcement calculated on the basis of the maximum tie force should extend over the complete span of the supporting beam. He also concluded that the effective width of the support is chosen as 0.75 times the column width for an external column and 0.5 times the column width for an internal column.

6.3 EFFECT OF VERTICAL TIES OR STANCHIONS

The problem of laterally loaded infilled frames has received the attention of many research workers, however, very little work has been done on the behaviour of such a structure under the effect of vertical loading. In this section the analysis of a framed panel is considered with emphasis to the influence of the vertical edge ties or stanchions.

Figure 6.8 shows the vertical stress distribution in the wall along the wall/beam interface. A noticeable feature of this distribution is the considerable reduction in the vertical stress concentration at the bottom corners of the wall. The magnitude of the maximum vertical stress is nearly one-sixth of that obtained for a simply supported composite beam without stanchions and about half that produced in the case of a wall on

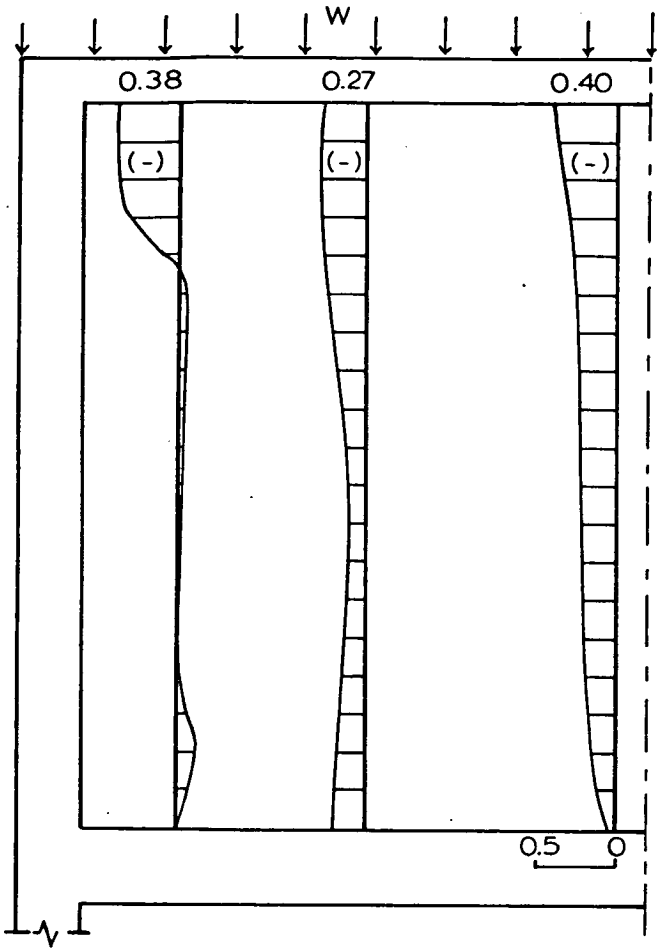

FIG. 6.4 HORIZONTAL STRESS DISTRIBUTION IN $\frac{\sigma x t}{W}$.

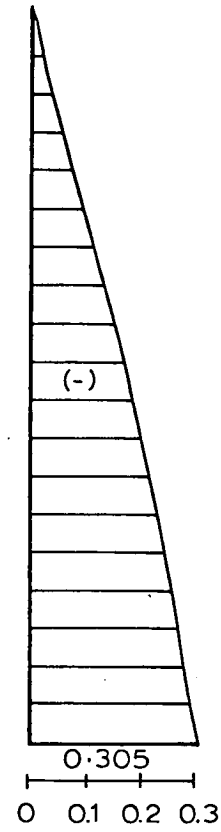

FIG. 6.5 AXIAL FORCE IN COLUMNS (IN T/W).

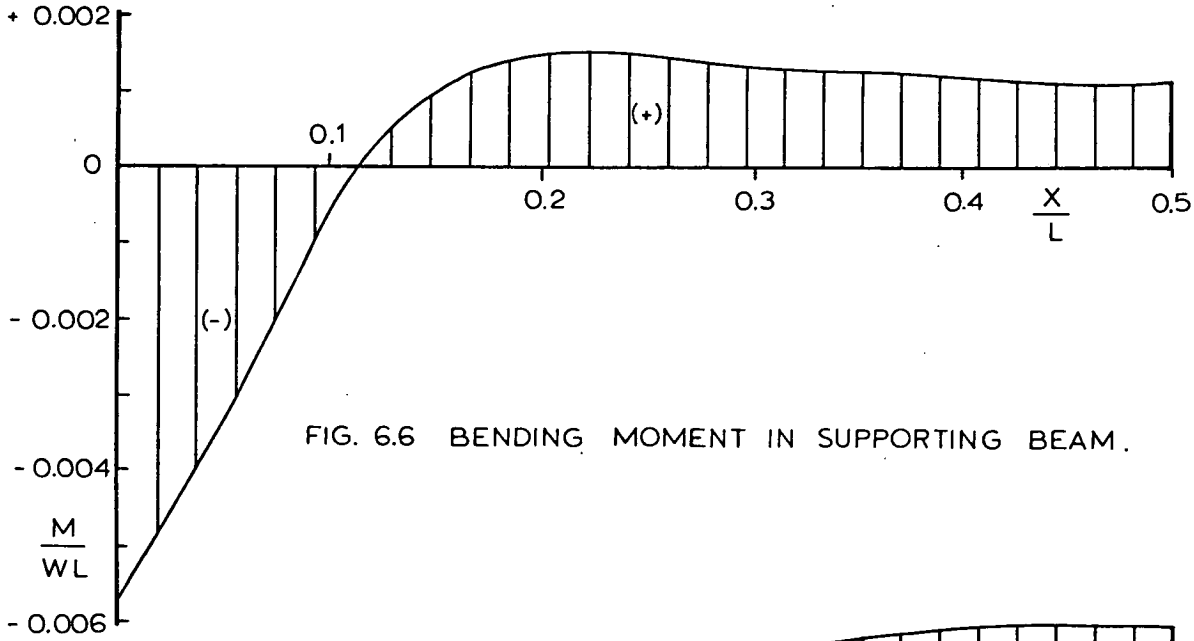

FIG. 6.6 BENDING MOMENT IN SUPPORTING BEAM.

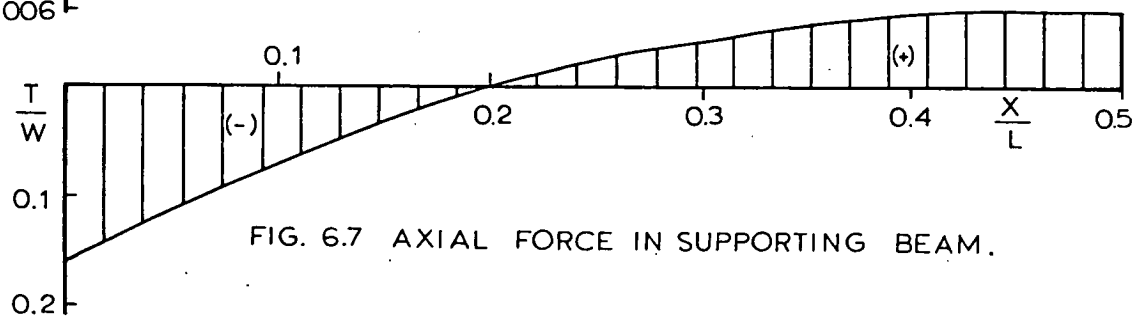

FIG. 6.7 AXIAL FORCE IN SUPPORTING BEAM.

beam of a finite support width. Table 6.1.

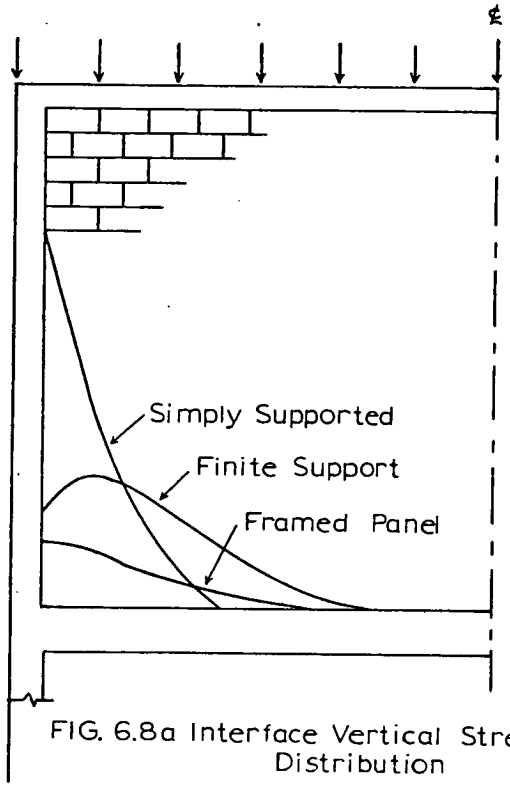

FIG. 6.8a Interface Vertical Stress Distribution

The insertion of vertical columns at the end of the wall has relieved the high local stresses in the panel over the supports. The axial force in the stanchions increases from the top of the wall to the supports as shown in Figure 6.5. The stanchions relieve the wall of vertical forces that are transmitted to them through the shearing stresses. Figure 6.9.

The magnitude of the shear stress along the common boundary between the wall and stanchion has been evaluated by Rosenhaupt and Sokal[7] for the case of an interior stanchion in a wall on continuous beam, as given by the following relationship :

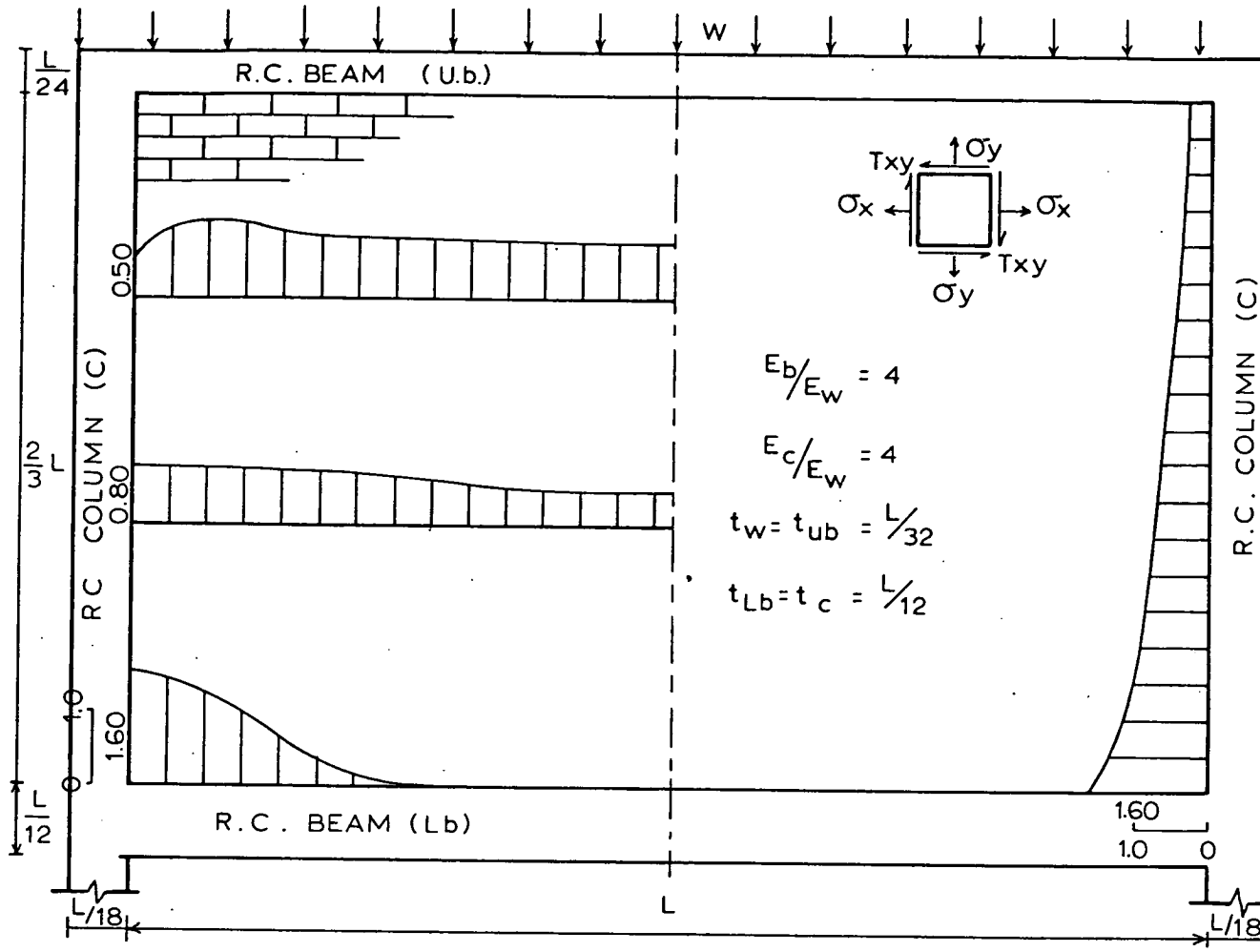

FIG. 6.8 VERTICAL STRESS DISTRIBUTION ($\frac{\sigma_y . t L}{W}$) IN INFILLED PANEL

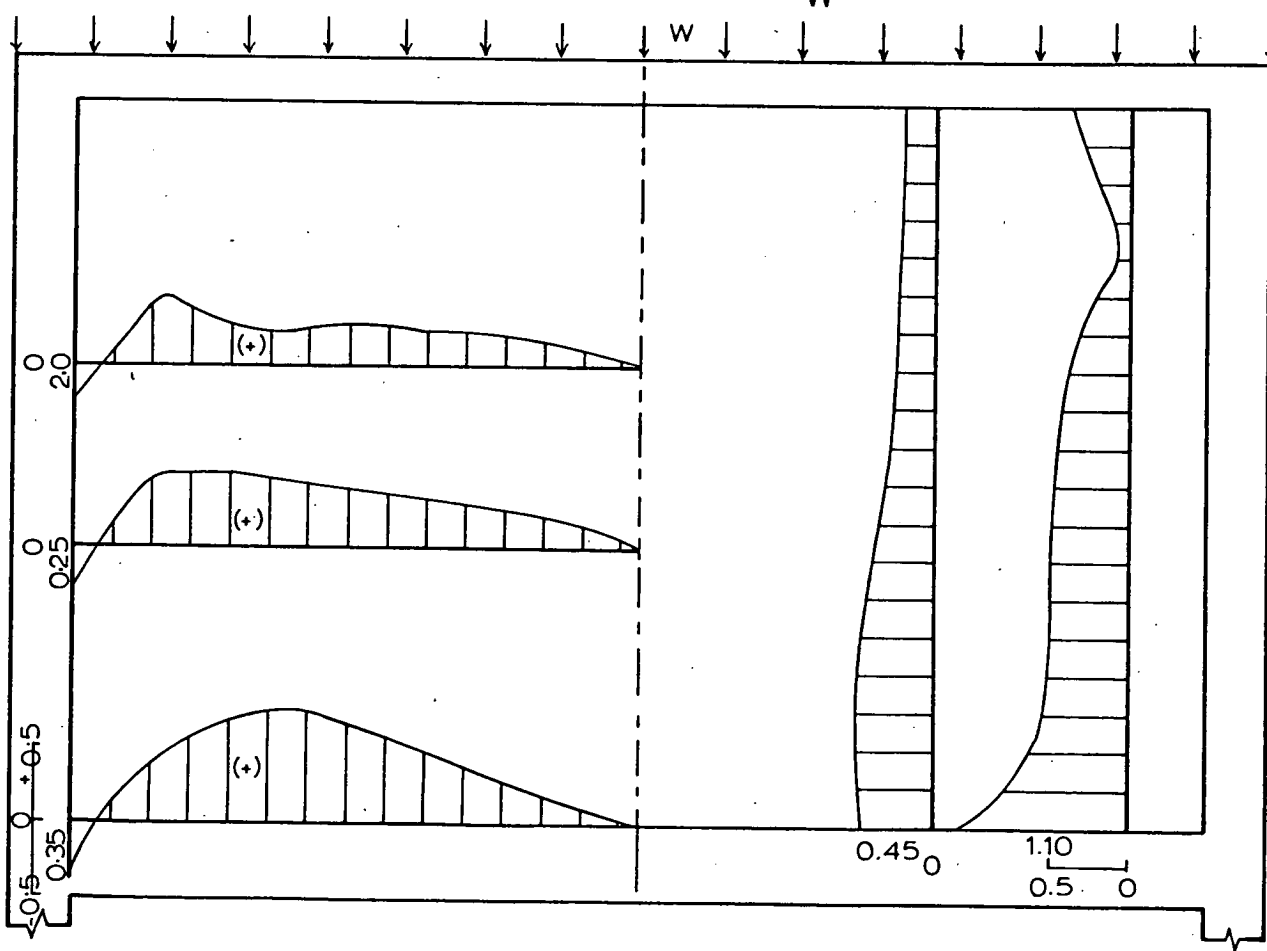

FIG. 6.9 SHEAR STRESS DISTRIBUTION ($\frac{\tau_{xy} t L}{W}$) IN INFILLED FRAME.

$$\tau = \frac{1}{2t} \cdot AE \cdot \frac{\Delta\varepsilon_y}{\Delta_y}$$

in which τ is the boundary shear stress, A and E are the sectional area of the stanchion and its elastic modulus respectively, $\Delta\varepsilon_y$ is the vertical strain in the stanchion and t is the wall thickness.

It follows that for the case of an end stanchion the shear can be shown to be equal to half that given above, namely :

$$\tau = \frac{1}{4t} \cdot AE \cdot \frac{\Delta\varepsilon_y}{\Delta_y}$$

From the distribution of the shear stress in the wall shown in Figure 6.9, it can be seen that it increases from top of the wall towards the supports where its maximum value occurs.

From above it follows that for the stanchions to be effective the above shear must be effectively transmitted to the stanchions and shear connectors may be used since it is unwise to rely upon bond only.

The substantial reduction in the vertical stress concentration will undoubtedly result in an increase in the failure resistance of the wall. This has been confirmed by results of tests carried out by Rosenhaupt[6] on vertically loaded masonry infill panels.

The distribution of the bending moment in the supporting beam shown in Figure 6.6 indicates hogging moments in the region of the supports due to the rigid joint between beam and stanchion, and sagging moment along a greater portion of the span. The magnitude of the midspan moment is much less than that produced in the case of a simply supported beam and this explains the reason for the comparatively low central deflection (Table 6.1).

The distribution of the axial force in the supporting beam follows the same trend as the bending moment distribution, Figure 6.7. This shows tensile forces along the central region of the span and compression near to the supports. The compression occurs as a result of the excessive hogging moment in the region of the supports.

6.4 EFFECT OF LOADING AT BEAM LEVEL

Most of the published works on the interaction between walls and their supporting beams deal with walls loaded at the top. There have been very few tests[21] conducted on wall panels loaded at the beam level. In practice loading at the beam level represents a floor loading.

The finite element analysis of this problem revealed that with the exception of the interface vertical stresses, the magnitudes and the distributions of the stresses in the wall and beam are almost of the same order in so far as the elastic stage is concerned (Figures 6.15 to 6.19).

Regarding the vertical stress distribution at the wall/beam interface it can be seen that very high tensile stresses have developed along the greater portion of the span and that the compressive stresses have concentrated near to the edge of the wall. The magnitude of the maximum tensile stress equals the applied stress and, surprisingly, the magnitude of the maximum vertical stress is the same as that induced in the case of loading at the top of the wall.

Failure of the interface joint to resist the vertical tensile stresses or the horizontal shear stress will reduce the frictional resistance and may cause separation and subsequently great loss in the composite action. As has been explained in Chapter 4 that the joint shear failure is not common in practical cases, it follows that for maintaining the composite action the interface tensile stresses may be resisted by either providing vertical tensile connectors between the wall and beam or by prestressing the composite beam.

The importance of the tensile connectors in the case of loading at the beam level has been affirmed by Ramesh et al[21]. From the results of tests carried out on brick panel walls on reinforced concrete beams, they showed that in all tests the first crack was observed at the junction of the wall and beam, because of the vertical tensile force coming at the junction. One of the tests failed by slipping of the vertical connectors indicating that the length of the connectors must be sufficient to provide the necessary bond strength. Another

test was reported to have failed by yielding of the tensile connectors.

Achyutha[22] suggested that the truss analogy method proposed by Rosenhaupt et al[24] can satisfactorily predict the stresses in the tensile connectors. However, Ramesh[21] showed that this may be valid only up to the formation of a crack at the junction of the wall and beam.

More detailed tests are required to confirm the results of these exploratory studies, for more economical design of the composite beam to be achieved.

6.5 THE BEHAVIOUR OF WALLS ON CONTINUOUS BEAMS

The supporting of walls on three point supports, will assist in preventing cracking due to foundation movements usually encountered in expansive soils or as a result of coal mining operations.

Typical results of stress distributions in a wall on continuous beam are shown in Figures 6.10 to 6.14. The wall analysed was assumed to be supported on a two-span point-supported continuous beam.

With reference to Figure 6.10, it can be seen that the vertical stress in the wall concentrates over the support points. The magnitude of the stress concentration over the exterior support is less than half that in a similar wall on

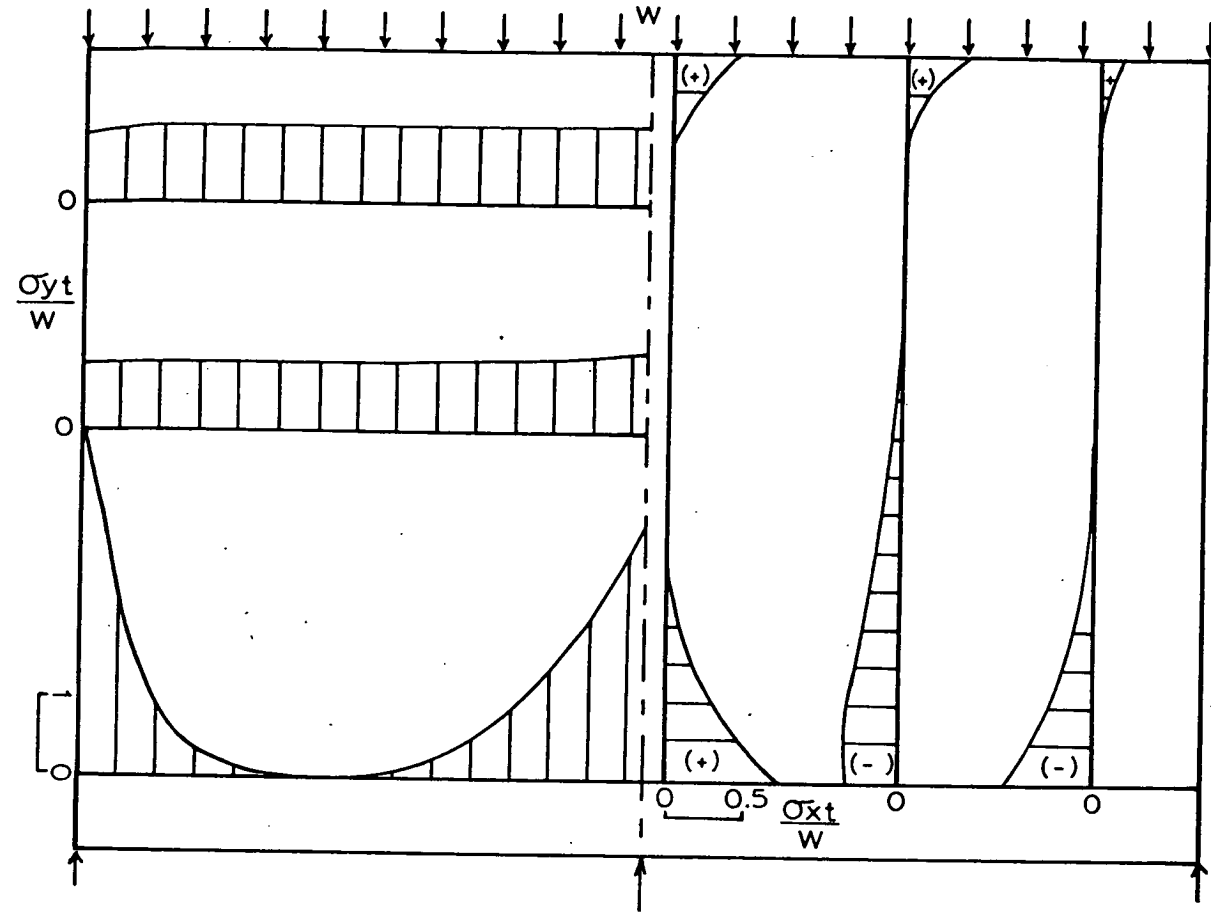

FIG. 6.10 VERTICAL AND HORIZONTAL STRESS DISTRIBUTIONS IN WALL ON CONTINUOUS BEAM.

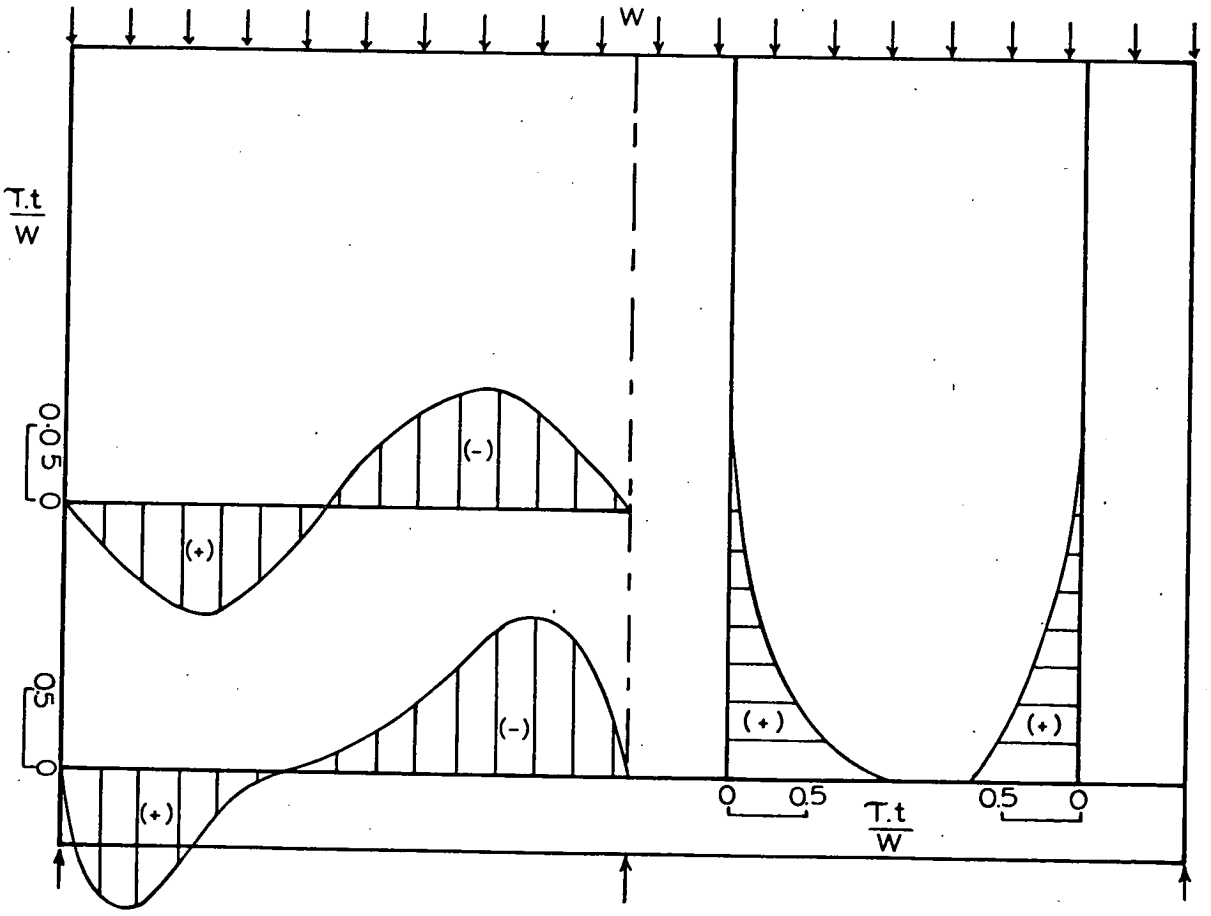

FIG. 6.11 SHEAR STRESS DISTRIBUTION IN WALL ON CONTINUOUS BEAM.

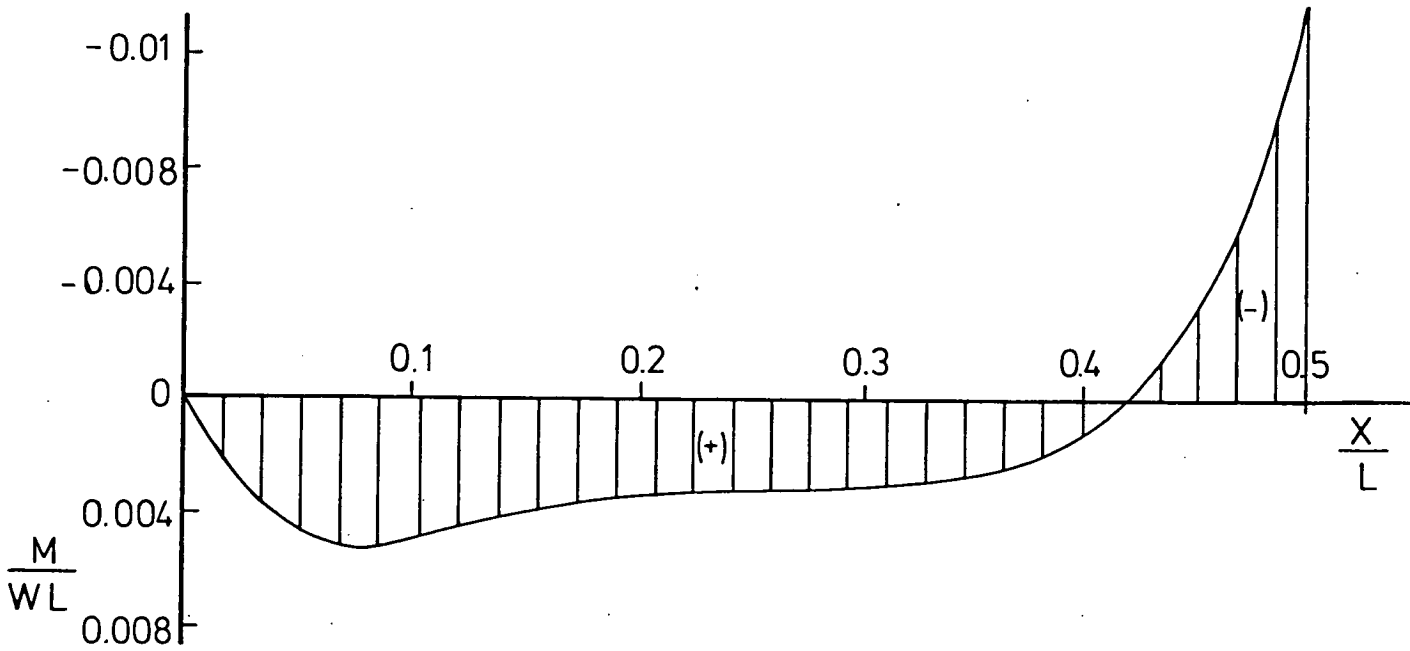

FIG. 6.12 BENDING MOMENT IN CONTINUOUS SUPPORTING BEAM.

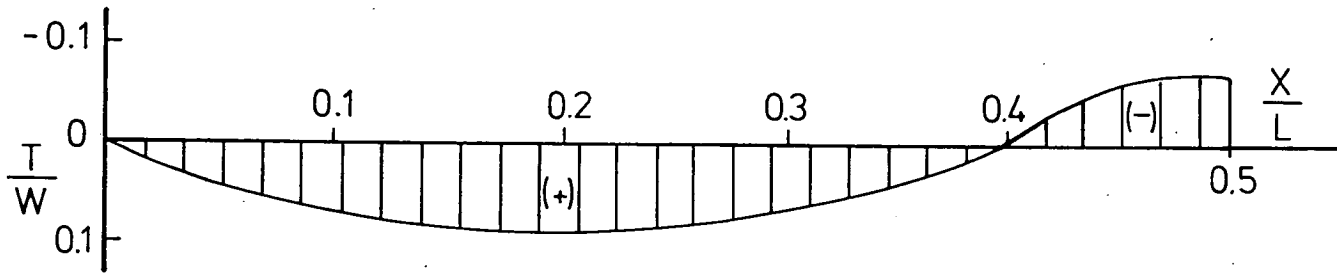

FIG 6.13 AXIAL FORCE IN CONTINUOUS SUPPORTING BEAM.

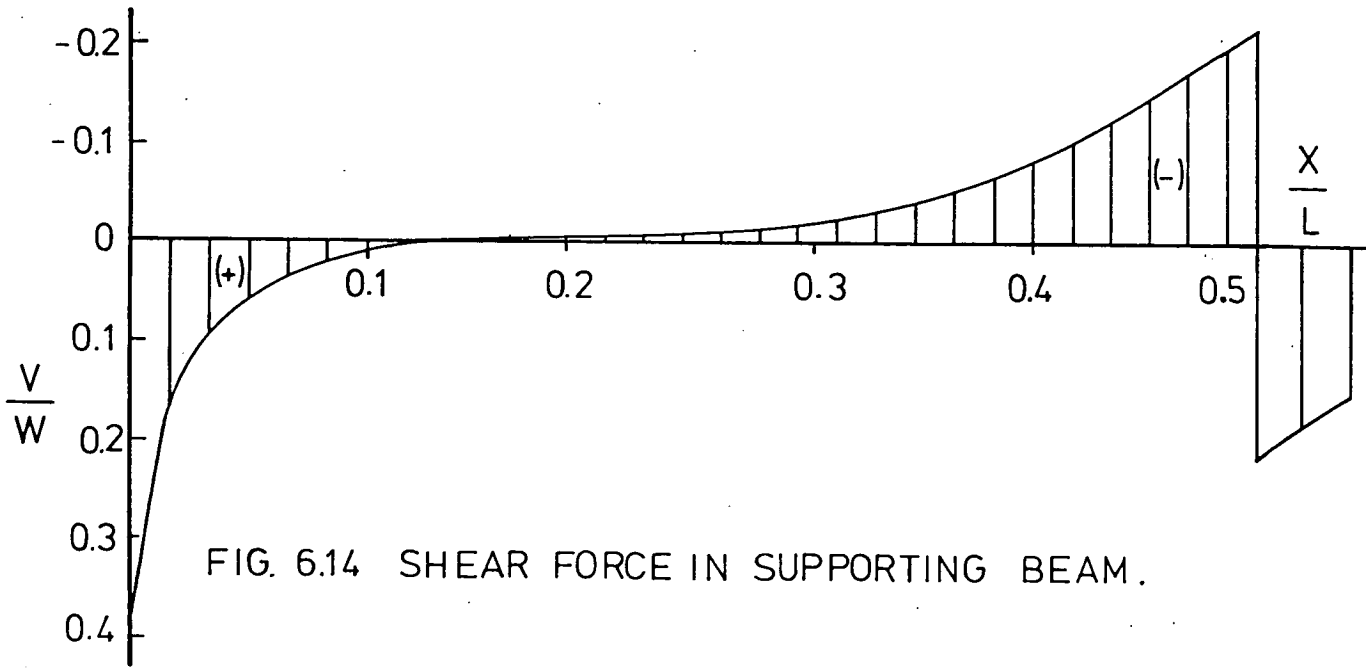

FIG. 6.14 SHEAR FORCE IN SUPPORTING BEAM.

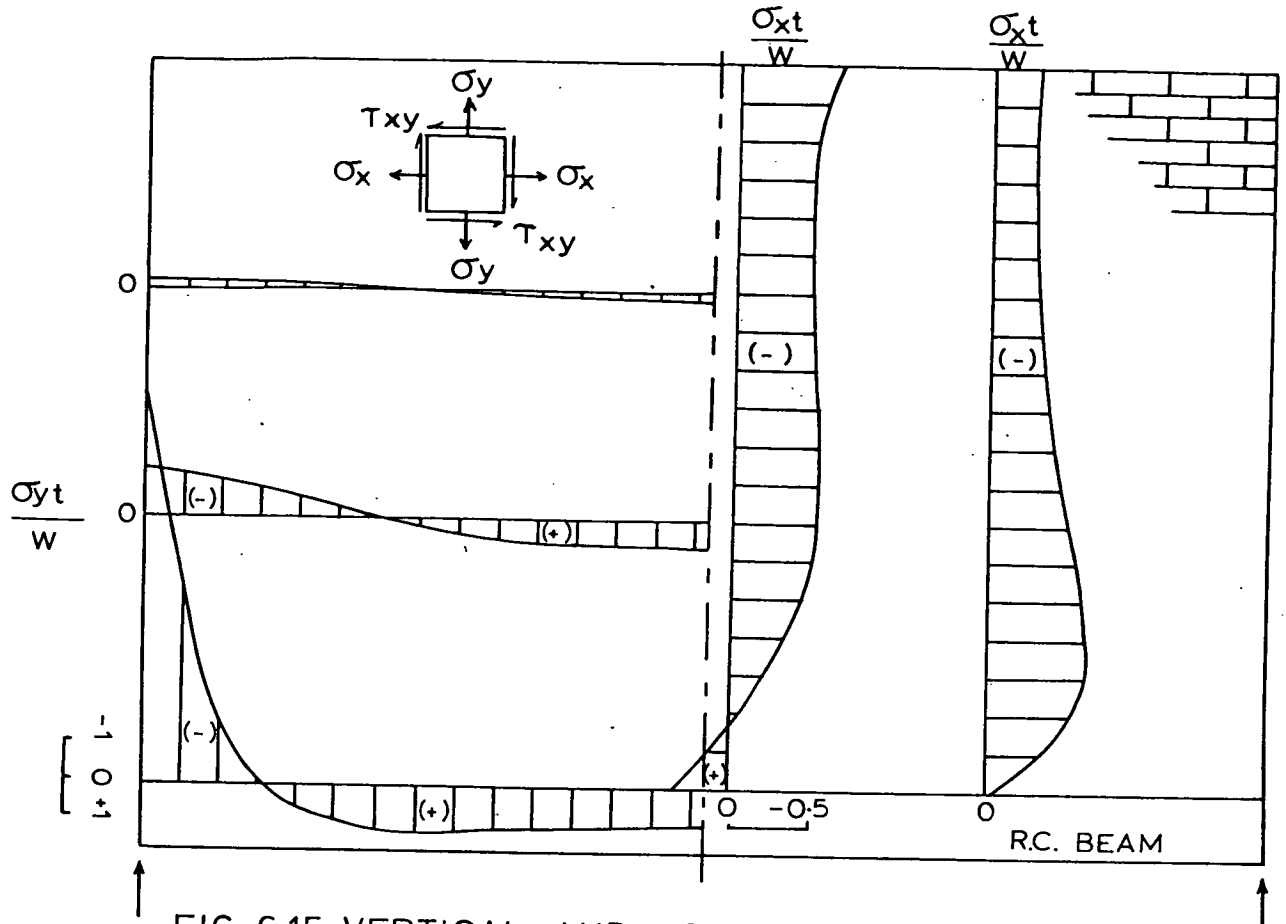

FIG. 6.15 VERTICAL AND HORIZONTAL STRESS DISTRIBUTIONS IN PANEL LOADED AT BEAM LEVEL.

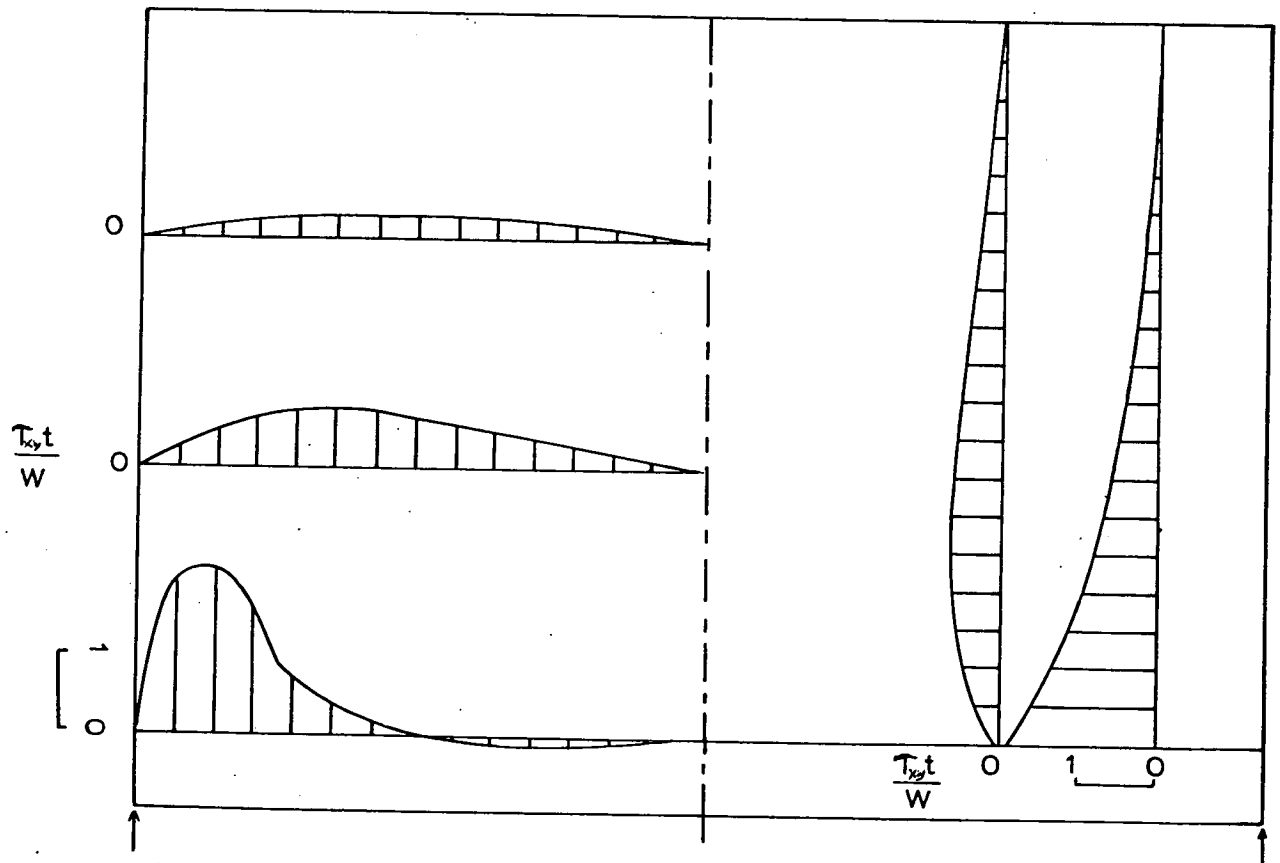

FIG. 6.16 SHEAR STRESS DISTRIBUTION IN PANEL LOADED AT BEAM LEVEL.

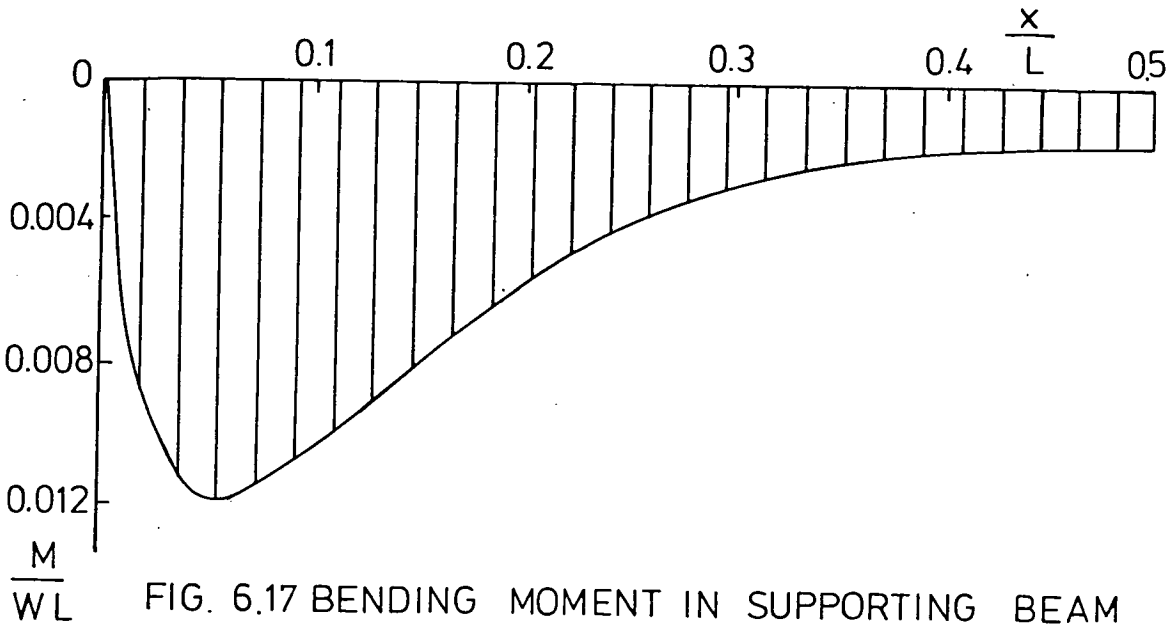

FIG. 6.17 BENDING MOMENT IN SUPPORTING BEAM WITH LOADING AT BEAM LEVEL.

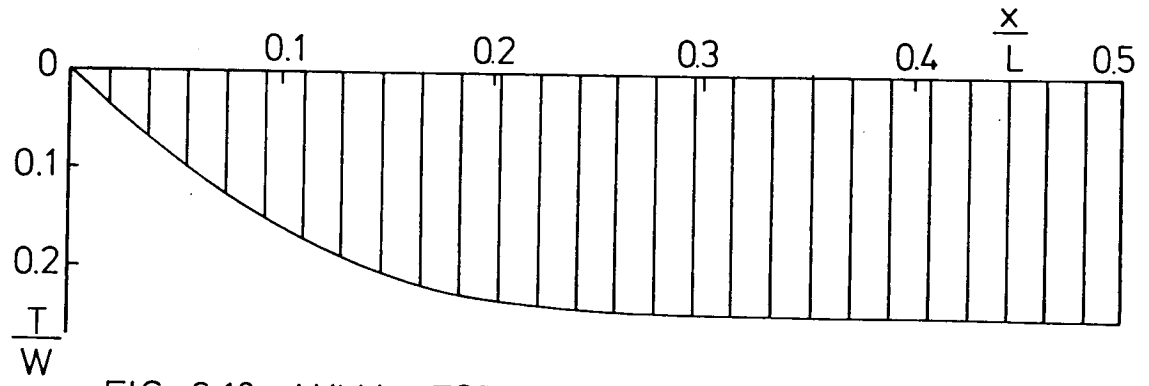

FIG. 6.18 AXIAL FORCE IN SUPPORTING BEAM WITH LOADING AT BEAM LEVEL.

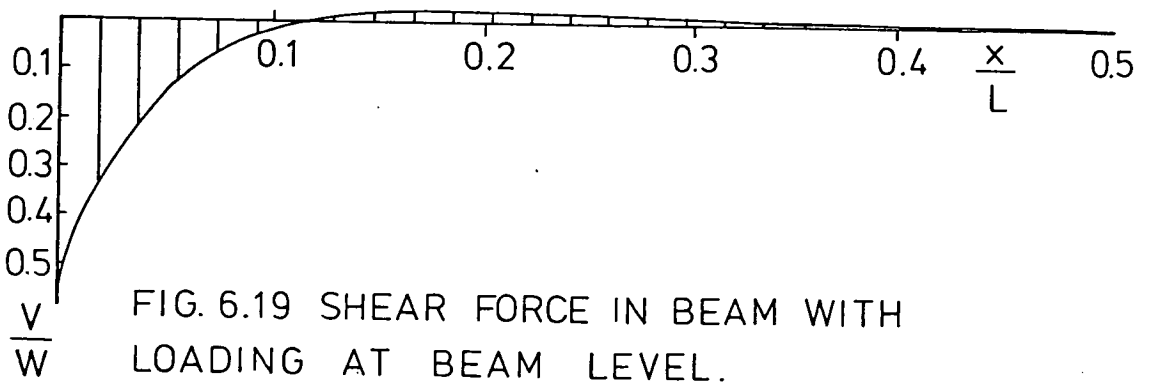

FIG. 6.19 SHEAR FORCE IN BEAM WITH LOADING AT BEAM LEVEL.

beam on two-points supports and is slightly higher than that over the interior support. However, the vertical loading on the beam along the central region of the span over the interior support is much higher than that over the end support. This is clearly evident from the shear force distribution in the supporting beam shown in Figure 6.14. This indicates that the magnitude of the interior reaction is 1.5 times that of the exterior reaction. However, it is to be noted that this is 30 per cent less than the magnitude of the same reaction in an elastic continuous beam. The latter, however, is 3.3 times that of the end support.

From results of tests on masonry walls on three-span reinforced concrete beams, it has been reported by Rosenhaupt and Sokal[7] that all measured reactions remained nearly equal until the first crack appeared after which the ratio of interior to end reaction began to increase and reached at the final stage of loading a value much lower than for an elastic beam. This was explained to be due to the loss of wall rigidity at the appearance of cracks.

The horizontal stress distribution in the wall is given in Figure 6.10. This shows tensile stresses at midspan along the wall height. These are balanced by axial compression in the supporting beam as shown in Figure 6.13. The couple formed by these forces induces the high hogging moment over the interior support as shown in Figure 6.12. It is seen that this is the

absolute maximum moment and that its magnitude is nearly half that in the elastic continuous beam.

6.6 ENCASTRE BEAM

Analysis of the composite beam with the ends of the supporting beam assumed as fixed has also been considered, the results are shown in Figures 6.20 to 6.22 and are summarized in Table 6.1.

The interface vertical stress distribution shown in Figure 6.20 indicates that the effect of the support fixity is to relieve the wall of the vertical stress concentration to less than half that when the beam is simply supported.

The most remarkable effect of the support fixity is the substantial hogging bending moment resulting from the restraints imposed upon the ends of the beam. However, the sagging moment is very much reduced compared to that in a simply supported beam. The effect of the composite action is shown by the fact that the magnitude of the fixed end moment in the composite beam is less than one-third that in a built-in beam.

6.7 COMPARISON OF RESULTS

Table 6.1 shows comparison of results for the particular five cases analysed above with those obtained for the simply

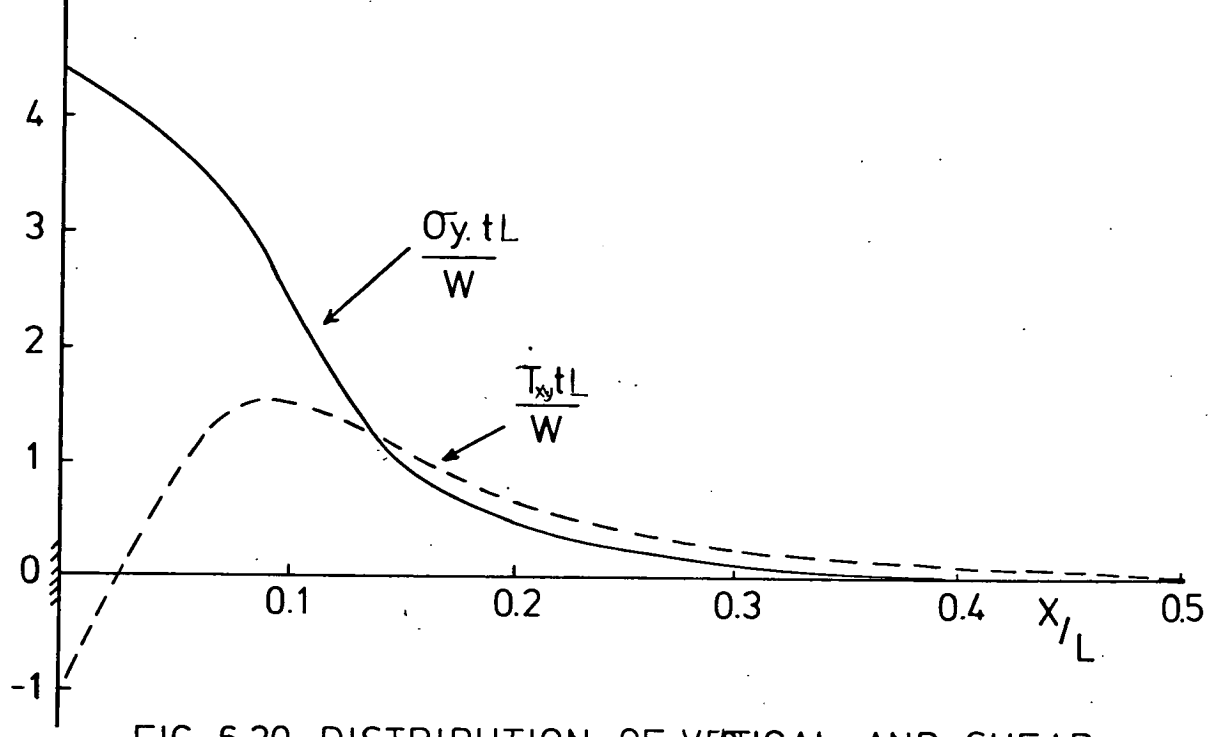

FIG. 6.20 DISTRIBUTION OF VERTICAL AND SHEAR STRESS AT WALL / BEAM INTERFACE.

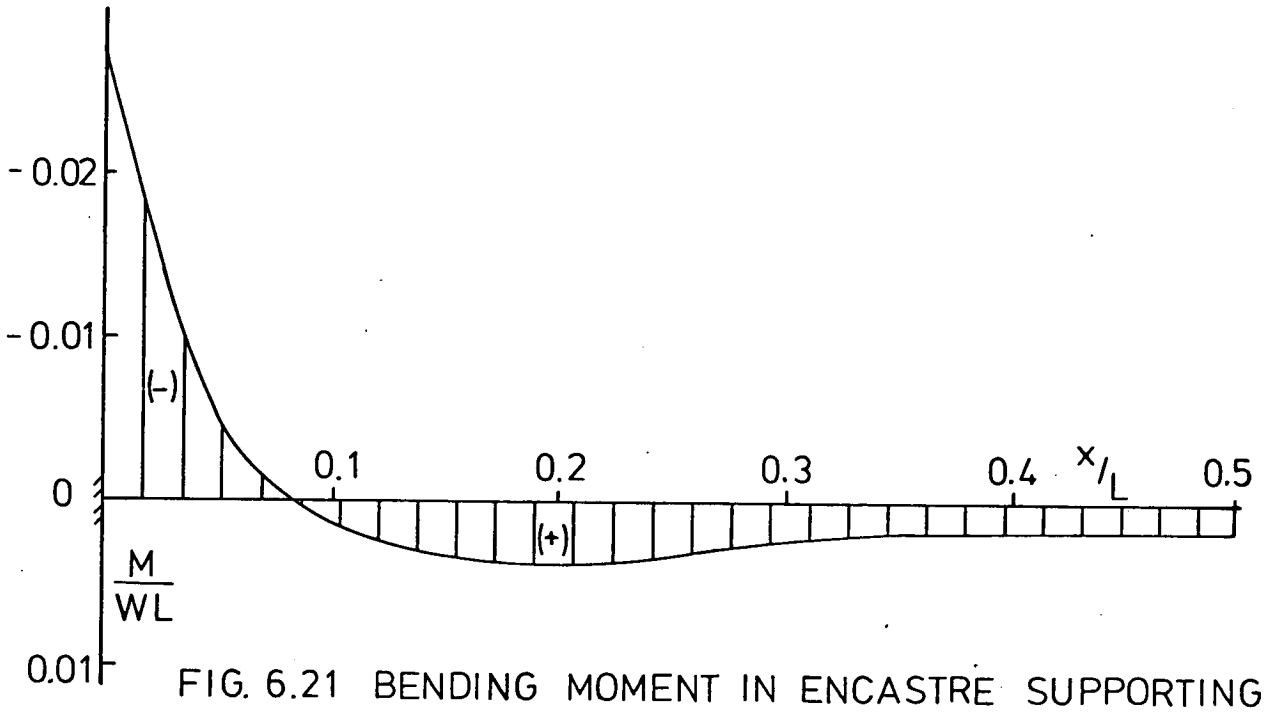

FIG. 6.21 BENDING MOMENT IN ENCASTRE SUPPORTING BEAM.

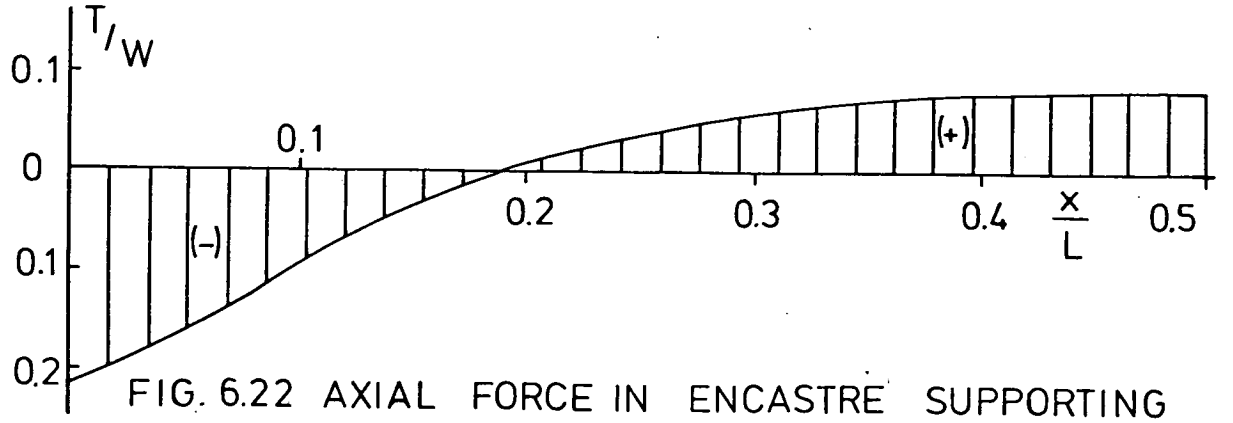

FIG. 6.22 AXIAL FORCE IN ENCASTRE SUPPORTING BEAM.

TABLE 6.1 COMPARISON OF RESULTS

BOUNDARY CONDITION	BENDING MOMENT $\frac{M}{WL} \times 10^{-4}$		AXIAL FORCE T/W		VERTICAL STRESS CONCENTRATION	MAXIMUM SHEAR STRESS $\frac{\tau . t}{\omega}$	CENTRAL DEFLECTION $\frac{\delta}{L} . 10^{-7}$
	ABSOLUTE MAXIMUM	MIDSPAN	ABSOLUTE MAXIMUM	MIDSPAN			
Support Width	-94.84	17.47	-0.177	0.077	3.0	1.30	6.72
Infill Frame	-61.09	12.43	-0.177	0.077	1.6	0.75	5.46
Load at Beam Level	117.13	16.29	0.247	0.247	10.0	2.20	16.36
Continuous Beam	-222.22	-222.22	0.086	-0.069	4.6	1.00	0.00
Encastre Beam	-258.38	16.08	-0.216	0.085	4.5	1.50	9.44
Simply Supported	117.00	15.86	0.251	0.251	10.0	2.20	16.04

supported case. Regarding the vertical stress concentration in the wall, Table 6.1 confirms that the simple support condition is the most severe support condition. It is seen that the magnitude of the stress concentration is the same for loading either on the beam level or on top of the wall. The least stress concentration is seen to be in the case where the panel is enclosed in a frame which shows the significance of the stanchions in relieving the wall from the vertical stress concentration. In cases where the supports are fixed or when the supporting beam is continuous, the stress concentration is seen to be less than half that in the simply supported case. As has been described earlier that the maximum vertical stress is the most predominant failure criterion before yielding of the supporting beam, it follows that introduction of any of these support conditions, in particular inclusion of vertical edge ties, will increase the ultimate strength of the composite beam over that in the simply supported case.

Table 6.1 also shows that with the exception of the continuous beam case the midspan bending moments are all positive and are of the same order of magnitude. The absolute maximum moment occurs at the supports when the ends of the beam are built-in and the maximum sagging moment occurs near the supports when the beam is simply supported.

A study of the last column of Table 6.1 shows that the presence of the vertical stanchions has reduced the central deflection to about one-third of that in the simply supported

beam.

It can be realized that in the foregoing analysis only one example has been analysed for each case and that no firm conclusions have been drawn on the basis of these results. However, it is suggested that the results have validity in that they all show that the point support leads to the most severe stress conditions and will be a safe assumption to make for the design procedure.

Further work, both experimental and analytical, should be made in these areas.

CHAPTER 7 : A DESIGN METHOD FOR COMPOSITE WALL-BEAMS

7.1 INTRODUCTION AND REVIEW OF THE EXISTING DESIGN METHODS

In this Chapter after a brief review of existing design methods is presented, proposals for the design of composite walls on steel or reinforced concrete beams are given. It is not intended that these proposals are finalized since the inclusion of design charts might well simplify the procedure.

(a) The Moment-Arm Method

This method has been suggested by Wood[2] and is only applicable to panels without openings. The method is based on the assumption of a reinforced panel as a whole, and it suggests that the amount of the steel reinforcement required in the supporting beam can be calculated by adopting a moment-arm of 2/3 x depth of wall with a limit of 0.7 x span. It has been shown by Wood that the method is conservative. This is because in actual practice there will be other features such as friction at the supports and cracking of concrete which will increase the apparent moment-arm.

(b) The Moment Coefficients Method

This has also been proposed by Wood[2] and it suggests that a design moment of WL/50 based on total load for brick panels where there are doors or window openings near the supports, and

WL/100 for panels where door or window openings are absent or occur at midspan. As a factor of safety, the design steel stress is limited to 109 N/mm^2 where the beam is propped up during the wall construction, and to 78 N/mm^2 where the beam is unsupported during wall construction.

In methods (a) and (b) the concrete or brick stresses and the deflections need not be calculated. However, the limitations imposed on both methods are that the height/span ratio should not be less than 0.6 x span, and that in the case of the moment coefficients method the beam depth/span ratio should be approximately (1/15 to 1/20). It is clear that the methods suffer from the lack of generalization since no account has been given to the variation in the wall/beam relative stiffness nor to the effect of the vertical stress concentration in the wall.

(c) Modified Moment Coefficient Method

To cater for the effect of the vertical stress concentration in the wall Wood and Simms[3] developed another design procedure based on modification of the moment coefficients method. They suggested that a reduction in the degree of the composite action, reflected in an increase in the beam bending moment, can occur as a result of the high compression stresses produced over the supports by the arching action inherent in composite behaviour. However, as the degree of the composite action is reduced the allowable stresses in the reinforcing steel can be increased.

On the basis of these concepts the following design equation has been proposed :

$$\text{R.F.} \propto \frac{(176 + K)\left[154 - \frac{K(K - 8)}{92}\right]}{3542}$$

in which the factor R accounts for the reduction in the average wall stress below the allowable, F is the stress reduction factor for slenderness of wall, and K is the bending moment factor.

The method is also limited to a minimum wall height/span ratio of 0.6 and a beam depth/span ratio between 1/15 to 1/20.

(d) Triangular-Load Distribution Method

A simple method[16] of designing the supporting beam is to consider that the loading on the beam is a superposition of triangular distribution of the wall loading and a horizontal component of the arch thrust (T') which is assumed to act at 22.5^{o} to the vertical (Figure 7.1). The vertical component of the thrust is W/2.

It must be remembered that with a single panel there is little justification for this simple method for there is no apparent external support for the bricks outside the triangle. The method also does not give any consideration to walls of great depth, since the bending moment deduced from the method is constant with varying wall height.

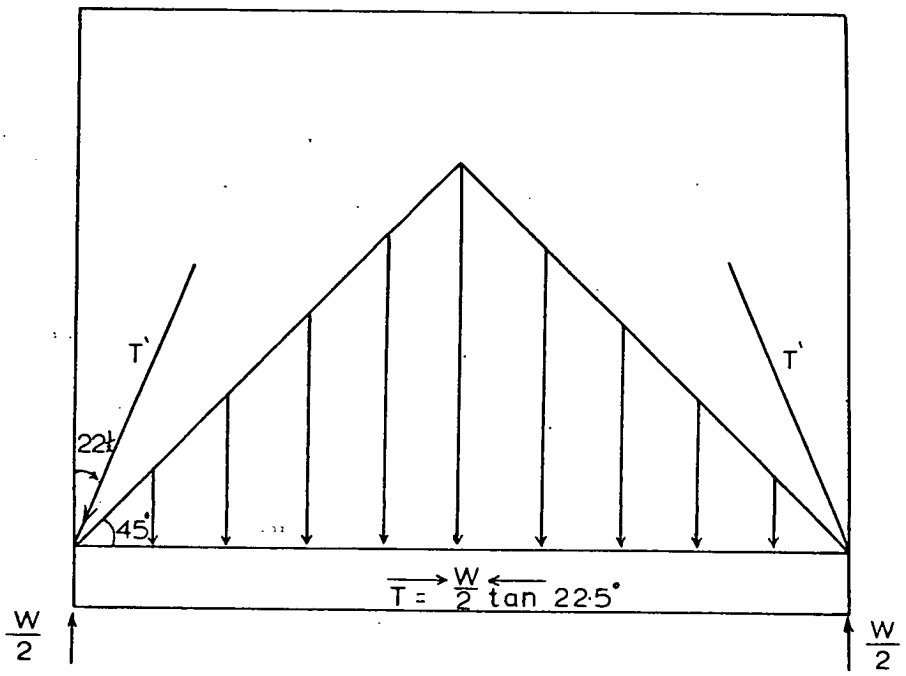

FIG. 7.1 GRAVITY LOADING FOR 45° SPREAD.

(e) B/20/5 Sub-Committee Design Recommendations

More recently an alternative design procedure at the ultimate limit state of masonry panels on steel beams has been proposed by the B/20/5 Sub-Committee[14,47,48,49,50] and has been included in the Draft Standard for the use of structural steel in buildings[51].

The method is based on satisfying two conditions : one ensuring that the beam is sufficiently stiff to avoid exceeding the design stress on the masonry panel, and the other ensuring that the beam is sufficiently strong to carry the loads upon it. It proposes that the design moment should be a super-position of the moment due to the beam self-weight and the

normal floor loading carried by the beam together with a moment of $W_w L/4K$ resulting from the wall loading. The total design moment, however, is limited to a minimum moment given by :

$$M_{min} \doteq \frac{0.22}{t^3 Lh} \cdot f_y \cdot \frac{(W_w \cdot \gamma_m)^4}{f_k}$$

where :

W_w is the sum of the design self weight of the panel and the design loads carried by the panel, in accordance with CPIII[52];

K is a relative stiffness parameter defined as $\frac{4\ L^3 t}{\sqrt{I}} \cdot \frac{E_w}{W_b}$;

f_k is the characteristics compressive strength of masonry ;

γ_m is a partial safety factor ;

f_y is the characteristics strength of the structural steel in beam ; and

h is the total depth of the beam.

The theory upon which the design method is based is that the length of contact along the wall/beam interface is governed by the relative stiffness (K), the stiffer the beam, the larger the length of contact.

The method appears to be conservative since it overestimates the bending moment by neglecting the effect of the interface horizontal shear force and by overestimating the contact length in the evaluation of the bending moment due to the wall loading.

7.2 FORMULATION OF A DESIGN PROCEDURE AT THE ULTIMATE LIMIT STATE

7.2.1 Design of Solid Brick Panel Walls on Simply Supported Steel Beams

In the design method two main requirements must be satisfied. These are :

(a) The maximum vertical stress in the panel should not exceed the brickwork design crushing strength.

(b) The bending and axial stresses in the beam should not exceed the design strength of steel.

Condition (a) - Maximum vertical stress in the wall is a limiting factor :

The minimum second moment of area (I_{min}) required to limit the brickwork stress to the design crushing strength (f_b) is given by rearranging equation (4.7.3) as :

$$I_{min} \leq \frac{h^3 t \beta^4 E_w}{(\frac{f_b L t}{W_w} - 1)^4 E_b} \qquad \ldots (7.1)$$

where W_w is the total applied load including the wall self-weight and f_b is the brickwork design crushing strength given by f'_c / γ_m in which f'_c is the characteristics compressive strength of brickwork and γ_m is a partial safety factor for the vocal compressive strength of the panel.

For a brick panel wall on a steel beam, E_w/E_b may be assumed equal to 1/30.

$$\therefore \quad I_{min} \propto \frac{h^3 t \beta^4}{30\left(\frac{f_b L t}{W_w} - 1\right)^4}$$

A beam designed by (7.2) satisfies the maximum vertical stress condition in the wall. To satisfy condition (b) it is necessary to check for the steel bending stresses.

Condition (b) - Check for beam bending stresses :

When the wall is stressed to the value of its material design strength, the value of the parameter R in equation (4.7.3) will be maximum and is given by :

$$R_{max} = \frac{1}{\beta}\left(\frac{f_b L t}{W_w} - 1\right) \qquad \ldots (7.3)$$

$$= 4\sqrt{\frac{h^3 t}{30\, I_{min}}} \qquad \ldots (7.4)$$

The maximum bending moment due to the self-weight of the wall and any superimposed load on it is given on substituting the value of R from (7.3) into equations (4.7.28), (4.7.30) and (4.7.32) for the three ranges of R. For a simplified moment expression the term γK may be neglected.

For $R \leqslant 5$

$$M_w = \frac{W_w^2(L - 10\ d\alpha)}{5 f_b\ Lt} \qquad \ldots (7.5)$$

Added to this is the moment due to the beam self weight and any additional floor loads assumed as uniformly distributed on the beam. This gives the total design moment as :

$$M_T = M_w + M_b = \frac{W_w^2(L - 10\ d\alpha)}{5 f_b\ Lt} + \frac{W_b L}{8} \qquad \ldots (7.6)$$

Similar expressions can be derived for the two ranges of R, namely :

For $5 < R < 7$

$$M_T = \frac{W_w^2(L - 8\ d\alpha)}{5.33\ f_b\ Lt} + \frac{W_b L}{8} \qquad \ldots (7.7)$$

And, for $R \geqslant 7$

$$M_T = \frac{W_w^2(L - 6\ d\alpha)}{6\ f_b\ Lt} + \frac{W_b L}{8} \qquad \ldots (7.8)$$

If f_{st} is the steel design strength, it follows that the section modulus required to satisfy the steel stress condition is given by :

$$Z \leq \frac{M_T}{f_{st}} \qquad \ldots (7.9)$$

where f_{st} is given by f_y/γ_m in which f_y is the characteristic strength of structural steel and γ_m is a partial safety factor.

M_T is obtained from equations (7.6) to (7.8) for the appropriate range of R. If a beam designed by condition (7.2) satisfies condition (7.9), then both design requirements of maximum vertical stress in the wall and maximum bending stresses in the beam, are satisfied. If condition (7.9) is not satisfied, only the maximum vertical stress requirement is met and the beam has to be redesigned for the steel stresses. This will be the case when the wall is not stressed up to its design strength f_b. A section is then chosen and the value of R is calculated as given by :

$$R = \sqrt[4]{\frac{h^3 t}{30\ I}}$$

This value of R is then substituted in equation (4.7.28), (4.7.30) or (4.7.32) according to the appropriate range of R, to give the moment due to W_w. To this is added the moment due to the beam self weight and the floor loading. The beam section modulus required to satisfy the bending stresses for

the three ranges of R, will be as follows :

$\underline{R \leqslant 5}$

$$Z \leqslant \frac{W_w(L - 10\ d\alpha)}{5\ f_s(1 + \beta R)} + \frac{W_b L}{8\ f_{st}} \qquad \ldots (7.10)$$

$\underline{5 < R < 7}$

$$Z \leqslant \frac{W_w(L - 8\ d\alpha)}{5.33\ f_s(1 + \beta R)} + \frac{W_b L}{8\ f_{st}} \qquad \ldots (7.11)$$

$\underline{R \geqslant 7}$

$$Z \leqslant \frac{W_w(L - 6\ d\alpha)}{6\ f_s(1 + \beta R)} + \frac{W_b L}{8\ f_{st}} \qquad \ldots (7.12)$$

The chosen section is then compared with that obtained by one of expressions (7.1) to (7.12). This is then used to calculate a new value of R which is substituted in the relevant of expressions (7.10) to (7.12) and a new section is obtained with which the last is compared. The iteration process is then continued until the last two values of Z are very near.

The moment due to the wall loading can be obtained from curves constructed for different values of R, h/L ratio and wall thickness. The general trend of these curves is shown in Figure (7.2).

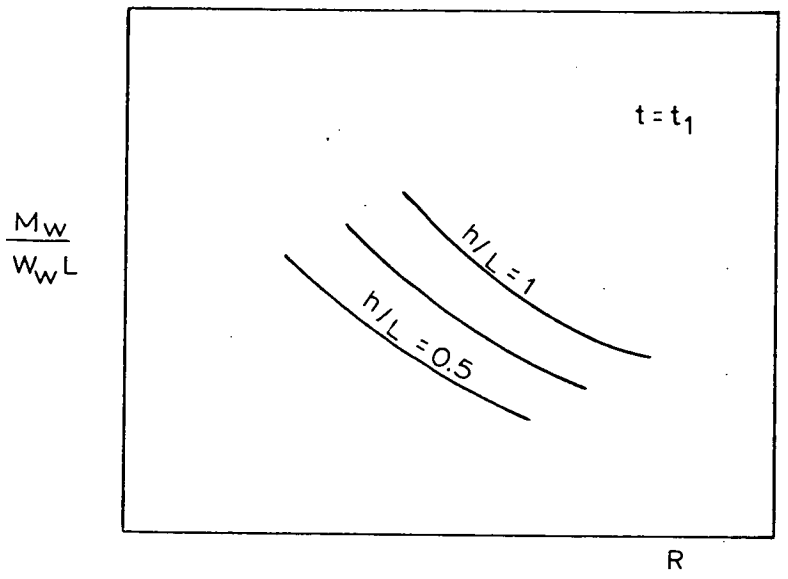

FIG. 7.2 Variation of Bending Moment due to Wall Loading with R and h/L for a Wall Thickness t_1.

The adequacy of the section must also be checked against the following :

(c) Tensile stress at midspan given by :

$$f_{st} = \frac{W_w}{A}\left(\alpha - \frac{\gamma ht}{30A}\right) + \frac{M_c}{Z} \qquad \ldots (7.13)$$

where M_c is the bending moment at midspan due to the wall loading and is obtained from equations (4.7.29), (4.7.31) or (4.7.33).

(d) Vertical shear at the supports, based on half the total load and the web gross area.

(e) Horizontal shear at the wall/beam interface. This is

checked for slipping at the interface joint. The check is provided by equation (4.7.16) for the coefficient of friction (μ) at the wall/beam interface.

$$\mu \geqslant W_w(\alpha - \frac{\gamma ht}{30A}) \qquad \ldots (7.14)$$

μ = 0.5 for brickwork wall on encased steel beam and

0.3 for brickwork wall on unencased steel beam.

If equation (7.14) is not satisfied shear connectors should be provided.

(f) The deflection at midspan which should not exceed L/300. This is checked by equation (4.7.37).

$$\delta = \frac{W_w L^3(3 + 10\,\beta R + 5\,\beta^2 R^2)}{240\,E_b I(1 + \beta R)^3} + \frac{3\,W_w L}{10\,E_w ht} -$$

$$\frac{W_w L^2 d(\alpha - \frac{\gamma ht}{30A})}{24\,E_b I} + \frac{W_b L^3}{384\,E_b I}$$

7.2.2 Design of Solid Brick Panel Walls on Simply Supported Reinforced Concrete Beams

The same design procedure is also applicable to the case of brick panels on reinforced concrete beams. In this case, however, the modular ratio (E_b/E_w) is taken as 4 and hence the minimum section of the beam required to limit the maximum

vertical stress in the panel to the brickwork design strength is given by :

$$I_{min} \propto \frac{h^3 t \beta^4}{4\left(\frac{f_b \cdot Lt}{W_w} - 1\right)^4} \qquad \ldots (7.15)$$

This is the required equivalent concrete section. It is assumed that the second moment of area of the equivalent section is calculated about its centroidal axis and that the concrete in tension is assumed to be ineffective.

Check for the adequacy of the chosen section in bending is performed by first computing the maximum bending moment in the beam for the corresponding value of R according to its appropriate range as in equations (7.6)to (7.8).

From this moment the section required to satisfy conditions (a) and (b) is given by the relationship according to the British Code[53] :

$$M_T = 0.15\, f_{cu}\, bd^2 \qquad \ldots (7.16)$$

And the area of reinforcing steel is computed by :

$$A_{st} = 0.3\, \frac{f_{cu}}{f_s}\, bd \qquad \ldots (7.17)$$

where f_{cu} is the characteristic cube strength of concrete and f_{st} is the stress in reinforcement.

Equations (7.16) and (7.17) are based on the section adopted in the British Code in which it is assumed that at flexural failure the average stress in the compressive zone is 0.6 f_{cu} and that the centre of compression is located at the mid-depth of this zone. The value adopted for the maximum depth of the compressive zone in the code of practice is one half of the effective depth.

If the beam designed by equation (7.16) and (7.17) satisfies (7.15) then it is adequate against the vertical stress condition in the wall and the bending stresses in the beam. If it does not, it must be redesigned for bending using the process of iteration. A section is chosen for which the required area of steel is calculated and consequently the value of R. This is used for the calculation of the bending moment due to the wall loading W_w, to which the moment due to the beam self weight and the floor loading is added. Equation (7.16) is used for the determination of the section which is then compared with the chosen section and by comparison and iteration the required section is obtained when the chosen and computed sections are nearly the same.

The remaining design steps are the same as those for the case of a steel beam.

7.2.3 Walls with Openings

The above design procedure may equally be applied to walls with central openings. However, in the case of a wall with offset door opening, it must be realized that the smaller section of the wall to the side of the opening must be designed to carry half of the applied load and that the beam bending moment is to be increased by 40 per cent over that in a beam supporting a similar solid wall. The beam must be checked for an axial force given by equation (5.13) as :

$$T = W_w(0.325 - 0.048\ K)$$

and for a deflection given by equation (5.16) as :

$$\delta = \frac{W_w L(3 + 10\ \beta R + 5\ \beta^2 R^2)}{} + \frac{0.75\ W_w L}{E_w h t} -$$

$$\frac{W_w L^3 d(\alpha - \gamma K)}{9.6\ E_b I} + \frac{W_b L^3}{154\ E_b I}$$

Beams designed by these methods have to be propped during construction.

Note : In the proposed design methods a great deal of simplification could be introduced by a suitable use of design charts. A suggestion for a proposed design chart has been made in Figure 7.2, but it is obvious that most of the proposed design equations could well be expressed in graphical forms, which will provide a more simpler design procedure.

CHAPTER 8 : CONCLUSIONS AND SUGGESTIONS FOR FUTURE RESEARCH

1. The wall and beam behave compositely as a tied arch. The wall takes the compression and the beam acts as a tie. The arching action in the wall causes the concentration of vertical compression above the beam support, and the concentration of these forces is the main cause of the wall failure before the steel in the supporting beam yields.

2. The ultimate resistance of the wall may be increased by either the use of bricks of high compressive strength at the bottom corners of the wall or by reinforcing of the bed joints over these localities.

3. Inclusion of vertical stanchions along the edges of the wall relieves the wall from the vertical stress concentration and would thus increase its ultimate carrying capacity.

4. The concentration of the vertical forces over the supports also results in high horizontal shear stress along the wall/beam interface and very near to the supports. For full composite action to develop this shear stress must be transmitted efficiently across the interface joint.

5. The maximum bending moment in the beam occurs very near to the supports and the vertical shear extends from the support section to about one-tenth to one-fifth of the span. The maximum axial force, however, occurs at midspan.

6. Two dimensionless parameters have been found to govern the stress distribution in the wall and the forces in the beam. These are the relative stiffness parameter ,

$$R = \sqrt[4]{\frac{h^3 t E_w}{I E_b}}$$

and the relative axial stiffness parameter,

$$K = \frac{h t E_w}{A E_b} .$$

The influence of R is much more pronounced than that of K. The vertical stress concentration over the supports increases with the increase of R as in the case of a flexible beam. However, a relatively stiff beam with low value of R results in the spread of the compressive forces towards the beam midspan thus relieving the wall from the stress concentration but increasing the bending moment in the supporting beam.

7. In walls with h/L ratio greater than unity, the stress distribution in the bottom part of the wall and the forces in the beam remain unaffected by the increase in the wall height.

8. Apart from a small increase in the maximum vertical stress over the supports, walls with central openings behave similarly to solid walls. The design recommendations for solid walls are also applicable to walls with central openings.

9. When a doorway occurs near to a support tensile stresses develop around the top corners of the opening. The ultimate resistance of such walls is nearly half that of solid walls or walls with central openings, which indicates a considerable loss in the degree of the composite action. This is also indicated by the excessive beam deflection which may be up to 2.5 times that of a beam supporting solid wall.

10. The finite element method has shown to be a very powerful numerical technique for providing a satisfactory solution to the composite structure under all possible boundary conditions, using the STRUDL computer program. On the basis of results obtained by this method, an approximate analysis has been proposed and a design procedure has been formulated.

Suggestion for Further Research

The present study has been concerned with the investigation of the interaction behaviour of walls on point-supported beams. This support condition has been shown to lead to the most severe stress distribution and consequently any design procedure based on this support condition will be conservative if adopted for structures with different support conditions. The aim of Chapter 6 was to reflect the effect of some of these support conditions on the behaviour of the composite beam. The preliminary analysis indicated beneficial effects

in the wall and beam, which if utilized will provide a more economical design. This, however, has to be confirmed by further analytical and experimental work which may cover the effect of the following :

1. Vertical stanchions or edge walls (framed panel);

2. Continuity of the supporting beam;

3. Column support;

4. Fixity of support.

The problem of the composite structure could be extended to include the effect of a composite box beam for which the walls can be assumed as a web and the slab and floor as the flanges. Great economy may be achieved in the design of such structures as a composite beam.

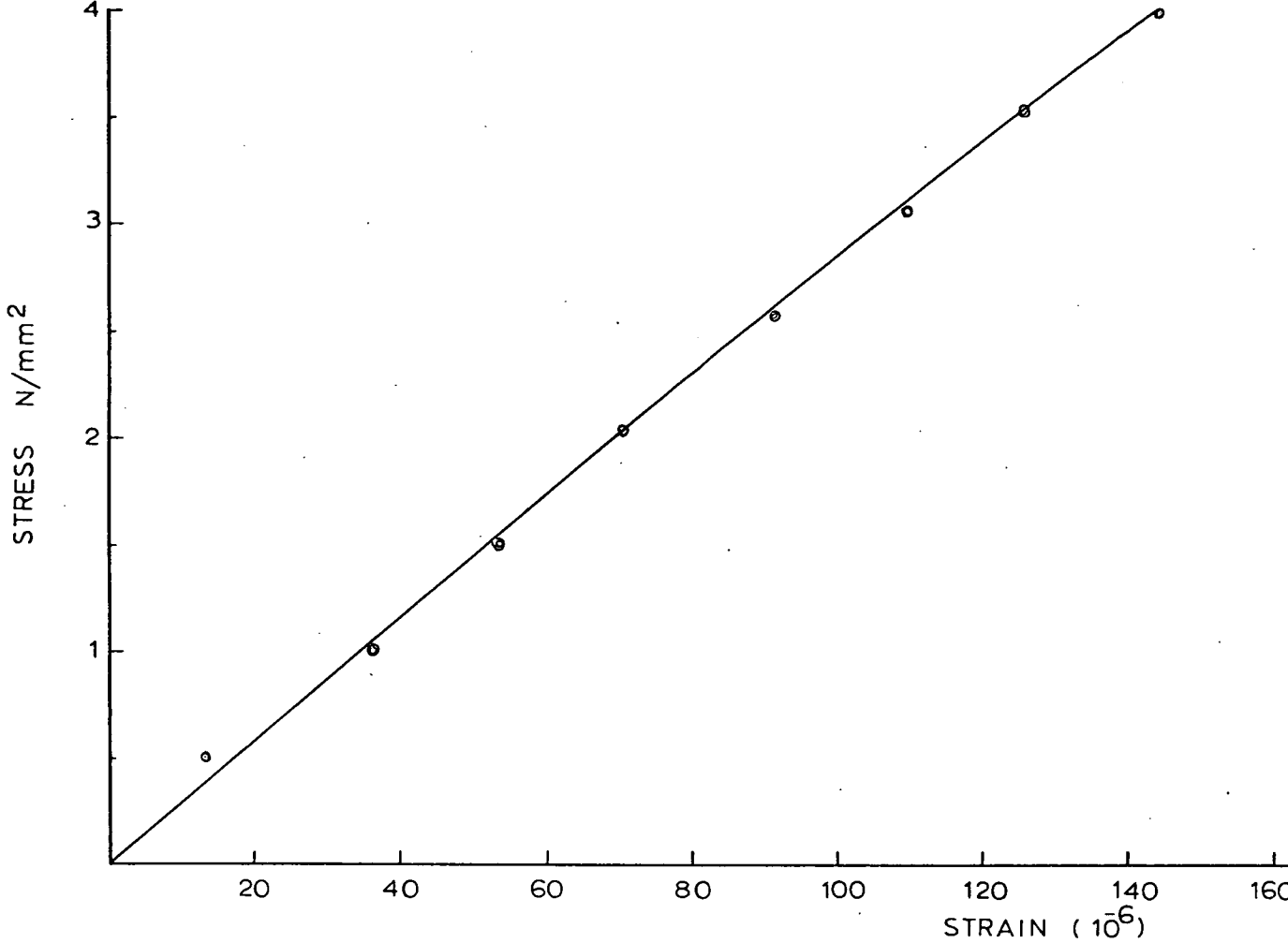

FIG (2A) STRESS-STRAIN CURVE FOR A CONCRETE PRISM IN AXIAL COMPRESSION

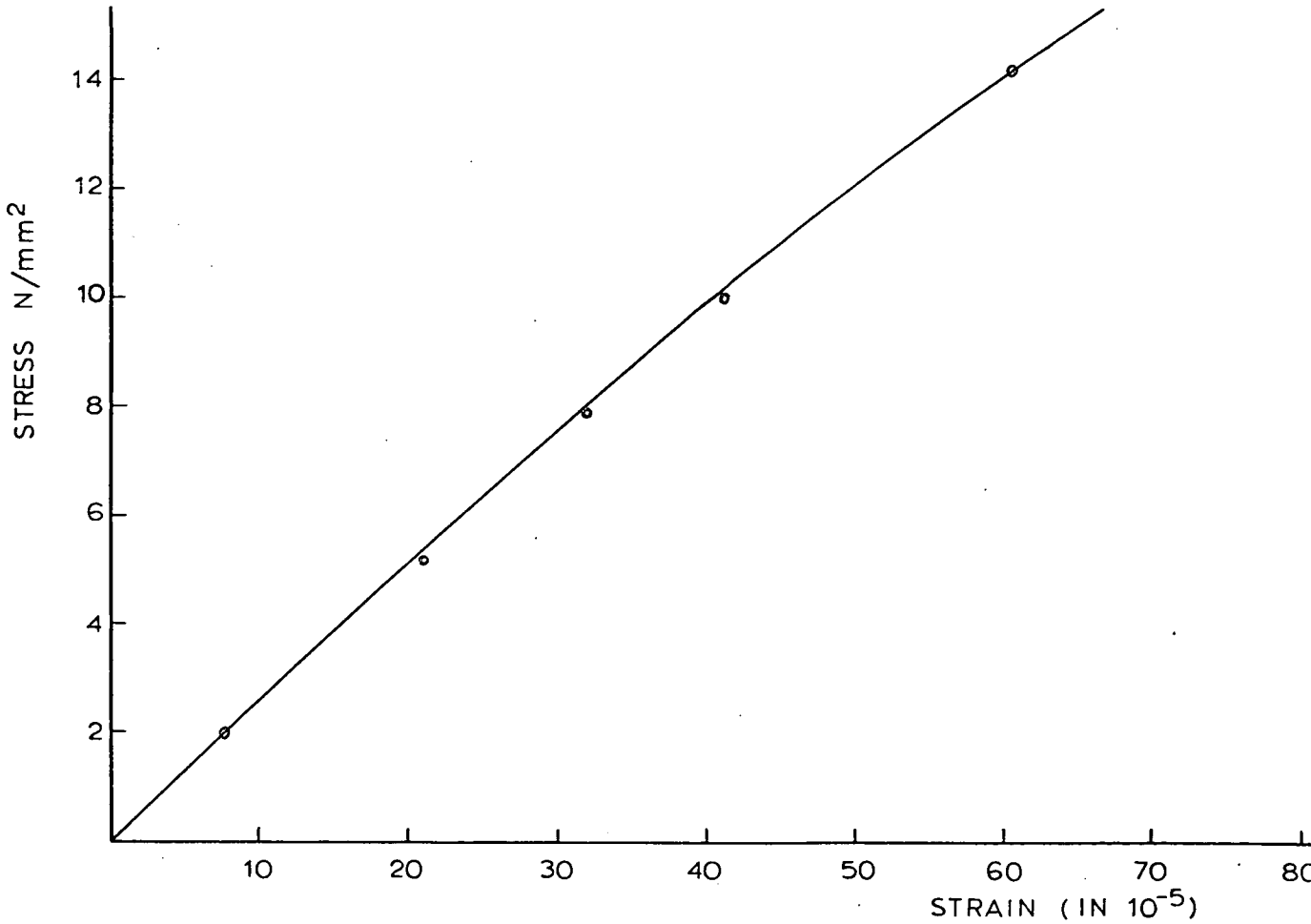

FIG (3A) STRESS-STRAIN CURVE FOR A 100mm CONCRETE CYLINDER

FIG. (4A) STRESS-STRAIN CURVE FOR BRICKWORK WALL SEGMENTS.

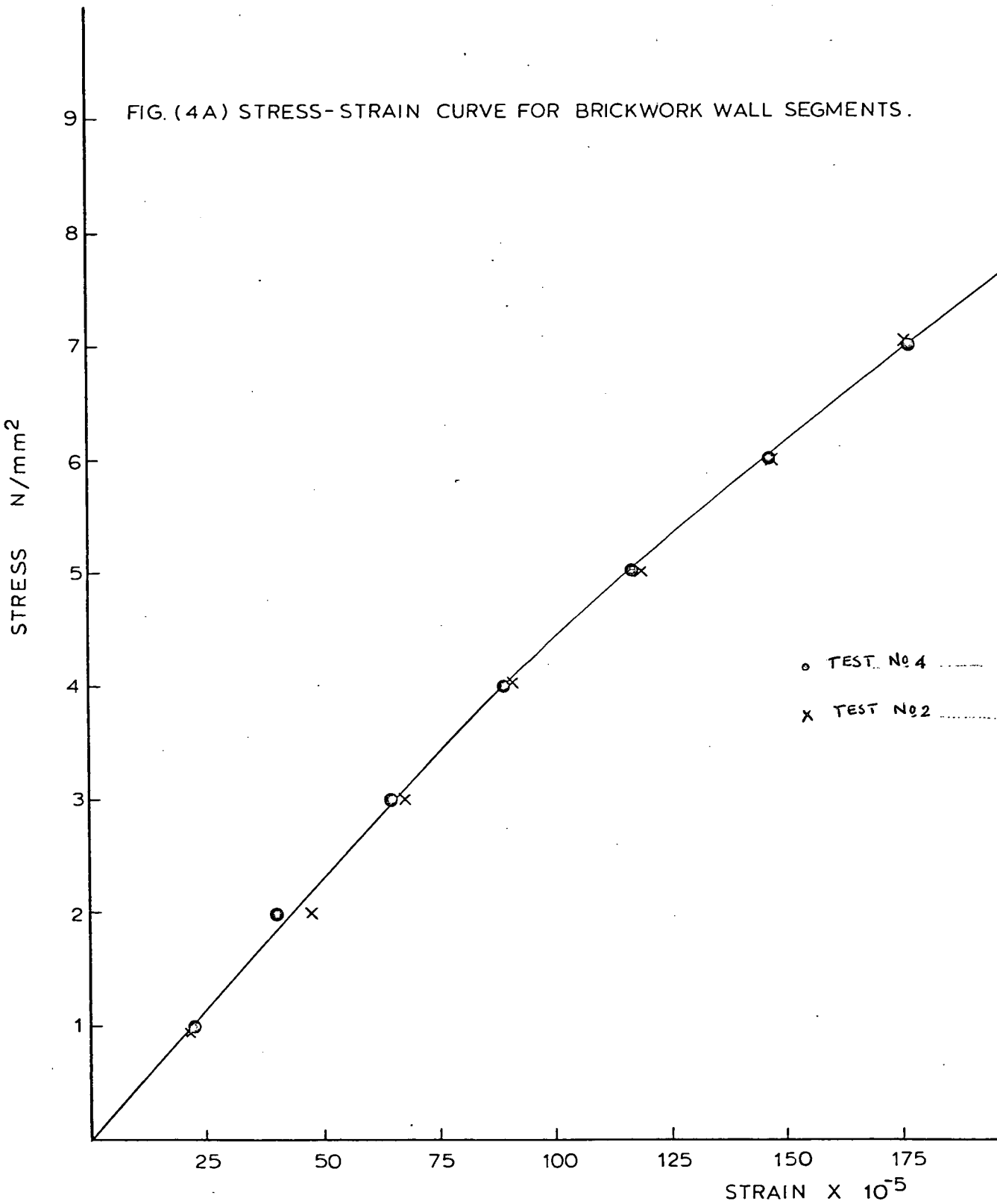

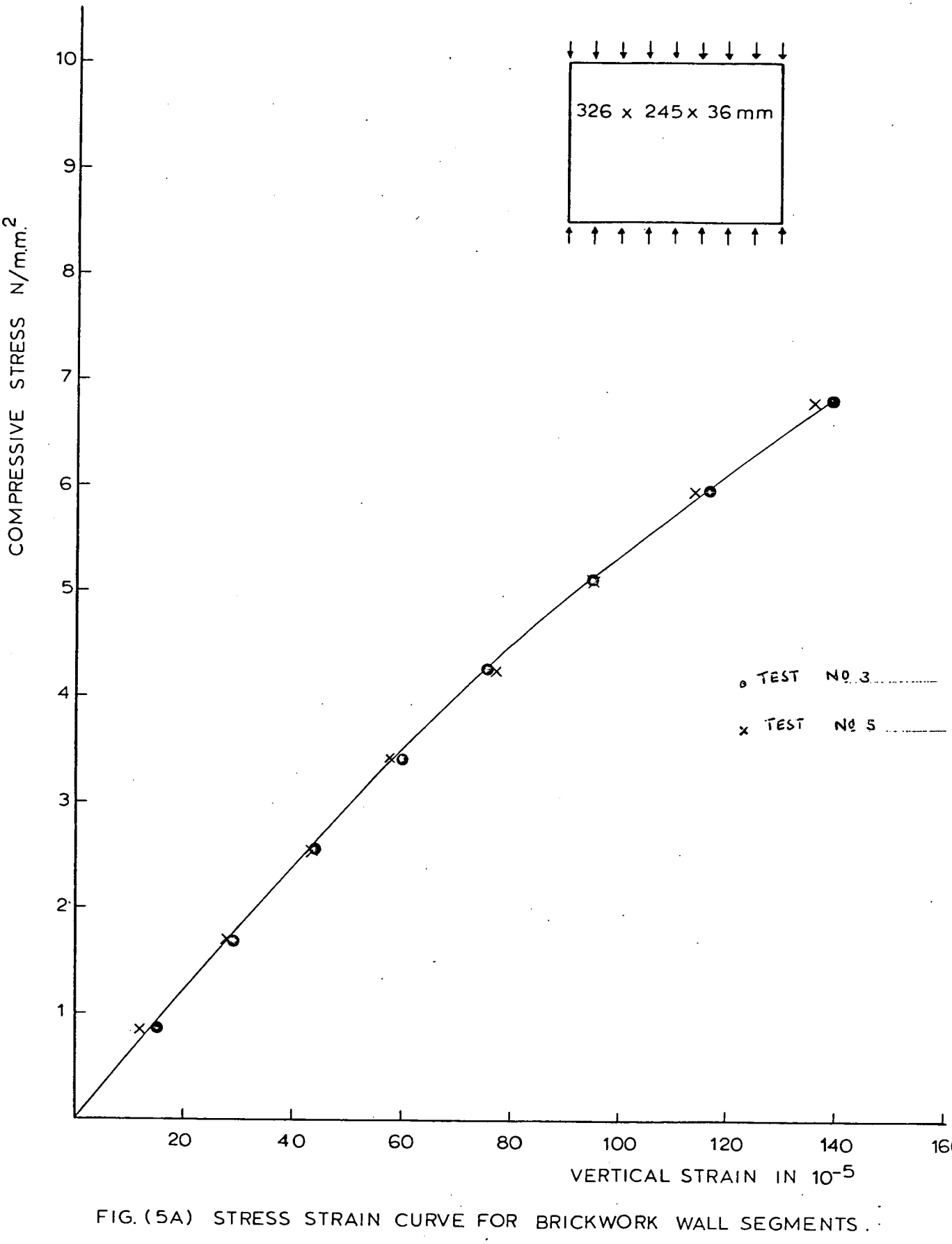

FIG. (5A) STRESS STRAIN CURVE FOR BRICKWORK WALL SEGMENTS.

REFERENCES

1. Mainstone, R J, "Studies in Composite Construction, Part III, Test on the New Government Offices, Whitehall Gardens", National Building Studies, Research Paper No 28, 1960.

2. Wood, R H, "Studies in Composite Construction, Part I, The Composite Action of Brick Panel Walls Supported on Reinforced Concrete Beams", National Building Studies, Research Paper No 13, 1952.

3. Wood, R H and Simms, L G, "A Tentative Design Method for the Composite Action of Heavily Loaded Brick Panel Walls Supported on Reinforced Concrete Beams", Building Research Station, CP 26/29, July 1969.

4. Rosenhaupt, S, "Stress in Point Supported Composite Walls", Proc of the American Concrete Institute, Vol 61, 1964, pp 795-809.

5. Rosenhaupt, S, "Elastic Analysis of Composite Walls - A General Theory", Bulletin Research Council of Israel, Vol 10c, 1961, pp 62-77.

6. Rosenhaupt, S, "Experimental Study of Masonry Walls on Beams", Proc ASCE ST DIV No ST3, June 1962, pp 137-166.

7. Rosenhaupt, S and Sokal, Y, "Masonry Walls on Continuous Beams", Proc ASCE ST DIV Vol 91, February 1965, pp 155-171.

8. Coull, A, "Composite Action of Walls Supported on Beams", Building Science, Vol 1, 1965-66, pp 259-270.

9. Plowman, J M, Sutherland, R J M and Couzens, M L, "The Testing of Reinforced Brickwork and Concrete Slabs Forming Box Beams", Structural Engineer, Vol 45, 1967, pp 379-393.

10. Colbourne, J R, "Studies in Composite Constructions : An Elastic Analysis of Wall/Beam Structure", CP 15/69, Building Research Station.

11. Burhouse, P, "Composite Action Between Brick Panel Walls and their Supporting Beams", Proc ICE, Vol 43, 1969, pp 175-194.

12. Yettram, A L and Hirst, M J S, "An Elastic Analysis for the Composite Action of Walls Supported on Simple Beams", Building Science, Vol 6, 1971, pp 151-159.

13. Levy, M and Spira, E, "Analysis of Composite Walls with and Without Openings", International Association for Bridges and Structural Engineers, Vol 33-I, 1973, pp 143-166.

14. Smith, B S and Riddington, J R, "The Design for Composite Action of Brickwork Walls on Steel Beams", 3rd International Brick-Masonry Conference, Essex, April 1973.

15. Male, D J and Arbon, P F, "A Finite Element Study of Composite Action in Walls Supported on Simple Beams", Building Science, Vol 6, 1971, pp 151-159.

16. Green, D R, "The Stress Analysis of Shear Walls", PhD Thesis, University of Glasgow, 1970.

17. Green, D R, "The Interaction of Solid Shear Walls and their Supporting Structures", Building Science, Vol 7, 1972, pp 239-248.

18. Saw, C B, "Linear Elastic Finite Element Analysis of Masonry Walls on Beams", Building Science Vol 9, 1974, pp 299-307.

19. Riddington, J R, "The Composite Behaviour of Walls Interacting with Flexural Members", PhD Thesis, University of Southampton, 1974.

20. Yettram, A L and Hirst, M J S, "An Elastic Analysis for the Composite Action of Walls Supported on Encastre Beams and Portal Frames", Building Science, Vol 9, 1974, pp 233-241.

21. Ramesh, C K, David, P S and Anjanayulu, E, "A Study of Composite Action in Brick Panel Wall Supported on Reinforced Concrete Beam", Indian Concrete Journal Vol 44, October 1970.

22. Achyutha, "Discussion of the Paper by Ramesh et al", Indian Concrete Journal Vol 45, No 5, May 1971.

23. Chandrashephara, K and Jacob, K A, "Photoelastic Analysis of Composite Action of Walls Supported on Beams", Building and Environment, Vol 11, 1976, pp 139-144.

24. Rosenhaupt, S and Muellor, G, "Openings in Masonry Walls on Settling Supports", Proc ASCE No ST3, June 1963, pp 107-131.

25. Rosenhaupt, S, Beresford, F D and Blakey, F A, "Test of a Post-Tensioned Concrete Masonry Wall", Proc ACI, Vol 64, 1967, pp 829-837.

26. Male, D J, "Discussion of the Papers by Burhouse", Proc ICE, Vol 44, 1969.

27. Raab, A R, "Discussion of the Papers by Rosenhaupt[4]", Proc ACI, Vol 61, 1964, pp 1685-1688.

28. Murthy, C K and Hendry, A W, "Comparative Tests on 1/3- and 1/6-Scale Model Brickwork Piers and Walls", Proc of the British Ceramic Society, No 4, July 1965.

29. Benjamin, J R and Williams, H A, "The Behaviour of One-Storey Brick Shear Walls", Journal of Structural Division, Proc ASCE, Paper 1723, July 1958.

30. Sinta, B P and Hendry, A W, "Splitting Failure of Brickwork as a Function of the Deformation Properties of Bricks and Mortar", British Ceramic Research Association, Technical Note No 86, May 1966.

31. Ruthburn, I C, "Wind Forces on a Tall Building", Proc ASCE, Vol 64(7), 1938.

32. Hrennikoff, A, "Solutions of Problems of Elasticity by the Framework Method", Journal of Applied Mechanics, ASME, December 1941, p A-169.

33. Sen, B R and Basayi, Prakash, "Determination of Elastic Constants for Concrete from Splitting Tests", Indian Concrete Journal (Bombay), Vol 36, No 7, July 1962, pp 249-252.

34. Desi, C S and Abel, J F, "Introduction to the Finite Method", Van Nostrand.

35. Smith, B S, Carter, C and Choudhury, J R, "The Diagonal Tensile Strength of Brickwork", The Structural Engineer, June 1970, No 6, Vol 48, pp 219-225.

36. Smith, B S and Rahman, K M K, "The Variation of Stresses in Vertically Loaded Brickwork Walls", Proc ICE, Vol 51, 1972.

37. Zeinkiewicz, O C and Cheung, Y K, "The Finite Element Method in Structural Continuum Mechanics", McGraw-Hill.

38. McLeod, I A, "New Rectangular Finite Element for Shear Wall Analysis", Journal of Structural Division, Proc ASCE, ST3, March 1969.

39. Pole, G M", Discussion of the Paper by McLeod", Proc ASCE, ST1, January 1970.

40. Logcher, R D, Conner J J and Nelson, M F, "ICES STRUDL-II, The Structural Design Language. Engineering Users Manual", Vol 2, Massachusetts Institute of Technology, Cambridge, Massachusetts.

41. Gilkey, C H, Fox, J D and Jones, T J, "Evaluation of STRUDL Finite Elements", Combustion Division, Report No EMD-72-1, Eight Semiannual Conference of the ICES Users Group, San Francisco, California, January 1972.

42. Hetenyi, M, "Beams on Elastic Foundations", University of Michigan Press, Ann Arbon, 1946.

43. Timosheuko, S Pand Goodier, J N, "Theory of Elasticity", Third Edition, McGraw-Hill.

44. Khoo, C L, "A Failure Criterion for Brickwork in Axial Compression", PhD Thesis, University of Edinburgh, 1972.

45. Cook, R D, "Concepts and Applications of Finite Element Analysis", John Wiley and Sons, Inc.

46. Smith, B S and Riddington, J R, "The Composite Behaviour of Masonry Wall on Steel Beam Structures", Proc of the First Canadian Masonry Symposium, June 1976.

47. Smith, B S, "Composite Action Between Walls and Beams", B/20/5, Sub-Committee, Technical Paper 47, University of Southampton, November 1972.

48. Smith, D G E and Johnson, R P, "The Interaction of Masonry Panels, Beams and Columns", B/20/5 Sub-Committee, Technical Paper 218, University of Warwick, March 1976.

49. Smith,D G E and Johnson, R P, "Derivation of the Design Method for Beams on Walls Presented in Technical Paper 47", B/20/5 Sub-Committee, Technical Paper 219, University of Warwick, March 1976.

50. Smith, D G E and Johnson, R P, "Walls on Beams, A Simplified Approach", B/20/5 Sub-Committee, Technical Paper 220, University of Warwick, March 1976.

51. CP 117: Part I, "Draft Standard for the Use of Structural Steel in Buildings Part 3 : Composite Construction", British Standard Institution, August 1976.

52. CP 111 : Part 2 : 1970, British Standard Code of Practice, Structural Recommendations for Loadbearing Walls, Part 2, British Standard Institution.

53. Bennet, E W, "Structural Concrete Elements", Chapman and Hall.